



University  
of Glasgow

Evans, Stephanie Kaye (2015) *Studies on the response to, and recovery from, rapamycin in Saccharomyces cerevisiae*. PhD thesis.

<http://theses.gla.ac.uk/6168/>

Copyright and moral rights for this thesis are retained by the author

A copy can be downloaded for personal non-commercial research or study, without prior permission or charge

This thesis cannot be reproduced or quoted extensively from without first obtaining permission in writing from the Author

The content must not be changed in any way or sold commercially in any format or medium without the formal permission of the Author

When referring to this work, full bibliographic details including the author, title, awarding institution and date of the thesis must be given

Studies on the response to, and  
recovery from, rapamycin in  
*Saccharomyces cerevisiae*

Stephanie Kaye Evans M.Sci.

Thesis submitted in fulfilment of the requirements for the Degree of Doctor of  
Philosophy

January 2015

School of Life Sciences,  
College of Medical, Veterinary and Life Sciences,  
University of Glasgow

© Stephanie Evans, January 2015

## Abstract

The Target of Rapamycin Complex 1 (TORC1) is a key and conserved regulator of cell growth and proliferation. The xenobiotic compound rapamycin is a potent inhibitor of TORC1 in yeast. The EGO complex, a non-essential activator of TORC1 is required for recovery of cells following rapamycin treatment. Why? Here, we find that rapamycin is in fact only a partial inhibitor of yeast TORC1; wild-type cells are able to maintain slow proliferation in the presence of high concentrations of the drug (*i.e.* concentrations multiple times the minimum inhibitory concentration). We find that this residual, rapamycin-insensitive, proliferation is dependent on the EGO complex and on TORC1 activity. We show that the ability of cells to maintain slow proliferation in the presence of rapamycin dictates their ability to recover. We find that rapamycin is not actively detoxified in yeast; instead, rapamycin is cleared by dilution-by-proliferation. The cell-associated intracellular pool of rapamycin is stable, decreasing only very slowly following washout of the drug and only diminishing at the rate of cell proliferation. The rapamycin-insensitive growth rate also persists long after rapamycin washout, indeed, until cells recover from the drug. The rapamycin-insensitive growth rate is not only able to quantitatively account for the observed kinetics of recovery from the drug in wild-type cultures, but also explains the severity of the *ego*- recovery defect.

We contributed to a large-scale genetic screen seeking mutants that, like *ego*-mutants, fail to recover from rapamycin treatment. We find that loss of any one of 10 proteins identified results in a rapamycin recovery defect and a slow rapamycin-insensitive growth rate. Our data propose important or novel roles of the core HOPS/CORVET complex, threonine biosynthesis, Vps15p, Vsp34p, Ccr4p and Dhh1p activities in modulating the activity or efficiency of TORC1.

Overall our results reveal that rapamycin is only a partial inhibitor of yeast TORC1, that persistence of the drug within the cell limits recovery and that rapamycin is not actively detoxified in yeast. Instead, recovery occurs due to dilution-by-proliferation and distribution of the drug among an increasing number of progeny cells. We also identify a set of potentially novel regulators of TORC1 activity.

# Table of Contents

|                                |  |    |
|--------------------------------|--|----|
| Abstract                       | 2  |    |
| Table of Contents              | 3  |    |
| List of Tables                 | 8  |    |
| List of Figures                | 9  |    |
| Acknowledgements               | 12   |    |
| Author's Declaration           | 13   |    |
| Contribution of Others to Data | 13   |    |
| List of Abbreviations          | 14   |    |
| 1                              | Introduction   | 15 |
| 1.1                            | TOR Complexes  | 15 |
| 1.2                            | Rapamycin  | 16 |
| 1.2.1                          | Detoxification of rapamycin in mammalian systems       | 16 |
| 1.2.2                          | Drug detoxification mechanisms in yeast                | 17 |
| 1.3                            | The Target of Rapamycin Complex 1                      | 18 |
| 1.3.1                          | Composition of TORC1                                   | 18 |
| 1.3.2                          | TORC1 localisation                                     | 18 |
| 1.4                            | Upstream of TORC1                                      | 20 |
| 1.4.1                          | TORC1 in response to environmental stress              | 21 |
| 1.4.2                          | TORC1 in response to nutrient cues                     | 22 |
| 1.4.2.1                        | The EGO Complex  | 22 |
| 1.4.2.2                        | The SEA Complex  | 23 |
| 1.4.2.3                        | Vam6p as a Guanine Exchange Factor for the EGO complex | 27 |
| 1.4.2.4                        | TORC1 activation by leucyl-tRNA synthetase             | 27 |
| 1.4.2.5                        | TORC1 regulation by PI(3,5)P2                          | 30 |
| 1.5                            | The mammalian Target Of Rapamycin 1 (mTORC1)           | 32 |
| 1.5.1                          | mTORC1 composition                                     | 32 |
| 1.5.2                          | mTORC1 in response to nutrient cues                    | 34 |
| 1.5.2.1                        | mTORC1 localisation                                    | 34 |
| 1.5.2.2                        | mTORC1 activation by Rheb                              | 34 |
| 1.5.2.3                        | mTORC1 activation by Rag GTPases and Ragulator         | 35 |
| 1.5.2.4                        | The 'inside-out' model of mTORC1 activation            | 37 |
| 1.5.2.5                        | Regulation of mTORC1 by GATOR                          | 40 |
| 1.5.2.6                        | Regulation of mTORC1 by Leucyl-rRNA synthetase         | 40 |
| 1.6                            | Downstream of yeast TORC1                              | 43 |
| 1.6.1                          | Regulation of translation initiation                   | 43 |
| 1.6.2                          | Regulation of ribosome biosynthesis                    | 43 |

|        |  |    |
|--------|--|----|
| 1.6.3  | Regulation of amino acid permeases at the cell surface _____   | 45 |
| 1.6.4  | Regulation of autophagy _____  | 46 |
| 1.6.5  | Regulation of starvation-induced gene transcription _____  | 47 |
| 1.6.6  | Sch9p and Tap42p _____   | 48 |
| 1.6.7  | Comparison of yeast down-stream functions of TORC1 with the<br>down-stream functions of mTORC1 _____ | 49 |
| 1.7    | Phenotype of <i>ego</i> - mutants _____  | 50 |
| 1.8    | Aims of this project _____   | 52 |
| 2      | Materials and Methods _____  | 53 |
| 2.1    | Growth conditions _____  | 53 |
| 2.2    | Yeast cultures _____   | 53 |
| 2.2.1  | Creating double mutants _____  | 53 |
| 2.3    | Transformation _____   | 56 |
| 2.3.1  | Bacterial transformation _____   | 56 |
| 2.3.2  | Yeast transformation _____   | 56 |
| 2.3.3  | Switching the kanamycin selection marker _____   | 56 |
| 2.4    | Sporulation and dissection _____   | 56 |
| 2.4.1  | Sporulation and dissection _____   | 56 |
| 2.4.2  | Determining the mating type _____  | 58 |
| 2.4.3  | Genotyping haploids with regards to auxotrophic markers _____  | 58 |
| 2.5    | Creating <i>kog1</i> $\Delta^{\text{ts}}$ haploids _____   | 58 |
| 2.6    | Spot assay for recovery _____  | 59 |
| 2.7    | Methylene blue staining _____  | 59 |
| 2.8    | Amino acid uptake _____  | 59 |
| 2.9    | Measuring culture densities and calculating the growth rate _____                                    | 60 |
| 2.9.1  | Culture density as measured by Coulter counter _____   | 60 |
| 2.9.2  | Culture density as measured by optical spectrometry _____  | 60 |
| 2.9.3  | Calculating the growth rate _____  | 60 |
| 2.10   | Autophagy assay _____  | 61 |
| 2.11   | Mass spectrometry _____  | 61 |
| 2.12   | Translation assay _____  | 62 |
| 2.13   | Measuring and predicting recovery time from rapamycin _____  | 63 |
| 2.13.1 | Experimentally measuring recovery time _____   | 63 |
| 2.13.2 | Predicting the recovery time _____   | 63 |
| 2.14   | Databases _____  | 64 |
| 2.14.1 | GO Term analysis _____   | 64 |
| 2.14.2 | Physical interaction analysis _____  | 64 |
| 2.15   | Sensitivity to rapamycin _____   | 64 |
| 2.16   | FM4-64 staining and confocal microscopy _____  | 65 |

|        |  |     |
|--------|--|-----|
| 2.16.1 | FM4-64 staining _____  | 65  |
| 2.16.2 | Confocal microscopy _____  | 65  |
| 2.17   | Statistics _____   | 65  |
| 3      | Testing various models that could explain why <i>ego</i> - mutants fail to recover from rapamycin treatment _____                        | 67  |
| 3.1    | Introduction _____   | 67  |
| 3.2    | Results _____  | 69  |
| 3.2.1  | Establishing the <i>ego</i> - phenotype under our laboratory conditions ____   | 69  |
| 3.2.2  | Methylene blue staining _____  | 70  |
| 3.2.3  | Uptake of amino acids _____  | 72  |
| 3.2.4  | Testing <i>gap1Δ</i> null mutants for recovery from rapamycin _____  | 80  |
| 3.2.5  | Testing recovery of <i>ego</i> - mutants from various TORC1 inactivating treatments _____  | 82  |
| 3.2.6  | Do known multidrug detoxification pathways have a role in recovery from rapamycin? _____   | 84  |
| 3.3    | Conclusion _____   | 88  |
| 4      | Rapamycin-insensitive TORC1 activity _____   | 94  |
| 4.1    | Introduction _____   | 94  |
| 4.2    | Results _____  | 95  |
| 4.2.1  | Wild-type cells proliferate in the presence of a high concentration of rapamycin (200 ng/mL) _____                                       | 95  |
| 4.2.2  | Rapamycin treatment induces autophagy in wild-type and in <i>ego1Δ</i> cells _____   | 102 |
| 4.2.3  | Proliferation of wild-type cells in various high concentrations of rapamycin _____   | 104 |
| 4.2.4  | Can <i>ego</i> - mutant cells proliferate in the presence of high concentrations of rapamycin? _____                                     | 105 |
| 4.2.5  | Does the proliferation rate of <i>ego1Δ</i> mutants vary with the concentration of rapamycin, when present at high concentrations? _____ | 107 |
| 4.2.6  | Are all subunits of the EGO complex required to support rapamycin-insensitive proliferation? _____                                       | 109 |
| 4.2.7  | Are Tor1p and Tco89p required for rapamycin-insensitive proliferation? _____   | 114 |
| 4.2.8  | Growth rate of <i>kog1<sup>ts</sup></i> in the presence of a high concentration of rapamycin _____                                       | 116 |
| 4.2.9  | Can yeast cells proliferate in the complete absence of Kog1p? ____   | 121 |
| 4.2.10 | Rapamycin-insensitive TORC1 activity is inhibited by caffeine ____   | 123 |
| 4.2.11 | Ego1p is required for rapamycin-insensitive translation _____  | 126 |
| 4.2.12 | Growth rate of <i>caf20Δ</i> and <i>eap1Δ</i> in the presence of a high concentration of rapamycin _____                                 | 128 |
| 4.2.13 | Do wild-type cultures of various genetic backgrounds have a rapamycin-insensitive growth rate? _____                                     | 129 |

|         |  |     |
|---------|--|-----|
| 4.3     | Conclusion _____   | 132 |
| 5       | Rapamycin-insensitive proliferation underpins recovery from rapamycin _____                          | 136 |
| 5.1     | Introduction _____   | 136 |
| 5.2     | Results _____  | 136 |
| 5.2.1   | Can we invoke a rapamycin recovery defect in wild-type cells? ____                                   | 136 |
| 5.2.2   | The rapamycin-insensitive growth rate persists following washout of the drug _____                   | 139 |
| 5.2.3   | Monitoring rapamycin in cells using mass spectrometry _____  | 141 |
| 5.2.4   | Can <i>ego</i> - mutants recover from rapamycin? _____   | 149 |
| 5.2.5   | Can we quantify the recovery time? _____   | 154 |
| 5.2.6   | How does the recovery time vary with concentration of rapamycin? _____                               | 156 |
| 5.2.7   | Does the rapamycin-insensitive growth rate explain the recovery time? _____                          | 160 |
| 5.2.8   | Does a rapamycin-insensitive growth rate correlate with recovery? _____                              | 164 |
| 5.3     | Conclusion _____   | 166 |
| 6       | Identifying other potential regulators of TORC1 _____  | 171 |
| 6.1     | Introduction _____   | 171 |
| 6.2     | Results _____  | 171 |
| 6.2.1   | Summary of the primary screen _____  | 171 |
| 6.2.2   | Analysis of the results of the primary screen _____  | 172 |
| 6.2.3   | GO Term enrichment in the primary mutant set _____   | 175 |
| 6.2.3.1 | GO term enrichment in the 'single-hit' mutant set _____  | 178 |
| 6.2.4   | Protein-protein interactions among the gene products of the mutant set from the primary screen _____ | 181 |
| 6.2.5   | Selection of mutants for secondary screening _____   | 183 |
| 6.2.6   | Secondary screen: Recovery from rapamycin _____  | 185 |
| 6.2.6.1 | Threonine biosynthesis mutants _____   | 186 |
| 6.2.6.2 | Endosomal trafficking mutants _____  | 186 |
| 6.2.6.3 | Regulation of transcription mutants _____  | 189 |
| 6.2.6.4 | Summary _____  | 189 |
| 6.2.7   | Tertiary screen I: Viability of null mutants in the presence of rapamycin _____                      | 189 |
| 6.2.8   | Tertiary screen II: Rapamycin-insensitive growth rate _____  | 191 |
| 6.2.8.1 | Threonine biosynthesis mutants _____   | 191 |
| 6.2.8.2 | Endosomal trafficking mutants _____  | 194 |
| 6.2.8.3 | Regulation of transcription mutants _____  | 196 |
| 6.2.8.4 | Summary _____  | 196 |

|        |  |     |
|--------|--|-----|
| 6.2.9  | Selectivity to rapamycin treatment _____   | 196 |
| 6.2.10 | Recovery from rapamycin of <i>ego1Δ pep3Δ</i> double mutants _____   | 198 |
| 6.2.11 | The rapamycin-insensitive growth rate of <i>hops/corvet- ego-</i><br>double mutants _____                                  | 200 |
| 6.2.12 | Could a vacuolar morphology defect explain the requirement of<br>the core HOPS/CORVET complex in rapamycin recovery? _____ | 202 |
| 6.3    | Conclusion _____   | 206 |
| 7      | Discussion _____   | 210 |
| 7.1    | Rapamycin does not fully inactivate TORC1 _____  | 210 |
| 7.2    | Is rapamycin-insensitive activity due to a subset of TORC1 not<br>bound to rapamycin? _____                                | 211 |
| 7.3    | The mechanism of rapamycin ‘detoxification’ _____  | 212 |
| 7.4    | Identifying other potential regulators of TORC1 _____  | 213 |
| 7.4.1  | Mutants of translational regulators _____  | 213 |
| 7.4.2  | Mutations of the HOM proteins _____  | 214 |
| 7.4.3  | The Vps15-Vps34 complex _____  | 214 |
| 7.4.4  | The core HOPS/CORVET complex _____   | 216 |
| 7.5    | How much TORC1 activity is insensitive to rapamycin? _____   | 219 |
| 7.6    | Does all nutrient signalling to TORC1 act via the EGO complex? ____  | 220 |
| 7.7    | Future work _____  | 221 |
| 7.7.1  | The large-scale genetic screen _____   | 221 |
| 7.7.2  | TORC1 activity _____   | 223 |
| 7.7.3  | Identify new regulators of TORC1 _____   | 224 |
| 7.7.4  | How does rapamycin enter the cell? _____   | 224 |
| 7.7.5  | What are the rapamycin-insensitive functions of TORC1? _____   | 225 |
| 7.8    | Conclusion _____   | 225 |
|        | References _____   | 226 |

## List of Tables

|           |  |     |
|-----------|--|-----|
| Table 2.1 | List of Strains used throughout the thesis_____  | 55  |
| Table 2.2 | List of the plasmids used in this thesis _____   | 57  |
| Table 3.1 | Methylene blue staining of cells treated with rapamycin _____  | 73  |
| Table 3.2 | Chronological lifespan of <i>ego</i> - mutants from Powers et al. (2006)_____  | 92  |
| Table 4.1 | Germination and proliferation of <i>kog1Δ</i> /WT diploids in the absence and presence of rapamycin (200 ng/mL) _____                  | 122 |
| Table 5.1 | Recovery from various concentrations of rapamycin with varying treatment times _____   | 153 |
| Table 5.2 | Comparison of the calculated slope of the recovery time to the observed rapamycin-insensitive doubling time _____                      | 165 |
| Table 6.1 | Null mutants identified from each run of the primary screen with a colony formation defect _____                                       | 173 |
| Table 6.2 | The number of null mutants identified across the three runs that were scored as having at least a mild rapamycin recovery defect _____ | 174 |
| Table 6.3 | The gene name and ORF number of mutants identified in at least two runs of the primary screen_____                                     | 176 |
| Table 6.4 | Enrichment of GO terms identified in our primary mutant set __   | 177 |
| Table 6.5 | The gene names for which the null mutants were significantly enriched in the primary screen by GO Term analysis _____                  | 179 |
| Table 6.6 | Enrichment of GO Terms of the mutant set found only in any one run of the primary screen _____   | 180 |
| Table 6.7 | Null mutants selected for secondary screening _____  | 184 |
| Table 6.8 | Percentage of cell death following exposure to rapamycin _____   | 192 |
| Table 6.9 | Summary of the results of the secondary screens _____  | 207 |

## List of Figures

|             |  |     |
|-------------|--|-----|
| Figure 1.1  | The components of TORC1 _____  | 19  |
| Figure 1.2  | The EGO complex _____  | 24  |
| Figure 1.3  | The SEA complex _____  | 26  |
| Figure 1.4  | Vam6p regulates TORC1 activity via the EGO complex _____   | 28  |
| Figure 1.5  | The leucyl-tRNA synthetase activates the EGO complex _____   | 29  |
| Figure 1.6  | The signalling molecule PI(3,5)P2 activates TORC1 _____  | 31  |
| Figure 1.7  | The components of mTORC1 and signalling by Rheb _____  | 33  |
| Figure 1.8  | The Rag GTPases regulate mTORC1 with the aid of the<br>Regulator complex _____                                       | 36  |
| Figure 1.9  | The V-ATPase promotes mTORC1 activity _____  | 39  |
| Figure 1.10 | The components, and signalling to mTORC1, of the GATOR<br>complex _____  | 41  |
| Figure 1.11 | Leucyl-tRNA synthetase promotes mTORC1 activity _____  | 42  |
| Figure 1.12 | The downstream TORC1 signalling pathway _____  | 44  |
| Figure 3.1  | Loss of any subunit of the EGO complex results in a rapamycin<br>recovery defect phenotype _____                     | 71  |
| Figure 3.2  | Uptake of amino acids following rapamycin treatment _____  | 75  |
| Figure 3.3  | Uptake of amino acids into wild-type and <i>gtr2Δ</i> cells relative<br>to their own uptake of untreated cells _____ | 77  |
| Figure 3.4  | Loss of Gap1p does not result in a rapamycin recovery defect ____  | 81  |
| Figure 3.5  | Testing sensitivity of yeast to caffeine _____   | 83  |
| Figure 3.6  | Recovery of <i>ego-</i> from TORC1 inactivating treatments _____   | 85  |
| Figure 3.7  | Recovery from rapamycin of null mutants involved in<br>multidrug resistance _____                                    | 87  |
| Figure 4.1  | Proliferation of wild-type cells in the constant presence of<br>rapamycin (200 ng/mL) _____                          | 97  |
| Figure 4.2  | The rapamycin-insensitive growth rate of wild-type cells is not<br>altered by previous exposure to rapamycin _____   | 99  |
| Figure 4.3  | Sensitivity of naïve or recovered wild-type cultures to various<br>concentrations of rapamycin _____                 | 101 |
| Figure 4.4  | Autophagy is induced upon treatment of yeast cells with high<br>concentrations of rapamycin _____                    | 103 |
| Figure 4.5  | Growth rate of wild-type cultures in various high<br>concentrations of rapamycin _____                               | 106 |
| Figure 4.6  | Proliferation of <i>ego1Δ</i> cells in the constant presence of<br>rapamycin (200 ng/mL) _____                       | 108 |
| Figure 4.7  | Growth rate of wild-type and <i>ego1Δ</i> cultures in various high<br>concentrations of rapamycin _____              | 110 |
| Figure 4.8  | The growth rate of <i>ego-</i> mutants in the presence of a high<br>concentration rapamycin _____                    | 112 |

|             |  |     |
|-------------|--|-----|
| Figure 4.9  | Growth rate of wild-type, <i>ego1Δ</i> and <i>gtr2Δ</i> cultures in 20 and 200 ng/mL rapamycin _____   | 113 |
| Figure 4.10 | Proliferation of <i>tor1Δ</i> and <i>tco89Δ</i> cells in the constant presence of rapamycin (200 ng/mL) _____  | 115 |
| Figure 4.11 | The growth rate of <i>tco89Δ</i> cells in 20 and 200 ng/mL rapamycin _____   | 117 |
| Figure 4.12 | Growth rate of <i>kog1<sup>ts</sup></i> in the constant presence of rapamycin (200 ng/mL) _____  | 119 |
| Figure 4.13 | Growth rate of <i>kog1<sup>ts</sup></i> in 20 and 200 ng/mL rapamycin _____  | 120 |
| Figure 4.14 | Growth rate of wild-type and <i>ego1Δ</i> cultures treated with a high concentration of rapamycin and sub-inhibitory concentration of caffeine _____           | 125 |
| Figure 4.15 | Translation rates of rapamycin and cycloheximide treated wild-type and <i>ego1Δ</i> mutant cells _____   | 127 |
| Figure 4.16 | The rapamycin-insensitive growth rates of <i>caf20Δ</i> and <i>eap1Δ</i> cultures in the presence of rapamycin (200 ng/mL) _____                               | 130 |
| Figure 4.17 | The rapamycin-insensitive growth rate of wild-type strains of various genetic backgrounds _____  | 131 |
| Figure 5.1  | Recovery of wild-type cells from rapamycin treatment in the presence of caffeine _____   | 138 |
| Figure 5.2  | Recovery of wild-type cells from rapamycin when expressing a caffeine resistant <i>tor1<sup>I1954V</sup></i> allele in the presence of caffeine ____           | 140 |
| Figure 5.3  | The rapamycin-insensitive growth rate of cultures maintains after washout of the drug _____  | 142 |
| Figure 5.4  | Recovery of wild-type and <i>ego1Δ</i> from 400 ng/mL rapamycin _____  | 144 |
| Figure 5.5  | Uptake of rapamycin into wild-type and <i>ego1Δ</i> cells _____  | 146 |
| Figure 5.6  | Cell associated rapamycin during a 'recovery phase' from rapamycin treatment _____   | 147 |
| Figure 5.7  | Increase in culture density during recovery from rapamycin _____   | 148 |
| Figure 5.8  | The total intracellular concentration of rapamycin present during the 'recovery phase' _____   | 150 |
| Figure 5.9  | Recovery of wild-type and <i>ego-</i> mutants from various concentrations of rapamycin _____   | 152 |
| Figure 5.10 | Observing cultures recovering from rapamycin treatment _____   | 155 |
| Figure 5.11 | Demonstrating how the lag time to recovery was determined ____   | 157 |
| Figure 5.12 | The time at which wild-type and <i>ego1Δ</i> cells recover from various concentrations of rapamycin _____  | 159 |
| Figure 5.13 | Extrapolating recovery time to the origin _____  | 161 |
| Figure 5.14 | The predicted and experimentally observed recovery times for wild-type and <i>ego1Δ</i> cultures from various high concentrations of rapamycin treatment _____ | 163 |
| Figure 5.15 | Recovery of <i>tor1Δ</i> , <i>eap1Δ</i> wild-type (W303, EG123), and <i>tco89Δ</i> from rapamycin treatment _____  | 167 |
| Figure 6.1  | Protein-protein interactions among the primary protein set ____  | 182 |

|             |  |     |
|-------------|--|-----|
| Figure 6.2  | Recovery from rapamycin of <i>hom2Δ</i> and <i>hom3Δ</i> mutants_____  | 187 |
| Figure 6.3  | Recovery from rapamycin of endosomal trafficking mutants____   | 188 |
| Figure 6.4  | Recovery from rapamycin of regulation of transcription<br>representatives_____   | 190 |
| Figure 6.5  | The rapamycin-insensitive growth rate of <i>hom2Δ</i> and <i>hom3Δ</i><br>mutant cultures _____  | 193 |
| Figure 6.6  | The rapamycin-insensitive growth rate of <i>pep3Δ</i> , <i>pep5Δ</i> ,<br><i>vps16Δ</i> , <i>vps33Δ</i> , <i>vps15Δ</i> , <i>vps34Δ</i> and <i>shp1Δ</i> mutant cultures____ | 195 |
| Figure 6.7  | The rapamycin-insensitive growth rate of <i>ccr4Δ</i> , <i>dhh1Δ</i> and<br><i>ctk1Δ</i> mutant cultures_____  | 197 |
| Figure 6.8  | The fold decrease in growth rate in the presence of rapamycin<br>compared to equivalent untreated cultures_____  | 199 |
| Figure 6.9  | Rapamycin recovery of <i>ego1Δ pep3Δ</i> double mutants from<br>various concentrations of the drug _____   | 201 |
| Figure 6.10 | The rapamycin-insensitive growth rate of <i>ego1Δ pep3Δ</i> double<br>mutant cultures _____  | 203 |
| Figure 6.11 | Representative images of FM4-64 staining in wild-type, <i>ego1Δ</i> ,<br><i>pep3Δ</i> , <i>ego1Δ pep3Δ</i> and <i>ypt7Δ</i> cells_____                                       | 205 |
| Figure 7.1  | The role of Hom2p and Hom3p in threonine biosynthesis and<br>their potential role in TORC1 activation_____   | 215 |
| Figure 7.2  | The upstream TORC1 signalling pathway showing the role of<br>the core HOPS/CORVET complex _____  | 217 |

## Acknowledgements

I would like to thank Dr. Joe Gray for presenting me with the opportunity to undertake such a fascinating project, with continued support and advice throughout the PhD. I express my gratitude also to the Biotechnology and Biological Sciences Research Council for funding this project.

I am grateful to Musab Bhutta, Christine Merrick, Lisa Blackwood, Sue Krause and Josie McGhie for their friendship and support over the last four years, it has been invaluable.

I would also like to thank Dr. Burgess of the University of Glasgow Polyomics Facility for his time and expertise with regards to optimising the mass spectrometer and enabling us to observe the cell-associated pool of rapamycin. These results proved incredibly important for the progress of the project. My gratitude also goes to Dr. McInerny for the use of the Coulter counter which provided a plethora of interesting results. I would also like to extend my thanks to Dr. Thumm, Dr. Powers, Dr. Kamada and Dr. Dokudovskaya for their kind donations of plasmids and yeast strains.

My deepest thanks goes to my family, Bev, Ian, Katie and Lizzie for their eternal love and support. And to Chris, for his immeasurable love and encouragement.

## **Author's Declaration**

I declare that the work presented in this thesis is my own, unless otherwise stated. It is entirely of my own composition and has not, in whole or in part, been submitted for another degree.

Stephanie Kaye Evans

January 2015

## **Contribution of Others to Data**

The data presented in Figure 5.5, Figure 5.6 and Figure 5.8 was carried out with the aid of Dr. Burgess and Dr. Weidt of the University of Glasgow Polyomics Centre. Optimisation of the conditions required to detect rapamycin by mass spectrometry and the running of samples on the mass spectrometer was carried out by Dr. Burgess and myself. The identification of rapamycin peaks and determination of signal intensities were carried out by Dr. Burgess or Dr. Weidt. Further analysis of the identified rapamycin signal peaks was carried out by myself.

The large-scale genetic screen, the results of which are analysed in Chapter 6, was carried out by Dr. Poon, Dr. Singer and Dr. Johnston at Dalhousie University, Canada, in collaboration with Dr. Gray. Scoring of colony formation was carried out by image analysis and Dr. Poon, all further analysis was carried out by myself.

## List of Abbreviations

|           |   |
|-----------|---|
| caf       | Caffeine  |
| CORVET    | class C cORe Vacuole and Endosomal Tethering                              |
| CPM       | Counts Per Minute   |
| EGO       | Exit from GrOwth arrest   |
| FBPase    | Fructose 1,6-bisphosphatase   |
| GAP       | GTPase Activating Protein   |
| GATOR     | Gap Activity TOwards Rags   |
| GEF       | Guanine nucleotide Exchange Factor  |
| GFP       | Green Fluorescent protein   |
| GSE       | Gap1 Sorting in the Endosome  |
| GTPase    | Guanosine TriPhosphatase  |
| HOPS      | HOmotypic fusion and Protein Sorting                                      |
| LRS       | Leucyl-tRna Synthetase  |
| PAS       | Pre-Autophagosomal Structure  |
| PtdIns(3) | Phosphatidylinositol 3-phosphate  |
| PI(3,5)P2 | Phosphatidylinositol 3,5-bisphosphate                                     |
| PDR       | Pleiotropic Drug Resistance   |
| rap       | Rapamycin   |
| ROS       | Reactive Oxygen Species   |
| SD        | Synthetic Defined media   |
| SDS PAGE  | SDS-PolyacrylAmide Gel Electrophoresis                                    |
| SEA       | SEh1 Associated   |
| SEACAT    | SEA Complex Activating Torc1  |
| SEACIT    | SEA Complex Inhibiting Torc1  |
| TAP       | Tandem Affinity Purification  |
| TORC1     | Target Of Rapamycin Complex 1   |
| TORC2     | Target Of Rapamycin Complex 2   |
| V-ATPase  | Vacuolar ATPase   |
| Vid       | Vacuole import and degradation  |
| YP        | Yeast extract and Peptone media   |
| YPD       | Yeast extract, Peptone and Dextrose media (note, glucose is used instead) |

# 1 Introduction

## 1.1 TOR Complexes

All eukaryotic cells contain two highly conserved Target Of Rapamycin Complexes, TORC1 and TORC2. For most organisms, the two complexes contain the same Tor protein (mTor in the case of mammals); however, *Saccharomyces cerevisiae* differs in that it has two copies of the TOR gene, *TOR1* and *TOR2* (Wullschleger et al. 2006). This *TOR* gene duplication is likely to have occurred during the whole yeast genome duplication (Wolfe & Shields 1997). Tor1p is exclusively found in TORC1 whilst Tor2p is predominantly associated with TORC2 but can also function in TORC1 (Loewith et al. 2002; Martin & Hall 2005).

The TOR Complexes regulate cell growth and proliferation in response to environmental conditions. TORC1 controls both cell growth (the increase in cell mass) and proliferation (the increase in cell number) predominantly in response to nutrient availability but also in response to environmental stresses (Takahara & Maeda 2012; De Virgilio & Loewith 2006b). External growth factors and hormones, for example insulin and insulin-like growth factors, also regulate mammalian mTORC1 (Wullschleger et al. 2006). TORC2 regulates the spatial growth of cells by regulating both the actin cytoskeleton and membrane organisation via sphingolipid biosynthesis (Loewith & Hall 2011). The mode of action of the TOR complexes appears to be conserved across eukaryotic cells (Schmelzle & Hall 2000).

Treatment of wild-type yeast cells with rapamycin results in cells entering a G0 arrest similar to that seen in starved cells (Barbet et al. 1996; Heitman et al. 1991; Zaragoza et al. 1998). The G0 arrest of wild-type cells induced by rapamycin treatment is reversible and cells are able to return to proliferation following removal of the “rapamycin block” (Dubouloz et al. 2005). However, null mutants have been identified that fail to resume proliferation following rapamycin treatment, for example loss of any component of the EGO complex (Binda et al. 2009; Dubouloz et al. 2005). The basis behind the failure of *ego*-mutants to recover from rapamycin treatment is currently unknown and is the major focus of the work described in this thesis.

## 1.2 Rapamycin

Rapamycin is a secondary metabolite of the soil-dwelling bacterium *Streptomyces hygroscopicus* from Easter Island (Vézina et al. 1975). Rapamycin is named after Easter Island, also known as Rapa Nui (Vézina et al. 1975). Rapamycin was originally identified as an antifungal agent due to its potent inhibition of yeast proliferation. It was soon discovered that the TOR1 complex was the intracellular target of the drug (Heitman et al. 1991). Rapamycin has therefore been extensively used to study the TORC1 pathway in numerous species. Rapamycin is a somewhat unusual drug with regards to its mode of action: to target and inactivate TORC1, rapamycin must first bind the cyclophilin protein Fpr1p (FKBP12 in mammals), a *cis-trans* prolyl isomerase thought to be important for protein folding (Heitman et al. 1991; Koltin et al. 1991). The *cis-trans* activity of Fpr1p is not required for TORC1 inhibition, instead the binary rapamycin-Fpr1p complex binds to Tor1p, thereby inhibiting TORC1 activity (Lorenz & Heitman 1995).

It was hoped that rapamycin could be used as a clinical antifungal agent, but was initially discounted due to undesirable side effects; it was found that rapamycin was also a potent inhibitor of proliferation of mammalian cells (Sehgal 2003). It was soon realised that inhibiting proliferation of mammalian cells meant that rapamycin could instead be used clinically as an immunosuppressant. Rapamycin (under its clinical name sirolimus) is currently used in a number of applications, including that as an immunosuppressant following transplant operations. It is hoped that rapamycin will also be used to treat cancer and metabolic diseases, for example diabetes (Benjamin et al. 2011; Sehgal 2003). The use of rapamycin to disrupt cancer cells in clinical trials has so far not proven successful; it would appear that the effectiveness of rapamycin is unpredictable with regards to the inhibition of proliferation (Benjamin et al. 2011).

### 1.2.1 Detoxification of rapamycin in mammalian systems

A number of cellular mechanisms exist in eukaryotic cells to overcome xenobiotic compounds and these mechanisms appear conserved across phyla. With regards to rapamycin detoxification, little is known about how this drug is

metabolised in cells, either yeast or mammalian. Some evidence has suggested that rapamycin is a substrate for the cytochrome P450 CYP3A4 enzyme in mammalian liver hepatocytes (Anzenbacher & Anzenbacherova 2001; Guengerich 1999; Li et al. 1995) but how non-hepatocyte mammalian cells degrade rapamycin, or indeed how rapamycin is transported to the liver in whole organisms remains unknown. It is possible that the cytochrome P450 CYP3A4 acts in collaboration with the efflux transporter P-glycoprotein (P-gp); extensive overlap in the substrates of CYP3A4 and P-gp have been reported, with rapamycin being one such substrate (see review: Linardi & Natalini 2006).

### 1.2.2 Drug detoxification mechanisms in yeast

Whilst a number of drug detoxification mechanisms exist in yeast, none so far has strongly identified rapamycin as a substrate. It is possible that rapamycin is detoxified in yeast either by being metabolised by cytochrome P450s (similar to the case thought to pertain in mammalian cells), targeted for sequestering in the vacuole through the addition of a glutathione tag or exported from the cell by members of the pleiotropic drug resistance pathway.

Physical metabolism of toxic substances can be carried out by two mechanisms in yeast: the cytochrome P450s and glutathione conjugation. Two cytochrome P450s have so far been identified in yeast, Erg5p and Erg11p (Erg11p is conserved across all phyla) (Kelly et al. 1997; Werck-reichhart & Feyereisen 2000). In yeast, the cytochrome P450s are involved in ergosterol biosynthesis in addition to their role as monooxygenases to metabolise toxic substances through hydroxylation (Bossche & Koymans 1998; Crešnar & Petrič 2011). The addition of a glutathione tag to toxic compounds results in sequestration into the vacuole, thus reducing the toxic effects. The conjugation of a xenobiotic compound with glutathione targets the compound for transport to the vacuole through GS-X pumps (Szczypka 1996).

A large network of proteins (over 20 have been identified) are involved in the export of toxic substances and are collectively known as the pleiotropic drug resistance network (PDR). The PDR network comprises of transcription factors, ABC transporter/efflux pumps and accessory proteins (Moye-Rowley 2003; Prasad & Goffeau 2012). Two of the earliest transcription factors to be identified were

Pdr1p and Pdr3p. Loss of Pdr1p results in profound drug hypersensitivity whereas loss of Pdr3p results in moderate hypersensitivity to xenobiotic compounds (Moye-Rowley 2003). One of the key downstream targets of Pdr1p was found to be the ABC efflux transporter Pdr5p (Moye-Rowley 2003; Prasad & Goffeau 2012). Not only is Pdr5p an exporter for xenobiotic compounds (for example cycloheximide) but it is also temporally regulated to export toxic metabolites that accumulate during cell growth (Moye-Rowley 2003; Prasad & Goffeau 2012). The ABC transporter pumps are able to export a wide range of seemingly unrelated substrates (Prasad & Goffeau 2012).

## **1.3 The Target of Rapamycin Complex 1**

### **1.3.1 Composition of TORC1**

The TOR Complexes were identified as the targets of the antifungal agent rapamycin. However, only TORC1 is inhibited by the presence of rapamycin and the TORC1 pathway is the focus of this thesis. The yeast Target of Rapamycin Complex 1 is composed of four subunits; Tor1p, Kog1p, Lst8p and Tco89p (Loewith et al. 2002; Reinke et al. 2004; Wedaman & Reinke 2003) (Figure 1.1). Kog1p and Lst8p are both essential proteins whilst Tor1p and Tco89p are not (Reinke et al. 2004). Tor1p is non-essential due to partial redundancy between Tor1p and Tor2p. In the absence of Tor1p, Tor2p is able to function in TORC1 and maintain some downstream function, however the redundancy is unidirectional and Tor1p is not able to function in place of Tor2p in the TORC2 complex (Loewith et al. 2002).

### **1.3.2 TORC1 localisation**

Numerous studies have been carried out to localise TORC1 within the cell (for example Alibhoy & Chiang 2010; Aronova & Wedaman 2007; Berchtold & Walther 2009; Brown et al. 2010; Binda et al. 2009; Kunz et al. 2000; Urban et al. 2007). It is generally agreed that Tor1p, Tco89p and Kog1p are bound to a membrane; however, some disagreement exists with regards to which membrane these proteins, and by inference TORC1, localises.

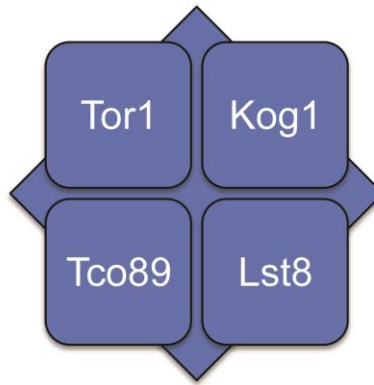


**Figure 1.1** The components of TORC1

TORC1 consists of four subunits, Tor1p, Kog1p, Tco89p and Lst8p. Kog1p and Lst8p are essential proteins whereas Tor1p and Tco89p are not. In the absence of Tor1p, Tor2p is able to function in TORC1 and maintain some downstream activity.

A number of studies have found TORC1 to be present at the plasma membrane, with some distinct puncta in the cytoplasm that could not always be associated with known structures (Alibhoy & Chiang 2010; Aronova & Wedaman 2007; Kunz et al. 2000). Li et al. (2006) also found Tor1p to be distributed in the cytoplasm in addition to localisation in the nucleus. Alternatively, studies have found components of TORC1 to be associated either with the vacuole or structures adjacent to the vacuole, most likely to be vesicles (Binda et al. 2009; Kira et al. 2014; Urban et al. 2007; Wedaman & Reinke 2003). It is now generally accepted that TORC1 mainly resides, and is active, at the cytoplasmic face of the vacuolar membrane (Loewith & Hall 2011). Through tethering the TORC1 downstream target Sch9p to the vacuole, Urban et al. (2007) were able to demonstrate that TORC1 is indeed active in this position.

More recent studies by Takahara & Maeda 2012 and Yan et al. 2012a have found that in response to certain stress conditions, the association of TORC1 with the vacuolar membrane is disrupted. Takahara & Maeda (2012) found that TORC1 was sequestered into stress granules in response to heat shock. The removal of TORC1 from the membrane is thought to prolong TORC1 inactivation during this stress. Yan et al. (2012a) also found that TORC1 was removed from the vacuolar membrane following activation of the Rho1p stress response. Binding of the Rho1p GTPase to TORC1 when activated (by Rom2p) due to stress environments resulted in disruption of TORC1 localisation at the vacuolar membrane (Yan et al. 2012a). It is possible that Rho1p targets TORC1 to stress granules, but this possibility has not yet been investigated. Again it appears that removal of TORC1 from the vacuolar membrane is a mechanism to prolong TORC1 inactivation, allowing cells time to recover from the initiating stress before resuming active growth and proliferation. These discoveries may explain why some groups found TORC1 to be distributed throughout the cytoplasm; the conditions of their experiments may have inadvertently resulted in activation of the environmental stress pathway.

## 1.4 Upstream of TORC1

TORC1 has been shown to respond to stimuli such as nutrient availability, heat shock, high temperature and redox stress (Loewith & Hall 2011). Little is currently known about how these environmental conditions are signalled to

TORC1 and the main focus of studies so far has been to understand the mechanism by which amino acid availability is sensed. A number of complexes and proteins that signal to TORC1 have been identified and will be discussed in more detail below. However, a number of gaps in our understanding of the TORC1 signalling pathway exist that are yet to be identified.

#### 1.4.1 TORC1 in response to environmental stress

A recent study suggests that spatiotemporal regulation of TORC1 occurs following heat shock (Takahara & Maeda 2012). Stress granules can form in yeast under conditions in which translation is stalled, such as a period of heat shock (Buchan & Parker 2009). The composition of stress granules can vary depending on the initiating stress, however often include ribosomal subunits, translation initiation factors, and proteins involved in cell signalling (Buchan & Parker 2009). Takahara & Maeda (2012) found that the TORC1 component Kog1p was associated with stress granules during a period of recovery following heat stress. The sequestering of TORC1 into stress granules is thought to maintain TORC1, and therefore the cell, in an inactive state during recovery from the heat stress to prevent DNA damage. Takahara & Maeda (2012) found that the length of time TORC1 remained inactive was dependent on the time it took for stress granule dissociation to occur following the re-initiation of translation. It is worth noting that TORC1 itself was inactivated in response to heat stress before being relocalised to the stress granules. The mechanism by which TORC1 is inactivated by heat shock remains elusive but could involve Rho1p (Takahara & Maeda 2012; Yan et al. 2012a; Yan et al. 2012b).

TORC1 appears to be a direct target of the small GTPase Rho1p in response to a number of environmental stresses that initiate the cell wall integrity signalling pathway (Yan et al. 2012a; Yan et al. 2012b). Activation of Rho1p GTPase by the GEF Rom2p (Ozaki et al. 1996) results in the binding of Rho1p to the Kog1p subunit of TORC1 in a region normally bound by Tap42p, a direct downstream target of TORC1 (Yan et al. 2012a). The interaction between Kog1p and Rho1p results in dissociation and subsequent activation of Tap42p leading to the induction of Tap42p downstream functions which includes stress induced gene transcription (Beck & Hall 1999a). Not only does Rho1p disrupt the interaction between Kog1p and Tap42p, but it also results in dissociation of TORC1 from the

membrane resulting in further inactivation of TORC1. The stress-induced binding of Rho1p to TORC1 was found to occur for less than 15 minutes, yet the reassociation of TORC1 to the membrane took approximately 90 minutes (Yan et al. 2012a; Yan et al. 2012b). It is possible that removing TORC1 from the vacuolar membrane provides an additional regulatory mechanism for the complex.

## 1.4.2 TORC1 in response to nutrient cues

### 1.4.2.1 The EGO Complex

The EGO complex (Exit from rapamycin-induced GrOwth arrest (Dubouloz et al. 2005)) was identified by the De Virgilio group and appears to activate TORC1 in response to amino acid availability (Binda et al. 2009; Dubouloz et al. 2005; Zhang et al. 2012). The EGO complex is a non-essential complex composed of four subunits: Ego1p, Ego3p, Gtr1p and Gtr2p (Binda et al. 2009; Dubouloz et al. 2005) (Figure 1.2A). When identifying proteins involved in amino acid permease trafficking Gao & Kaiser (2006) also identified all four members of the EGO complex in conjunction with a fifth protein, Ltv1p, which they termed the GSE complex. However, it is the four-subunit EGO complex that is generally regarded as an activator of TORC1 (Loewith & Hall 2011). Loss of any member of the EGO complex results in an inability to resume proliferation following rapamycin treatment. This phenotype will form the basis of this thesis.

The Gtr1p and Gtr2p subunits of the EGO complex are Ras-related GTPases (Hirose et al. 1998; Sekiguchi et al. 2001) that can activate TORC1 (Binda et al. 2009; Dubouloz et al. 2005) (Figure 1.2A & B). The binding of GTP and GDP to Gtr1p and Gtr2p regulates TORC1 activity, but in a complicated way; when Gtr1p is bound to GTP and Gtr2p is bound to GDP the EGO complex activates TORC1 whereas when Gtr1p is bound to GDP and Gtr2 is bound to GTP TORC1 is inactivated (Binda et al. 2009; Kira et al. 2014). Ego1p is thought to anchor the EGO complex to the vacuolar membrane through myristoylation of the N-terminus (Gao et al. 2005). Indeed, Gao et al. (2005) found Gtr1p to be soluble and localised to the cytosol in mutants lacking Ego1p. Ego3p is also thought to be required for assembly and localisation of the EGO complex at the vacuole (Zhang et al. 2012). Ego3p exists as a homodimer in cells (Zhang et al. 2012)

and it is thought that this dimerisation is necessary for localisation of Ego3p to the vacuolar membrane and for its interaction with the membrane anchor Ego1p (Zhang et al. 2012). It would appear that the localisation of Gtr2p is dependent on the presence of Gtr1p (Sekiguchi et al. 2001), and the localisation of Gtr1p to the membrane is dependent on the presence of Ego1p (Gao et al. 2005). The correct formation of the EGO complex is therefore dependent on the presence of every subunit (Sekiguchi et al. 2014).

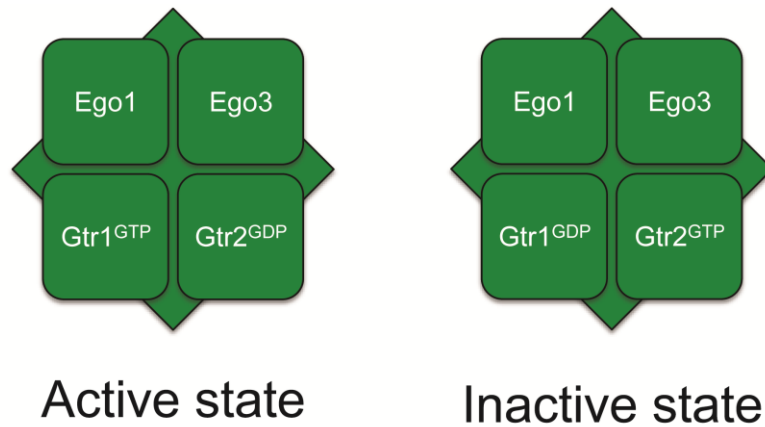
The non-essential nature of the EGO complex suggests that it is not necessarily the only mechanism by which TORC1 is activated by nutrient sensing. Stracka et al. (2014) have found that the EGO complex activates TORC1 in response to a high quality nitrogen source but the presence of elevated levels of glutamine were able to sustain TORC1 activity in a Gtr1/2p independent manner. However, potential alternative activators of TORC1 in response to nutrients remain elusive; as will be seen below, nearly all nutrient dependent regulators of TORC1 identified so far appear to act, at least in part, via the EGO complex.

#### **1.4.2.2 The SEA Complex**

The SEh1 Associated (SEA) complex is an eight subunit complex that localises to the vacuolar membrane and has been found to regulate TORC1 activity in a nutrient dependent manner (Dokudovskaya et al. 2011; Neklesa & Davis 2009; Panchaud et al. 2013b). The eight subunits (Iml1p (Sea1p), Npr2p, Npr3p, Seh1p, Sec13p, Sea2p, Sea3p and Sea4p) of the SEA complex form two functional sub-complexes, containing either three or five of the SEA proteins, that have different roles with regards to modulating TORC1 activity (Dokudovskaya et al. 2011; Neklesa & Davis 2009; Panchaud et al. 2013a). The Iml1p-Npr2p-Npr3p sub-complex inhibits TORC1 activity and is called SEACIT (SEA Complex Inhibiting Torc1) (Figure 1.3A & B). The other five membered sub-complex promotes TORC1 activity and is called SEACAT (SEA Complex Activating Torc1) (Panchaud et al. 2013a) (Figure 1.3A & B) The two sub-complexes will be discussed in more detail below.

The SEACIT components Npr2p and Npr3p (as a complex together) were originally identified by Neklesa & Davis (2009) following a genome-wide screen to identify potential regulators of TORC1.

A



B

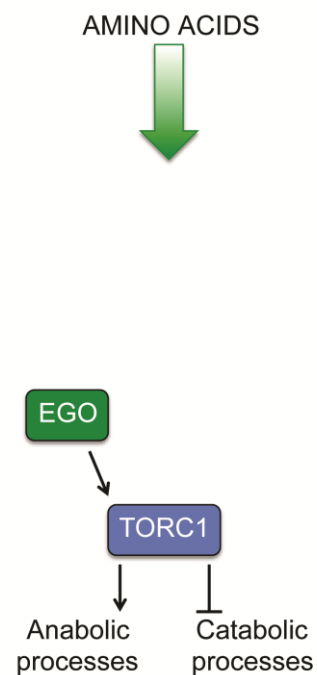


### Figure 1.2 The EGO complex

A: The EGO complex consists of four subunits Ego1p, Ego3p, Gtr1p and Gtr2p all of which are non-essential. Ego1p and Ego3p tether the EGO complex to the vacuolar membrane whilst Gtr1p and Gtr2p are GTPases that regulate TORC1 activity. When Gtr1p is bound to GTP and Gtr2p is bound to GDP the EGO complex is active. When the inverse is true the EGO complex is inactive.

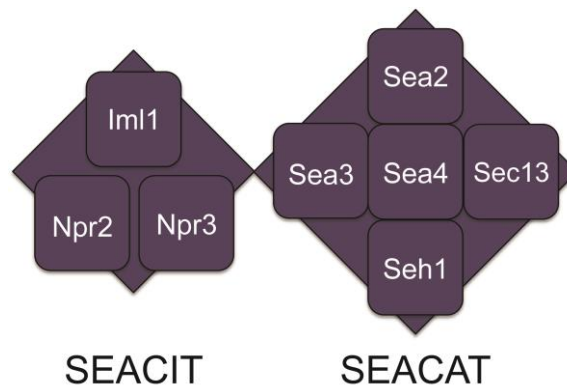
B: Under conditions of plentiful nutrients Gtr1p is bound to GTP whilst Gtr2p is bound to GDP and promotes TORC1 activity. The EGO complex is inactive under starvation conditions.

Npr2p and Npr3p were subsequently found to be associated with the other six SEA complex proteins as part of the larger SEA complex structure (Dokudovskaya et al. 2011) (Figure 1.3A). Neklesa & Davis (2009) found that Npr2p and Npr3p acted upstream of TORC1 and promoted its activity. The Npr2-Npr3 complex was found to be required for TORC1 inhibition in response to poor nutrient conditions; cells lacking either Npr2p or Npr3p failed to respond correctly to starvation conditions by maintaining active TORC1 (Neklesa & Davis 2009). Loss of the Iml1p SEACIT subunit results in cells with high TORC1 activity, compared to that of wild-type cells, as assayed by Sch9p phosphorylation (Panchaud et al. 2013b). It was found that Iml1p, Npr2p and Npr3p co-localised in a trimeric complex that is tethered at the vacuolar membrane through the tethering properties of Iml1p (Dokudovskaya et al. 2011; Panchaud et al. 2013b; Wu & Tu 2011).

It is thought that the SEACIT complex acts as a GTPase-Activating Protein (GAP) towards the Gtr1p subunit of the EGO complex. Localisation of SEACIT to the vacuolar membrane is dependent on the presence of the EGO complex (Panchaud et al. 2013b) and loss of either Gtr1p or Gtr2p negated the increase in TORC1 activity seen in cells lacking a member of the SEACIT complex (Panchaud et al. 2013b). Overproduction of Iml1p resulted in a decrease in GTP-associated Gtr1p leading to the conclusion that Iml1p has GAP activity towards Gtr1p (Panchaud et al. 2013b). It is therefore thought that SEACIT acts as an inhibitor of the EGO complex to regulate the activity of TORC1 (Figure 1.3B).

It appears that the members of SEACAT act redundantly to promote TORC1 activity and in cells lacking all of Sea2p, Sea3p and Sea4p or in cells lacking Seh1p a reduction in TORC1 activity is observed (Panchaud et al. 2013a; Panchaud et al. 2013b). The reduction of TORC1 activity in cells lacking SEACAT is dependent on the presence of SEACIT leading to a model in which SEACAT acts as an inhibitor of SEACIT which in turn acts as an inhibitor of the EGO complex (and therefore TORC1 activity) (Panchaud et al. 2013a) (Figure 1.3B). More research is required to confirm the role, and mechanism of action, of the SEACIT and SEACT complexes in the TORC1 signalling pathway.

A



B

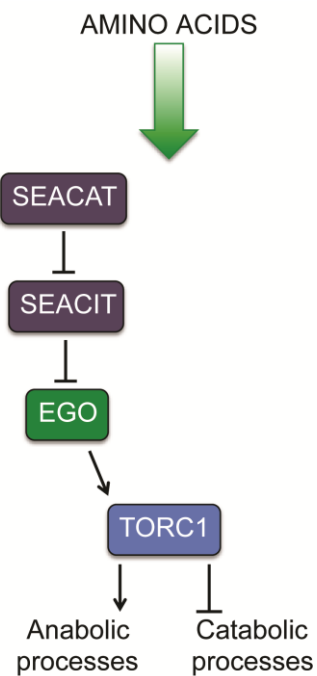


### Figure 1.3 The SEA complex

A: The SEA complex consists of eight subunits which are divided into two functional sub-complexes. SEACIT (SEA Complex Inhibiting Torc1) consists of Iml1p, Npr2p and Npr3p. SEACAT (SEA Complex Activating Torc1) consists of Sea2p, Sea3p, Sea4p, Seh1p and Sec13p. Iml1p tethers the whole SEA complex to the cytoplasmic face of the vacuolar membrane.

B: In the presence of nutrients the SEACAT complex inhibits the SEACIT complex which has GAP activity towards EGO. The inhibition of the SEACIT complex thus promotes TORC1 activity when cells are in conditions of plentiful nutrients.

### 1.4.2.3 Vam6p as a Guanine Exchange Factor for the EGO complex

Functional GTPases require both a GAP and a Guanine Exchange Factor (GEF) to moderate their activity. Iml1p acts as a GAP towards Gtr1p (Panchaud et al. 2013b); Vam6p acts as a GEF towards Gtr1p (Binda et al. 2009) (Figure 1.4). It is currently thought that the GTP-bound status of Gtr1p overrides that of Gtr2p with regards to TORC1 activity. Vam6p (Vps39p) was originally identified in the TORC1 signalling pathway by Zurita-Martinez et al. (2007) following a screen searching for null mutations that were synthetic lethal or had reduced fitness in combination with a null *tor1Δ* mutation. Vam6p is a member of the HOPS complex (Homotypic fusion and Protein Sorting) which is involved in membrane trafficking to the vacuole (Solinger & Spang 2013). It is not known whether the role of Vam6p as a GEF to Gtr1p is carried out as part of the HOPS complex or as an additional separate role of the protein. It is possible that the HOPS complex has a role in TORC1 activity, especially as loss of any member of the core HOPS complex was identified as being synthetic lethal in combination with a *tor1Δ* null mutation (Zurita-Martinez et al. 2007).

### 1.4.2.4 TORC1 activation by leucyl-tRNA synthetase

The leucyl-tRNA synthetase has also been found to have a role in regulating TORC1 activation, again via the EGO complex. Bonfils et al. (2012) found that the leucyl-tRNA synthetase, Cdc60p, interacts with the Gtr1p subunit of the EGO complex in a leucine dependent manner. Bonfils et al. (2012) propose a model in which charged leucyl-tRNA synthetase binds to Gtr1p, via the Cdc60p editing domain CP1, to prevent GTP hydrolysis of Gtr1p thus maintaining TORC1 activity (Figure 1.5). It appears that Cdc60p does not possess obvious GAP or GEF activity domains or functions; rather it behaves as an inhibitor of GAP activity towards Gtr1p, performed by an as yet unknown protein. No interaction between Cdc60p and Gtr2p has been observed (Bonfils et al. 2012) suggesting a second protein could be involved in maintaining Gtr2p in the GDP bound form to promote TORC1 activity. Alternatively, it is possible that through its interaction with Gtr1p, Cdc60p is in close enough proximity to aid hydrolysis of Gtr2p-GTP (Segev & Hay 2012). It is unclear why so far only a leucyl tRNA-synthetase has been identified that modulates TORC1 activity.

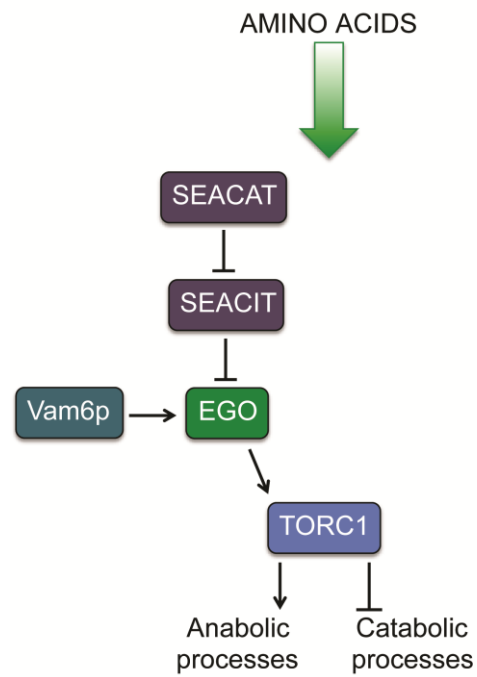


**Figure 1.4 Vam6p regulates TORC1 activity via the EGO complex**

The Vam6p component of the HOPS complex has GEF activity towards Gtr1p of the EGO complex. Under conditions of plentiful nutrients Vam6p activates the EGO complex which in turn activates TORC1.

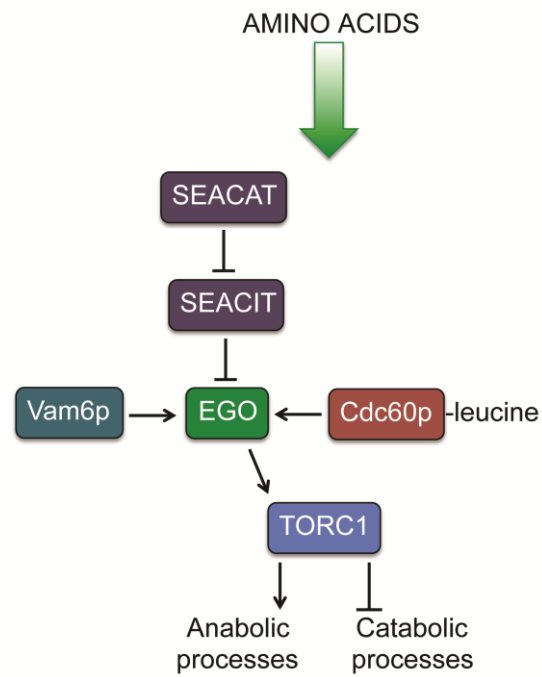


**Figure 1.5 The leucyl-tRNA synthetase activates the EGO complex**

In the presence of leucine the charged leucyl-tRNA synthetase (Cdc60p) interacts with the Gtr1p sub-unit of the EGO complex to prevent GTP hydrolysis. Inhibition of GTP hydrolysis by Cdc60p maintains the EGO complex in an active state resulting in active TORC1.

One possibility is that leucine is used as a ‘master sensor’ for the state of all amino acids within the cell due to it being the most frequently used amino acid in the yeast proteome (Bonfils et al. 2012). Another possibility is that Cdc60p is one of the most abundant aminoacyl-tRNA synthetases and this may account for its predominant role (Bonfils et al. 2012). A third possibility is that multiple other tRNA-synthetases interact with TORC1 but that these interactions have yet to be identified.

#### 1.4.2.5 TORC1 regulation by PI(3,5)P2

It would appear that the majority of research into upstream regulators of TORC1 activity has found the EGO complex to be key for proper TORC1 regulation. However, the EGO complex is not essential in yeast, whereas TORC1 activity is (Barbet et al. 1996; Dubouloz et al. 2005; Heitman et al. 1991). The viability of cells lacking the EGO complex suggests that there must be alternative methods of activating TORC1 other than via the EGO complex, a deduction also proposed by Stracka et al. (2014). One such alternative signalling molecule has been found to regulate TORC1 activity: the signalling phospholipid PI(3,5)P2 (Phosphatidylinositol 3,5-bisphosphate) (Jin et al. 2014) (Figure 1.6). Jin et al. (2014) found that null *fab1Δ* mutants, which are unable to synthesise PI(3,5)P2, were hypersensitive to the effects of rapamycin. The method by which PI(3,5)P2 potentially regulates TORC1 has not been fully identified, however Jin et al. (2014) propose three methods by which PI(3,5)P2 could regulate TORC1. (1) It is possible that PI(3,5)P2 directly activates TORC1 through direct binding of the TORC1 subunit Kog1p. (2) It is possible that PI(3,5)P2 acts as a platform on the vacuolar membrane for the localisation of TORC1, its regulators and downstream targets, for example the EGO complex and Sch9p (the latter of which was found to directly interact with PI(3,5)P2) (Jin et al. 2014). (3) Activity of the vacuolar V-ATPase may be required to signal amino acid availability to TORC1; a role of the V-ATPase in signalling to mTORC1 has been identified and will be discussed later. Activity of the V-ATPase requires the correct acidification of the vacuole which is lost in cells lacking PI(3,5)P2.

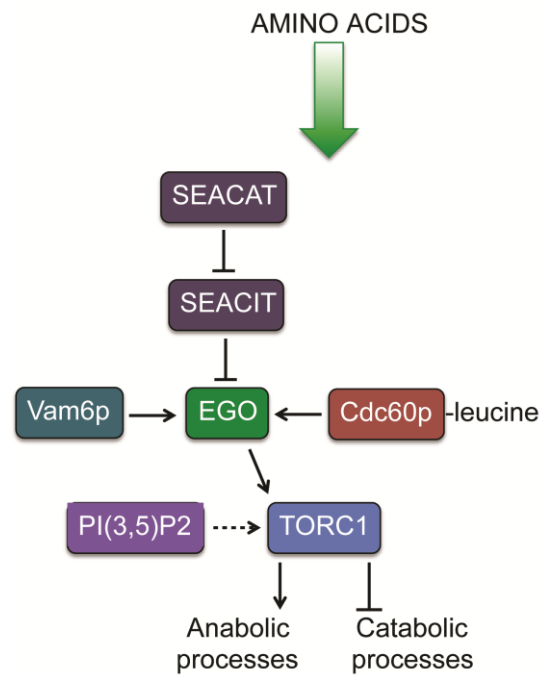


**Figure 1.6 The signalling molecule PI(3,5)P2 activates TORC1**

Through a currently unknown mechanism (hence a dashed line), the presence of PI(3,5)P2 is required for TORC1 activity. It is possible PI(3,5)P2 directly interacts with Kog1p to promote TORC1 activity, or is a landing pad to bring TORC1, upstream regulators and downstream effectors together.

Whilst an involvement of V-ATPase activity in the yeast TORC1 signalling pathway has not been uncovered so far, instability of the V-ATPase has been reported in cells lacking Ego1p (Gao et al. 2005) suggesting that the function of the V-ATPase and the EGO complex could be linked, either for vacuole stability or for TORC1 signalling.

## **1.5 The mammalian Target Of Rapamycin 1 (mTORC1)**

The conserved TORC1 signalling pathway is present in every eukaryotic species tested (Wullschleger et al. 2006). Whilst some elements of the mTORC1 pathway appear to be conserved with those found in yeast, a number of differences in the regulation of mTORC1 appear to have occurred.

### **1.5.1 mTORC1 composition**

The mammalian Target Of Rapamycin Complex 1, mTORC1, comprises of mTOR, Raptor which is the mammalian homolog of yeast Kog1p, mLST8 which is the mammalian homolog of yeast Lst8p, PRAS40 and Deptor (Jewell & Guan 2013; Laplante & Sabatini 2009) (Figure 1.7A).

In addition to regulation by nutrient availability, mTORC1 is also regulated by stress, energy levels, hormones and growth factors such as insulin and insulin-like growth factors (Wullschleger et al. 2006). The TSC1-TSC2 complex is central in regulating mTORC1 in response to external factors, for example growth factors. The TSC1-TSC2 complex acts as a GAP towards the TORC1 activator Rheb thus promoting mTORC1 activity (Inoki & Guan 2006) (Figure 1.7B). The regulation of mTORC1 in response to nutrient availability and the similarities with the yeast TORC1 signalling pathway will be considered in more detail here.

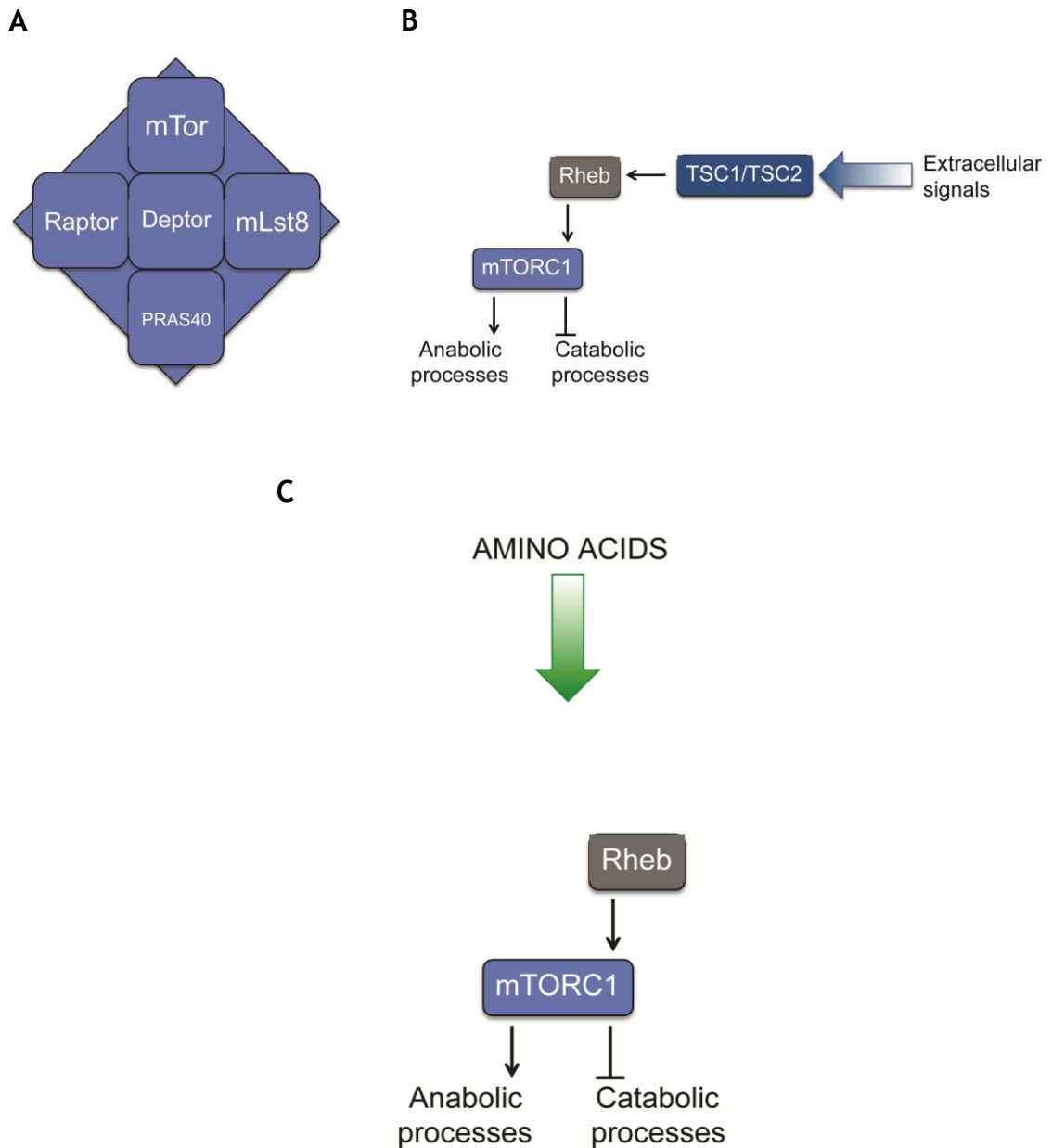


**Figure 1.7 The components of mTORC1 and signalling by Rheb**

A: mTORC1 comprises of five subunits: mTOR, Raptor, Deptor, mLst8 and PRAS40. Raptor is the mammalian homolog of Kog1p in yeast and mLst8 is the mammalian homolog of yeast Lst8p.

B: Rheb activates mTORC1 in response to activation by the TSC1-TSC2 complex which is in turn regulated by the presence of extracellular signals for example hormones and growth factors.

C: Translocation of mTORC1, in response to amino acids, to lysosomal membranes containing active Rheb results in activation of mTORC1.

## 1.5.2 mTORC1 in response to nutrient cues

### 1.5.2.1 mTORC1 localisation

Relocalisation of mTORC1 within the cell is an important mechanism of regulation for mTORC1 activation. mTORC1 is membrane bound, most likely to that of the lysosome (the functional equivalent of the yeast vacuole) (Korolchuk et al. 2011; Poüs & Codogno 2011). It appears that the intracellular position of the lysosomes carrying mTORC1 also affect the activity of mTORC1. Korolchuk et al. (2011) suggest that when nutrients are abundant, mTORC1 is located on lysosomes near the plasma membrane possibly where the upstream signals of mTORC1 are located. However, when cells are starved of amino acids the lysosomes bearing mTORC1 are found to be perinuclear; which Korolchuk et al. (2011) believe may aid the fusion of autophagosomes to lysosomes. Korolchuk et al. (2011) also found that reactivation of mTORC1 after starvation was hindered in cells that were unable to relocate the mTORC1 bound lysosomes to the cell periphery. Whilst the physical localisation of the lysosomes within a cell appears to regulate mTORC1 activity, the physical relocation of mTORC1 onto the membrane is also a crucial regulatory tool as will be discussed in more detail in the next section.

### 1.5.2.2 mTORC1 activation by Rheb

mTORC1 is activated by the small GTPase Rheb, located on the lysosomal membrane (Long et al. 2005; Sancak et al. 2007) (Figure 1.7C). Unlike yeast TORC1, mTORC1 activity is partially moderated by its translocation onto the lysosomal membrane where Rheb resides (Binda et al. 2009; Korolchuk et al. 2011; Sancak et al. 2010; Sancak et al. 2008). This translocation occurs only in response to the presence of amino acids and is not dependent on the activity status of Rheb or the presence of growth factors (Sancak et al. 2010). Under starvation conditions, when mTORC1 is inactive, mTOR1 is found distributed throughout the cytoplasm in small puncta (Sancak et al. 2008). Following amino acid stimulation mTOR1 is relocalised to the perinuclear region as well as to large lysosomal structures. On the other hand Korolchuk et al. (2011) found mTORC1 to be associated with lysosomes at the cell periphery upon the addition of amino acids. Korolchuk et al. (2011) found that the peripheral localisation of lysosomes containing mTORC1 is not sufficient to activate the complex in the

absence of upstream signals yet tethering mTORC1 to lysosomes (and only lysosomes) is sufficient to override amino acid starvation with regards to mTORC1 activity, but not regulation by insulin (Sancak et al. 2010). Regulation of mTORC1 by Rheb is not conserved with budding yeast: they lack an equivalent Rheb gene (Wullschleger et al. 2006).

### 1.5.2.3 mTORC1 activation by Rag GTPases and Ragulator

The translocation of mTORC1 onto the lysosomal membrane in response to amino acid stimulation is regulated by the Rag GTPases, which are orthologous to the Gtr proteins in yeast (Sancak et al. 2010; Sancak et al. 2008). Four Rag GTPases have been identified in mammalian cells; RagA and RagB are orthologs of Gtr1p and RagC and RagD are orthologs of Gtr2p (Hirose et al. 1998; Yang et al. 2013). As observed in yeast, the Rag GTPases exist in heterodimers to signal to mTORC1; RagA or RagB associates with RagC or RagD (Kim et al. 2008). The Rag GTPases reside on a lysosomal membrane in an apparently amino acid independent manner (Sancak et al. 2010). Again, as seen in yeast when RagA/RagB are bound to GTP and RagC/RagD are bound to GDP mTORC1 activity is promoted (Figure 1.8A).

The Ragulator complex aids the Rag GTPases in their regulation of mTORC1 (Figure 1.8B). The Ragulator complex was originally identified as a trimeric complex comprising of p18, p14 and MP1 that are encoded by *LAMTOR1*, *LAMTOR2* and *LAMTOR3* respectively (Sancak et al. 2010). A further two proteins were identified that function in the Ragulator complex and were subsequently termed LAMTOR4 (C7orf59) and LAMTOR5 (HBXIP) (Bar-Peled et al. 2012) (Figure 1.8C). The Ragulator complex appears to have two roles with regards to regulating the Rag GTPases that are discussed below.

One role of the Ragulator complex is to tether the Rag GTPases to the lysosomal membrane (Sancak et al. 2010) and Ragulator is therefore thought to have a similar role to that of the Ego proteins in yeast. Indeed, Kogan et al. (2010) and Zhang et al. (2012) found that there is high structural conservation between the p14-MP1 heterodimer and the homodimer of Ego3p, suggesting that Ego3p and the p14-MP1 heterodimer have potentially conserved functions.

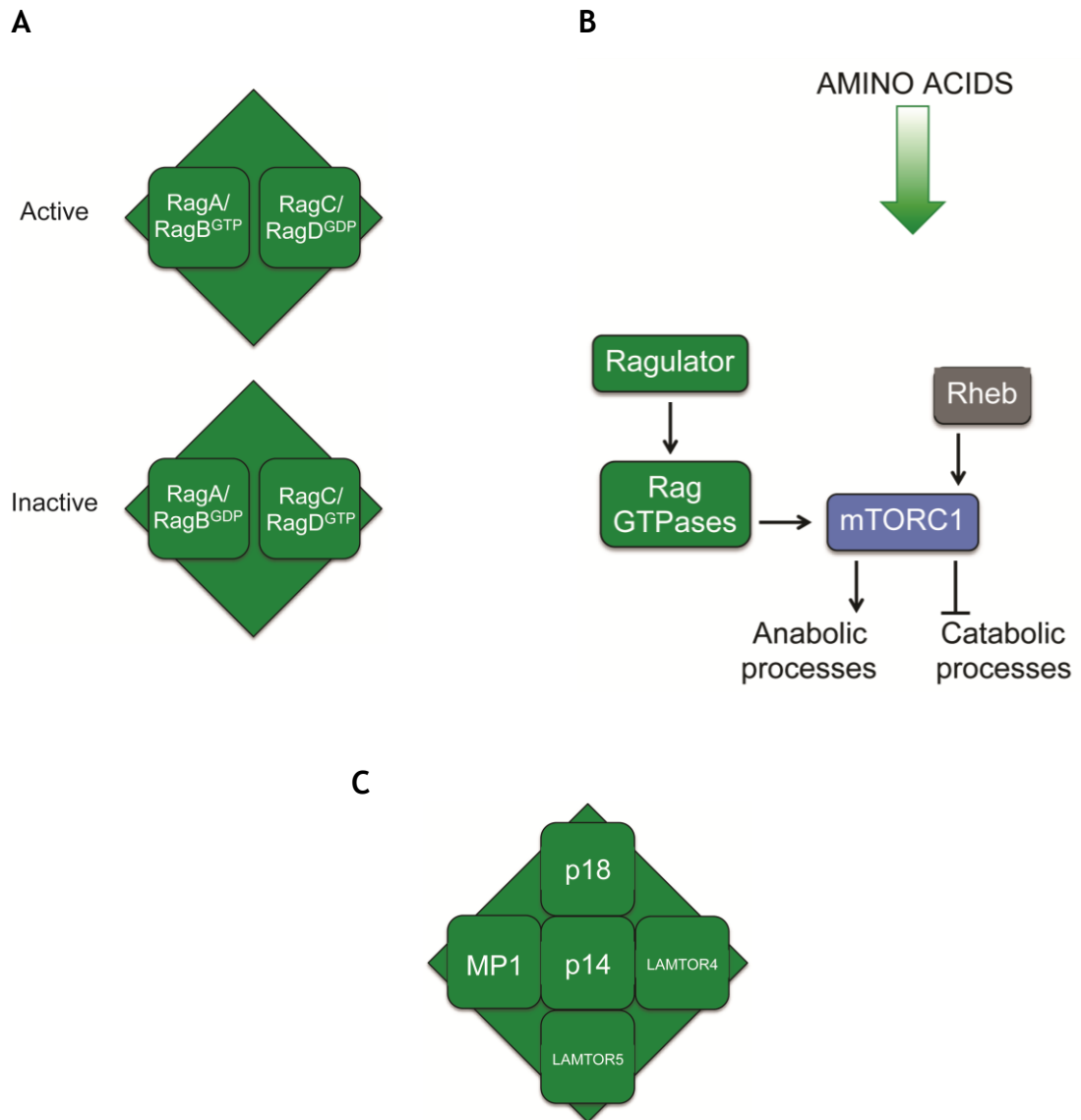


**Figure 1.8 The Rag GTPases regulate mTORC1 with the aid of the Ragulator complex**

A: Mammalian cells have four Rag GTPases which form heterodimers; RagA or RagB associates with RagC or RagD. When active, RagA/RagB is bound to GTP whilst RagC/RagD is bound to GDP.

B: When amino acids are abundant, the Rag GTPases promote TORC1 activity by relocating mTORC1 to lysosomes containing active Rheb. The Rag GTPases are tethered to the lysosomal membrane via interaction with the Ragulator complex. The Ragulator complex also promotes TORC1 activity by acting as a GEF to the RagA/RagB GTPases thus maintaining their activity.

C: The Ragulator complex comprises of five subunits which appear to be separated into two heterodimers, MP1-p14 and LAMTOR4-LAMTOR5 which are tethered by p18. The p18 subunit also tethers the Ragulator complex to the lysosomal membrane.

The p18 subunit of the Ragulator holds the two heterodimers, p14-MP1 and LAMTOR4-LAMTOR5 together thus creating the pentameric complex. The P18 subunit also binds Ragulator to the Rag GTPases and is the subunit through which the Ragulator-Rag GTPases are tethered to the lysosome (Bar-Peled et al. 2012; Nada et al. 2009; Sancak et al. 2010). Sancak et al. (2010) found that interactions, both within the trimeric Ragulator complex, and between the trimeric Ragulator and Rag GTPases were not affected in response to amino acid availability. Bar-Peled et al. (2012) however, did not find this to be the case with regards to the pentameric Ragulator complex. Bar-Peled et al. (2012) found that under starvation conditions the interaction between Ragulator and Rag GTPases was strengthened, yet in the presence of amino acids these interactions were weakened. The interaction between Ragulator and mTORC1 increased upon amino acid stimulation, consistent with mTORC1 activation (Bar-Peled et al. 2012). The interaction between p14, p18 and MP1 (the trimeric Ragulator) and between the Rag GTPases did not appear to alter in response to amino acid availability. In cells lacking the Ragulator complex, mTORC1 is inactive due to the inability of the Rag GTPases, and therefore mTORC1, to reside at the lysosome, even when stimulated with amino acids (Sancak et al. 2010).

A second role of the pentameric Ragulator complex is to act as a GEF towards RagA/RagB thus maintaining active TORC1 (Bar-Peled et al. 2012) (Figure 1.8B). Sancak et al. (2010) found that the p18 subunit (of p18, p14 and MP1 that were tested) specifically interacted with the RagB-RagD GTPase heterodimer *in vitro*. More research into the potential GEF properties of the Ragulator complex is required. It appears that the human ortholog of Vam6p (hVPS39), which has a role as a GEF for Gtr1p in yeast (Binda et al. 2009), does not have a role in mammalian mTORC1 signalling (Bar-Peled et al. 2012).

#### 1.5.2.4 The 'inside-out' model of mTORC1 activation

It is known that the TORC1 and mTORC1 pathways respond to nutrients, in particular amino acid availability, but how nutrients are sensed remains uncertain. A model has been proposed in mammalian cells in which amino acids are sensed by an 'inside-out' mechanism. This 'inside-out' model suggests that amino acid accumulation in the lysosome triggers signalling to, and activation of,

mTORC1 (Zoncu et al. 2011) (Figure 1.9). It is thought that the activity of the V-ATPase, *i.e.* the ATP hydrolysis of V1 and associated rotation of the stalk sub-complex, signals to mTORC1 via interaction with, and regulation of, the Ragulator complex (Zoncu et al. 2011). The V1 domain of the V-ATPase has been shown to interact with the Rag GTPases and both the V1 and V0 domains of the V-ATPase have been shown to directly associate with the Ragulator complex through the P18 subunit (Zoncu et al. 2011). It appears that the interaction between V1, Ragulator and Rag GTPases varies depending on the internal concentration of amino acids: the interaction is strengthened under deprived amino acid conditions and is weakened when amino acids are plentiful (Bar-Peled et al. 2012; Zoncu et al. 2011).

Bar-Peled et al. (2012) propose two possibilities to explain the variation in interaction strength between the V-ATPase complex, the Ragulator complex and the Rag GTPases in response to the intracellular concentration of amino acids. One possibility is that the Ragulator-Rags are found in two states, either interacting weakly or strongly with each other, depending on amino acid availability. Deprivation of amino acids results in a strong interaction between Ragulator and the Rag GTPases, preventing the binding of the Rag GTPases to mTORC1 and therefore resulting in reduced mTORC1 activity. When cells are stimulated with amino acids, the Ragulator complex promotes the binding of GTP to RagA and RagB leading to a conformational change, this change could potentially weaken the interaction between Ragulator and the Rag GTPases and expose an mTORC1 binding site thus promoting mTORC1 activation. A second proposal by Bar-Peled et al. (2012) suggests that the regulated interaction between Ragulator and Rag GTPases may be required for transition of the Rag GTPases on and off the lysosomal membrane. The tight binding of Ragulator to the Rag GTPases during starvation conditions could tether them to the lysosomal membrane. In the presence of amino acids the interaction between the Ragulator and Rag GTPases weakens and therefore could allow the Rag GTPases to dissociate from the lysosome, bind to mTORC1 and shuttle the complex back to the lysosomal membrane where it can be activated by Rheb. More work is required to determine whether either of these models can explain the changes in interaction intensity between the upstream signalling complexes of the mTORC1 pathway in response to amino acid availability.

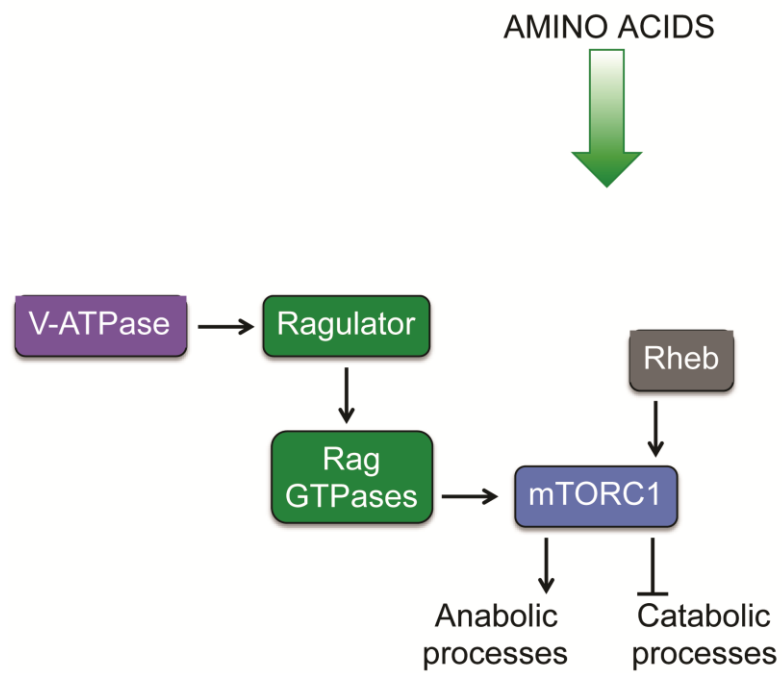


**Figure 1.9 The V-ATPase promotes mTORC1 activity**

It is thought that the V-ATPase complex signals nutrient availability via the ‘inside-out’ model in which amino acid accumulation in the vacuole drives activity of the V-ATPase. Active V-ATPase is able to promote Ragulator activity and thus mTORC1 activity via the Rag GTPases.

### 1.5.2.5 Regulation of mTORC1 by GATOR

A further complex in the mTORC1 amino acid sensing pathway has also been identified, the GATOR complex (Gap Activity TOWards Rags) which is proposed to down regulate mTORC1 activity (Bar-Peled et al. 2013). The GATOR complex comprises of eight subunits and exists as two sub-complexes: GATOR1 (Depdc5, Nprl2 and Nprl3) and GATOR2 (Mios, Wdr24, Wdr59, Seh1L and Sec13) (Bar-Peled et al. 2013) (Figure 1.10A). The GATOR complex shows functional similarity to the SEA complex identified in yeast, which is also split into two function-based sub-complexes SEACIT (GATOR1) and SEACAT (GATOR2) (Bar-Peled et al. 2013; Panchaud et al. 2013a). The GATOR complex is tethered to the lysosomal membrane through the DEPDC5 subunit (Bar-Peled et al. 2013). The two sub-complexes of GATOR have distinct roles; it appears that GATOR2 acts to inhibit the action of GATOR1 which in turn has GAP activity towards RagA/RagB thus down-regulating mTORC1 activity under unfavourable growth conditions (Bar-Peled et al. 2013; Panchaud et al. 2013a) (Figure 1.10B).

### 1.5.2.6 Regulation of mTORC1 by Leucyl-tRNA synthetase

As has been identified in yeast, a role for the leucyl-tRNA synthetase (LRS) in regulating mTORC1 activity has been found in mammalian cells. Han et al. (2012) found that LRS specifically interacts with both raptor and mTOR and is required for the relocalisation of mTORC1 to the lysosome. It was also found that LRS directly interacts with RagD-GTP to promote GTP hydrolysis (Han et al. 2012), this is in contrast to the discovery that Cdc60p interacts with Gtr1p in yeast (Bonfils et al. 2012). The interaction of LRS with RagD, which did not require t-RNA charging, appears to occur in a leucine-dependent manner and results in LRS functioning as a GAP for RagD, thus promoting mTORC1 activity (Figure 1.11). It would appear that LRS is also able to respond to isoleucine stimulation in activating mTORC1, suggesting that LRS may be a central amino acid sensor within the cell (Han et al. 2012).

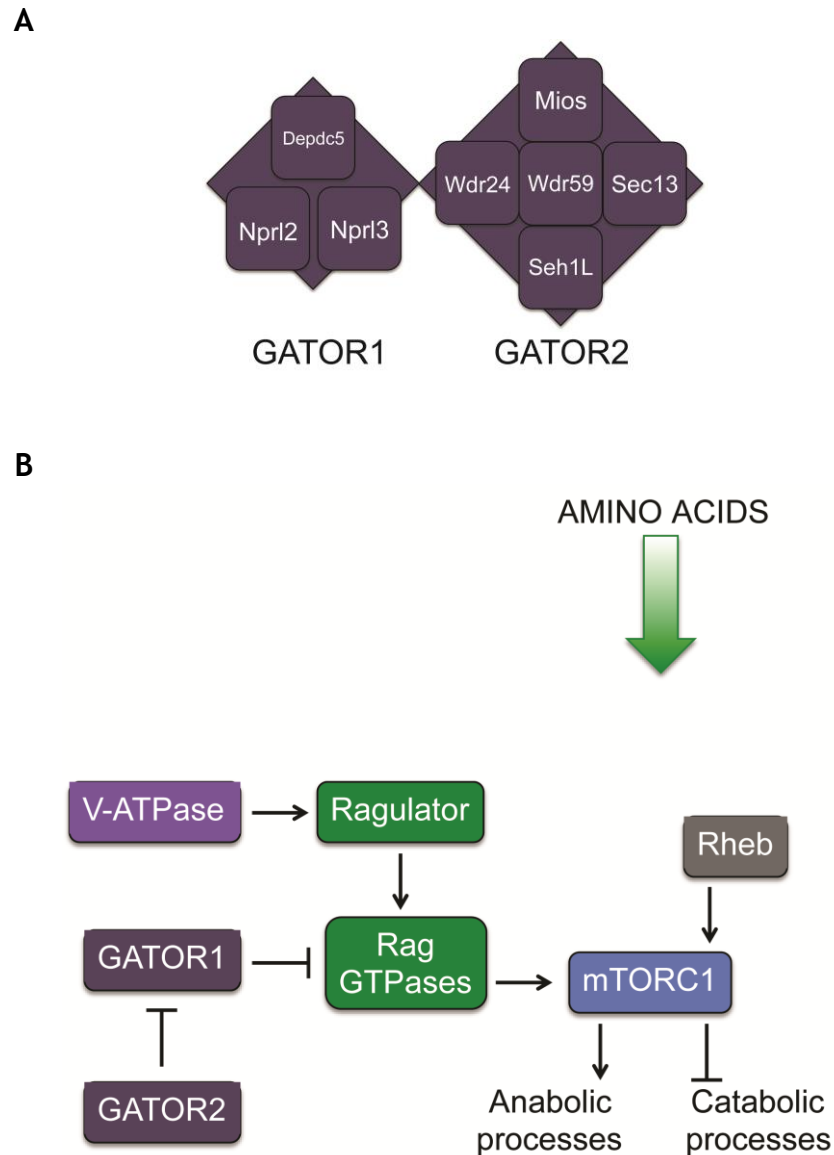


**Figure 1.10 The components, and signalling to mTORC1, of the GATOR complex**

A: The GATOR complex is comprised of eight subunits that are split into two functional sub-complexes: GATOR1 and GATOR2. GATOR1 consists of Depdc5, Nprl2 and Nprl3 whilst GATOR2 consists of Mios, Wdr24, Wdr59, Sec13 and Seh1L. The GATOR complex is tethered to the lysosomal membrane by the Depdc5 subunit.

B: Under optimal growth conditions, the GATOR2 sub-complex inhibits the activity of the GATOR1 sub-complex. GATOR1 has GAP activity towards the Rag GTPases and can therefore down-regulate their activity, and as such that of mTORC1, when starved of amino acids.

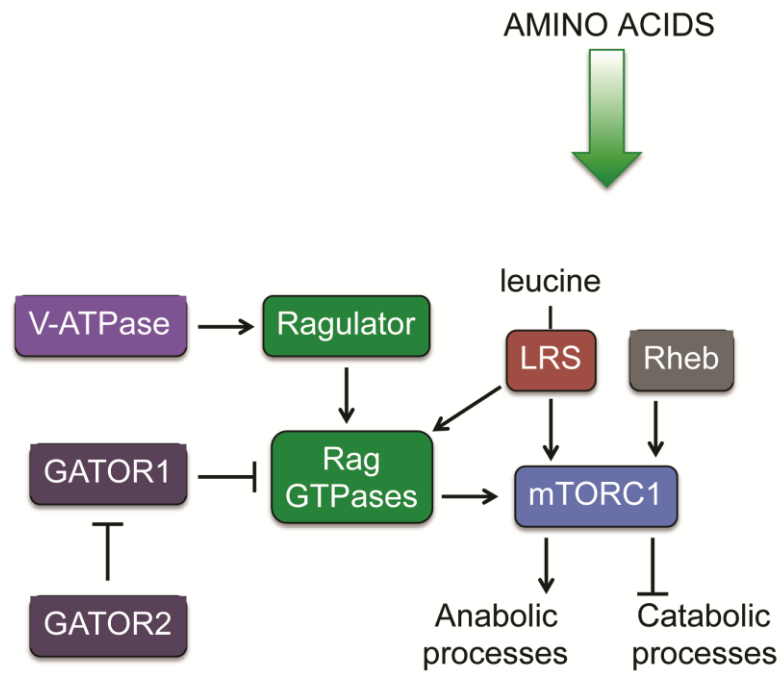


**Figure 1.11 Leucyl-tRNA synthetase promotes mTORC1 activity**

When charged with leucine, the leucyl-tRNA synthetase (LRS) is able to interact with both mTORC1 and RagD. LRS has GAP activity towards RagD thus maintaining mTORC1 activity under optimal growth conditions.

## 1.6 Downstream of yeast TORC1

TORC1 regulates cell growth and proliferation in response to nutrient availability and environmental stresses. When amino acids are plentiful, TORC1 is active and promotes anabolic processes such as the initiation of translation, ribosome biosynthesis and the expression of specific, high-affinity amino acid permeases at the cell surface (De Virgilio & Loewith 2006b). Inactivation of TORC1 results in the promotion of catabolic processes, including the induction of autophagy, the up-regulation of starvation induced gene transcription and the switch from specific to general amino acid permeases at the cell surface (Beck et al. 1999; De Virgilio & Loewith 2006b). The inactivation of TORC1 culminates in cells entering a quiescent-like G<sub>0</sub> state (Barbet et al. 1996; Rohde et al. 2001). The majority of studies investigating the down-stream functions of TORC1 involve either starving cells of amino acids or treating them with rapamycin.

### 1.6.1 Regulation of translation initiation

The initiation of translation is regulated by TORC1 and is inhibited in cells treated with rapamycin (Barbet et al. 1996; Urban et al. 2007). A study by Cherkasova & Hinnebusch (2003) has shown that rapamycin treatment leads to phosphorylation of the translation initiation factor eIF2 $\alpha$ , resulting in its inactivation and the subsequent inhibition of protein synthesis (Figure 1.12). Berset et al. (1998) demonstrated that rapamycin treatment results in the degradation of the translation initiation factor eIF4G, possibly through loss of its interaction with eIF4E. The loss of interaction between eIF4G and eIF4E can result from the activation of eIF4E binding proteins (4E-BPs) that disrupt the interaction between eIF4G and eIF4E to inhibit translation (Figure 1.12). It is thought that the activation of 4E-BP1 is the mechanism by which mTORC1 inhibits translation in mammalian cells (Feldman et al. 2009) (see later).

### 1.6.2 Regulation of ribosome biosynthesis

The biogenesis of ribosomes is a major consumer of cellular energy (Martin et al. 2006) and TORC1 activity is required to maintain transcription of genes encoding ribosomal proteins, as well as synthesising and processing 35S precursor mRNA (Li et al. 2006; Powers & Walter 1999).

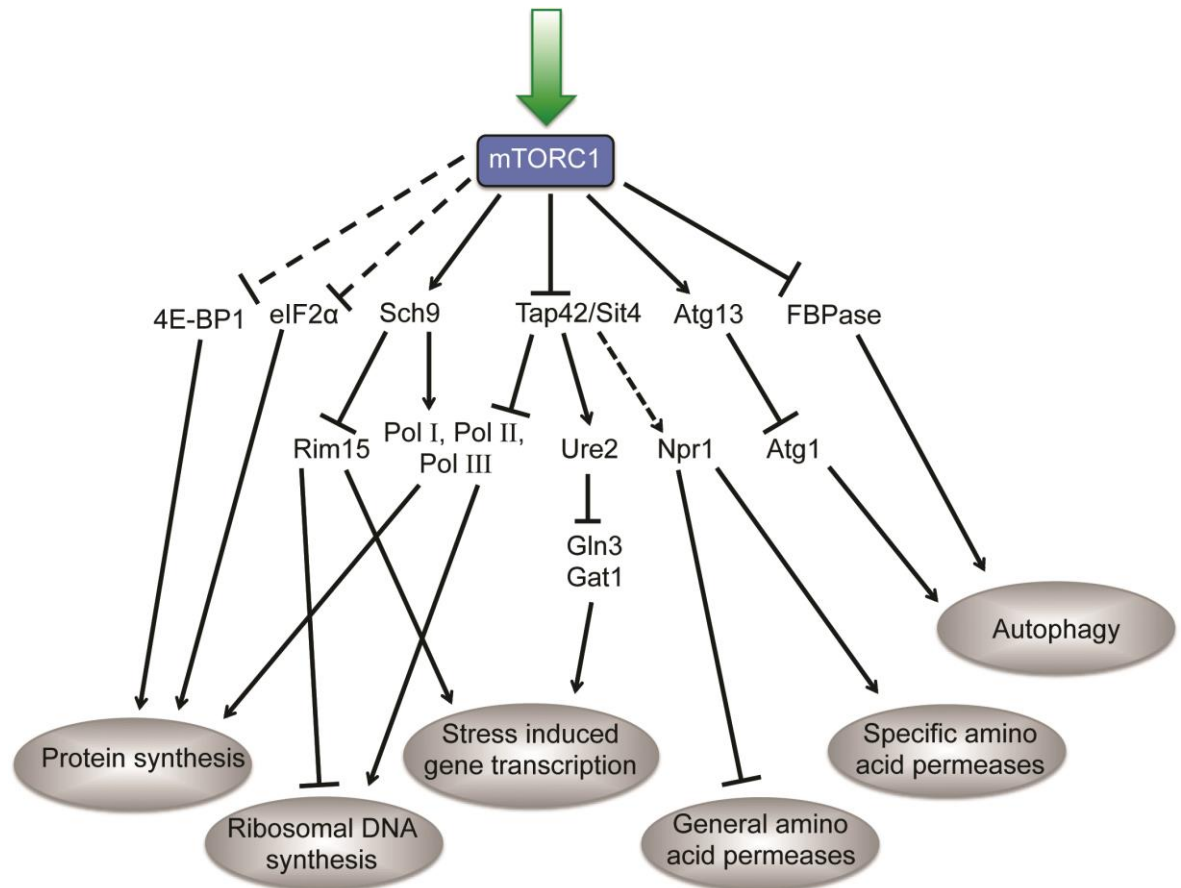


**Figure 1.12 The downstream TORC1 signalling pathway**

Active TORC1 promotes anabolic activities (including protein synthesis, transcription of ribosomal DNA, and the expression of specific amino acid permeases at the cell surface) and prevents catabolic activities (the induction of stress induced gene transcription, the induction of autophagy and the expression of general amino acid permeases at the cell surface). When TORC1 is inactive, due to poor amino acid and nutrient availability, anabolic processes are down-regulated and catabolic processes are promoted.

Dashed lines represent interactions that are not well established and may involve additional proteins.

Cells treated with rapamycin, or starved for nitrogen, show an immediate reduction in the transcription of ribosomal protein mRNA that does not require *de novo* protein synthesis (Cardenas et al. 1999; Hardwick et al. 1999; Neklesa & Davis 2009; Powers & Walter 1999) (Figure 1.12). The down-regulation of genes encoding proteins involved in ribosome biogenesis is due to inhibition of Pol I and Pol III and a reduction in the activity of Pol II at ribosomal gene promoters (Powers & Walter 1999). Li et al. (2006) found that shuttling of the Tor1p protein in and out of the nucleus played a role in the regulation of 35S mRNA transcription. Under optimal growth conditions Tor1p was found to be localised in the nucleus and associated with the 35S rDNA promoter region. However, in cells treated with rapamycin, Tor1p dissociates from the 35S promoter region and exits the nucleus (Li et al. 2006). It is thought that the TORC1 downstream targets, Sch9p and Tap42p activate synthesis of ribosomal protein mRNA; this will be discussed later.

### 1.6.3 Regulation of amino acid permeases at the cell surface

Exponentially growing cells consume a large amount of energy and require nutrients, such as amino acids, to maintain growth. Extracellular amino acids can be imported to supplement those made by the yeast themselves, or in the case of auxotrophs, provide nutrients which the cell cannot make. Exponentially growing cells express specific high-affinity amino acid permeases at the cell surface (De Virgilio & Loewith 2006b) for example the tryptophan and histidine permeases Tat2p and Hip1p; conversely cells in starvation conditions instead express general low-affinity amino acid permeases at the cell surface, an example being Gap1p (Beck et al. 1999b) (Figure 1.12). Specific and general amino acid permeases are inversely regulated at the level of protein sorting and stability in response to nutrient (amino acid, nitrogen or carbon) availability (Beck et al. 1999b; Schmidt et al. 1998). In exponentially growing cells, specific amino acid permeases are transported to, and are active at, the plasma membrane. Under TORC1 inactivating conditions, the specific amino acid permeases are removed from the plasma membrane, transported to the vacuole and degraded (Beck et al. 1999b). When cells are in optimal growth conditions, general amino acid permeases are cycled to the vacuole and degraded immediately following synthesis due to ubiquitination by Npi1p (Springael & André 1998). When TORC1 is inactivated, Gap1p is phosphorylated by Npr1p

protecting it from ubiquitination and allowing the accumulation of Gap1p at the cell surface (Beck et al. 1999b; Schmidt et al. 1998). The localisation of Gap1p at the cell surface replaces the specific permeases (e.g., Tat2p) which are degraded in the vacuole (Beck et al. 1999b; Schmidt et al. 1998). The up-regulation of Gap1p at the cell surface appears to occur in conjunction with the increase in complex sphingolipid synthesis upon TORC1 inactivation due to phosphorylation of Orm1p and Orm2p by Npr1p (Shimobayashi et al. 2013). The exact mechanism by which Npr1p is regulated by TORC1 is unclear (Jacinto et al. 2001), but it is likely that Tap42p is involved (Schmidt et al. 1998). In the absence of TORC1 activity, Npr1p is rapidly dephosphorylated leading to the degradation of Tat2p and the expression of general amino acid permeases at the cell surface (Schmidt et al. 1998).

#### 1.6.4 Regulation of autophagy

Autophagy is a process utilised by cells to increase the availability of free amino acids and as such is increased upon TORC1 inactivation, a response normally reserved for starvation conditions (Raught et al. 2001; Zaman et al. 2008). When cells are in conditions of plentiful nutrients, and TORC1 is active, autophagy is repressed. However, when TORC1 is inactivated, autophagy is induced leading to the creation of autophagic bodies that are transported to the vacuole and the contents degraded (Shin & Huh 2011); continued autophagy results in cells containing enlarged vacuoles (Brown et al. 2010). The phosphorylation of Atg13p by TORC1 regulates autophagy (Kamada et al. 2000; Kamada et al. 2010) (Figure 1.12). When TORC1 is active Atg13p is phosphorylated preventing it from interacting with Atg1p. When TORC1 is inactivated however, Atg13p is rapidly dephosphorylated and binds to Atg1p resulting in an active Atg13p-Atg1p complex that promotes PAS formation (Pre-Autophagosomal Structure) (Kamada et al. 2000; Kamada et al. 2010; Shin & Huh 2011). The formation of the PAS also appears to involve the phosphatidylinositol 3-phosphate (PtdIns(3)) kinase complex I which is composed of Vps34p, Vps15p, Atg6p and Atg14p (Obara & Ohsumi 2011; Suzuki & Ohsumi 2010). The human homolog of Vps34p, hVps34, is thought to be involved in mTORC1 signalling via a currently unknown mechanism (Yang et al. 2013).

TORC1 has also been shown to regulate autophagy in response to glucose starvation. Fructose 1,6-bisphosphatase (FBPase) is induced upon glucose starvation and targets cargo proteins to the vacuole via the Vid pathway (vacuole import and degradation) (Alibhoy & Chiang 2010). Depriving cells of glucose results in the interaction of TORC1 with FBPase, predominantly via Tco89p, thus preventing degradation of FBPase and allowing cargo proteins to be transported to the vacuole (Figure 1.12). Upon TORC1 reactivation, FBPase is released from TORC1 promoting the degradation of FBPase and subsequently inhibiting the Vid pathway (Alibhoy & Chiang 2010; Brown et al. 2010).

### 1.6.5 Regulation of starvation-induced gene transcription

As described above, the inactivation of TORC1 results in a general decrease in protein synthesis. In contrast, the transcription of genes involved in the Nitrogen Discrimination Pathway have been found to be up-regulated following nitrogen starvation or rapamycin treatment (Beck & Hall 1999; Cardenas et al. 1999; Hardwick et al. 1999). The GATA transcription factors Gln3p and Gat1p have been identified to regulate starvation-induced gene translation (Beck & Hall 1999; Cardenas et al. 1999; Hardwick et al. 1999) (Figure 1.12). Treatment of cells with rapamycin causes a rapid increase in the transcription of genes regulated by Gln3p and Gat1p; within 10 minutes of rapamycin treatment a 10-fold increase in some gene transcripts is seen (Beck & Hall 1999). Hardwick et al. (1999) found that the strongest effects on starvation induced gene transcription occurred within 15-30 minutes following the addition of rapamycin, suggesting that the regulation of these genes does not depend on *de novo* protein synthesis. Indeed, it was found that under conditions in which TORC1 is inactive, Gln3p and Gat1p are localised to the nucleus and are relocated to the cytoplasm upon TORC1 reactivation (Beck & Hall 1999; Hardwick et al. 1999). Gln3p has been shown to be tethered to the cytoplasm by interaction with Ure2p which is regulated by TORC1 (Beck & Hall 1999). Under conditions in which TORC1 is active Ure2p is phosphorylated by the TORC1 downstream targets Tap42p/Sit4p which results in it binding to, and retaining, Gln3p in the cytoplasm. When TORC1 is inactivated, Ure2p is rapidly dephosphorylated resulting in its dissociation from Gln3p and the transportation of Gln3p to the nucleus (Beck & Hall 1999; Cardenas et al. 1999; Hardwick et al. 1999). Ure2p is found in the cytoplasm regardless of TORC1 activity status (Beck & Hall 1999).

### 1.6.6 Sch9p and Tap42p

The majority of the downstream TORC1 functions identified so far are mediated through two branches of TORC1 signalling: Sch9p and Tap42p. The induction of autophagy however occurs via direct phosphorylation of Atg13p and appears independent of Sch9p or Tap42p (Kamada et al. 2010).

Dephosphorylation of Sch9p (a result of inactive TORC1) results in the down-regulation of protein synthesis (Huber et al. 2009) and ribosome biogenesis (Jorgensen & Rupeš 2004). Active Sch9p inhibits the function of several downstream transcriptional repressors for example Maf1p, Stb3p, Dot6p and Tod6p that predominantly regulate the expression of ribosomal genes (Huber et al. 2009). When Sch9p is inactivated by dephosphorylation, ribosomal gene transcripts are decreased leading to an overall decrease in protein synthesis. Sch9p also directly interacts with Rim15p to inhibit stress responses by tethering Rim15p in the cytoplasm (Wanke et al. 2008). Rim15p is a central regulator in the adaptation of cells to poor nutrient conditions and is controlled by a number of upstream regulators, one of which is TORC1 via Sch9p (Swinnen et al. 2013). Upon activation, Rim15p is translocated to the nucleus and promotes transcription factors (for example Msn2p and Msn4p) that initiate stress induced gene transcription (Swinnen et al. 2013) (Figure 1.12). It has recently been shown that recruitment of Sch9p to the vacuolar membrane requires PI(3,5)P<sub>2</sub> which could implicate PI(3,5)P<sub>2</sub> in having a downstream function of TORC1, in addition to its potential activating activity (Jin et al. 2014).

The release of Tap42p from TORC1 results in its inactivation and the induction of stress-induced gene transcription partially via regulation of the transcription factors Msn2p and Msn4p that target stress response genes (Düvel et al. 2003). The translocation of the transcription factor Gln3p to the nucleus following TORC1 inactivation is possibly regulated by Tap42p/Sit4p (Beck & Hall 1999; Düvel et al. 2003) (Figure 1.12). The phosphorylation of Npr1p and therefore switch from specific to general amino acid permeases at the cell surface is also under the control of Tap42p by a currently unknown mechanism (Schmidt et al. 1998) (Figure 1.12). When active, Tap42p is found in a trimeric complex with a second regulatory subunit and a catalytic subunit (most often Sit4p in TORC1 signalling) but this association is disrupted by the presence of rapamycin or when

TORC1 is inactive (Di Como & Arndt 1996). A point mutation in *TAP42* (*tap42-11*) or overexpression of Sit4p can render cells semi-resistant to the effects of rapamycin (Di Como & Arndt 1996).

### 1.6.7 Comparison of yeast down-stream functions of TORC1 with the down-stream functions of mTORC1

Due to the essential and conserved nature of the TORC1 signalling pathway, the fundamental downstream functions are similar across all eukaryotic cells. The mTORC1 pathway regulates cell growth and proliferation predominantly through the regulation of protein synthesis. The downstream proteins regulated by mTORC1 are also involved in regulating other cell growth and proliferation signalling pathways, for example c-Myc is a transcription factor regulated by mTORC1 that subsequently regulates genes involved in cell growth (Schmelzle & Hall 2000). In cases where regulation is lost, the downstream pathways of mTORC1 have been implicated in cancer development (Guertin & Sabatini 2007; Schmelzle & Hall 2000).

Regulation of protein synthesis by mTORC1 is predominantly governed by two signalling branches originating from direct targets of mTORC1; those downstream of S6 Kinase (S6K) (the homolog of Sch9p) and those downstream of 4E-BP1 (Inoki & Guan 2006; Laplante & Sabatini 2009; Raught et al. 2001; Schmelzle & Hall 2000). When the S6 Kinase is active, following phosphorylation by mTORC1, S6K promotes mRNA biogenesis, cap-dependent translation and the translation of ribosomal proteins (Laplante & Sabatini 2009; Raught et al. 2001). When mTORC1 is inactivated, S6K is dephosphorylated leading to inhibition of protein synthesis, similar to that seen in yeast cells. It is worth noting that mTORC1 is not the only method by which S6K is phosphorylated and it is thought that S6K is a central regulator of protein synthesis in response to various environmental cues (Raught et al. 2001).

In addition to regulation by S6K, the regulation of translation by mTORC1 is also carried out via the eIF4E Binding Protein 1 (4E-BP1) (Raught et al. 2001). Translation initiation factors are required to aid the start of translation in mammalian cells and help guide the ribosome to the 5' end of the mRNA. Two such translation initiation factors are eIF4E and eIF4G (Feldman et al. 2009). To

enable translation to start, eIF4E and eIF4G must be bound together at the 5' cap of mRNA. Translation can be inhibited by the binding of 4E-BP1 to eIF4E thus preventing the interaction between eIF4G and eIF4E (Feldman et al. 2009). When phosphorylated by mTORC1 4E-BP1 is unable to interact with eIF4E and translation is permitted. When mTORC1 activity is lost, 4E-BP1 is dephosphorylated and is therefore able to compete with eIF4G and prevent translation (Feldman et al. 2009).

As mentioned previously, it was hoped that rapamycin could be used clinically to inhibit cancerous cells but clinical trials resulted in inconsistent responses to rapamycin treatment. Studies carried out by Feldman et al. (2009) and Thoreen et al. (2009) using novel ATP-inhibitors of mTORC1 have found that rapamycin is in fact an incomplete inhibitor of mTORC1 activity, especially with regards to the phosphorylation of 4E-BP1. Feldman et al. (2009) and Thoreen et al. (2009) used different ATP-inhibitors of mTORC1 (pp242 or Torin1 respectively) and found that the dephosphorylation of 4E-BP1 was much more dramatic following treatment with the ATP-inhibitors than that following treatment with rapamycin. The identification of potential substrate selectivity with regards to mTORC1 inhibition in the presence of rapamycin could lead to a number of novel downstream targets and functions of mTORC1 being identified that were overlooked in cells treated with rapamycin.

One such example of a down-stream function of mTORC1 that could be further understood by using alternative mTORC1 inhibitors is the role of mTORC1 in the induction of autophagy. The role of yeast TORC1 in initiating autophagy is clear, however the role of mTORC1 in inducing autophagy is less so. Thoreen et al. (2009) found that mammalian cells treated with rapamycin resulted in a weak induction of autophagy, however cells treated with Torin1 resulted in a strong induction of autophagy. The mechanism by which mTORC1 regulates autophagy remains unclear but it is possible that phosphorylation, by mTORC1, of ULK1 and ATG13 may be involved (Jewell & Guan 2013).

## 1.7 Phenotype of *ego-* mutants

Loss of any component of the EGO complex (which we term *ego-*) in yeast results in cells that are unable to resume proliferation following rapamycin treatment

(Binda et al. 2009; Dubouloz et al. 2005). Part of the aims of this project are to understand why loss of the EGO complex results in a rapamycin recovery defect. A number of prior studies have been carried out to investigate the phenotype of *ego-* mutants, especially in response to rapamycin treatment and are discussed below.

Key phenotypes of TORC1 signalling have been compared between wild-type and *ego-* mutants in the absence or presence of rapamycin. Firstly, the phosphorylation of the TORC1 downstream target Sch9p was observed in wild-type and *ego-* cells either during exponential growth or following rapamycin treatment. Through the use of a gel-shift assay Binda et al. (2009) found that cells lacking any component of the EGO complex had lower basal TORC1 activity compared to that of wild-type cells. The low TORC1 activity in *ego-* mutants was comparable to cells lacking Tco89p, a component of TORC1 (Binda et al. 2009). Upon TORC1 inactivation, either following rapamycin or caffeine treatment, a complete dephosphorylation of Sch9p was observed and appeared similar in both wild-type and *ego-* cells.

Dubouloz et al. (2005) tested the response of *ego-* mutants to a number of hallmarks of inactive TORC1 and compared to wild-type cells. Dubouloz et al. (2005) concluded that mutants lacking the EGO complex appeared to respond to rapamycin treatment in a manner similar to that of wild-type cells. The hallmarks of inactive TORC1 tested included the transcription of stress response genes, the accumulation of glycogen, the induction of autophagy and the inhibition of protein synthesis (Dubouloz et al. 2005). A number of these conditions were also tested following a “recovery period” in which cells were washed into fresh media following treatment with rapamycin and incubated. Consistent with the inability of *ego-* mutants to resume proliferation following rapamycin treatment (*i.e.* the rapamycin recovery defect), hallmarks of inactive TORC1 also failed to recover (*i.e.* return to the state found in untreated cells), including low protein synthesis rate, autophagy and high glycogen levels. By contrast, these hallmarks had returned to basal levels in wild-type cells following removal of rapamycin (Dubouloz et al. 2005). Shin & Huh (2011) also found that autophagy was maintained longer in nitrogen-starved *gtr2Δ* cells than in wild-type cells; they concluded that the maintenance of autophagy was a result of weak TORC1 activity in *gtr2Δ* cells (Nicolas Panchaud et al. 2013) and

therefore an inability to efficiently reactivate TORC1 following the accumulation of amino acids from the autophagy process. If null mutants of the EGO complex appear to respond in a manner similar to that of wild-type cells when treated with rapamycin why do *ego*- cells fail to recover from rapamycin treatment?

## 1.8 Aims of this project

The EGO complex has been identified as an upstream regulator of yeast TORC1, indeed nearly every mechanism of TORC1 activation in yeast appears to converge on the EGO complex. Whilst null mutants of the EGO complex are viable and appear to have no strong phenotype, following treatment with rapamycin null mutants of the EGO complex fail to recover (Binda et al. 2009; Dubouloz et al. 2005). This project aims to explore the origin of the rapamycin recovery defect.

The mechanism by which rapamycin is detoxified in yeast (and for the most part mammalian cells) is not known. We will explore what happens to the intracellular pool of rapamycin in yeast following a rapamycin treatment period.

Finally, upstream regulators of yeast TORC1 in response to nutrients remain elusive and knowledge of the amino acid signalling pathway in yeast is not as well developed as that of mammalian cells (itself still far from complete). We will attempt to identify potential novel regulators of TORC1 by identifying null mutants that phenocopy loss of the EGO complex.

## 2 Materials and Methods

### 2.1 Growth conditions

All chemicals were purchased from Sigma (Dorset, UK) unless otherwise specified.

Cells were grown in either rich or selective synthetic minimal media as required. Rich media (YPD) comprised of yeast extract (1%), peptone (2%) and glucose (2%), solid media was created through the addition of agar (2%). Synthetic media (SD) was created using Difo yeast nitrogen base with the addition of glucose (2%) and the appropriate nutrients. Media lacking carbon (YP) comprised of yeast extract (1%) and peptone (2%).

Unless otherwise stated overnight liquid cultures were grown at room temperature with agitation, experimental growth temperatures were as stated in the results section. Cultures grown on solid media were incubated at either 28°C or 30°C unless otherwise stated.

### 2.2 Yeast cultures

All yeast haploid cultures used (except where specified) were in the BY4743 genetic background. Diploids were obtained from the yeast deletion collection in which every non-essential gene has replaced with a KanMX4 cassette (Giaever et al. 2002). Note that a “magic marker” cassette is also present in the background of this deletion collection which can confer leucine and histidine prototrophy in the *MATa* haploid, the auxotrophic state of leucine and histidine was not tested (Tong et al. 2001). See Table 2.1 for a list of all strains used.

#### 2.2.1 Creating double mutants

Double mutants were created by patching two null mutants of interest, with opposite mating types and differing drug resistance markers (see 2.3), onto a plain YPD plate and incubating at 30°C overnight. The resulting colony was patched onto selective media to select for diploids resistant to both G418 and Nat. Diploids were subsequently sporulated and dissected (see 2.4.1).

| Strain Number | Genetic Background | Mutation               | Genotype   |
|---------------|--------------------|------------------------|--|
| 5549          | BY4743             | <i>atg11Δ</i>          | <i>MAT? his3Δ leu2Δ ura3Δ atg11Δ::KanMX4</i>             |
| 5550          | BY4743             | <i>atg11Δ</i>          | <i>MAT? his3Δ leu2Δ ura3Δ lys2Δ atg11Δ::KanMX4</i>       |
| 5551          | BY4743             | <i>atg11Δ</i>          | <i>MAT? his3Δ leu2Δ ura3Δ atg11Δ::KanMX4</i>             |
| 5283          | BY4743             | <i>caf20Δ</i>          | <i>caf20Δ::KanMX4</i>                                    |
| 5284          | BY4743             | <i>caf20Δ</i>          | <i>caf20Δ::KanMX4</i>                                    |
| 5285          | BY4743             | <i>caf20Δ</i>          | <i>caf20Δ::KanMX4</i>                                    |
| 5563          | BY4743             | <i>ccr4Δ</i>           | <i>MAT? his3Δ leu2Δ ura3Δ lys2Δ ccr4Δ::KanMX4</i>        |
| 5564          | BY4743             | <i>ccr4Δ</i>           | <i>MAT? his3Δ leu2Δ ura3Δ met15Δ lys2Δ ccr4Δ::KanMX4</i> |
| 5565          | BY4743             | <i>ccr4Δ</i>           | <i>MAT? his3Δ leu2Δ ura3Δ lys2Δ ccr4Δ::KanMX4</i>        |
| 5605          | BY4743             | <i>ctk1Δ</i>           | <i>ctk1Δ::KanMX4</i>                                     |
| 5606          | BY4743             | <i>ctk1Δ</i>           | <i>ctk1Δ::KanMX4</i>                                     |
| 5607          | BY4743             | <i>ctk1Δ</i>           | <i>ctk1Δ::KanMX4</i>                                     |
| 5568          | BY4743             | <i>dhh1Δ</i>           | <i>MAT? his3Δ leu2Δ ura3Δ lys2Δ dhh1Δ::KanMX4</i>        |
| 5569          | BY4743             | <i>dhh1Δ</i>           | <i>MAT? his3Δ leu2Δ ura3Δ lys2Δ dhh1Δ::KanMX4</i>        |
| 5570          | BY4743             | <i>dhh1Δ</i>           | <i>MAT? his3Δ leu2Δ ura3Δ lys2Δ dhh1Δ::KanMX4</i>        |
| 5245          | BY4743             | <i>eap1Δ</i>           | <i>eap1Δ::KanMX4</i>                                     |
| 5246          | BY4743             | <i>eap1Δ</i>           | <i>eap1Δ::KanMX4</i>                                     |
| 5247          | BY4743             | <i>eap1Δ</i>           | <i>eap1Δ::KanMX4</i>                                     |
| 4839          | BY4743             | <i>ego1Δ</i>           | <i>MATa his3Δ leu2Δ ura3Δ met15Δ ego1Δ::KanMX4</i>       |
| 4840          | BY4743             | <i>ego1Δ</i>           | <i>MATa his3Δ leu2Δ ura3Δ met15? lys2Δ ego1Δ::KanMX4</i> |
| 4841          | BY4743             | <i>ego1Δ</i>           | <i>MATa his3Δ leu2Δ ura3Δ lys2Δ met15Δ ego1Δ::KanMX4</i> |
| 4851          | BY4743             | <i>ego1Δ</i>           | <i>MATa his3Δ leu2Δ ura3Δ met15Δ ego1Δ::Nat</i>          |
| 5617          | BY4743             | <i>ego1Δ pep3Δ</i>     | <i>ego1Δ::Nat pep3Δ::KanMX4</i>                          |
| 5618          | BY4743             | <i>ego1Δ pep3Δ</i>     | <i>ego1Δ::Nat pep3Δ::KanMX4</i>                          |
| 5619          | BY4743             | <i>ego1Δ pep3Δ</i>     | <i>ego1Δ::Nat pep3Δ::KanMX4</i>                          |
| 4821          | BY4743             | <i>ego3Δ</i>           | <i>MATa his3Δ leu2Δ ura3Δ lys2Δ ego3Δ::KanMX4</i>        |
| 4822          | BY4743             | <i>ego3Δ</i>           | <i>MATa his3Δ leu2Δ ura3Δ lys2Δ ego3Δ::KanMX4</i>        |
| 4823          | BY4743             | <i>ego3Δ</i>           | <i>MATa his3Δ leu2Δ ura3Δ met15Δ ego3Δ::KanMX4</i>       |
| 1384          | By4743             | <i>gap1Δ</i>           | <i>MATa his3Δ leu2Δ met15Δ ura3Δ gap1Δ::KanMX4</i>       |
| 4824          | BY4743             | <i>gtr1Δ</i>           | <i>MATa his3Δ leu2Δ ura3Δ lys2Δ gtr1Δ::KanMX4</i>        |
| 4825          | BY4743             | <i>gtr1Δ</i>           | <i>MATa his3Δ leu2Δ ura3Δ met15Δ gtr1Δ::KanMX4</i>       |
| 4826          | BY4743             | <i>gtr1Δ</i>           | <i>MATa his3Δ leu2Δ ura3Δ lys2Δ gtr1Δ::KanMX4</i>        |
| 4831          | BY4743             | <i>gtr2Δ</i>           | <i>MATa his3Δ leu2Δ ura3Δ lys2Δ gtr2Δ::KanMX4</i>        |
| 4832          | BY4743             | <i>gtr2Δ</i>           | <i>MATa his3Δ leu2Δ ura3Δ met15Δ gtr2Δ::KanMX4</i>       |
| 4833          | BY4743             | <i>gtr2Δ</i>           | <i>MATa his3Δ leu2Δ ura3Δ lys2Δ gtr2Δ::KanMX4</i>        |
| 5537          | BY4743             | <i>hom2Δ</i>           | <i>MAT? his3Δ leu2Δ ura3Δ hom2Δ::KanMX4</i>              |
| 5538          | BY4743             | <i>hom2Δ</i>           | <i>MAT? his3Δ leu2Δ ura3Δ hom2Δ::KanMX4</i>              |
| 5539          | BY4743             | <i>hom2Δ</i>           | <i>MAT? his3Δ leu2Δ ura3Δ hom2Δ::KanMX4</i>              |
| 5659          | BY4743             | <i>hom3Δ</i>           | <i>hom3Δ::KanMX4</i>                                     |
| 5660          | BY4743             | <i>hom3Δ</i>           | <i>hom3Δ::KanMX4</i>                                     |
| 5661          | BY4743             | <i>hom3Δ</i>           | <i>hom3Δ::KanMX4</i>                                     |
| 4922          | BY4743             | <i>kog1Δ pkog1-105</i> | <i>kog1Δ::KanMX4 pkog1<sup>ts</sup></i>                  |
| 5225          | BY4743             | <i>npl3Δ</i>           | <i>npl3Δ::KanMX4</i>                                     |
| 5235          | BY4743             | <i>npl3Δ</i>           | <i>npl3Δ::KanMX4</i>                                     |
| 5236          | BY4743             | <i>npl3Δ</i>           | <i>npl3Δ::KanMX4</i>                                     |

|      |        |               |   |
|------|--------|---------------|---|
| 5332 | BY4743 | <i>pep3Δ</i>  | <i>MATa his3Δ leu2Δ ura3Δ met15Δ pep3Δ::KanMX4</i>        |
| 5333 | BY4743 | <i>pep3Δ</i>  | <i>MATa his3Δ leu2Δ ura3Δ met15? pep3Δ::KanMX4</i>        |
| 5334 | BY4743 | <i>pep3Δ</i>  | <i>MATa his3Δ leu2Δ ura3Δ met15Δ pep3Δ::KanMX4</i>        |
| 3180 | BY4743 | <i>pep5Δ</i>  | <i>pep5Δ::KanMX4</i>                                      |
| 5543 | BY4743 | <i>pib2Δ</i>  | <i>MAT? his3Δ leu2Δ ura3Δ lys2Δ pib2Δ::KanMX4</i>         |
| 5544 | BY4743 | <i>pib2Δ</i>  | <i>MAT? his3Δ leu2Δ ura3Δ pib2Δ::KanMX4</i>               |
| 5545 | BY4743 | <i>pib2Δ</i>  | <i>MAT? his3Δ leu2Δ ura3Δ lysΔ pib2Δ::KanMX4</i>          |
| 5581 | BY4743 | <i>shp1Δ</i>  | <i>MAT? his3Δ leu2Δ ura3Δ met15Δ lys2Δ shp1Δ::KanMX4</i>  |
| 5582 | BY4743 | <i>shp1Δ</i>  | <i>MAT? his3Δ leu2Δ ura3Δ met15Δ shp1Δ::KanMX4</i>        |
| 5583 | BY4743 | <i>shp1Δ</i>  | <i>MAT? his3Δ leu2Δ ura3Δ shp1Δ::KanMX4</i>               |
| 5555 | BY4743 | <i>snx4Δ</i>  | <i>MAT? his3Δ leu2Δ ura3Δ snx4Δ::KanMX4</i>               |
| 5556 | BY4743 | <i>snx4Δ</i>  | <i>MAT? his3Δ leu2Δ ura3Δ lys2Δ snx4Δ::KanMX4</i>         |
| 5557 | BY4743 | <i>snx4Δ</i>  | <i>MAT? his3Δ leu2Δ ura3Δ lys2Δ snx4Δ::KanMX4</i>         |
| 4420 | BY4743 | <i>tco89Δ</i> | <i>MATa his3Δ leu2Δ ura3Δ met15Δ lys2Δ tco89Δ::KanMX4</i> |
| 4424 | BY4743 | <i>tco89Δ</i> | <i>MATa his3Δ leu2Δ ura3Δ met15Δ tco89Δ::KanMX4</i>       |
| 4490 | BY4743 | <i>tor1Δ</i>  | <i>MATa his3Δ leu2Δ ura3Δ lys2? met15? tor1Δ::KanMX4</i>  |
| 4837 | BY4743 | <i>vam6Δ</i>  | <i>MATa his3Δ leu2Δ ura3Δ lys2Δ vam6Δ::KanMX4</i>         |
| 4838 | BY4743 | <i>vam6Δ</i>  | <i>MATa his3Δ leu2Δ ura3Δ met15Δ vam6Δ::KanMX4</i>        |
| 5499 | BY4743 | <i>vam6Δ</i>  | <i>his3Δ leu2Δ ura3Δ vam6Δ::nat</i>                       |
| 5675 | BY4743 | <i>vam7Δ</i>  | <i>vam7Δ::KanMX4</i>                                      |
| 5676 | BY4743 | <i>vam7Δ</i>  | <i>vam7Δ::KanMX4</i>                                      |
| 5379 | BY4743 | <i>vps15Δ</i> | <i>MATa his3Δ leu2Δ ura3Δ vps15Δ::KanMX4</i>              |
| 5380 | BY4743 | <i>vps15Δ</i> | <i>MATa his3Δ leu2Δ ura3Δ vps15Δ::KanMX4</i>              |
| 5381 | BY4743 | <i>vps15Δ</i> | <i>MATa his3Δ leu2Δ ura3Δ vps15Δ::KanMX4</i>              |
| 5351 | BY4743 | <i>vps16Δ</i> | <i>MATa his3Δ leu2Δ ura3Δ met15Δ vps16Δ::KanMX4</i>       |
| 5352 | BY4743 | <i>vps16Δ</i> | <i>MATa his3Δ leu2Δ ura3Δ lys2Δ vps16Δ::KanMX4</i>        |
| 5353 | BY4743 | <i>vps16Δ</i> | <i>MATa his3Δ leu2Δ ura3Δ vps16Δ::KanMX4</i>              |
| 5763 | BY4743 | <i>vps33Δ</i> | <i>vps33Δ::KanMX4</i>                                     |
| 5764 | BY4743 | <i>vps33Δ</i> | <i>vps33Δ::KanMX4</i>                                     |
| 5765 | BY4743 | <i>vps33Δ</i> | <i>vps33Δ::KanMX4</i>                                     |
| 2474 | BY4743 | <i>vps34Δ</i> | <i>his3Δ leu2Δ ura3Δ vps34Δ::KanMX4</i>                   |
| 0161 | W303   | Wild-type     | <i>MATa</i>   |
| 0205 | EG123  | Wild-type     | <i>MATa</i>   |
| 1367 | BY4743 | Wild-type     | <i>MATa his3Δ leu2Δ ura3Δ met15Δ</i>                      |
| 5599 | BY4743 | <i>yke2Δ</i>  | <i>yke2Δ::KanMX4</i>                                      |
| 5600 | BY4743 | <i>yke2Δ</i>  | <i>yke2Δ::KanMX4</i>                                      |
| 5601 | BY4743 | <i>yke2Δ</i>  | <i>yke2Δ::KanMX4</i>                                      |
| 4842 | BY4743 | <i>ypt7Δ</i>  | <i>MATa his3Δ leu2Δ ura3Δ met15Δ ypt7Δ::KanMX4</i>        |
| 4843 | BY4743 | <i>ypt7Δ</i>  | <i>MATa his3Δ leu2Δ ura3Δ met15Δ ypt7Δ::KanMX4</i>        |
| 5434 | BY4743 | <i>ypt7Δ</i>  | <i>ypt7Δ::KanMX4</i>                                      |

**Table 2.1 List of Strains used throughout the thesis**

All strains used throughout the thesis are shown, in alphabetical order by mutation. The mating type and auxotrophic markers are shown if known, a ? indicates unknown information. Note that the background strain BY4743 is the diploid background from which the haploid cells were generated.

Resulting dissected haploids were tested for G418 and Nat sensitivity and double null mutants confirmed by their resistance to both drugs.

## **2.3 Transformation**

### **2.3.1 Bacterial transformation**

Chemically competent DH $\alpha$  cells (Invitrogen, Paisley, UK) were transformed following the manufactures instructions.

### **2.3.2 Yeast transformation**

Exponentially growing overnight cultures were transformed using a standard lithium acetate protocol as set out in Gietz et al. (1995). Table 2.2 shows a list of the plasmids used in this study and the references from which the plasmids were obtained.

### **2.3.3 Switching the kanamycin selection marker**

To change the KanMX4 selection marker to that of Nat (nourseothricin), exponentially growing haploid cultures were transformed with a PCR amplified Nat cassette. The PCR product was amplified from a plasmid created by Goldstein & McCusker (1999) to replace the KanMX4 cassette by homologous recombination with a cassette conferring alternative drug resistance, in this case Nat resistance. Following the transformation procedure, instead of plating directly onto selective plates, cultures were plated onto plain YPD and incubated overnight at 30°C. The following day colonies were replica plated onto selective Nat plates and incubated overnight at 30°C. Cells which had undergone homologous recombination were confirmed by both their ability to grow in the presence of Nat and their loss of resistance to G418.

## **2.4 Sporulation and dissection**

### **2.4.1 Sporulation and dissection**

Diploid cells were incubated in liquid sporulation media (potassium acetate (0.3%), raffinose (0.02%)) at room temperature until tetrads were observed by microscopy (usually 2-3 days).

| Plasmid number | Backbone plasmid | Gene  | Reference               |
|----------------|------------------|---|-------------------------|
| pG514          | pRS316           | <i>kog1-105</i><br>( <i>kog1<sup>ts</sup></i> ) | (Nakashima et al. 2008) |
| pG535          | pRS316           | <i>PGK1-GFP</i>                                 | (Welter et al. 2010)    |
| pG497          | ?                | 3HA- <i>TOR1</i>                                | (Reinke et al. 2006)    |
| pG498          | ?                | 3HA- <i>tor1<sup>L1957V</sup></i>               | (Reinke et al. 2006)    |

**Table 2.2 List of the plasmids used in this thesis**

The plasmids used during the course of this thesis, listed in alphabetical order for the gene they carry. The reference from which the plasmids were obtained is also shown. ? indicates that the plasmid backbone is unknown.

Cells were pelleted, resuspended in zymolyase (0.5 mg/mL) and incubated at 30°C for 10-12 min before ice-cold Tris-sorbitol (Tris (10 mM), sorbitol (1 M)) was added. Dissections were carried out on YPD 4% agar plates (unless otherwise stated).

#### 2.4.2 Determining the mating type

The mating types for newly created haploids were determined by mating the null mutant haploids to the ‘a’ and ‘α’ mating tester strains on YPD plates and incubating at 30°C overnight. The resulting culture was patched onto synthetic dropout media lacking any amino acid supplements and again incubated overnight at 30°C. The mating type of the haploid of interest was determined by observing complementation between the mating tester and the haploid of interest on the dropout media; the mating type was inferred from that of the mating tester if complementation, and therefore colony formation, was observed.

#### 2.4.3 Genotyping haploids with regards to auxotrophic markers

The genotype of specific auxotrophic markers was also determined for freshly created haploids. Haploid cells were patched onto synthetic media lacking either methionine or lysine and plates incubated at 30°C overnight. Haploids were prototrophic for the marker of interest if colony formation was observed and auxotrophic if the cultures failed to grow on the selective media. Note, these strains also contain the “magic marker” cassette which confers leucine and histidine prototrophy depending on the mating type of the cell (Tong et al. 2001). The phenotype of haploids with regards to leucine and histidine was not tested.

### 2.5 Creating *kog1*Δ<sup>ts</sup> haploids

Heterozygous diploid *kog1*Δ/*KOG1* cells were transformed with a plasmid borne temperature sensitive *kog1*<sup>ts</sup> allele (*pkog1*<sup>ts</sup> (Table 2.2) (Nakashima et al. 2008)) and sporulated as described in 2.4.1. Tetrads were dissected onto YPD 4% agar plates and *kog1*Δ null mutants carrying *pkog1*<sup>ts</sup> were identified by their ability to grow in the presence of G418. To induce the temperature-sensitive phenotype

*kog1Δ-pkog1<sup>ts</sup>* cultures were grown for a day prior to the experimental start at either the permissive (22°C) or non-permissive (37°C) temperature during which they were maintained in exponential growth by dilution into fresh YPD media when necessary.

## 2.6 Spot assay for recovery

When in exponential growth phase, cultures were normalised by OD<sub>600nm</sub>, as specified in the Figure legends, and drugs added at the concentrations stipulated. Cultures were incubated at room temperature or 28°C with agitation as specified, unless otherwise stated. Cells were washed three times in fresh media (unless otherwise specified) by pelleting cells through centrifugation followed by resuspension in fresh YPD media (unless otherwise stated). Ten-fold serial dilutions were created into fresh YPD which were spotted (5 µL) onto YPD plates and incubated at either 28°C or 30°C for two days after which the plates were scanned.

## 2.7 Methylene blue staining

Exponentially growing cultures were treated (or not) with rapamycin (200 ng/mL) for the times stipulated. Aliquots of culture were mixed with methylene blue (final concentration 0.02% w/v) and spotted onto a glass slide. Control cultures of heat-killed cells (85°C for 10 minutes) were also included. Staining was observed by microscopy and a minimum of 200 cells were counted per sample.

## 2.8 Amino acid uptake

Exponentially growing cultures were treated (or not) with rapamycin (200 ng/mL). Cultures were normalised to an OD<sub>600nm</sub> of ~0.25 in 1 mL, pelleted and concentrated in YPD (75 µL) to which <sup>35</sup>S labeled methionine and <sup>35</sup>S labeled methionine cysteine (22 µCi) (EasyTag EXPRESS<sup>35</sup>S Protein Labeling Mix, Perkin Elmer, Massachusetts, USA) was added and cells incubated at room temperature for 5 minutes. Cultures were washed six times with ice-cold methionine (75 mM) and cysteine (75 mM) using micro centrifuge filters (Corning Costar, Sigma-Aldrich, Dorset, UK). Retained cell-associated radiation was measured by

Scintillation counter (Beckman Coulter, High Wycombe, UK). Control samples of medium alone, *i.e.* YPD containing no cells, and to which radiation was added were also included; the Count Per Minute (CPM) measurement from these controls was subtracted from the CPM of each sample.

## **2.9 Measuring culture densities and calculating the growth rate**

### **2.9.1 Culture density as measured by Coulter counter**

Exponentially growing cultures were treated (or not) in YPD and incubated at room temperature with agitation. To measure the culture density at specified times, aliquots of each culture were removed and sonicated for 5 sec before being added to 10 mL isoton liquid. The volume of sonicated culture added to the isoton was dependent on the density of the culture and was adjusted to ensure the number of cells present was within the accurate detection range; the cell numbers counted per culture were subsequently normalised. The number of cells counted per sample, within a size range of 2.51-8.58  $\mu\text{m}$ , were measured by a Coulter counter in 500  $\mu\text{L}$  samples, three repeats were measured per sample and the average calculated. The mean cell size was measured between 3.258-8.436  $\mu\text{m}$ .

### **2.9.2 Culture density as measured by optical spectrometry**

Exponentially growing cultures were treated (or not) in YPD and incubated at 28°C with agitation. At specified times, samples were removed and the culture density measured at OD<sub>600nm</sub>.

### **2.9.3 Calculating the growth rate**

The culture density measurements at each time point, either determined by Coulter counter or optical spectrometry, were converted into the  $\log_2$  and the growth rate was determined as the linear regression line (using the Excel slope function) of two observed culture density measurements between two specified time points, as specified in the Figure legends. The growth rate was calculated during a period when the growth rate was stable.

## 2.10 Autophagy assay

Cells expressing a plasmid-borne copy of *PGK1-GFP* were chemically lysed according to Welter et al. (2010), briefly: Cell pellets normalised for  $OD_{600nm}$  were collected by centrifugation and resuspended in ice-cold water (1 mL) to which lysis buffer (150  $\mu$ L; NaOH (1.85 M),  $\beta$ -mercaptoethanol (7.5% v/v)) was added, mixed by vortex and samples incubated on ice for 10 min. Ice-cold TCA (150  $\mu$ L of 50% TCA w/v) was added and the samples incubated for a further 10 min on ice before being centrifuged at full speed for 10 min. Precipitated pellets were washed twice in ice-cold acetone (1 mL), dried at room temperature then resuspended in SDS sample buffer (Tris-HCl pH 6.8 (50 mM), SDS (2% w/v), glycerol (10% v/v),  $\beta$ -mercaptoethanol (1% v/v), bromophenol blue) and stored at  $-20^{\circ}$ C.

Proteins were separated on a NuPAGE 12% Bis-Tris gel with MES running buffer (Invitrogen, Paisley, UK) and transferred to a PVDF membrane according to manufactures instructions. Membranes were probed with an anti-GFP primary antibody (Santa Cruz, Heidelberg, Germany) and a hydrogen peroxidase secondary antibody was used. Development was carried out using an ECL development kit (GE Healthcare) according to the manufacturer's instructions. Bands were visualised by autoradiography.

## 2.11 Mass spectrometry

Exponentially growing cultures were treated (or not) with rapamycin (400 ng/mL). At each time point cell pellets equivalent to 10  $OD_{600nm}$  units were collected by centrifugation. To extract rapamycin, the cell pellets were washed three times in ice-cold water before cells were lysed by vortexing in 200  $\mu$ L ice-cold water and an equal volume of glass beads for six cycles of 30 sec vortex and 30 sec on ice. Rapamycin was extracted five times into neat ethyl acetate (250  $\mu$ L) (Fisher, Loughborough, UK) by vortexing for 30 sec prior to centrifugation for 2 min at 16,000 g. The organic layers were collected and pooled.

*The following description was provided by Dr. Burgess of the University of Glasgow Polyomics Facility who optimised the mass spectrometry procedure (in collaboration with myself).*

Mass spectrometry was carried out at the University of Glasgow Polyomics Facility and consisted of: Extracted sample (10  $\mu$ L) was injected onto an Ultimate 3000 RSLC system (Thermo, Hemel Hempstead, UK) equipped with an Acclaim 5 $\mu$ m 2.1 x 150 mm C18 column. The separation gradient ran from 5% acetonitrile, 95% water to 50% acetonitrile, 50% water in 20 minutes, followed by a wash at 95% acetonitrile, 5% water for 6 minutes and 6 minutes reequilibration at 95% water, 5% acetonitrile. Mass spectrometry detection was performed on a Q-Exactive (Thermo, Hemel Hempstead, UK) in negative ionization mode at 70,000 resolution. Identity of rapamycin was confirmed by retention time, mass and fragment pattern matching to an authentic standard. Quantification was performed using Quan Browser version 2.2 (Thermo, Hemel Hempstead, UK) and was carried out by Dr. Burgess and Dr. Weidt at the University of Glasgow Polyomics Facility.

## 2.12 Translation assay

Following treatment of exponentially growing cultures, a cell pellet equivalent to  $\sim 2$  OD<sub>600nm</sub> units was collected and resuspended in SD lacking methionine (1 mL). <sup>35</sup>S-labeled methionine and <sup>35</sup>S-labeled cysteine (22  $\mu$ Ci) (EXPRE<sup>35</sup>S<sup>35</sup>S Protein Labeling Mix, Perkin Elmer, Massachusetts, USA) was added and cells incubated at room temperature for 10 min with shaking. Cells were pelleted and lysed using NaOH (1 M) in solution with methionine (10 mM) and cysteine (10 mM) with  $\beta$ -mercaptoethanol (0.5% v/v) and incubated on ice for 10 min. Ice-cold TCA (final concentration 10% w/v) was added and samples incubated on ice for a further 10 min. TCA precipitable material was washed three times in ice-cold acetone before being resuspended in SDS buffer (see 2.10). Peptide-associated radiation was measured by scintillation counter (Beckman Coulter, High Wycombe, UK). Media-only controls to which radiation was added and the TCA extraction procedure performed were included; the subsequent CPM obtained from the control was subtracted from the CPM of each sample.

## 2.13 Measuring and predicting recovery time from rapamycin

### 2.13.1 Experimentally measuring recovery time

Exponentially growing cultures were treated with rapamycin for two hours in YPD at room temperature with agitation. Following the two hour ‘treatment phase’, cells were washed three times in fresh YPD (as explained in 2.6) (rapamycin washout), inoculated into fresh medium and incubated at room temperature with agitation for a ‘recovery phase’. During a 48 hour recovery phase, the culture density was measured by Coulter counting (as explained in 2.9). The culture density of untreated cultures and those in the continuous presence of rapamycin were also measured as controls. The recovery time was measured as the lag time for the growth rate of recovering cultures to switch from that resembling continuously treated cultures to that of untreated cultures; this is explained in more detail in Chapter 5.

### 2.13.2 Predicting the recovery time

The recovery time of cultures from various concentrations of rapamycin was calculated using the following formula:

$$t^R = t^{DT} \times \log_2 [\text{rap}]_{\text{treatment}} + a$$

|        |                                   |  |
|--------|-----------------------------------|--|
| where: | $t^R$                             | predicted recovery time (hrs)  |
|        | $t^{DT}$                          | observed doubling time in the constant presence of a high concentration of rapamycin (far in excess of the minimum inhibitory concentration) (hrs) |
|        | $[\text{rap}]_{\text{treatment}}$ | the concentration of rapamycin in the media during the treatment phase (ng/mL)   |
|        | $a$                               | constant (hrs), a “fudge-factor” derived from the best fit of the initial trajectory of $t^R$ to the experimentally observed recovery times        |

The context of this equation is explained in more detail in Chapter 5.

## 2.14 Databases

### 2.14.1 GO Term analysis

To identify potentially enriched GO terms within our dataset of null mutants identified in a primary screen (see Chapter 6 for more detail) we utilised the Saccharomyces Genome Database's (SGD) GO Term finder program ([www.yeastgenome.org/cgi-bin/GO/goTermFinder.pl](http://www.yeastgenome.org/cgi-bin/GO/goTermFinder.pl)). This program searches a query list of genes to identify enriched GO terms within that set compared to those known in the background. Enrichment is determined by statistical significance with a cut-off limit of  $p < 0.01$  (note p-values are automatically calculated using a Bonferroni Correction to reduce the potential for false positives due to the requirement of multiple hypothesis testing). The GO Term Finder searches were carried out in January 2014, the website warns that due to regular updates and additions to GO terms, the results of a particular search may vary depending on the time between repeats.

### 2.14.2 Physical interaction analysis

To test for any known physical interactions within our dataset we utilised the Osprey software (Breitkreutz et al. 2003). The information Osprey uses to visualise known interactions within a query set of proteins is derived from the Saccharomyces Genome Database. It is worth noting that the Osprey software does not appear to have been updated for some time and more recently identified interactions between proteins are not shown.

## 2.15 Sensitivity to rapamycin

Exponentially growing cultures were normalised for  $OD_{600nm}$  in YPD and incubated in the presence of various concentrations of rapamycin in a 24 well plate at 28°C with agitation. An endpoint assay was carried out measuring the  $OD_{600nm}$  6 hours after the addition of rapamycin. The  $OD_{600nm}$  of cultures was normalised to that of untreated controls.

## 2.16 FM4-64 staining and confocal microscopy

### 2.16.1 FM4-64 staining

To visualise vacuoles within the cell, exponentially growing cultures were treated (or not) with rapamycin and incubated at 28°C with agitation for the time specified in the Figure legend. Aliquots of each culture were concentrated in YPD (50 µL; with rapamycin where appropriate) to which the vacuolar stain FM4-64 (2 µM final concentration) was added. Cells were incubated for 30 minutes at 30°C in the dark. YPD (1 mL; with or without rapamycin) was added and cells pelleted. The pellets were resuspended into YPD media (5 mL; with or without rapamycin) and incubated in the dark at 28°C with agitation for 90 minutes. Following the incubation period cells were washed once with water (1 mL), resuspended in complete synthetic media (25 µL) and kept on ice in the dark until microscopy analysis. Note: Cells were resuspended in synthetic media to be observed by microscopy to reduce the potential for background autofluorescence.

### 2.16.2 Confocal microscopy

A Zeiss Confocor LSM510 confocal microscope was used to detect FM4-64 staining within cells. An argon laser was used with an excitation wavelength between 505 and 530 nm and an emission wavelength of 560 nm. All images were taken using a 63x oil-immersed objective. A merge of the bright field and fluorescent image will be shown. Backgrounds were adjusted to increase visibility of the stain.

## 2.17 Statistics

*Error Bars:* All quantitative experiments were repeated at least three times and the average calculated. Error bars denote the standard error of the mean (S.E.M.) which was calculated from the following formula:

$$\text{S.E.M.} = \frac{\text{SD}}{\sqrt{N}}$$

|        |        |                            |
|--------|--------|----------------------------|
| where: | S.E.M. | standard error of the mean |
|        | SD     | standard deviation         |
|        | N      | number of replicates       |

*p-values*: Statistical significance was calculated using Student's t-test. The tests were carried out using a two-tailed, type three test between two results. A two-tailed, type three t-test is used to determine whether two means are different from each other, regardless of the direction, and when the two samples are of unequal variance. Statistical significance was applied when the p-value was less than 0.05.

### 3 Testing various models that could explain why *ego*- mutants fail to recover from rapamycin treatment

#### 3.1 Introduction

The EGO complex, which consists of four subunits; Ego1p, Ego3p, Gtr1p and Gtr2p, is currently thought to be an activator of TORC1 in response to nutrient availability (Binda et al. 2009; Dubouloz et al. 2005; Gao & Kaiser 2006). TORC1 activity is essential for yeast proliferation. However the EGO complex is not essential: null mutants are viable. Yet, null mutants lacking any of the four members of the complex appear to be completely unable to recover from rapamycin treatment (Binda et al. 2009; Dubouloz et al. 2005).

Why does loss of the EGO complex result in a selective failure to recover from rapamycin treatment? Here, we consider four models that could explain the phenotype seen in *ego*- mutants in response to rapamycin and are set out below.

##### Loss of Viability Model

Selective loss of viability in the presence of rapamycin has been shown to occur in mutants defective in the cell wall integrity pathway (Krause & Gray 2002). It is possible that this is also the case for cells lacking the EGO complex.

##### Permease Switch Model

One physiological effect of inactive TORC1 is the exchange of specific (e.g. Tat2p) for general (e.g. Gap1p) amino acid permeases at the cell surface (Beck et al. 1999). The EGO complex could be required for the trafficking of general amino acid permeases in yeast.

It is possible that *ego*- mutants are able to internalise the specific amino acid permeases but fail to express the general amino acid permeases at the cell surface when treated with rapamycin. This failure would result in cells lacking any amino acid permeases at the cell surface following rapamycin treatment. Whilst loss of amino acid permeases at the cell surface of prototrophic strains may not have dramatic consequences, the laboratory strains used are auxotrophic for a number of amino acids. Due to the inability of auxotrophic

cells to synthesise all the amino acids they require, the presence of amino acid permeases at the cell surface is of great importance. The lack of amino acid permeases at the cell surface of rapamycin treated *ego-* mutant cells could result in *ego-* mutants entering a state of starvation. This prolonged starvation state would present as an inability to recover from rapamycin treatment.

There is some controversy regarding the role of the EGO complex in the transport of Gap1p to the cell surface. Gao & Kaiser (2006) showed that the EGO complex (which they termed the GSE complex in association with a fifth protein Ltv1p) is required to transport Gap1p to the plasma membrane upon transfer of cells to poor nitrogen sources. However, Binda et al. (2009) found that *ego-* mutants were able to transport Gap1p to the plasma membrane when given a poor nitrogen source. Binda et al. (2009) suggested that the difference between the two studies was due to the strain backgrounds used; the strain used by Gao & Kaiser (2006) carried a loss-of-function allele at the *PER1* locus which has been associated with abnormal responses of amino acid permeases to nitrogen signals. The strains used throughout this thesis are wild-type at the *PER1* locus.

It is also possible that the EGO complex is required, not necessarily for transport, but for activity of the general amino acid permeases at the cell surface. If this were the case, rapamycin treatment of *ego-* mutants would also result in *ego-* cells arresting in a permanent state of starvation and thus appearing unable to recover from rapamycin.

#### **TORC1 Reactivation Model**

It is possible that the EGO complex is selectively required to reactivate TORC1 from any inactivated state, induced either chemically or by nutrient starvation. If the EGO complex is required to reactivate TORC1 following rapamycin treatment, loss of the EGO complex would result in cells with constitutively inactive TORC1 following exposure to the drug. Such cells would be unable to recover from rapamycin treatment.

#### **Rapamycin Detoxification Model**

The EGO complex could be required for detoxification of rapamycin in yeast, either in association with a known detoxification mechanism or via a novel

process. If the EGO complex is required for detoxification of rapamycin, we predict that loss of the complex would result in a build-up of the drug within *ego-* cells resulting in continued TORC1 inactivation and prolonged G0 arrest, even when the drug is removed from the extracellular medium. Very little is currently known about how rapamycin is detoxified in yeast cells. The only known detoxification mechanism for rapamycin occurs primarily in the human liver and involves the cytochrome P450 CYP3A4 (Anzenbacher & Anzenbacherova 2001; Guengerich 1999; Li et al. 1995).

In this chapter we set out to test the above models.

## 3.2 Results

### 3.2.1 Establishing the *ego-* phenotype under our laboratory conditions

The phenotype of mutants lacking any of the four components of the EGO complex in response to rapamycin treatment was tested. This was carried out to establish the phenotype of *ego-* mutants in response to rapamycin treatment in our strain background and under our laboratory conditions.

Heterozygous diploids were purchased from the Yeast Deletion Collection (in which every non-essential gene has been replaced with a KanMX4 cassette (Giaever et al. 2002)) and sporulated. The resulting tetrads were dissected to produce fresh haploids. A number of fresh haploids were created for each null mutant to reduce the potential for second site mutations within the strains and therefore ensure that the phenotype observed is a result of loss of the particular gene of interest only. Dissected tetrads resulted in viable robust colonies for all spores with a 2:2 segregation of G418 sensitive and resistant colonies (data not shown); G418 resistance identified cells that were null mutants for the gene of interest.

At least two tetrads were dissected per *ego-* mutant and of these at least three independent mutant haploids were tested for their ability to recover from rapamycin treatment. Exponentially growing cultures were treated (or not) with rapamycin (200 ng/mL) for two hours after which cells were washed three times in fresh media and spotted onto a YPD plate. We found that all mutant

segregants behaved identically and representatives of each *ego*- mutant can be seen in Figure 3.1.

We found that wild-type cells were able to recover from a two-hour rapamycin treatment (Figure 3.1). However, cells lacking any one of the four subunits of the EGO complex (Ego1p, Ego3p, Gtr1p or Gtr2p) failed to resume proliferation within two days following removal of the drug (Figure 3.1). The recovery defect is profound. We have confirmed that mutant cells in our background strain lacking the gene of any one member of the EGO complex fail to recover from rapamycin treatment under our laboratory conditions.

### 3.2.2 Methylene blue staining

Loss of viability of *ego*- mutants when treated with rapamycin could explain why we fail to observe recovery of *ego*- cells following removal of the drug from the media. We employed the metabolic viability stain methylene blue to test whether cells remain alive both in the constant presence of rapamycin or following rapamycin washout. Methylene blue is able to cross the plasma membrane of both live and dead cells. In live yeast cells, methylene blue can be reduced resulting in loss of the blue colour whilst dead cells are unable to metabolise the dye and stain blue (Painting & Kirsop 1990).

Due to the similarity in phenotype observed for all four *ego*- knockout strains we tested *ego1Δ* and *gtr2Δ* cells as representatives of *ego*- mutants and examined the viability of cells treated with rapamycin. Exponentially growing cultures in YPD were treated with rapamycin (200 ng/mL) for 24 hours; at various time points samples were taken, exposed to methylene blue and cell staining observed by microscopy. Cultures were also treated with rapamycin for two hours after which cells were washed three times with fresh media and inoculated into YPD for 24 hours after which cells were stained with methylene blue.

As can be seen in Table 3.1 wild-type cells did not stain with methylene blue up to and at 24 hours after the introduction of rapamycin and at 24 hours after washout of rapamycin following a two-hour treatment.

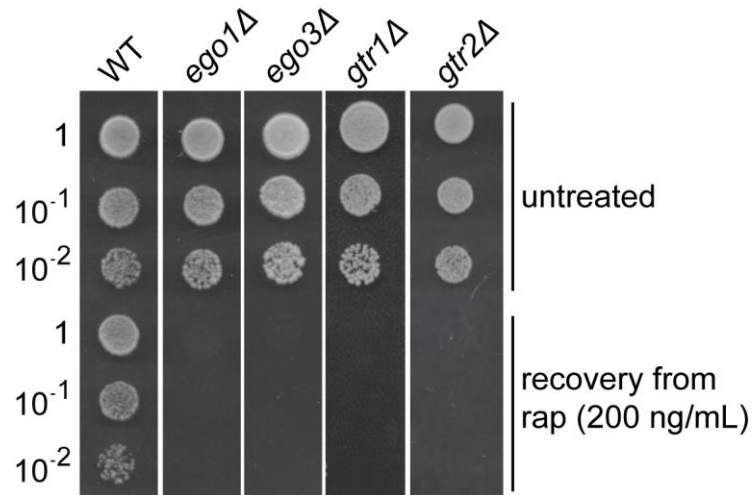


**Figure 3.1 Loss of any subunit of the EGO complex results in a rapamycin recovery defect phenotype**

Exponentially growing cultures of wild-type, *ego1Δ*, *ego3Δ*, *gtr1Δ* and *gtr2Δ* cells were treated (or not) at an OD<sub>600nm</sub> of ~0.1 for two hours with rapamycin (200 ng/mL) in YPD at room temperature with agitation. Cells were collected and washed three times in fresh YPD after which ten-fold serial dilutions were created and spotted (5 μL) onto a YPD plate which was incubated at 28°C for two days prior to scanning.

We also found that neither *ego1Δ* nor *gtr2Δ* cells stained blue up to 24 hours in the constant presence of rapamycin, nor at 24 hours after the removal of the drug following a two-hour rapamycin treatment. We did not observe the presence of any significant number of ‘ghost’ cells for any treatment or at any time point measured. Ghost cells appear flat and white as a result of loss of integrity, usually a result of lysis, which prevents retention of methylene blue within the cell.

To ensure that dead cells indeed stain positive with methylene blue, control samples of heat killed cells were stained with methylene blue. Samples of wild-type, *ego1Δ* and *gtr2Δ* cultures that had been treated with rapamycin for four hours (to ensure the viability stain was effective in the presence of the drug) were heated to 85°C for 10 minutes before being exposed to methylene blue.

As seen in Table 3.1 we found that over 99% of heat treated wild-type, *ego1Δ* and *gtr2Δ* cells showed strong staining with methylene blue. We conclude that methylene blue is effective in our wild-type, *ego1Δ* and *gtr2Δ* cells and that the presence of rapamycin does not interfere with the staining of dead cells.

We conclude that the rapamycin recovery defect seen in *ego*- mutants is unlikely to result from cell death, at least as measured by methylene blue staining.

### 3.2.3 Uptake of amino acids

It would appear that cell death in the presence of rapamycin is unlikely to explain the recovery defect seen in *ego*- mutants. Testing the ability of *ego*-mutant cells to actively import amino acids will provide a second independent test of viability.

If loss of the EGO complex results in cell death following rapamycin treatment we would expect to see little or no uptake of amino acids into *ego*- cells following treatment with the drug. Measuring the ability of *ego*- cells to import amino acids would also begin to test the permease switch model, which predicts that *ego*- mutants are unable to import amino acids following rapamycin treatment.

|   |     | Strain |              |              |
|---|-----|--------|--------------|--------------|
|   |     | WT     | <i>ego1Δ</i> | <i>gtr2Δ</i> |
| Time after<br>introduction<br>of rapamycin<br>(hrs) | 0   | <1     | <1           | <1           |
|   | 2   | <1     | <1           | <1           |
|   | 4   | <1     | <1           | <1           |
|   | 6   | <1     | <1           | <1           |
|   | 24  | <1     | <1           | <1           |
| Time following<br>2 hr rapamycin<br>treatment (hrs) | 0   | <1     | <1           | <1           |
|   | 3   | <1     | <1           | <1           |
|   | 6   | <1     | <1           | <1           |
|   | 24  | <1     | <1           | <1           |
| Heat Treated  | >99 | >99    | >99          |              |

**Percentage cells stained  
with methylene blue**

**Table 3.1 Methylene blue staining of cells treated with rapamycin**

Exponentially growing wild-type, *ego1Δ* and *gtr2Δ* cultures were treated (or not) with rapamycin (200 ng/mL) in YPD and incubated at room temperature with agitation. Treated cultures were either maintained in the presence of the drug or following two hours after the introduction of rapamycin cells were washed three times in fresh media after which they were incubated at room temperature with agitation to recover. All cultures were maintained in an exponential growth phase for the duration of the experiment. Samples of wild-type, *ego1Δ* and *gtr2Δ* cells that had been exposed to rapamycin for four hours were killed by heating to 85°C for 10 min. Cells were exposed to methylene blue and staining observed by microscopy. A minimum of 200 cells were counted for each of 3 replicates.

If *ego-* mutants fail to express active general amino acid permeases at the cell surface following rapamycin treatment, we would also expect to see no uptake of amino acids into rapamycin treated *ego-* cells. If neither the loss of viability nor permease switch model applies to *ego-* mutants, then we would expect to see no difference in amino acid uptake between rapamycin treated wild-type and *ego-* mutant cells.

We measured the uptake of a mix of  $^{35}\text{S}$ -labelled methionine and  $^{35}\text{S}$ -labelled cysteine into exponentially growing cells in YPD that were either untreated or continuously treated with rapamycin (200 ng/mL) for two, six or 24 hours at room temperature with agitation. Cultures were maintained in the exponential growth phase for the duration of the experiment by dilution into the appropriate medium.

As seen in Figure 3.2 there was no difference in the uptake of amino acids between untreated wild-type and untreated *ego1Δ* mutant cells. However, a subtle but significant ( $p=0.02$ ) defect in the ability of untreated *gtr2Δ* cells to import amino acids was observed relative to untreated wild-type cells (Figure 3.2).

It would appear that loss of Ego1p does not affect amino acid import under our standard laboratory conditions (Figure 3.2). On the other hand, the lower uptake of amino acids by untreated *gtr2Δ* cells compared to that of wild-type cells suggests that amino acid permeases are not expressed correctly or are not fully active under normal conditions in a *gtr2Δ* mutant (Figure 3.2). This could be because Gtr2p is specifically required for trafficking, or activity, of amino acid permeases to the cell surface under normal conditions. Alternatively it is possible that Gtr2p is required for all cellular trafficking, which includes amino acid permeases to the plasma membrane.

Treatment of all cultures with rapamycin resulted in a decrease in the import of radiolabelled amino acids compared to that of untreated cultures (Figure 3.2). We found that the uptake of radiolabelled amino acids into *ego1Δ* cells at both two and six hours following rapamycin treatment was not significantly different to radiolabelled amino acid uptake into the equivalently treated wild-type cells ( $p=0.63$  and  $0.20$  respectively) (Figure 3.2).

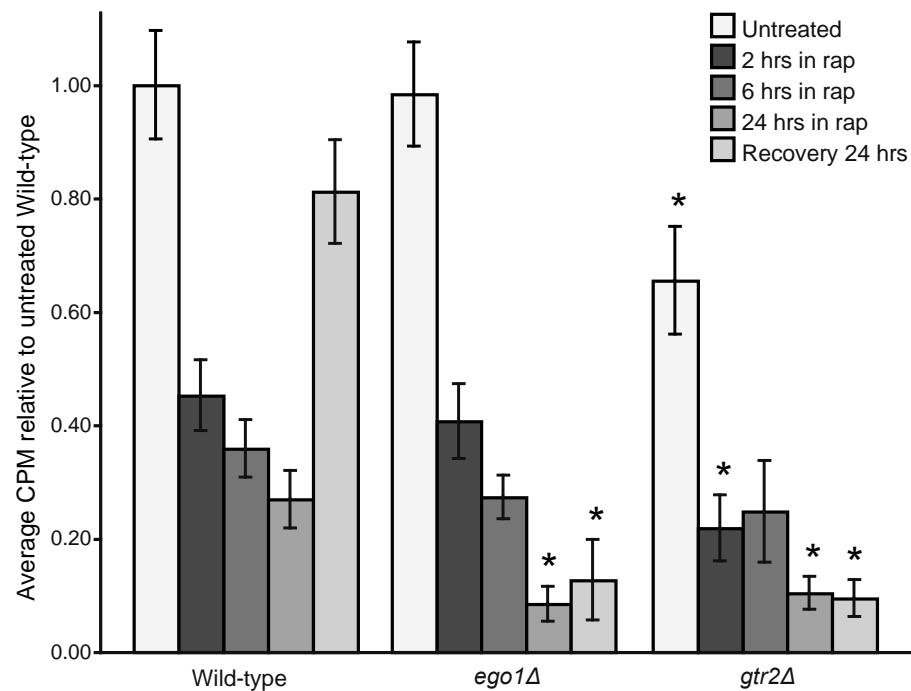


### Figure 3.2 Uptake of amino acids following rapamycin treatment

The  $OD_{600nm}$  of exponentially growing wild-type, *ego1Δ* and *gtr2Δ* cultures was normalised to an  $OD_{600nm}$  of ~0.1 in YPD, cultures were treated (or not) with rapamycin (200 ng/mL) and incubated at room temperature with agitation. All cultures were maintained in an exponential growth phase for the duration of the experiment by dilution into appropriate medium. At two, six and 24 hours after the introduction of rapamycin or 24 hours following rapamycin washout (washout occurred two hours after the introduction of the drug) cell pellets, normalised to an  $OD_{600nm}$  of ~0.25, were resuspended in YPD containing a mix of  $^{35}S$ -labelled methionine and  $^{35}S$ -labelled cysteine (0.4 MBq) and incubated for five minutes at room temperature. Cells were washed six times with ice-cold methionine (75 mM) and cysteine (75 mM); retained radiation was measured using a scintillation counter and expressed as counts per minute (CPM) relative to that for the average untreated wild-type cells (39,398 CPM). Control readings of media with radiation ranged from 1,042 to 4,748 CPM. N=6 independent cultures; error bars denote S.E.M.; \*  $p < 0.05$  relative to equivalently treated wild-type cells.

The uptake of radiolabelled amino acids into *gtr2Δ* cells was significantly lower following a two hour rapamycin treatment compared to that of wild-type cells after two hours in rapamycin ( $p=0.16$ ) (Figure 3.2). After six hours in the presence of rapamycin the uptake of radiolabelled amino acids into *gtr2Δ* cells was not significantly different to radiolabelled amino acid uptake into equivalently treated wild-type cells ( $p=0.32$ ) (Figure 3.2).

It is possible that *gtr2Δ* cells may respond normally to rapamycin treatment but have a general defect in amino acid uptake under all conditions. We asked whether the fold decrease in amino acid import differed between wild-type and *gtr2Δ* cells up to six hours in the presence of rapamycin. We normalised the uptake of radiolabelled amino acids into two and six hour rapamycin treated *gtr2Δ* cells to that of untreated *gtr2Δ* cells. We found that the fold decrease in radiolabelled amino acid uptake into *gtr2Δ* cells in the presence of rapamycin was not significantly different to that of wild-type cells for either a two hour or six hour treatment ( $p=0.3$  and  $0.9$  respectively) (Figure 3.3).

We have observed that the trend in amino acid uptake by *ego1Δ* and *gtr2Δ* mutants occurred as wild-type cells up to and at six hours following the introduction of rapamycin. The ability of *ego1Δ* and *gtr2Δ* mutants to import amino acids in the presence of rapamycin suggests that *ego-* cells are indeed viable in the presence of the drug. The ability of *ego-* cells to import amino acids following rapamycin treatment and the lack of methylene blue staining in the presence of the drug leads us to conclude that loss of cell viability is unlikely to explain the inability of *ego-* mutants to recover from rapamycin treatment.

We have observed a difference in the ability of *ego1Δ* and *gtr2Δ* to import amino acids, both into untreated cells and cells that have been exposed to rapamycin for two hours. The significant decrease in uptake of amino acids by two hour rapamycin treated *gtr2Δ* cells, compared to equivalently treated wild-type cells, suggests that we cannot rule out the possibility that the general amino acid permeases are being incorrectly expressed in rapamycin-treated *gtr2Δ* cells and that this could explain the inability of at least a subset of *ego-* mutants to recover from rapamycin treatment.

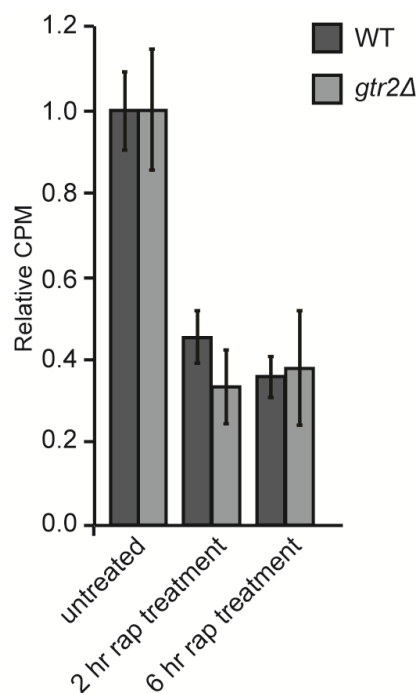


**Figure 3.3 Uptake of amino acids into wild-type and *gtr2Δ* cells relative to their own uptake of untreated cells**

The wild-type and *gtr2Δ* mutant amino acid uptake results from Figure 3.2 with the counts per minute (CPM) of rapamycin treated cells expressed relative to their own untreated CPM (36,753 CPM for WT and 25,630 CPM for *gtr2Δ*). N=6 independent cultures; error bars denote S.E.M.

However, the inability of *ego*- mutants to recover from rapamycin treatment is shared between all four *ego*- null mutants (Figure 3.1). We also measured the uptake of amino acids into *ego1Δ* cells and find that there is no significant difference in the uptake of amino acids into rapamycin-treated *ego1Δ* cells compared to equivalently treated wild-type cells (Figure 3.2). We can therefore conclude that whilst there appears to be a difference in the requirement of different subunits of the EGO complex for permease trafficking, the ability of rapamycin treated *ego1Δ* cells to import amino acids in a manner similar to rapamycin treated wild-type cells suggests that the permease switch model is unlikely to explain the shared *ego*- mutant phenotype with regards to rapamycin recovery.

Amino acid uptake was also measured in recovering cells; exponentially growing wild-type, *ego1Δ* and *gtr2Δ* cultures were treated with rapamycin (200 ng/mL) for two hours at room temperature with agitation after which cells were washed three times in fresh media and incubated at room temperature with agitation to recover. Radiolabelled amino acid uptake was measured 24 hours after the transferral of rapamycin-treated cells into fresh media. All cultures were maintained in an exponential growth phase for the duration of the experiment by dilution into fresh media.

Consistent with wild-type cells being able to recover from rapamycin treatment, we found that the uptake of the radiolabelled amino acids into recovering wild-type cells was not significantly different to that of untreated wild-type cells 24 hours after the removal of rapamycin ( $p=0.16$ ) (Figure 3.2).

Following washout of rapamycin (“recovery”), uptake of radiolabelled amino acids into cells lacking either Ego1p or Gtr2p did not resemble that of untreated cells (Figure 3.2); again, these results are consistent with the inability of *ego*- mutants to recover following rapamycin treatment (as seen in Figure 3.1). Not only did the uptake of radiolabelled amino acids into *ego1Δ* and *gtr2Δ* cells after a “recovery period” not resemble that of untreated cells, we also found that the uptake of radiolabelled amino acids into cells following a “recovery period” was lower than the radiolabelled amino-acid uptake measured following a six hour rapamycin treatment (Figure 3.2). It would appear that, with regards to amino acid uptake, *ego1Δ* and *gtr2Δ* cells recovering from rapamycin behave

differently to those that are in the constant presence of rapamycin for up to six hours.

We have observed that the uptake of radiolabelled amino acids into *ego1Δ* and *gtr2Δ* cells after a “recovery period” is lower than that of cells in the constant presence of rapamycin (for up to six hours) (Figure 3.2). The uptake of amino acids into wild-type, *ego1Δ* and *gtr2Δ* cells that had been maintained in the continuous presence of rapamycin for 24 hours was also measured to compare the uptake of recovering cells and those exposed to rapamycin for a long time. We found that all cultures were able to import the radiolabelled amino acid mix following 24 hours in the presence of rapamycin, however *ego1Δ* and *gtr2Δ* mutants imported significantly less compared to wild-type cells ( $p=0.006$  or  $p=0.01$  respectively) (Figure 3.2). These results could be a result of loss of viability in the continuous presence of rapamycin for an extended period of time; however, the methylene blue viability stain data would suggest that this is not the case (Table 3.1). Alternatively, in the continued presence of rapamycin *ego1Δ* and *gtr2Δ* mutants could be overreacting or responding aberrantly to the effects of the drug.

In conclusion, we have found that loss of the EGO complex does not appear to impinge on the ability of *ego-* cells to import amino acids following rapamycin treatment. It is doubtful that lack of amino acid permeases at the cell surface following rapamycin treatment explains the inability of all *ego-* mutants to recover from rapamycin treatment. However, we have made two unexpected observations. Firstly we show that there appears to be a difference between Ego1p and Gtr2p with regards to their role in permease trafficking. Second, it would appear that *ego-* mutants overreact, compared to wild-type cells, to the continued presence of rapamycin for 24 hours. It is noteworthy that the overreaction to the continued presence of the drug is also shared with *ego-* cells recovering for 24 hours from a two hour treatment with rapamycin. It is possible that the altered states (as observed by amino acid uptake) of *ego-* cells in the continued presence of rapamycin for 24 hours and of *ego-* cells recovering from rapamycin treatment for 24 hours could hint at why *ego-* mutants fail to recover from rapamycin treatment.

### 3.2.4 Testing *gap1Δ* null mutants for recovery from rapamycin

TORC1 activity is controlled by nutrient sensing; therefore it is possible that there is a threshold of intracellular nutrient availability below which TORC1 remains inactive. If there is a modest decrease in the availability of amino acids detected in *ego-* mutants and the sensed availability lies just under this threshold it could result in *ego-* mutants with constitutively inactive TORC1 following rapamycin treatment. This situation may apply to *gtr2Δ* mutants in particular.

If a modest decrease in sensed amino acids explains the inability of *ego-* mutant cells to recover from rapamycin treatment we would expect that a severe reduction in amino acid uptake would be sufficient to result in an inability of cells to recover from rapamycin. As described earlier, Gap1p is the predominant general amino acid permease presented at the cell surface following TORC1 inactivation (Beck et al. 1999). We would therefore predict that loss of Gap1p would result in a dramatic reduction in the uptake, and therefore intracellular availability, of amino acids following rapamycin treatment. If amino acid availability needs to be above a certain threshold, at which the *ego-* mutants are on the edge, we would predict that a *gap1Δ* null mutant should fail to recover from rapamycin treatment.

We tested the ability of a *gap1Δ* null mutant, in the same strain background as our wild-type and the *ego-* mutants, to recover from rapamycin treatment. Wild-type, *ego1Δ* and *gap1Δ* cells were treated with rapamycin for two hours after which cells were washed three times in fresh YPD and spotted to a plain YPD plate to recover. As seen in Figure 3.4 wild-type cells were able to recover from rapamycin treatment as seen previously (Figure 3.1). As expected, loss of Ego1p resulted in cells that were unable to recover from rapamycin treatment (Figure 3.4). We found that *gap1Δ* cells were able to recover from rapamycin treatment in a manner indistinguishable from that of wild-type cells (Figure 3.4). These results suggest that the presence of Gap1p in the plasma membrane is not required for yeast to recover from rapamycin treatment. The results also imply that a threshold of amino acid uptake does not explain why *ego-* mutants fail to recover from rapamycin.

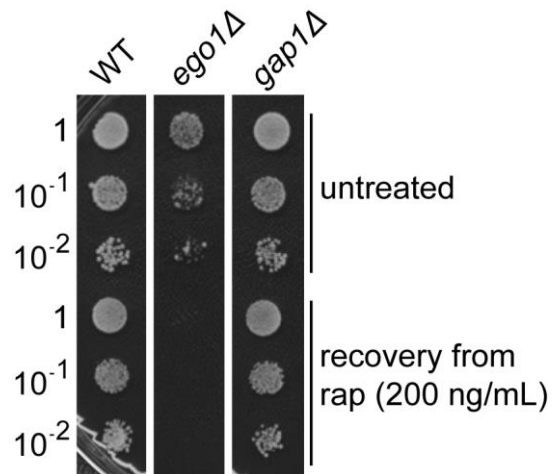


**Figure 3.4** Loss of Gap1p does not result in a rapamycin recovery defect  
Exponentially growing wild-type, *ego1Δ* and *gap1Δ* cultures at an OD of ~0.1 were treated (or not) with rapamycin (200 ng/mL) in YPD at room temperature with agitation for two hours. Cells were washed three times in fresh media; ten-fold serial dilutions were created and spotted (5  $\mu$ L) onto a YPD plate which was incubated at 30°C for two days.

### 3.2.5 Testing recovery of *ego*- mutants from various TORC1 inactivating treatments

If the TORC1 reactivation model explains the inability of *ego*- mutants to recover from rapamycin, we would predict that *ego*- mutants should fail to recover from *any* treatment that results in inactivation of TORC1; for example using nutrient starvation or caffeine treatment (Beck et al. 1999; Reinke et al. 2006; Wanke et al. 2008). We wished to test the ability of *ego1Δ* and *gtr2Δ* to recover from a concentration of caffeine that is inhibitory for *ego*- mutants as well as from a period of carbon or nitrogen starvation.

To determine what concentration caffeine is inhibitory to *ego*- mutant cells we first tested the ability of an *ego1Δ* mutant to form colonies in the presence of various concentrations of caffeine. Exponentially growing wild-type and *ego1Δ* cultures were normalised to an OD<sub>600nm</sub> of ~0.1 in YPD from which ten-fold serial dilutions were created and spotted to YPD plates containing various concentrations of caffeine (0-9 mM). Plates were incubated at 30°C for two days. As seen in Figure 3.5 wild-type cells were able proliferate in the presence of all concentrations of caffeine tested. We found that *ego1Δ* mutants were able to proliferate as effectively as wild-type on plain YPD plates and were able to proliferate in the presence of 3 mM caffeine, albeit *ego1Δ* cells appeared more sensitive to the effects of 3 mM caffeine than wild-type cells (Figure 3.5). A small amount of growth was observed for the most concentrated *ego1Δ* culture in the presence of 6 mM caffeine and no growth was observed for *ego1Δ* cells in the presence of 9 mM caffeine (Figure 3.5). We conclude that 9 mM caffeine is sufficient to fully inhibit proliferation, and thus to fully inactivate TORC1 in *ego*-mutants.

To test whether *ego*- mutants were able to recover from caffeine treatment, exponentially growing wild-type, *ego1Δ* and *gtr2Δ* cultures were treated with rapamycin (200 ng/mL) or caffeine (9 mM) for two hours after which cells were washed three times in YPD and spotted to a YPD plate which was incubated at 30°C to recover. As seen previously (Figure 3.1) we found that wild-type cells were able to recover from rapamycin treatment whereas *ego1Δ* and *gtr2Δ* mutants were unable to do so (Figure 3.6).

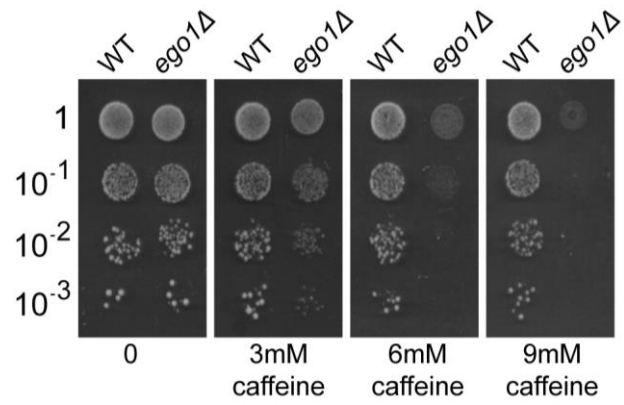


**Figure 3.5 Testing sensitivity of yeast to caffeine**

Exponentially growing wild-type and *ego1Δ* cultures were normalised to an  $OD_{600nm}$  of  $\sim 0.1$  in YPD. Ten-fold serial dilutions were created in YPD and spotted (5  $\mu$ L) onto either a plain YPD plate or plates containing caffeine (3, 6 or 9 mM) which were incubated at 30 °C for two days.

However, we found that wild-type, *ego1Δ* and *gtr2Δ* mutants were all able to recover from a two hour treatment with caffeine (Figure 3.6).

We also tested the ability of *ego-* mutants to recover from physiological conditions known to inhibit TORC1 activity. Exponentially growing cultures of wild-type, *ego1Δ* and *gtr2Δ* cells in YPD were washed three times in either SD-AA (for nitrogen starvation) or YP (for carbon starvation) media and subsequently inoculated into their respective drop-out media and incubated at room temperature with agitation for two hours. After the two hour incubation, ten-fold serial dilutions were created in YPD and spotted on to a YPD plate to recover at 30°C for two days. As seen in Figure 3.6 we found that *ego1Δ* and *gtr2Δ* cells were able to recover, as wild-type, from a period of either carbon or nitrogen starvation.

The ability of *ego-* mutants to resume proliferation following alternative TORC1 inhibiting treatments suggests that a general loss of the EGO complex does not compromise TORC1 reactivation under the conditions tested above. These results suggest that the TORC1 reactivation model is unlikely to explain the rapamycin recovery defect of *ego-* mutants. It is possible that the EGO complex is selectively required for recovery of rapamycin via some other drug selective mechanism, for example detoxification of rapamycin itself or removal of the rapamycin-Fpr1p complex from TORC1.

### **3.2.6 Do known multidrug detoxification pathways have a role in recovery from rapamycin?**

Could the EGO complex be required for rapamycin detoxification? If rapamycin is cleared from yeast by known drug detoxification mechanisms, which may depend on the EGO complex, we would predict that loss of the mechanism involved in rapamycin detoxification, for example cytochrome P450s or the pleiotropic drug resistance (PDR) pathway, would phenocopy the loss of *ego-* mutants.

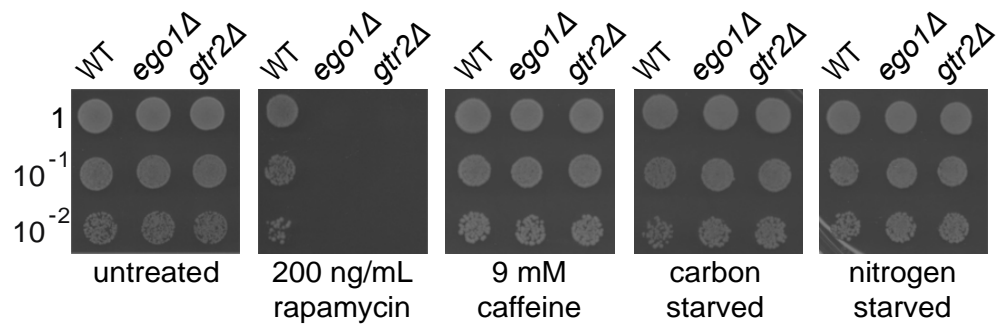


**Figure 3.6 Recovery of *ego-* from TORC1 inactivating treatments**

Exponentially growing wild-type, *ego1Δ* and *gtr2Δ* cultures at an  $OD_{600nm}$  of  $\sim 0.1$  were untreated, treated with rapamycin (200 ng/mL) or caffeine (9 mM) in YPD and incubated at room temperature for two hours with agitation. Cells were washed three times into fresh YPD and ten-fold serial dilutions were spotted (5  $\mu$ L) onto a plain YPD plate. Alternatively, cultures at an  $OD_{600nm}$  of  $\sim 0.1$  were pelleted and cells resuspended in media lacking either carbon or nitrogen. This was repeated twice more before cells were inoculated into the relevant drop-out media and incubated at room temperature for two hours with agitation. Ten-fold serial dilutions were created in YPD and spotted (5  $\mu$ L) onto a plain YPD plate. Plates were incubated at 30°C for 2 days.

Little is known about how rapamycin is detoxified in cells. Some evidence from mammalian systems suggests that rapamycin can be detoxified in liver by the cytochrome P450 CYP3A4 (Anzenbacher & Anzenbacherova 2001; Guengerich 1999; Li et al. 1995). Yeast contain two cytochrome P450's: Erg5p (which is non-essential) and Erg11p (which is essential). *DAP1* encodes an accessory protein that is required for the function of Erg11p (Mallory et al. 2005). We tested whether loss of *ERG5* or *DAP1*, which should also compromise Erg11p function, affects recovery from rapamycin.

A number of large-scale genome-wide genetic screens have been carried out using rapamycin. Studies carried out by Butcher et al. (2006) found that overexpression of three pleiotropic resistance genes (*PDR16*, *PDR17*, and *PDR3*) resulted in a potential reduction in sensitivity to rapamycin. Hillenmeyer et al. (2008) also performed a large-scale screen and found that loss of 252 genes, out of 510 genes they classed as being involved in multidrug resistance, resulted in hypersensitivity to rapamycin. Whilst Hillenmeyer et al. (2008) did not specify which null 'multidrug resistance' mutants resulted in rapamycin sensitivity, they alluded that *PDR1* and *PDR5* were included in their 'multidrug resistance' set. It is possible therefore that pleiotropic drug resistance (PDR) pathways have a role in rapamycin detoxification. Therefore, we also tested the ability of *pdr1Δ*, *pdr3Δ* and *pdr5Δ* mutants to recover from rapamycin treatment. Pdr1p and Pdr3p are transcription factors that regulate the ABC transporter proteins, an example of which is Pdr5p (Moye-Rowley 2003).

Exponentially growing cultures of wild-type, *ego1Δ*, *erg5Δ*, *dap1Δ*, *pdr1Δ*, *pdr3Δ* and *pdr5Δ* cells in the BY4743 strain background were treated with rapamycin (200 ng/mL) in YPD for two hours at 28°C with agitation. Cells were washed three times in fresh YPD and ten-fold serial dilutions were spotted onto a YPD plate which was incubated at 28° for two days.

We found that wild-type cells were able to recover from a two-hour rapamycin treatment whereas *ego1Δ* mutants failed to recover (Figure 3.7). It would appear that loss of either Erg5p or Dap1p does not compromise recovery from rapamycin and cells behaved as wild-type (Figure 3.7). Furthermore, loss of any one of Pdr1p, Pdr3p or Pdr5p did not compromise recovery from rapamycin treatment; the PDR null mutants tested all behaved as wild-type (Figure 3.7).

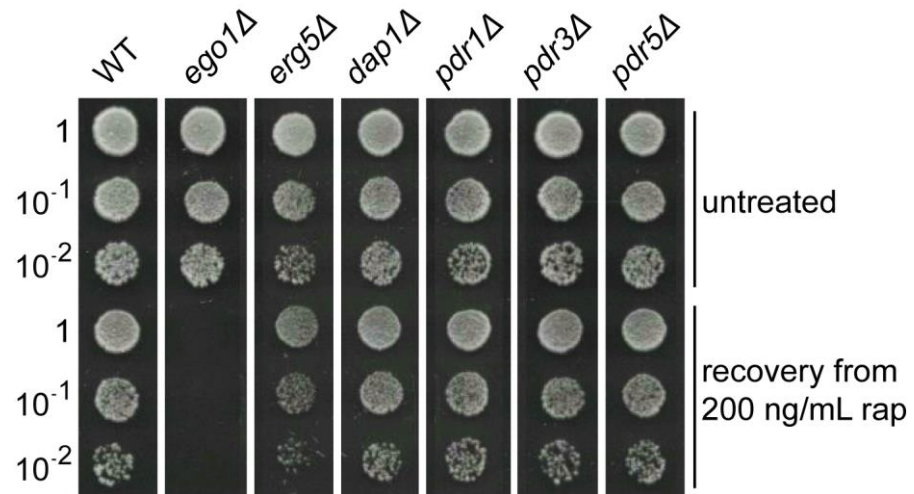


**Figure 3.7 Recovery from rapamycin of null mutants involved in multidrug resistance**

Exponentially growing cultures of wild-type, *ego1Δ*, *pdr1Δ*, *pdr3Δ*, *pdr5Δ*, *erg5Δ* and *dap1Δ* cells at an  $OD_{600nm}$  of  $\sim 0.1$  were treated (or not) with rapamycin (200 ng/mL) in YPD at 28°C for two hours with agitation. Cells were washed three times with fresh media after which ten-fold serial dilutions were created and spotted (5  $\mu$ L) onto a YPD plate which was incubated at 28°C for 2 days.

The lack of a rapamycin recovery defect phenotype for any mutant involved in known drug detoxification pathways tested suggests it is unlikely that classical multidrug resistance pathways have a role in detoxification of rapamycin in yeast. It is worth noting that only a small subset of proteins involved in multidrug resistance have been tested here. If the EGO complex is required for detoxification of rapamycin it may do so via proteins not tested here, require the involvement of more than one detoxification method, do so via a novel detoxification method or some combination thereof. We cannot therefore exclude the rapamycin detoxification model to explain why *ego*- mutants fail to recover from rapamycin treatment, but it would appear that rapamycin detoxification is unlikely to involve the cytochrome P450's or the pleiotropic drug resistance mechanisms alone.

### 3.3 Conclusion

The work carried out in this chapter was undertaken to test the four models we proposed that could explain the rapamycin recovery defect observed in mutants lacking the EGO complex.

#### Loss of Viability Model

Initially we proposed that loss of viability of *ego*- mutants in response to rapamycin could explain the inability of *ego*- cells to recover from rapamycin treatment. It would appear that this model is incorrect. The use of the methylene blue viability stain showed that *ego*- cells did not stain up to and at 24 hours after the introduction of rapamycin nor at 24 hours after washout of the drug. We also found that amino acid uptake by *ego*- mutants was no different to that of wild-type cells six hours after the introduction of rapamycin. Due to the profound nature of the recovery defect, if cells died in the presence of rapamycin we would have expected to see some evidence of this in either the methylene blue staining or amino acid uptake.

We therefore conclude that loss of the EGO complex does not result in cell death following exposure to rapamycin.

#### Permease Switch Model

Our second model speculated that the amino acid permease switch from specific

permeases to general permeases upon TORC1 inactivation is not completed in *ego-* mutants, resulting in cells in a permanent state of starvation and thus G0 arrest. We find that *ego1Δ* cells are able to import amino acids in a manner similar to that of wild-type cells up to and at six hours after the introduction of rapamycin. Whilst we find that the overall import of amino acids is lower into two-hour rapamycin-treated *gtr2Δ* mutants, compared to wild-type, the fold decrease in uptake is not statistically significant between the two strains. It is likely that the low uptake of amino acids into *gtr2Δ* cells following a two hour rapamycin treatment is a result of a general defect in uptake of amino acids into *gtr2Δ* cells. The trend in amino acid uptake into *ego-* mutants does not appear to be different to that for wild-type cells up to six hours after the addition of rapamycin. This would suggest that amino acid permeases are present at the cell surface of *ego-* cells treated with rapamycin and it is unlikely that *ego-* mutants are starving in the presence of the drug.

It is worth noting that, whilst it would appear that amino acids are imported into rapamycin treated *ego-* cells, we did not confirm that the permease switch took place in these cells. It would be worth confirming in rapamycin-treated *ego-* mutants that the specific amino acid permeases were degraded and that general amino acid permeases were expressed at the cell surface. Two complimentary assays could be carried to confirm the switch had in fact occurred. Firstly, the abundance of the specific amino acid permease Tat2p could be monitored over time, following the addition of rapamycin, by western blot analysis (Beck et al. 1999). This would test if all Tat2p permease protein had been degraded and therefore none should be present at the cell surface. To test if Gap1p, a general amino acid permease, is transported to the cell surface following rapamycin treatment, the localisation of GFP tagged Gap1p could be monitored by fluorescent microscopy. Furthermore, AZC is a toxic proline analogue that is imported by the Gap1p permease (Andréasson et al. 2004). Sensitivity to AZC of cells that had been treated with rapamycin could be tested; if rapamycin treated cells failed to grow in the presence of AZC it would indicate that Gap1p is indeed present and active at the cell surface.

It is possible that six hours in rapamycin is not long enough for the permease switch to have occurred. Evidence from Beck et al. (1999) would suggest that this is not the case. Beck et al. (1999) found that the specific amino acid

permease Tat2p was almost completely degraded following a one hour rapamycin treatment. We would therefore expect the amino acid permease turnover to have occurred by our two hour time measurement and certainly by six hours.

To ensure the levels of amino acids being sensed in *ego*- mutants were not near a limiting threshold required for TORC1 activity we tested the ability of a *gap1Δ* null mutant to recover from rapamycin treatment. If the intracellular concentration of amino acids detected is crucial for recovery of yeast from rapamycin treatment we would have expected a *gap1Δ* null mutant (in which amino acid import should be severely compromised upon rapamycin treatment) to have a recovery defect as seen in *ego*- mutants. We did not find this to be the case. Loss of Gap1p did not affect the ability of cells to recover from rapamycin treatment. The wild-type phenotype of *gap1Δ* mutants suggests that merely lowering the intracellular amino acid concentration does not impact the ability of yeast cells to recover from rapamycin treatment.

By measuring the uptake of amino acids following rapamycin treatment, we would conclude that the permease switch model does not explain the rapamycin recovery defect of *ego*- mutants.

### **TORC1 Reactivation Model**

If the EGO complex is required for TORC1 reactivation following any condition which inactivated the complex, we would expect to see the same recovery defect in *ego*- mutants following any TORC1 inactivating treatment. We find that *ego*- mutants are in fact able to recover from all chemical and conditional TORC1 inactivating treatments tested, with the exception of rapamycin. These results suggest that loss of the EGO complex does not result in a complete inability to reactivate TORC1 and that the recovery defect observed in *ego*- mutants is a rapamycin-selective phenotype.

An alternative physiological method of inactivating TORC1 is to grow cultures to saturation, resulting in nutrient limitation. A genome-wide study by Powers et al. (2006) investigated the chronological life span of ~4800 null mutants by growing cells to saturation in complete synthetic media and at various time points transferring aliquots to fresh media and observing the ability of cells to

resume proliferation as measured by OD<sub>600nm</sub>. All four null mutants of the EGO complex were included in this screen and Powers et al. (2006) found that all four null mutants were able to resume proliferation as efficiently as wild-type cultures, even after five weeks in stationary phase (Table 3.2). These results support our conclusion that loss of the EGO complex does not result in an inability of *ego-* cells to reactivate TORC1 *per se* in order to resume proliferation.

### **Rapamycin Detoxification Model**

Yeast have a number of mechanisms for detoxifying xenobiotics, these include the pleiotropic drug resistance pathway and cytochrome P450s. We speculated that the EGO complex could be required to detoxify rapamycin. Loss of proteins from the PDR or cytochrome P450 drug resistance mechanisms did not compromise recovery from rapamycin treatment. However, both mechanisms involve a large number of proteins and it is likely that redundancy occurs within each system. Large-scale studies have hinted that overexpression or loss of multidrug resistance genes affects sensitivity of yeast to rapamycin; however, to our knowledge, no specific study to date has investigated the method by which rapamycin is detoxified in yeast. We therefore cannot rule out the possibility that the EGO complex is required for detoxification of rapamycin; however, if it does, it is likely to be via a mechanism not tested here.

### **Summary**

Four models were presented that could explain the inability of *ego-* mutants to resume proliferation following treatment with rapamycin. We find that the *ego-* rapamycin recovery defect phenotype cannot be explained by loss of viability, loss of general amino acid permeases at the cell surface nor an inability of *ego-* mutants to reactivate TORC1 from an inactive state.

We have, however, discovered that the inability of *ego-* cells to recover from rapamycin treatment is a rapamycin-selective phenotype. The rapamycin recovery defect phenotype of *ego-* mutants could therefore be a result of inadequate rapamycin detoxification by an unknown mechanism in *ego-* cells.

| Gene        | 1 week | 2 weeks | 5 weeks |
|-------------|--------|---------|---------|
| <i>EGO1</i> | 1.082  | 1.231   | 0.980   |
| <i>EGO3</i> | 0.901  | 2.996   | 3.745   |
| <i>GTR1</i> | 1.145  | 2.472   | 0.974   |
| <i>GTR2</i> | 1.099  | 1.073   | 1.292   |

**Table 3.2 Chronological lifespan of *ego*- mutants from Powers et al. (2006)**

Data taken from Powers et al. (2006) in which cultures were grown to saturation phase in complete synthetic liquid media. An aliquot of cells was transferred into fresh media at 1, 2 and 5 weeks after saturation and the ability to resume proliferation was assessed by spectrometry measuring OD<sub>600nm</sub>. Viability was determined relative to the mean viability for the deletion collection at each time point.

Alternatively, it is possible that the EGO complex is selectively required for the uncoupling of the rapamycin-Fpr1p intermediate complex from the TOR1 complex. Loss of the EGO complex would therefore result in rapamycin irreversibly bound to TORC1.

Whilst the majority of published studies on the EGO complex have been carried out using rapamycin treatments for up to six hours (Binda et al. 2009; Dubouloz et al. 2005) we have measured amino acid uptake following 24 hours in the constant presence of rapamycin into wild-type and *ego*- mutants. To our surprise, we found that the uptake of amino acids into 24 hour treated *ego*-mutants was significantly lower than that of wild-type cells treated for 24 hours with rapamycin. It was interesting to observe that *ego*- cells that had undergone a period of “recovery” (from a two hour treatment of rapamycin) also had a lower amino acid uptake that was not significantly different to the uptake of amino acids into cells that had been exposed to rapamycin for 24 hours. The similarity between the amino acid uptake of *ego*- mutants following a 24 hour rapamycin treatment and those that were in a “recovery period” for 24 hours could hold clues as to why null mutants of the EGO complex fail to recover from rapamycin treatment.

## 4 Rapamycin-insensitive TORC1 activity

### 4.1 Introduction

In the previous chapter, we showed that the rapamycin recovery defect observed in *ego-* mutants is a rapamycin selective phenotype. We tested four hypotheses that could explain the inability of *ego-* mutants to recover from rapamycin; two were discounted: the loss of viability model and the permease switch model. It is possible however that the EGO complex is selectively required for TORC1 reactivation following rapamycin treatment or for detoxification of rapamycin or both.

Inactivation of TORC1 results in a number of physiological changes within a yeast cell including: the down-regulation of translation, the induction of autophagy, the phosphorylation of Sch9p and the switch from specific to general amino acid permeases at the cell surface (De Virgilio & Loewith 2006b). Null *ego-* mutants appear to behave as wild-type cells following exposure to rapamycin for up to six hours; as assayed by the down regulation of translation, the induction of autophagy (Dubouloz et al. 2005) and the phosphorylation of Sch9p (Binda et al. 2009). So why do *ego-* mutants fail to recover from rapamycin treatment? We found that following a longer exposure to rapamycin (24 hours), the *ego-* mutants showed a lower rate of amino acid uptake compared to that of wild-type cells. This altered amino acid uptake rate following a longer exposure to the drug was also evident when the *ego-* mutants had been treated with rapamycin for a short time (two hours), washed into fresh media and incubated for 24 hours, *i.e.* while attempting to recover. This observation hints that *ego-* mutant cells may indeed respond differently to rapamycin compared to wild-type cells.

During the course of our studies we observed that wild-type cells were able to proliferate, albeit slowly, in the continuous presence of a high concentration of rapamycin (200 ng/mL) *i.e.* a concentration far exceeding the minimum inhibitory concentration of ~3-5 ng/mL that fully induces phenotypes associated with inactivated TORC1 (Neklesa & Davis 2008). It is generally thought that rapamycin is a complete inhibitor of proliferation in yeast. Barbet et al. (1996) and Heitman, et al. (1991) concluded that high concentrations of rapamycin

inhibit the proliferation of cells in the JK9-3d strain background. Upon closer inspection of the literature we found that some groups have in fact observed residual proliferation of cells in the presence of high concentrations of rapamycin (in the BY4743 background as is used here), but have not commented on it (for example Dubouloz et al. (2005) and Neklesa & Davis (2008)). Is it possible that rapamycin does not fully inhibit proliferation of yeast cells, at least in the BY4743 background?

Note; throughout the rest of this thesis, unless otherwise stated, the term ‘high concentration’ of rapamycin is indicative of a concentration at or above 20 ng/mL, *i.e.* at least four times the minimum inhibitory concentration of the drug in wild-type cells.

## 4.2 Results

### 4.2.1 Wild-type cells proliferate in the presence of a high concentration of rapamycin (200 ng/mL)

To begin to characterise the proliferation of wild-type cells in the presence of high concentrations of rapamycin we monitored the culture density in a population of wild-type cells over a period of 12 hours following the addition of rapamycin (200 ng/mL). We used a Coulter particle counter to measure cell number; a Coulter counter is able to detect the absolute number of cells in a given volume of sample regardless of changes in cell size or shape that can occur following rapamycin treatment (Loewith & Hall 2011).

Exponentially growing wild-type cultures in YPD were treated (or not) with rapamycin (200 ng/mL) at time 0 in YPD and incubated at room temperature with agitation. At two hour intervals, starting at time 0, the culture density was measured by Coulter counter for up to 12 hours after the addition of rapamycin. Cultures were maintained in an exponential growth phase for the duration of the experiment by dilution into the appropriate medium if necessary; the culture density was subsequently adjusted by the appropriate dilution factor. The results are expressed as semi-Log<sub>2</sub> plots of relative culture density with time after the addition of rapamycin. The steady-state growth rate is also shown and

was calculated as a reciprocal of the doubling time between two and 12 hours after the introduction of rapamycin.

As seen in Figure 4.1A untreated wild-type cultures maintained a logarithmic growth rate over the 12 hour time-course. Within the first two hours of rapamycin treatment we found that the growth rate of wild-type cultures slowed compared to the growth rate of untreated wild-type cultures (Figure 4.1A).

Following the two hour transition period, rapamycin treated wild-type cultures maintained a steady growth rate for the remaining 10 hours monitored, a growth rate that was slower than that of untreated wild-type cultures; we call this the 'rapamycin-insensitive growth rate' (Figure 4.1A). Due to the stable nature of the rapamycin-insensitive growth rate between two and 12 hours after the introduction of the drug we were able to calculate the growth rates of untreated and rapamycin treated wild-type cultures. As seen in Figure 4.1B we found that treatment of wild-type cultures with rapamycin resulted in a decrease in growth rate to ~34% that of untreated wild-type cultures. It would appear that under our laboratory conditions wild-type cells are able to maintain proliferation in the presence of 200 ng/mL rapamycin, albeit at a slower residual rate compared to that of untreated wild-type cells.

It is possible that the growth rate of wild-type cultures in the continued presence of rapamycin is due to a mixed population of cells - those that are completely inhibited by rapamycin and those that are resistant to the drug. The results seen in Figure 4.1A however would argue against this possibility. The growth rate of rapamycin treated wild-type cultures is constant between two and 12 hours after the introduction of rapamycin, and within each time point interval. If a mixed population of rapamycin sensitive and resistant cells were present we would expect the growth rate of the rapamycin treated culture to increase over time due to an increasing proportion of rapamycin resistant cells, with time, within the population. We do not see this trend within the data (Figure 4.1A).

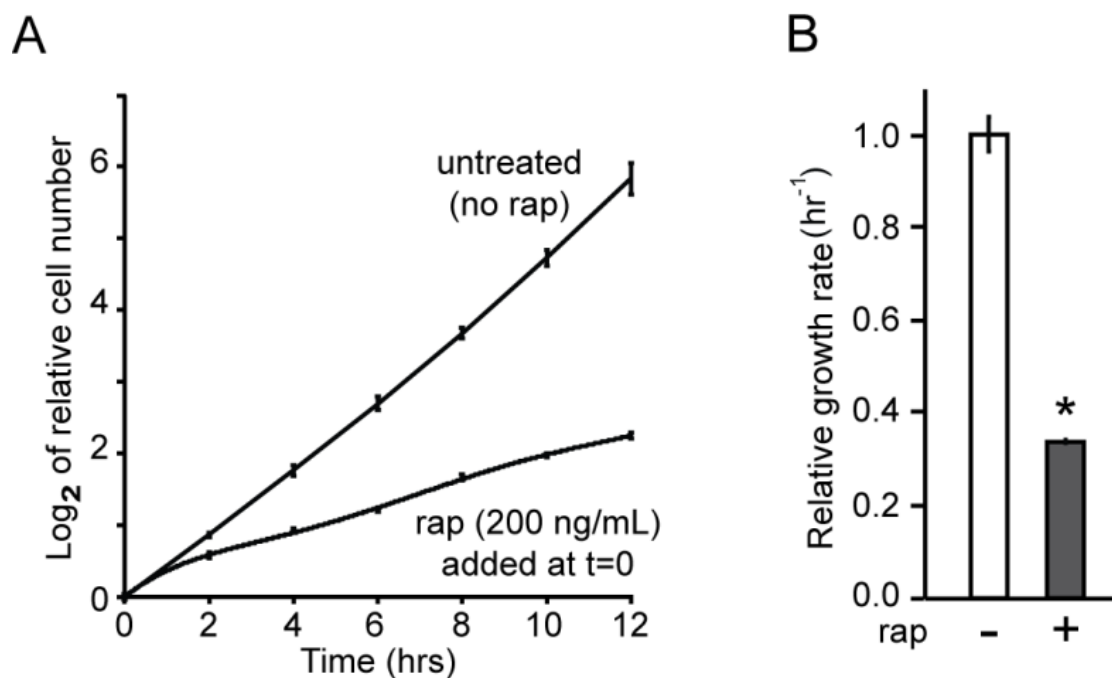


**Figure 4.1 Proliferation of wild-type cells in the constant presence of rapamycin (200 ng/mL)**

A: Exponentially growing wild-type cultures in YPD were normalised to an  $OD_{600nm}$  of  $\sim 0.025$ , treated (or not) with rapamycin (200 ng/mL) at time 0 and incubated at room temperature with agitation. The culture density was measured by Coulter counter every two hours up to 12 hours after the addition of rapamycin. The  $\text{Log}_2$  of the relative cell number compared to the average number of cells at time 0 was calculated and plotted. A polynomial line of best fit with an order of 5 is shown for wild-type cells in the presence of rapamycin. Error bars denote S.E.M.

B: The growth rate of wild-type cultures was calculated between two and 12 hours (between which the rapamycin-insensitive growth rate was stable) and calculated relative to the average growth rate of untreated wild-type cultures ( $0.5 \text{ hr}^{-1}$ ).  $N=4$  independent cultures; error bars denote S.E.M.; \*  $p=0.0004$  relative to untreated wild-type.

To test for any changes in cell population, we examined the growth rate of wild-type cultures in the presence of rapamycin that had previously been exposed to the drug and allowed to recover. We predict that if a subset of rapamycin resistant cells are present in the population, the rapamycin sensitivity of the wild-type culture as a whole would decrease following a number of cycles of rapamycin treatment and recovery.

Wild-type cultures were treated with rapamycin (200 ng/mL) for 24 hours in YPD at 28°C with agitation. Cells were washed three times in fresh YPD and spotted onto a plain YPD plate to recover at 28°C. Cells that had recovered from the first rapamycin treatment were retreated with rapamycin (200 ng/mL) for a further 24 hours at 28°C with agitation and cells were again washed and plated for recovery and incubated at 28°C. Exponentially growing cultures of naïve (never been treated with rapamycin), once recovered and twice recovered wild-type cells were treated (or not) with rapamycin (200 ng/mL) in YPD at 28°C with agitation. The culture density was measured at three and six hours after the introduction of rapamycin by spectrometry at OD<sub>600nm</sub> and the growth rate calculated. We chose to measure culture density at three and six hours after the introduction of rapamycin due to the stability of the rapamycin-insensitive growth rate between these times (Figure 4.1A). The growth rates of rapamycin-treated cultures were calculated relative to the growth rate of the equivalent untreated culture.

As seen in Figure 4.2 we found that the residual growth rates, in the presence of a high concentration of rapamycin, of wild-type cultures that had previously been exposed to rapamycin, either once or twice, was not significantly different to that of naïve wild-type cultures treated with rapamycin for the first time ( $p=0.20$  and  $0.69$ ). It would appear that exposure to rapamycin does not result in selection for rapamycin-resistant cells under the conditions of our experiment. The slow residual growth rate of wild-type cultures in the presence of a high concentration of rapamycin is therefore likely to reflect slow residual proliferation of all the cells in the culture.

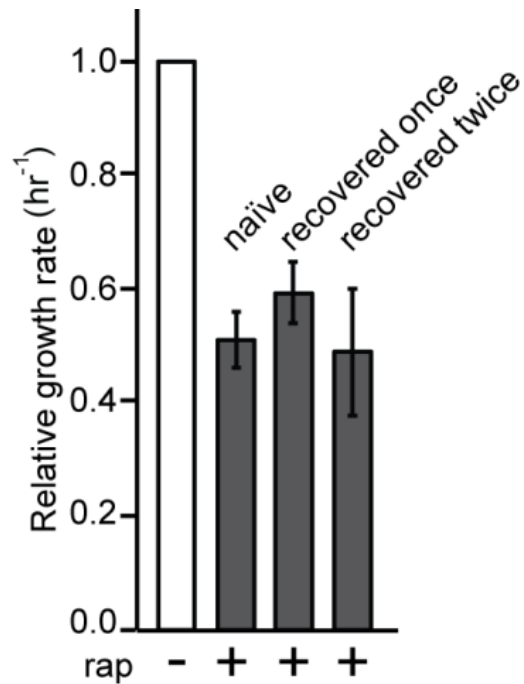


**Figure 4.2** The rapamycin-insensitive growth rate of wild-type cells is not altered by previous exposure to rapamycin

Exponentially growing wild-type cultures were normalised to an  $OD_{600nm}$  of  $\sim 0.05$  and treated with rapamycin (200 ng/mL) for 24 hours at 28°C with agitation. Cells were washed three times using fresh YPD and the cultures plated onto a YPD plate to recover at 30°C. These recovered cells were inoculated into YPD and when in exponential growth phase normalised to an  $OD_{600nm}$  of  $\sim 0.05$  and re-treated for a further 24 hours with rapamycin (200 ng/mL) in YPD at 28°C with agitation. Cells were washed three times using fresh YPD and plated onto a YPD plate to recover at 30°C. Untreated (naïve) cells, those that had been previously treated once or twice with rapamycin were then grown to exponential growth phase and normalised to an  $OD_{600nm}$  of  $\sim 0.04$  and treated (or not) with rapamycin (200 ng/mL). The culture density was measured by spectrometry at  $OD_{600nm}$  at three and six hours after the introduction of rapamycin and the growth rate calculated. The growth rates are expressed relative to their equivalent untreated culture (0.7 hr<sup>-1</sup>, 0.8 hr<sup>-1</sup> and 0.8 hr<sup>-1</sup> for naïve, recovered once and recovered twice). N=3 independent cultures; error bars denote the S.E.M.

Finally, we tested if the minimum inhibitory concentration of rapamycin is altered in wild-type cells that had recovered from a previous rapamycin treatment (200 ng/mL). Exponentially growing wild-type cultures were treated with rapamycin (200 ng/mL) in YPD at 28°C with agitation for 24 hours after which cells were washed three times in fresh YPD, spotted onto a YPD plate and incubated at 30°C. Naïve and recovered wild-type cells in an exponential growth phase were treated (or not) with rapamycin (5, 7.5 or 10 ng/mL) in YPD and incubated at 28°C with agitation for six hours. An end-point assay was used to test rapamycin sensitivity by measuring the change in culture density by spectrometry at OD<sub>600nm</sub> following the six hour incubation period. Each endpoint OD<sub>600nm</sub> measurement is expressed relative to the average OD<sub>600nm</sub> of the respective untreated culture.

As seen in Figure 4.3 we found that there was no significant difference between the sensitivity to rapamycin of naïve wild-type cells and those that had recovered from previous treatment with the drug ( $p=0.96$  in 5 ng/mL, 0.70 in 7.5 ng/mL and 0.55 in 10 ng/mL rapamycin). These results suggest that recovery from rapamycin does not select for rapamycin-resistant mutants under the conditions of our experiment.

We have identified that wild-type yeast cells are able to maintain some significant proliferation in the presence of a high concentration of rapamycin (200 ng/mL), albeit at a slower rate than that of untreated cells. It is unlikely that the residual proliferation observed is a result of ineffective rapamycin; we observed a decrease in the proliferation rate of wild-type cells treated with 7.5-10 ng/mL rapamycin (compared to that of untreated cells), a concentration at least 20 times lower than the concentration used to measure the growth rate of cultures. The residual proliferation of wild-type cells therefore appears to be a robust, inherent behaviour of wild-type cells and is not a result of ineffective rapamycin or, that we see, of rapamycin-resistant cells. We use the term 'rapamycin-insensitive growth rate' to describe the residual growth of cultures in the presence of rapamycin.

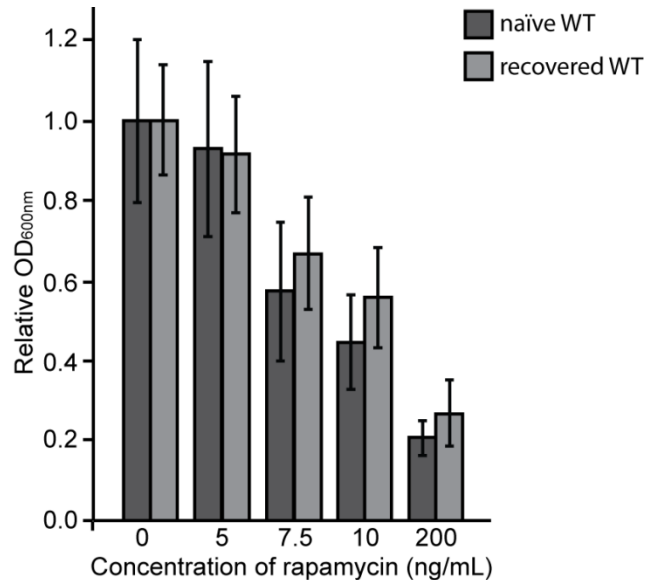


**Figure 4.3 Sensitivity of naïve or recovered wild-type cultures to various concentrations of rapamycin**

Exponentially growing wild-type cultures were normalised to an OD<sub>600nm</sub> of ~0.05 and treated with rapamycin (200 ng/mL) for 24 hours in YPD at 28°C with agitation. After 24 hours in the presence of the drug, cells were washed three times in fresh YPD and spotted onto a YPD plate which was incubated at 28°C for two days. Exponentially growing naïve wild-type cells (those that had not been previously exposed to rapamycin) and wild-type cells that had recovered from a 24 hour treatment were normalised to an OD<sub>600nm</sub> of ~0.1 to which rapamycin was added (5, 7.5 or 10 ng/mL), untreated control cultures were also included. Cultures were incubated at 28°C with agitation for six hours after which the OD<sub>600nm</sub> was measured and expressed relative to the average OD<sub>600nm</sub> of untreated cultures (0.34 OD<sub>600nm</sub> for naïve and 0.16 OD<sub>600nm</sub> for recovered cultures). N=3 independent cultures; error bars denote S.E.M.

#### 4.2.2 Rapamycin treatment induces autophagy in wild-type and in *ego1Δ* cells

It is possible that we see continued, albeit slow, proliferation of wild-type cells in the presence of 200 ng/mL rapamycin due to an abnormal response to the drug, and therefore ineffective TORC1 inactivation. We measured the induction of autophagy, a hallmark of inactive TORC1, to ensure that our drug treatment was effective at inactivating TORC1 in wild-type cells. We used a plasmid borne Pgk1-GFP construct (Welter et al. 2010) to assay autophagy. Pgk1p is a housekeeping protein that is expressed throughout the cytosol under normal conditions; upon the induction of autophagy Pgk1-GFP is transported to the vacuole. The Pgk1 component of the fusion is degraded in the vacuole whilst the GFP fragment is resistant to vacuolar proteases (Welter et al. 2010). By probing for the presence of free GFP on a western blot we can determine whether or not autophagy has occurred.

Cultures of wild-type and *ego1Δ* cells expressing a plasmid borne Pgk1-GFP construct were grown overnight in selective media. Once in an exponential growth phase the cultures were treated (or not) with rapamycin (20, 50, 100 or 200 ng/mL) in YPD at 28°C with agitation for six hours. Normalised cell pellets were collected, lysed using NaOH with 2-Mercaptoethanol on ice and proteins from whole cell lysates were separated by SDS PAGE. Separated proteins were transferred to a membrane and probed with an anti-GFP antibody followed by a secondary antibody conjugated to horseradish peroxidase.

As seen in Figure 4.4 we found that we were able to detect the full Pgk1-GFP construct, but no free GFP, in untreated wild-type cells, consistent with no autophagy occurring under these conditions (Figure 4.4A). We found that autophagy was induced in wild-type cells treated with rapamycin (200 ng/mL) (Figure 4.4A) suggesting that treatment of wild-type cells with 200 ng/mL rapamycin results in inactive TORC1. We also tested whether lower concentrations of rapamycin were able to induce autophagy in wild-type cells. As seen in Figure 4.4A, the presence of free GFP was detected in wild-type cells following treatment with any high concentration of rapamycin tested (*i.e.* a concentration of rapamycin 20 ng/mL or above). The extent of free GFP also appears comparable regardless of the high concentration tested (Figure 4.4A).

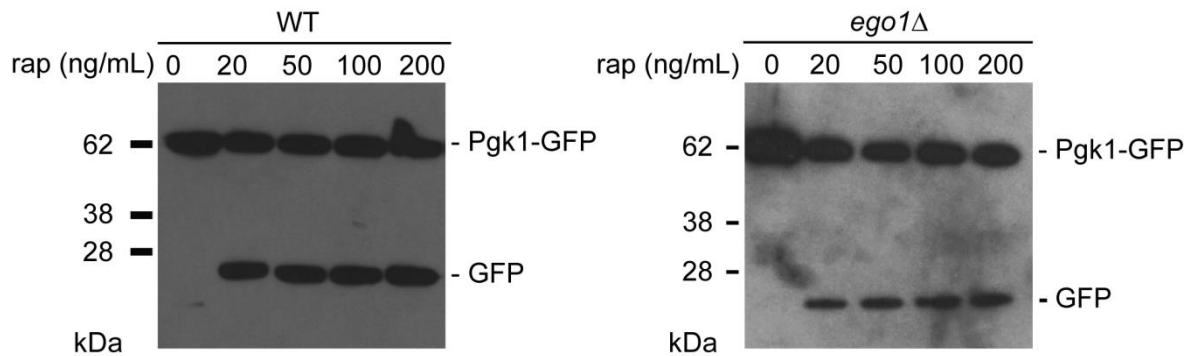


**Figure 4.4** Autophagy is induced upon treatment of yeast cells with high concentrations of rapamycin

A: Wild-type cells expressing a plasmid borne Pgk1-GFP construct were grown overnight in selective media. The following day, cultures in an exponential growth phase were normalised to an  $OD_{600nm}$  of  $\sim 0.25$  which were pelleted and washed once in water before being resuspended in YPD. Cultures were treated (or not) with rapamycin (20, 50, 100 or 200 ng/mL) and incubated at  $28^{\circ}C$  with agitation for six hours. Cells were lysed and proteins separated from whole cell lysates by SDS PAGE, transferred to a membrane and probed with an anti-GFP antibody. Detection was carried out using a secondary antibody conjugated to horseradish peroxidase and an ECL detection kit.

B: Null *ego1Δ* mutant cells expressing a plasmid borne Pgk1-GFP construct were grown overnight in selective media. The following day cultures in an exponential growth phase were normalised to an  $OD_{600nm}$  of  $\sim 0.2$  which were pelleted and resuspended in YPD. Cultures were treated (or not) with rapamycin (20, 50, 100 or 200 ng/mL) and incubated at  $28^{\circ}C$  with agitation for six hours. Cells were lysed and proteins separated from whole cell lysates by SDS PAGE, transferred to a membrane and probed with an anti-GFP antibody. Detection was carried out using a secondary antibody conjugated to horseradish peroxidase and an ECL detection kit.

*Note: These experiments were carried out independently on separate days; therefore results between each strain should not be compared, only those results from treatments within the same strain are comparable.*

The induction of autophagy in wild-type cells following treatment with 20-200 ng/mL rapamycin suggests that TORC1 is being inactivated in these cultures. The residual rapamycin-insensitive growth rate is therefore unlikely to be a result of ineffective TORC1 inhibition either because of altered drug or altered response to the drug. The similarity between the free GFP signals observed in wild-type cells when treated with rapamycin within a range of 20 ng/mL to 200 ng/mL suggests that TORC1 is inactivated to a similar extent within this rapamycin concentration range. Concentrations of rapamycin above at least 20 ng/mL completely induce autophagy, a hallmark of low TORC1 activity.

We also tested whether a rapamycin treatment range of 20-200 ng/mL was sufficient to fully induce autophagy in *ego1Δ* cells. As seen in Figure 4.4B we only observed the full Pgk1-GFP construct in untreated *ego1Δ* cells, suggesting that TORC1 is sufficiently active in untreated *ego1Δ* cells to fully inhibit autophagy, despite loss of the EGO complex. We found that autophagy was induced in rapamycin treated *ego1Δ* cells and that the presence of free GFP was comparable between all concentrations tested (Figure 4.4B). These results suggest that a concentration of 20 ng/mL is enough to inactivate TORC1 in *ego1Δ* cells. We therefore conclude that concentrations of rapamycin above 20 ng/mL are sufficient for TORC1 inactivation in both wild-type and *ego1Δ* cells.

#### 4.2.3 Proliferation of wild-type cells in various high concentrations of rapamycin

We have demonstrated that wild-type cells are able to proliferate slowly in the presence of 200 ng/mL rapamycin, a high concentration at which TORC1 is inhibited, as measured by the induction of autophagy (Figure 4.4A). We found that treatment with 20 ng/mL rapamycin was sufficient to induce autophagy in wild-type cells to an apparently similar extent as treatment with 200 ng/mL rapamycin. It is possible that the slow rapamycin-insensitive growth rate observed in wild-type cultures at 200 ng/mL of drug is a result of rapamycin-inhibited TORC1, or is a result peculiar to that particular concentration of the drug, e.g. potential off-target effects. In the former case, we expect the same, measurable residual growth at all high concentrations of rapamycin; in the latter case, residual growth would vary with concentration of the drug, even when present at high levels.

Exponentially growing wild-type cultures were treated (or not) with rapamycin (20, 50, 100 or 200 ng/mL) in YPD and incubated at room temperature with agitation. The culture density was measured by Coulter counter at two hour intervals, from time 0 (the addition of rapamycin) to 12 hours after the introduction of rapamycin. Cultures were maintained in an exponential growth phase for the duration of the experiment by dilution into the appropriate medium where necessary and the culture density measured was adjusted by the appropriate dilution factor. The growth rate was calculated between two and 12 hours after the introduction of rapamycin, *i.e.* when the rapamycin-insensitive growth rate is stable, and expressed relative to the average untreated growth rate.

As seen in Figure 4.5 the growth rate of wild-type cultures treated with 200 ng/mL rapamycin is approximately 34% of that seen in untreated cultures. Treatment with lower concentrations of rapamycin, between 20 and 100 ng/mL, did not result in a growth rate different to that of cultures in 200 ng/mL rapamycin (Figure 4.5). It would appear that all high concentrations of rapamycin tested result in the same residual rapamycin-insensitive growth rate.

We conclude that rapamycin treatment of 20 ng/mL and above is sufficient to induce the rapamycin-insensitive growth rate of wild-type cultures. These results are consistent with concentrations of rapamycin above 20 ng/mL being sufficient for the induction of autophagy. The consistency of the rapamycin-insensitive growth rate of wild-type cultures treated with any high concentration of the drug suggests that the rapamycin-insensitive growth rate is a true phenotype of wild-type cultures treated with high concentrations of rapamycin.

#### 4.2.4 **Can *ego*- mutant cells proliferate in the presence of high concentrations of rapamycin?**

Published data suggests that hallmarks of inactive TORC1 do not appear to differ in *ego*- mutants compared to wild-type cells following short treatments with rapamycin (Binda et al. 2009; Dubouloz et al. 2005). We have identified a new phenotype of yeast in response to rapamycin: the rapamycin-insensitive proliferation rate. Is the EGO complex required to maintain this rapamycin-insensitive proliferation?

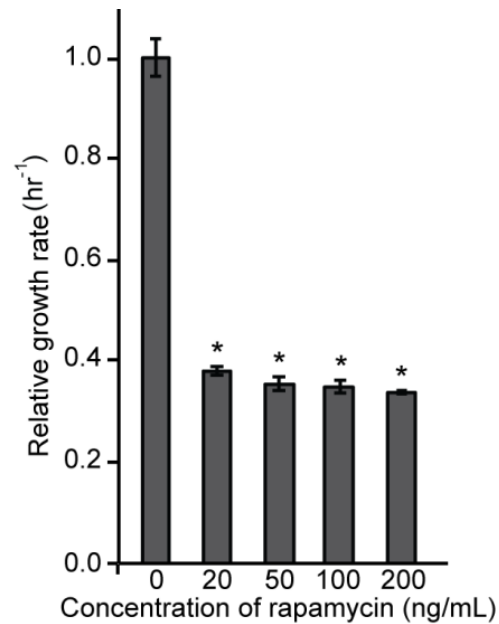


**Figure 4.5 Growth rate of wild-type cultures in various high concentrations of rapamycin**

Exponentially growing cultures of wild-type cells at an  $OD_{600nm}$  of  $\sim 0.025$  were treated (or not) with rapamycin (20-200 ng/mL) in YPD and incubated at room temperature with agitation. The culture density was measured by Coulter counter every two hours from time 0 (the introduction of rapamycin) to 12 hours after the addition of rapamycin. The growth rate was calculated for each culture between two and 12 hours after the introduction of rapamycin and expressed relative to the untreated wild-type growth rate ( $0.5 \text{ hr}^{-1}$ ).  $N=4$  independent cultures; error bars denote S.E.M.; \*  $p<0.05$  relative to the untreated growth rate.

Exponentially growing *ego1Δ* mutant cultures were treated (or not) with rapamycin (200 ng/mL) in YPD and incubated at room temperature with agitation. The culture density was measured by Coulter counter at two-hour intervals, from time 0 (the addition of rapamycin) to 12 hours after the introduction of rapamycin. Results are expressed as a semi-Log<sub>2</sub> plot of the relative culture density with time. The steady state growth rate of untreated and rapamycin treated *ego1Δ* cultures, calculated between two and 12 hours after the introduction of rapamycin, is also shown relative to that of untreated wild-type cultures from Figure 4.1B which were measured in parallel.

We found that the growth rate of untreated *ego1Δ* cultures was not significantly different to that of untreated wild-type cultures ( $p=0.95$ ) (Figure 4.6B), suggesting that the EGO complex is not limiting for proliferation under normal conditions. The *ego1Δ* mutant cultures took approximately two hours to slow their growth rate in response to rapamycin after which a slow steady growth rate was observed for the remainder of the experiment (Figure 4.6A). We found that the stable growth rate of *ego1Δ* cultures in the presence of rapamycin was significantly slower than that of wild-type cultures growing in the continued presence of the drug ( $p=1.61E-07$ ) (Figure 4.6B). We conclude that cells lacking Ego1p respond differently to the presence of rapamycin than do wild-type cells and that Ego1p is required to support residual rapamycin-insensitive proliferation. We have therefore identified a novel phenotype in which *ego1Δ* cells behave differently to wild-type cells when treated with rapamycin and one that is evident within two hours after the introduction of the drug.

#### **4.2.5 Does the proliferation rate of *ego1Δ* mutants vary with the concentration of rapamycin, when present at high concentrations?**

We have shown that the rapamycin-insensitive growth rate of *ego1Δ* mutants is significantly slower than that of wild-type cultures when treated with 200 ng/mL rapamycin. We have also shown that the rapamycin-insensitive growth rate of wild-type cells is independent of the external concentration of rapamycin. Is the same also true for *ego1Δ* cells?

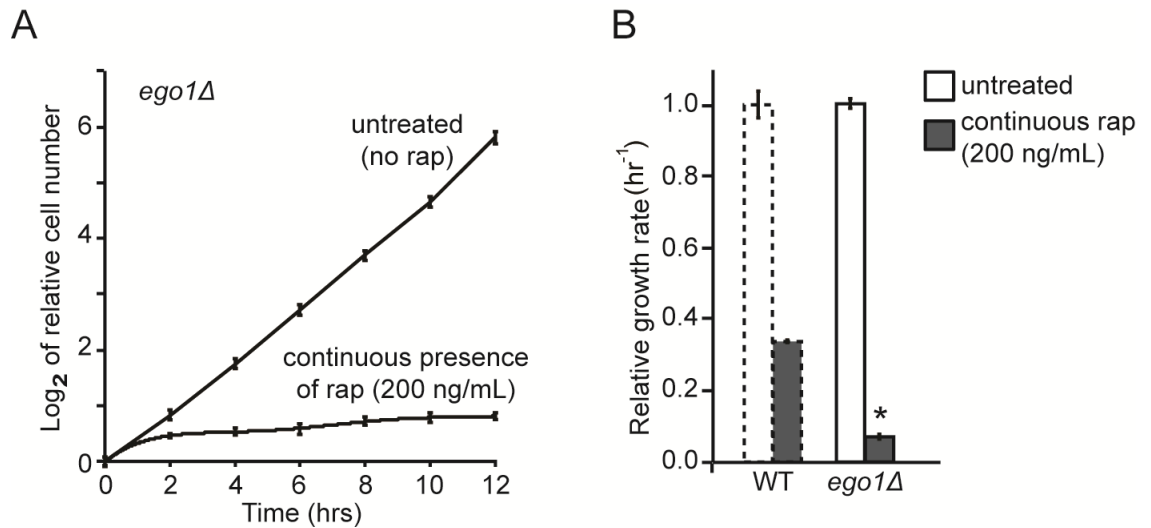


**Figure 4.6 Proliferation of *ego1Δ* cells in the constant presence of rapamycin (200 ng/mL)**

A: Exponentially growing *ego1Δ* cultures in YPD were normalised to an OD<sub>600nm</sub> of ~0.025, treated (or not) with rapamycin (200 ng/mL) at time 0 and incubated at room temperature with agitation. The culture density was measured by Coulter counter every two hours from time 0 (the introduction of rapamycin) to 12 hours after the addition of rapamycin. The Log<sub>2</sub> of culture density between two and 12 hours was calculated relative to the average culture density at time 0 and plotted. A polynomial line of best fit with an order of 5 is shown for *ego1Δ* cells in the presence of rapamycin. Error bars denote S.E.M.

B: The growth rates of *ego1Δ* cultures were calculated between two and 12 hours (when the rapamycin-insensitive growth rate was stable) and calculated relative to the average growth rate of untreated wild-type cultures (0.5 hr<sup>-1</sup>) from Figure 4.1B (indicated by a dashed border) which were measured in parallel. N=4 independent cultures; error bars denote S.E.M.; \* p=1.6x10<sup>-7</sup> relative to rapamycin treated wild-type cultures.

Exponentially growing *ego1Δ* cultures were treated (or not) with rapamycin (20, 50, 100 or 200 ng/mL) in YPD and incubated at room temperature with agitation. The culture density was measured by Coulter counter every two hours from time 0 (the addition of rapamycin) to 12 hours after the introduction of rapamycin. Cultures were maintained in an exponential growth phase for the duration of the experiment by dilution into the appropriate medium when necessary and the culture density measured was adjusted by the appropriate dilution factor. The growth rate was calculated between two and 12 hours after the introduction of rapamycin (when the rapamycin-insensitive growth rate is stable) and expressed relative to the average untreated growth rate of wild-type cultures measured in 4.2.3 (these experiments were carried out in parallel).

As seen in Figure 4.7 we found that the rapamycin-insensitive growth rate of *ego1Δ* cultures was extremely low for all concentrations of rapamycin tested, and did not appear to vary with an increasing concentration of the drug in the medium. The growth rate of rapamycin treated *ego1Δ* cultures was significantly slower than that for the equivalently treated wild-type cultures at each concentration of rapamycin tested ( $p=0.005$  for 20 ng/mL, 0.02 for 50 ng/mL, 0.009 for 100 ng/mL and 0.006 for 200 ng/mL) (Figure 4.7).

The similarity in growth rate of *ego1Δ* cultures treated with various concentrations of rapamycin, as observed for wild-type cultures, again suggests that the lowest concentration of the drug tested is enough to maximally inhibit TORC1.

#### **4.2.6 Are all subunits of the EGO complex required to support rapamycin-insensitive proliferation?**

We have identified that cells lacking Ego1p have a significantly slower proliferation rate in the presence of rapamycin than that of rapamycin treated wild-type cells. Loss of any one of the four components of the EGO complex results in a failure to recover from rapamycin treatment (Figure 3.1). Are all members of the EGO complex also required to support rapamycin-insensitive proliferation? We measured the growth rate of rapamycin treated cultures of *ego3Δ*, *gtr1Δ* and *gtr2Δ* mutants to test whether they too show a growth rate defect in the presence of the drug.

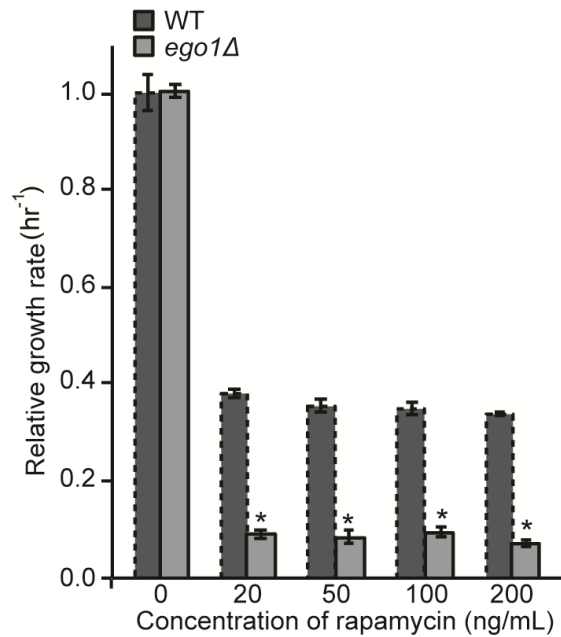


**Figure 4.7 Growth rate of wild-type and *ego1Δ* cultures in various high concentrations of rapamycin**

Exponentially growing *ego1Δ* cultures at an  $OD_{600nm}$  of  $\sim 0.025$  were treated (or not) with rapamycin (20-200 ng/mL) in YPD and incubated at room temperature with agitation. The culture density was measured by Coulter counter every two hours from time 0 (the introduction of rapamycin) to 12 hours after the addition of rapamycin. The growth rate was calculated for each culture between two and 12 hours after the introduction of rapamycin and expressed relative to the untreated wild-type growth rate from Figure 4.5 ( $0.5 \text{ hr}^{-1}$ ), which were measured in parallel. The growth rate of wild-type cells in various concentrations of rapamycin, and carried out in parallel, from Figure 4.5 (indicated by a dashed border) is included as a comparison.  $N=4$  independent cultures; error bars denote S.E.M.; \*  $p < 0.05$  relative to equivalently treated wild-type.

Exponentially growing cultures of wild-type, *ego3Δ*, *gtr1Δ* and *gtr2Δ* cells were treated (or not) with rapamycin (200 ng/mL) for 12 hours in YPD at room temperature with agitation. The culture density was measured by Coulter counter every two hours, from time 0 (the introduction of rapamycin) to 12 hours after the introduction of the drug. The growth rate of each culture was calculated between two and 12 hours after the introduction of rapamycin. Growth rates are expressed relative to the average growth rate of untreated wild-type cultures.

We found that the growth rate of any untreated *ego*- mutant was no different to the growth rate of untreated wild-type cultures ( $p=0.39$  for *ego3Δ*,  $0.56$  for *gtr1Δ* and  $0.61$  for *gtr2Δ* compared to untreated wild-type) (Figure 4.8). These results are consistent with loss of the EGO complex not limiting growth in nutrient rich conditions. In the presence of rapamycin, we found that loss of any one of the EGO complex components resulted in a significantly slower growth rate compared to wild-type cultures in the constant presence of rapamycin ( $p=0.045$  for *ego3Δ*,  $0.048$  for *gtr1Δ* and  $0.03$  for *gtr2Δ*) (Figure 4.8). We conclude that a slow rapamycin-insensitive growth rate, compared to that of wild-type cultures, is shared with all null mutants of the EGO complex.

We also measured the growth rate of *gtr2Δ* cultures treated with 20 ng/mL and 200 ng/mL rapamycin to determine whether the rapamycin-insensitive growth rate in these mutants is independent of the concentration of rapamycin tested, as was seen for *ego1Δ* mutants. Exponentially growing wild-type, *ego1Δ* and *gtr2Δ* cultures were treated (or not) with rapamycin (20 or 200 ng/mL) in YPD and incubated at 28°C with agitation for six hours. The culture density was measured by spectrometry (at  $OD_{600nm}$ ) at three and six hours after the introduction of rapamycin; the growth rate was calculated between these time points and expressed relative to the average growth rate of untreated wild-type cultures.

As seen in Figure 4.9 we found that the rapamycin-insensitive growth rate of *gtr2Δ* cultures was the same at both concentrations of rapamycin tested (20 and 200 ng/mL) ( $p=0.23$ ).

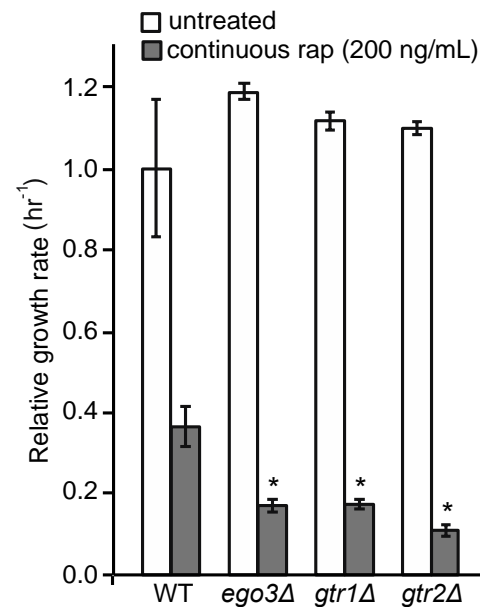


**Figure 4.8** The growth rate of *ego*-mutants in the presence of a high concentration rapamycin

Exponentially growing WT, *ego3Δ*, *gtr1Δ* and *gtr2Δ* cultures were normalised to an OD<sub>600nm</sub> of ~0.02 and treated (or not) with rapamycin (200 ng/mL) in YPD and incubated at room temperature. The culture density was measured every two hours from time 0 (the introduction of rapamycin) during the course of 12 hours by Coulter counter. The growth rates were calculated between two and 12 hours after the introduction of rapamycin and expressed relative to the average untreated wild-type (0.3 hr<sup>-1</sup>). N=3 independent cultures for WT and 4 for all remaining cultures; error bars denote S.E.M.; \* p<0.05 relative to rapamycin treated wild-type cells.

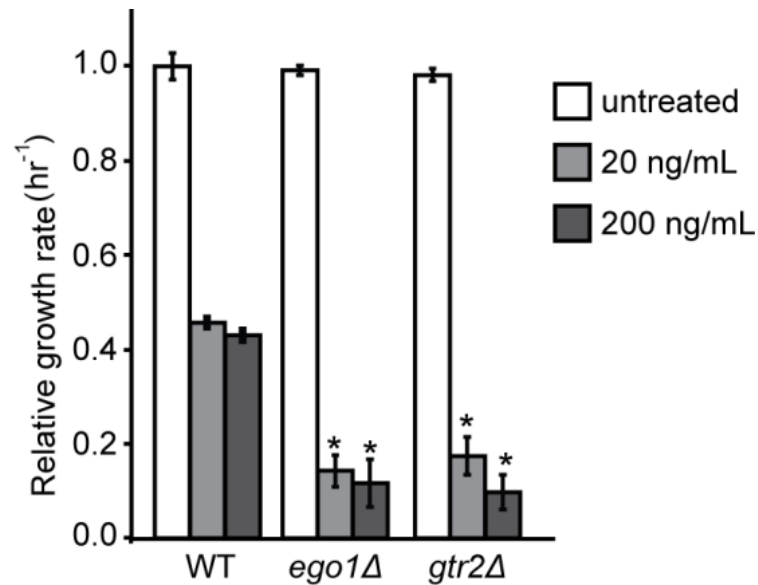


**Figure 4.9** Growth rate of wild-type, *ego1Δ* and *gtr2Δ* cultures in 20 and 200 ng/mL rapamycin

Exponentially growing wild-type, *ego1Δ* and *gtr2Δ* cultures were normalised to an  $OD_{600nm}$  of  $\sim 0.05$  for untreated cultures or  $\sim 0.1$  for treated cultures. Normalised cultures were treated (or not) with rapamycin (20 or 200 ng/mL) in YPD and incubated at  $28^{\circ}C$  with agitation for six hours. The  $OD_{600nm}$  was measured at three and six hours after the introduction of rapamycin and the growth rate calculated. Growth rates are expressed relative to the average growth rate of untreated wild-type cultures ( $0.6 \text{ hr}^{-1}$ ).  $N=4$  independent cultures for *ego1Δ*, 3 for wild-type and *gtr2Δ*; error bars denote S.E.M.; \*  $p < 0.05$  relative to equivalently treated wild-type cultures.

The similarity in the reduced rapamycin-insensitive growth rates of *ego1Δ* and *gtr2Δ* cultures (compared to that of wild-type cultures) in concentrations of rapamycin above 20 ng/mL suggests that the reduced rapamycin-insensitive growth rate of *ego1Δ* and *gtr2Δ* cultures in any high concentration of rapamycin is likely to apply for all *ego*- null mutants.

#### 4.2.7 Are Tor1p and Tco89p required for rapamycin-insensitive proliferation?

We have found that the EGO complex is important for full rapamycin-insensitive proliferation. The EGO complex is a known activator of TORC1 and TORC1 activity is partly compromised in cells lacking the EGO complex (Binda et al. 2009; Dubouloz et al. 2005). Could rapamycin only partly inhibit yeast TORC1? It is now known that rapamycin is an incomplete inhibitor of mammalian mTORC1 (Feldman et al. 2009; Thoreen et al. 2009). What if rapamycin-insensitive TORC1 activity drives the rapamycin-insensitive proliferation of yeast cells? If this is the case we would predict that any condition that compromises TORC1 activity, either genetically or chemically, would also result in a slow rapamycin-insensitive growth rate phenotype. TORC1 contains two specific and non-essential subunits, Tor1p and Tco89p; are these TORC1 specific proteins required for rapamycin-insensitive proliferation?

Exponentially growing wild-type, *tor1Δ*, and *tco89Δ* cultures were treated (or not) with rapamycin (200 ng/mL) for 12 hours in YPD at room temperature with agitation. The culture density was measured by Coulter counting every two hours and the growth rate determined between two and 12 hours after the introduction of the drug. Growth rates were calculated relative to the average untreated wild-type growth rate.

As seen in Figure 4.10 we found no significant difference in the growth rate of untreated cultures for either *tor1Δ* or *tco89Δ* mutants compared to that of wild-type cultures ( $p=0.41$  for *tor1Δ* and  $0.69$  for *tco89Δ*). When treated with rapamycin we observed a statistically significant reduction in the proliferation rate of cells lacking either Tor1p or Tco89p compared to rapamycin treated wild-type cells ( $p=0.04$  and  $0.02$  respectively) (Figure 4.10).

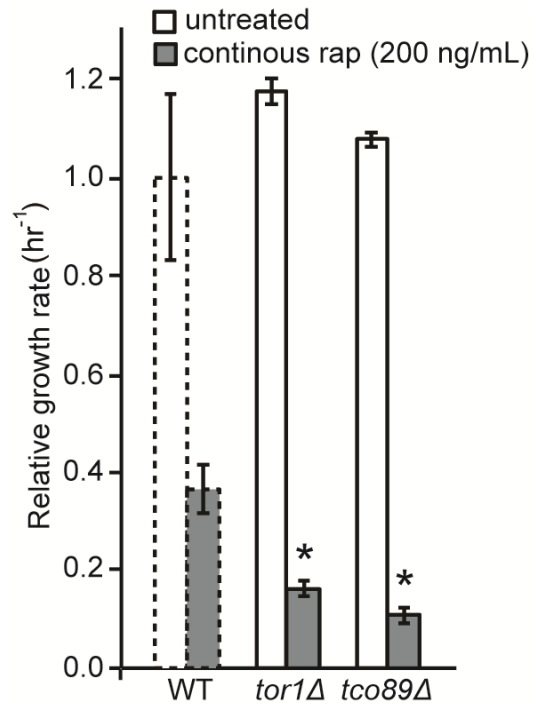


**Figure 4.10 Proliferation of *tor1Δ* and *tco89Δ* cells in the constant presence of rapamycin (200 ng/mL)**

Exponentially growing *tor1Δ* and *tco89Δ* cultures were normalised to an  $OD_{600nm}$  of  $\sim 0.02$  and treated (or not) with rapamycin (200 ng/mL) in YPD at room temperature. A Coulter counter was used to measure the culture density every two hours and the growth rate was calculated between two and 12 hours after the introduction of rapamycin. Growth rates were calculated relative to the average untreated wild-type ( $0.3 \text{ hr}^{-1}$ ) from Figure 4.8 (indicated by a dashed border), which were measured in parallel.  $N=3$  independent cultures for wild-type and 4 for all remaining cultures; error bars denote S.E.M.; \*  $p < 0.05$  relative to the rapamycin-insensitive growth rate of wild-type cultures.

These results suggest that in the presence of rapamycin Tor1p and Tco89p are required to maintain residual proliferation. These results are consistent with rapamycin failing to fully inactivate TORC1 and residual TORC1 activity driving at least part of the residual proliferation.

We also measured the growth rate of *tco89Δ* cultures treated with 20 and 200 ng/mL rapamycin to determine whether the rapamycin-insensitive growth rate is independent of the high concentration of rapamycin used. Exponentially growing *tco89Δ* cultures were treated (or not) with rapamycin (20 and 200 ng/mL) in YPD at 28°C with agitation. The culture density was measured by spectrometry at OD<sub>600nm</sub> at three and six hours after the introduction of rapamycin and the growth rate was determined between these time points. The growth rate was calculated relative to the growth rate of untreated wild-type cultures from Figure 4.9 which were measured in parallel. The growth rate of untreated and rapamycin treated (20 and 200 ng/mL) *ego1Δ* mutants from Figure 4.9 were also measured in parallel and are included as controls.

We found that the rapamycin-insensitive growth rate of *tco89Δ* mutants was not significantly different ( $p=0.60$ ) when *tco89Δ* cultures were treated with either 20 or 200 ng/mL rapamycin (Figure 4.11). These results show that for *tco89Δ* mutants, as for *ego-* mutants, the rapamycin-insensitive growth rate is consistent regardless of the concentration of rapamycin tested.

#### 4.2.8 Growth rate of *kog1<sup>ts</sup>* in the presence of a high concentration of rapamycin

Kog1p is the only specific and essential subunit of TORC1 (Loewith et al. 2002). Due to the essential nature of *KOG1* we used a plasmid borne temperature sensitive allele of *kog1<sup>ts</sup>* (Nakashima et al. 2008) to reduce basal TORC1 activity at the non-permissive temperature. Heterozygous diploid *kog1Δ/KOG1* cells were transformed with *pkog1<sup>ts</sup>*, sporulated and dissected on YPD plates to produce *kog1Δ* haploid cells containing *pkog1<sup>ts</sup>* (termed *kog1<sup>ts</sup>*). The temperature sensitive *kog1<sup>ts</sup>* allele was introduced into a *kog1Δ* null mutant to ensure all TORC1 complexes contained the mutated Kog1p protein.

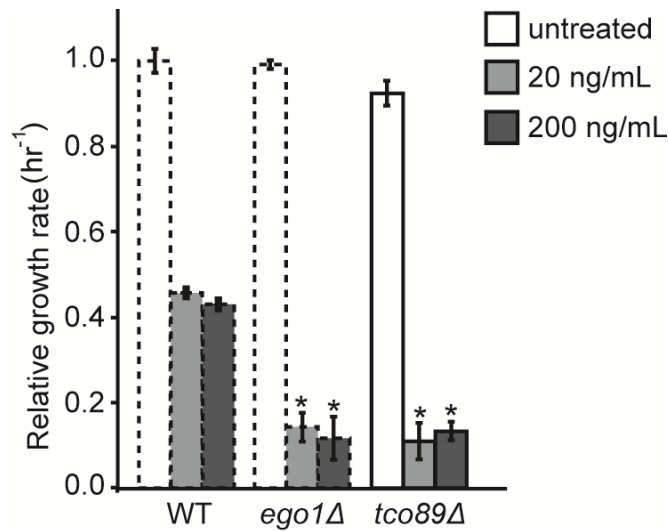


**Figure 4.11** The growth rate of *tco89Δ* cells in 20 and 200 ng/mL rapamycin. Exponentially growing *tco89Δ* mutant cultures were normalised to an OD<sub>600nm</sub> of ~0.05 for untreated cultures or ~0.1 for treated cultures. Normalised cultures were treated (or not) with rapamycin (20 or 200 ng/mL) in YPD and incubated at 28 °C with agitation for six hours. The OD<sub>600nm</sub> was measured at three and six hours after the introduction of rapamycin and the growth rate calculated. Growth rates are expressed relative to the average untreated wild-type (0.6 hr<sup>-1</sup>) from Figure 4.9 which were measured in parallel. The untreated and rapamycin-induced growth rates of wild-type and *ego1Δ* from Figure 4.9 are included as a comparison and were measured in parallel. Data already shown in Figure 4.9 is indicated by a dashed border. N=3 independent cultures for wild-type and 4 for *ego1Δ* and *tco89Δ*; error bars denote S.E.M.; \* p<0.05 relative to equivalently treated wild-type culture.

Wild-type and *kog1<sup>ts</sup>* cultures were grown in YPD at both the permissive (22°C) and non-permissive (37°C) temperature with agitation for 24 hours. Cultures were maintained in an exponential growth phase by dilution, as required, into fresh YPD. Exponentially growing cultures were treated (or not) with rapamycin (200 ng/mL) in YPD and incubated at the respective temperature for a further 12 hours. The culture density was measured by Coulter counter and the growth rate of each culture calculated between two and 12 hours after the addition of rapamycin. Growth rates were calculated relative to the average untreated wild-type growth rate of cultures at 22°C.

As seen in Figure 4.12 there was no significant difference ( $p=0.11$ ) between the growth rate of untreated wild-type and *kog1<sup>ts</sup>* cultures at the permissive temperature. These results suggest that the temperature-sensitive *kog1<sup>ts</sup>* allele is functional at the permissive temperature. We found that at the non-permissive temperature there was a significant difference ( $p=0.02$ ) in the growth rate of untreated *kog1<sup>ts</sup>* cultures compared to untreated wild-type cultures suggesting that Kog1p activity, and by inference TORC1 activity, is lower in *kog1<sup>ts</sup>* cells at 37°C (Figure 4.12).

At both the permissive and non-permissive temperature we observed a significantly slower growth rate for *kog1<sup>ts</sup>* cultures treated with rapamycin compared to rapamycin treated wild-type cultures ( $p=0.02$  at 22°C and 0.004 at 37°C) (Figure 4.12). These results suggest that Kog1p, and thus TORC1 activity, is required to maintain proliferation in the presence of rapamycin.

We also determined the growth rate of *kog1<sup>ts</sup>* cultures in the presence of 20 ng/mL and 200 ng/mL rapamycin. Exponentially growing *kog1<sup>ts</sup>* cultures were treated (or not) with rapamycin (20 or 200 ng/mL) in YPD and incubated at 28°C with agitation. The  $OD_{600nm}$  of each culture was measured at three and six hours following the introduction of rapamycin and the growth rate calculated. The growth rates of untreated and rapamycin treated wild-type cultures, shown in Figure 4.9, were measured in parallel and all growth rates were calculated relative to that of the average untreated wild-type cultures. A modest but significant ( $p=0.02$ ) growth defect was observed for untreated *kog1<sup>ts</sup>* cultures incubated at 28°C compared to that of untreated wild-type cultures (Figure 4.13).

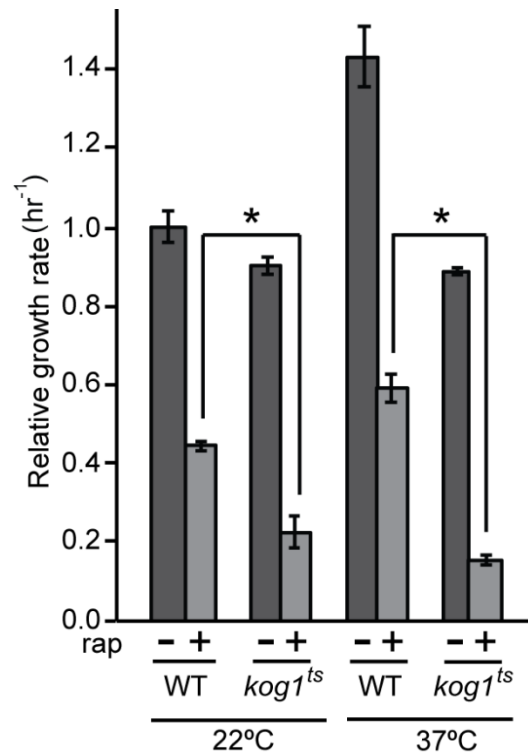


**Figure 4.12 Growth rate of *kog1<sup>ts</sup>* in the constant presence of rapamycin (200 ng/mL)**

Wild-type and *kog1Δ-pkog1<sup>ts</sup>* (*kog1<sup>ts</sup>*) cultures were grown at both the permissive (22°C) and non-permissive (37°C) temperature for 24 hours in YPD; cultures were diluted with fresh media to maintain an exponential growth phase when necessary. Following a 24 hour pre-treatment at the respective temperature, cultures were normalised to an OD<sub>600nm</sub> of ~0.025, treated (or not) with rapamycin (200 ng/mL) in YPD and maintained at their respective temperatures with agitation. The culture density was measured by Coulter counter every two hours from time 0 to 12 hours after the addition of rapamycin. The growth rate was calculated between two and 12 hours following the introduction of rapamycin and calculated relative to the average untreated wild-type growth rate at 22°C (0.39 hr<sup>-1</sup>). N=3 independent cultures; error bars denote S.E.M.; \* p<0.05

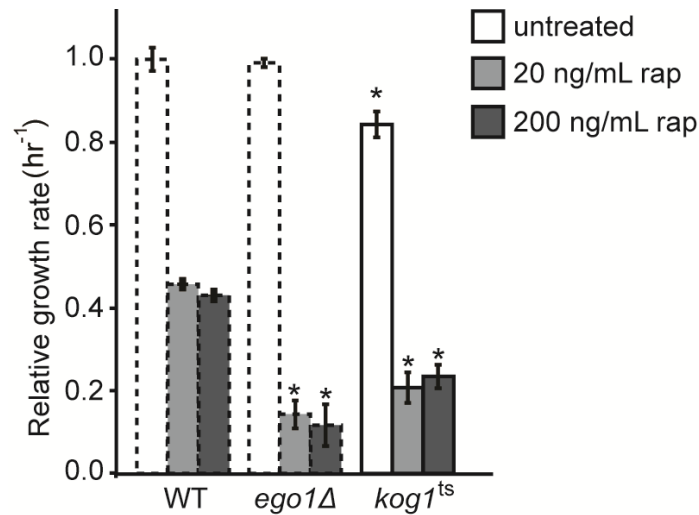


**Figure 4.13 Growth rate of *kog1<sup>ts</sup>* in 20 and 200 ng/mL rapamycin**

Exponentially growing wild-type, *ego1Δ* and *kog1<sup>ts</sup>* mutant cultures were normalised to an  $OD_{600nm}$  of  $\sim 0.05$  for untreated cultures or  $\sim 0.1$  for treated cultures. Normalised cultures were treated (or not) with rapamycin (20 or 200 ng/mL) for six hours in YPD and incubated at  $28^{\circ}C$  with agitation. The  $OD_{600nm}$  was measured at three and six hours after the introduction of rapamycin and the growth rate calculated. Growth rates are expressed relative to the average untreated wild-type ( $0.6 \text{ hr}^{-1}$ ). Note: The untreated and rapamycin-insensitive growth rates of wild-type and *ego1Δ* have previously been shown in Figure 4.9, as indicated by dashed borders.  $N=3$  independent cultures for wild-type and *kog1<sup>ts</sup>* and 4 for *ego1Δ*; error bars denote S.E.M.; \*  $p<0.05$  relative to equivalently treated wild-type cultures.

The growth rates of *kog1<sup>ts</sup>* cultures in the presence of either 20 ng/mL or 200 ng/mL rapamycin were not significantly different from each other ( $p=0.60$ ) (Figure 4.13). Consistent with all strains tested so far, we find that the rapamycin-insensitive growth rate of *kog1<sup>ts</sup>* is the same regardless of the concentration of rapamycin tested.

#### 4.2.9 Can yeast cells proliferate in the complete absence of Kog1p?

It has been proposed that TORC1 activity is absolutely required for yeast to proliferate. A study carried out by Loewith et al. (2002) demonstrated that cells expressing *KOG1* under a galactose promoter slowed proliferation following the addition of glucose to the medium (within 12-15 hours after initiating the GAL shut-off). If TORC1 activity is absolutely required for yeast proliferation it would provide strong evidence that rapamycin is not a complete inhibitor of TORC1. To determine whether cell proliferation is absolutely dependent on TORC1 activity we assayed, by microscopy, the ability of *kog1Δ* null mutant cells to proliferate following dissection from heterozygous diploids.

Heterozygous *kog1Δ/KOG1* diploids were sporulated and the resulting tetrads dissected onto both plain YPD plates and YPD plates containing a high concentration of rapamycin (200 ng/mL). The ability of each spore to proliferate was monitored by microscopy over three days. One day after dissection, we found that 50% of the spores had formed small colonies on the plain YPD plate (Table 4.1). These colonies were subsequently confirmed as being wild-type cells by their sensitivity to G418 (data not shown). We found that 10% of dissected cells (all *kog1Δ* by inference) had undergone 1-3 doublings within the first day but did not proliferate further after that (Table 4.1). The remaining 40% of dissected spores (all *kog1Δ* by inference) failed to divide even once during the three days monitored (Table 4.1). These results suggest that Kog1p, and thus the TOR1 complex, may be absolutely required for proliferation of yeast cells.

| Days after dissection | YPD            |               |                  | YPD & rapamycin (200 ng/mL) |               |                  |
|-----------------------|----------------|---------------|------------------|-----------------------------|---------------|------------------|
|                       | 0 doublings    | 1-3 doublings | colony formation | 0 doublings                 | 1-3 doublings | colony formation |
| 1                     | 40%<br>(16/40) | 10%<br>(4/40) | 50%<br>(20/40)   | 53%<br>(19/36)              | 25%<br>(9/36) | 22%<br>(8/36)    |
| 2                     | 40%<br>(16/40) | 10%<br>(4/40) | 50%<br>(20/40)   | 50%<br>(18/36)              | 3%<br>(1/36)  | 47%<br>(17/36)   |
| 3                     | 40%<br>(16/40) | 10%<br>(4/40) | 50%<br>(20/40)   | 50%<br>(18/36)              | 0%<br>(0/36)  | 50%<br>(18/36)   |

**Table 4.1 Germination and proliferation of *kog1Δ*/WT diploids in the absence and presence of rapamycin (200 ng/mL)**

Heterozygous *kog1Δ*/KOG1 diploid cells were inoculated into liquid sporulation media and incubated at room temperature with agitation. Digested tetrads were dissected onto either plain YPD plates or YPD plates containing rapamycin (200 ng/mL) which were incubated at 30°C. The ability of cells to divide was observed by microscopy every day for three days and the number of doublings scored. The percentage of cells per score is recorded, with the fraction of the total spores recorded underneath.

We found that 20% of *kog1Δ* mutant spores were able to divide a few times on YPD within the first day following dissection. To test whether this short, limited burst of proliferation was a result of inherited Kog1p, and thus potentially active TORC1, via meiosis we also dissected *kog1Δ/KOG1* tetrads in the presence of rapamycin (200 ng/mL) to reduce any potential remaining TORC1 activity. Three days after dissection, we found that 50% of spores were able to produce colonies, albeit more slowly than those dissected onto a plain YPD plate (these colonies were all subsequently confirmed as wild-type cells by their inability to grow in the presence of G418 (data not shown)). The remaining 50% of spores (all *kog1Δ* by inference) completely failed to proliferate during the three days monitored (Table 4.1). It is therefore likely that any initial proliferation of *kog1Δ* cells on the plain YPD plate was due to inherited Kog1p protein (and thus active TORC1) following meiosis of the heterozygous diploid.

We conclude that Kog1p, and thus TORC1 activity, is absolutely essential for yeast to proliferate. Furthermore, we find that all 18 independent wild-type spores tested were slowly able to form colonies when germinated in the presence of a high concentration of rapamycin. This observation further supports our conclusion that rapamycin is not a complete inhibitor of yeast TORC1 activity.

#### 4.2.10 Rapamycin-insensitive TORC1 activity is inhibited by caffeine

It appears from our analysis of mutants with reduced TORC1 activity that the rapamycin-insensitive growth rate of yeast cultures is a result of residual TORC1 activity. Caffeine has been shown to preferentially inhibit TORC1 in yeast in a manner different to that of rapamycin (Reinke et al. 2006; Wanke et al. 2008). We therefore utilised a sub-inhibitory concentration of caffeine to reduce TORC1 activity in wild-type cells and observed the consequence on the proliferation rate in the presence and absence of rapamycin.

Exponentially growing cultures of wild-type and *ego1Δ* cells were treated (or not) with rapamycin (200 ng/mL), caffeine (3 mM) or both in YPD and incubated at room temperature with agitation. The culture density was measured by Coulter counter every two hours up to 12 hours after the introduction of the

drugs. The growth rate of each culture was calculated between two and 12 hours after the introduction of the drugs and expressed relative to the average growth rate of untreated wild-type cultures.

As seen in Figure 4.14 the growth rate of wild-type cultures treated with a sub-inhibitory concentration of caffeine was no different to that of untreated cultures ( $p=0.70$ ). We found that treatment with a high concentration of rapamycin alone resulted in a reduced growth rate in wild-type cells consistent with our previous results (Figure 4.1B). When treated with both a sub-inhibitory concentration of caffeine and a high concentration of rapamycin we observed a significantly slower growth rate of wild-type cultures compared to that of cultures treated with rapamycin alone ( $p=4 \times 10^{-6}$ ) (Figure 4.14). These results further support our view that the rapamycin-insensitive growth rate is dependent on TORC1 activity and that rapamycin does not fully inhibit TORC1.

The growth rate of cultures of *ego1Δ* mutants in the presence of rapamycin, caffeine or both was also measured. We found that the growth rate of *ego1Δ* cultures in the presence of a sub-inhibitory concentration of caffeine alone was significantly slower than that of untreated *ego1Δ* cultures ( $p=0.02$ ) and was not significantly different to the growth rate of wild-type cultures treated with rapamycin ( $p=0.50$ ) (Figure 4.14). The treatment of *ego1Δ* cultures with combined caffeine and rapamycin almost completely abolished the rapamycin-insensitive growth rate of *ego1Δ* cultures ( $p=0.01$  compared to rapamycin treated *ego1Δ* cultures). These results are consistent with our model that the rapamycin-insensitive growth rate is at least partially or wholly dependent on TORC1 activity. These results also suggest that the slow rapamycin-insensitive growth rate of *ego1Δ* cultures is a result of lower basal TORC1 activity, as demonstrated by their hypersensitivity to caffeine.

Overall, we have found that yeast cells maintain slow proliferation in the presence of high concentrations of rapamycin. Loss of the EGO complex results in a slow rapamycin-insensitive proliferation rate, which is likely due to reduced basal TORC1 activity in these cells. The ability of cells to maintain proliferation in the presence of rapamycin suggests that the drug is not a complete inhibitor of TORC1 activity; cells lacking TORC1 activity (as assayed in *kog1Δ* null mutants) are unable to proliferate.

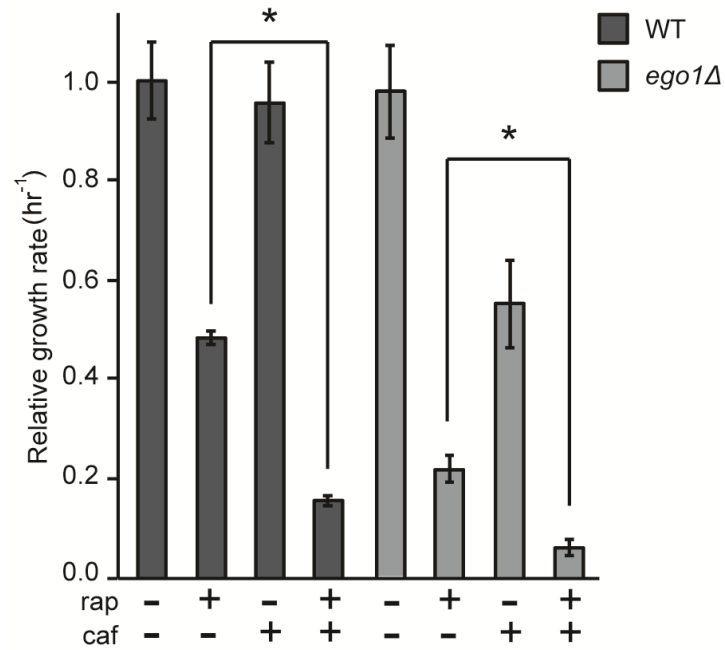


**Figure 4.14 Growth rate of wild-type and *ego1Δ* cultures treated with a high concentration of rapamycin and sub-inhibitory concentration of caffeine**  
 Exponentially growing wild-type and *ego1Δ* cultures, normalised to an  $OD_{600nm}$  of  $\sim 0.025$ , were untreated or treated with rapamycin (200 ng/mL), caffeine (3 mM) or both in YPD. All cultures were incubated at room temperature with agitation for 12 hours. The culture density was measured by Coulter counter every two hours from time 0 (the addition of the drugs). The growth rate was calculated between two and 12 hours after the introduction of the drugs and calculated relative to the average growth rate of untreated wild-type cultures ( $0.4 \text{ hr}^{-1}$ ).  $N=4$  independent cultures; error bars denote S.E.M.; \*  $p < 0.05$ .

For the remainder of this chapter, we will explore the potential origin of the slow rapamycin-insensitive growth rate of *ego*- mutants in more detail.

#### 4.2.11 Ego1p is required for rapamycin-insensitive translation

What could cause the slow rapamycin-insensitive growth rate in *ego*- mutants? Results published by Binda et al. (2009) and Dubouloz et al. (2005) have found that rapamycin appears to induce most TORC1-related physiological changes normally in mutants lacking the EGO complex. A key downstream function of TORC1 activity in supporting proliferation is the promotion and maintenance of protein synthesis (Barbet et al. 1996). It is possible that the reduced rapamycin-insensitive proliferation rate of *ego1Δ* mutants is a consequence of reduced translation rates within these cells. To test this possibility we measured the translation rate in wild-type and *ego1Δ* cells treated (or not) with rapamycin.

Exponentially growing wild-type and *ego1Δ* cultures were untreated, treated with rapamycin (200 ng/mL) or cycloheximide (25 μg/mL) in YPD at room temperature with agitation for six hours. Treatment of yeast with cycloheximide inhibits translation initiation (Obrig & Culp 1971) and therefore was included as a negative control for translation rates. After six hours, cultures were normalised for OD<sub>600nm</sub>, pelleted and resuspended in SD-methionine which was supplemented with a mix of <sup>35</sup>S-labelled methionine and <sup>35</sup>S-labelled cysteine (0.4 MBq) (hereafter referred to as radiolabelled amino acids). Cultures were incubated in the presence of the radiolabelled amino acid mix at room temperature with agitation for 10 minutes. Cells were subsequently chemically lysed on ice, TCA was added to precipitate peptides and peptide samples washed three times with ice-cold acetone. Radiation retained within precipitated peptides was measured by scintillation counter.

We found that the rate of incorporation of radiolabelled amino acids into peptides from untreated wild-type and untreated *ego1Δ* cells was not significantly different (p=0.61) (Figure 4.15) suggesting that translation rates are similar in these untreated cells. Treatment with cycloheximide, which abolishes translation in yeast, was included as a negative control. Treatment of both wild-type and *ego1Δ* mutants with cycloheximide resulted in a barely detectable level of precipitated radiolabel (Figure 4.15).

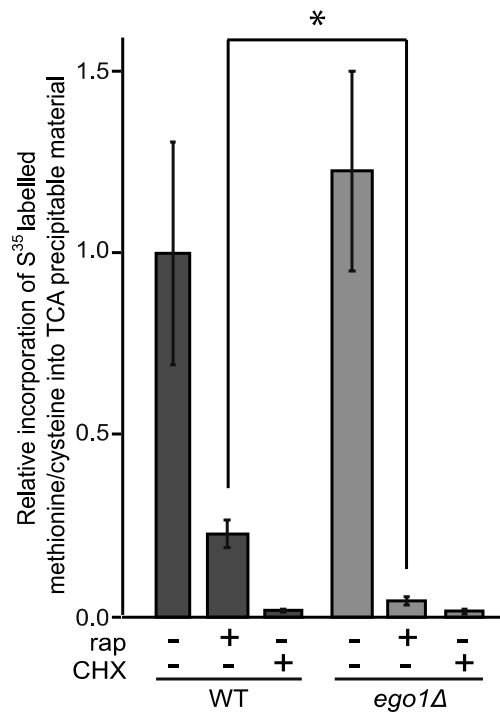


**Figure 4.15 Translation rates of rapamycin and cycloheximide treated wild-type and *ego1Δ* mutant cells**

Exponentially growing wild-type and *ego1Δ* cultures were untreated (at an  $OD_{600nm}$  of  $\sim 0.05$ ), treated with rapamycin (200 ng/mL) (at an  $OD_{600nm}$  of  $\sim 0.2$ ) or cycloheximide (25  $\mu$ g/mL) (at an  $OD_{600nm}$  of  $\sim 0.4$ ) in YPD at room temperature with agitation for six hours. After the six hour treatment period cultures were normalised to an  $OD_{600nm}$  of  $\sim 0.4$  and resuspended in SD-methionine containing a mix of  $^{35}S$ -labelled methionine and  $^{35}S$ -labelled cysteine (0.4 MBq) and incubated for 10 min at room temperature with agitation. Cells were chemically lysed on ice and peptides precipitated using TCA on ice. Retained radiation in TCA precipitable material was measured by Scintillation counter and calculated relative to that of the average untreated wild-type (143,545 CPM). Control readings of media with radiation ranged from 249 to 600 CPM. N=6, three technical repeats of three independent cultures; error bars denote S.E.M.; \*  $p < 0.05$

Treatment of wild-type cells with rapamycin resulted in a decrease in the detection of peptide-associated radiolabelled amino acids (Figure 4.15). The reduction of  $^{35}\text{S}$ -radiolabel detection from wild-type cells suggests that the translation rate is decreased in rapamycin treated cells, consistent with reduced TORC1 activity. We found that rapamycin treated *ego1Δ* cells had a significantly lower incorporation of radiolabelled amino acids into peptides compared to that of rapamycin treated wild-type cells ( $p=0.04$ ). Indeed, the incorporation of radiolabel into peptides from rapamycin treated *ego1Δ* cells was not significantly different to that of cycloheximide treated *ego1Δ* cells ( $p=0.12$ ) (Figure 4.15). These results suggest that the translation rate of rapamycin treated *ego1Δ* mutants is reduced to basal levels in the presence of the drug. It appears that residual TORC1 activity in rapamycin treated cells is required to maintain translation that in turn is likely to support rapamycin-insensitive proliferation.

#### 4.2.12 Growth rate of *caf20Δ* and *eap1Δ* in the presence of a high concentration of rapamycin

Rapamycin is an incomplete inhibitor of mTORC1 (Feldman et al. 2009; Thoreen et al. 2009), our results suggest that yeast TORC1 is not completely inhibited by rapamycin either. The regulation of the translation inhibitor 4E-BP1 (eIF4E Binding Protein) is one known rapamycin insensitive function of mTORC1 (Feldman et al. 2009; Thoreen et al. 2009). Caf20p and Eap1p are thought to perform the function of 4E-BP1 in yeast, which do not appear to have direct homologs of 4E-BP1 (Altmann et al. 1997; Cosentino et al. 2000; Thomas & Hall 1997). We measured the rapamycin-insensitive growth rate of null mutants lacking either Eap1p or Caf20p to test whether loss of either of these two proteins affects the rapamycin-insensitive growth rate.

Exponentially growing cultures of wild-type, *ego1Δ*, *caf20Δ* and *eap1Δ* cells were treated (or not) with rapamycin (200 ng/mL) in YPD and incubated at 28°C with agitation. At three and six hours following the introduction of rapamycin the density of each culture was measured by spectrometry at  $\text{OD}_{600\text{nm}}$  and the growth rate determined between these two time points. The growth rate of all cultures were calculated relative to the average untreated growth rate of wild-type cultures.

As seen in Figure 4.16 we found no significant difference between the growth rates of untreated *ego1Δ*, *caf20Δ* or *eap1Δ* mutants compared to that of untreated wild-type cultures ( $p=0.55$  for *ego1Δ*,  $0.054$  for *caf20Δ* and  $0.16$  for *eap1Δ*). We found that the growth rate of *caf20Δ* mutants treated with rapamycin was not significantly different ( $p=0.43$ ) to that of wild-type cultures (Figure 4.16). However, we found that the growth rate of rapamycin treated *eap1Δ* was significantly slower ( $p=0.008$ ) compared to that of wild-type cultures. The slow rapamycin-insensitive growth rate of *eap1Δ* cultures was not significantly different to that of rapamycin treated *ego1Δ* cultures ( $p=0.15$ ) (Figure 4.16). These results suggest that Eap1p is required to maintain the wild-type rapamycin-insensitive growth rate. These results are also consistent with Eap1p supporting a rapamycin-insensitive function. It is possible that Eap1p functions downstream of TORC1 via a currently unknown mechanism that is insensitive to rapamycin treatment.

#### 4.2.13 Do wild-type cultures of various genetic backgrounds have a rapamycin-insensitive growth rate?

So far all the yeast strains we have examined have been in the BY4743 genetic background. However, it is possible that the discovery of a rapamycin-insensitive growth rate is a phenomenon of the BY4743 genetic background. We measured the rapamycin-insensitive growth rate of wild-type strains in two alternative genetic backgrounds, W303 and EG123.

Exponentially growing cultures of wild-type (BY4743, W303 or EG123 genetic background) and *ego1Δ* (BY4743 genetic background) cells were treated (or not) with rapamycin (200 ng/mL) in YPD at 28°C with agitation. The culture density was measured by spectrometry at  $OD_{600nm}$  at three and six hours after the introduction of rapamycin and the growth rate calculated.

As seen in Figure 4.17 we found that wild-type cultures in both the W303 and EG123 genetic backgrounds were able to maintain some proliferation in the presence of rapamycin. It would appear that the W303 wild-type cultures were hypersensitive to rapamycin and had a significantly slower rapamycin-insensitive growth rate in the presence of 10 ng/mL of the drug compared to that of equivalently treated BY4743 wild-type cultures ( $p=0.002$ ) (Figure 4.17).

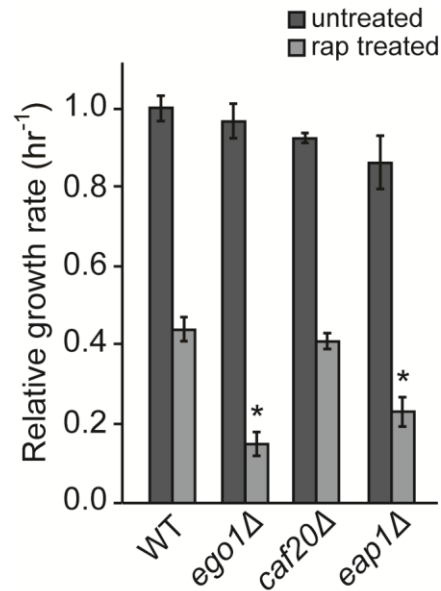


**Figure 4.16** The rapamycin-insensitive growth rates of *caf20Δ* and *eap1Δ* cultures in the presence of rapamycin (200 ng/mL)

Exponentially growing cultures of wild-type, *ego1Δ*, *caf20Δ* and *eap1Δ* cells were normalised to an OD<sub>600nm</sub> of ~0.05 and untreated or normalised to an OD<sub>600nm</sub> of ~0.1 and treated with rapamycin (200 ng/ml) in YPD and incubated at 28°C with agitation. The culture density was measured at three and six hours after the introduction of rapamycin by spectrometry at OD<sub>600nm</sub> and the growth rate calculated between these time points. The growth rate of each culture was calculated relative to the average untreated wild-type growth rate (0.6 hr<sup>-1</sup>). N=10 independent cultures for wild-type cultures, 8 for *ego1Δ* cultures and 3 for *caf20Δ* and *eap1Δ* cultures. Error bars denote S.E.M.; \* p<0.05 compared to equivalently treated wild-type culture.

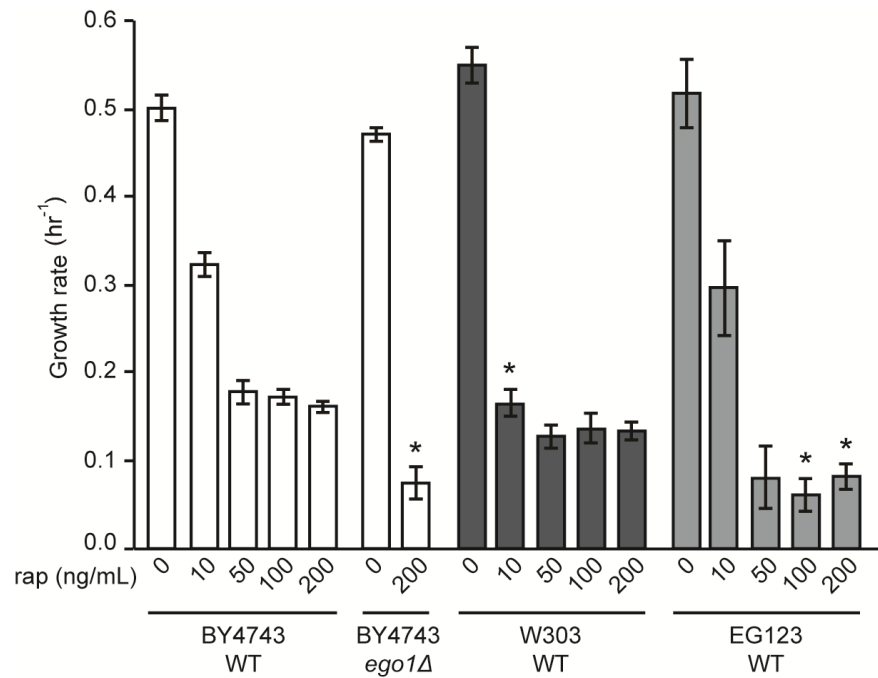


**Figure 4.17 The rapamycin-insensitive growth rate of wild-type strains of various genetic backgrounds**

Exponentially growing cultures of wild-type (BY4743, W303 or EG123 genetic backgrounds) and *ego1Δ* (BY4743 background) cells were normalised to an  $OD_{600nm}$  of  $\sim 0.1$ . Normalised cultures were treated (or not) with rapamycin (10, 50, 100 or 200 ng/mL) and incubated at 28°C with agitation for six hours. The culture density was measured by spectrometer at  $OD_{600nm}$  three and six hours after the introduction of rapamycin and the growth rate calculated between these time points. N=3 independent cultures. Error bars denote S.E.M.; \*  $p < 0.05$  relative to the equivalently treated wild-type BY4743 strain.

However at concentrations above 50 ng/mL rapamycin, the rapamycin-insensitive growth rate of W303 wild-type cultures was not significantly different to those of the BY4743 wild-type cultures ( $p=0.06$  in 50 ng/mL, 0.15 in 100 ng/mL and 0.10 in 200 ng/mL rapamycin) (Figure 4.17). We found that the rapamycin-insensitive growth rate of the EG123 wild-type cultures was not significantly different to that of BY4743 wild-type cultures in the presence of 10 or 50 ng/mL rapamycin ( $p=0.68$  in 10 ng/mL and 0.1 in 50 ng/mL rapamycin) (Figure 4.17). However, in concentrations of rapamycin greater than 50 ng/mL, the rapamycin-insensitive growth rate of EG123 wild-type cultures appears slower than those of equivalently treated BY4743 wild-type cultures ( $p=0.01$  in 100 ng/mL and 0.02 in 200 ng/mL rapamycin) (Figure 4.17). We therefore conclude that all wild-type strains tested are able to maintain proliferation in the constant presence of high concentrations of rapamycin, albeit at a slower rate compared to untreated cultures. It would appear that sensitivity to low concentrations of rapamycin is different with regards to the strain background. The growth rate of cultures in the presence of high concentrations of rapamycin (in this case concentrations of 50 ng/mL and above) also appears to be slower in the EG123 wild-type cultures compared to those of the BY4743 or W303 wild-type cultures.

### 4.3 Conclusion

In this chapter, we have identified a novel phenotype of yeast in response to rapamycin; the rapamycin-insensitive proliferation. The ability of yeast to maintain proliferation in the constant presence of rapamycin suggests that rapamycin is not a complete inhibitor of TORC1 in yeast. The use of alternative mTORC1 inhibitors (which, unfortunately, are not effective in yeast (Liu et al. 2012)) has shown that mTORC1 is not completely inhibited by rapamycin treatment; rapamycin-treated mammalian cells exhibit a milder phenotype than those treated with alternative inhibitors (Feldman et al. 2009; Thoreen et al. 2009). The results presented here suggest that yeast TORC1 more closely resembles mTORC1 than previously thought.

We find that the rapamycin-insensitive growth rate of yeast cultures is observable when growth rates are calculated from the culture density, as measured by Coulter counter or as measured by optical spectrometry. We also

find that a slow rapamycin-insensitive growth rate is observed when cultures are incubated at room temperature, 28°C or 37°C. The observation of a rapamycin-insensitive growth rate is not specific to the BY4743 genetic background; we have also observed residual growth of wild-type cultures in the W303 and EG123 strain backgrounds in the presence of high concentrations of rapamycin.

To confirm that TORC1 is not fully inactivated in rapamycin-treated yeast cells we established the phenotype of cells that lacked the essential TORC1 component Kog1p. We found that freshly dissected *kog1Δ* mutant cells failed to proliferate one day after dissection. A short burst of proliferation was seen for 20% of *kog1Δ* mutants within the first day; however, this was rapamycin inhibitable and is thus likely to be due to intact TORC1 being inherited by meiosis and sustaining limited proliferation. No proliferation was observed for *kog1Δ* mutants that were dissected onto plates containing a high concentration of rapamycin. The phenotype of cells lacking Kog1p demonstrates that yeast cells are unable to proliferate in the complete absence of Kog1p and by inference, TORC1 activity. That we see proliferation occurring in both wild-type and *ego-* mutants in the presence of rapamycin strongly suggests that some residual TORC1 activity remains following treatment with high concentrations of the drug.

We find that there is a significant difference in the rapamycin-insensitive growth rates of wild-type and *ego-* mutant cultures; *ego-* mutants proliferate much slower in the presence of rapamycin. This slow rapamycin-insensitive growth rate of *ego-* mutants appears to be the first phenotype identified in which *ego-* mutants differ to wild-type cultures in response to short rapamycin treatment times - a clear growth rate defect can be observed within six hours after the addition of rapamycin.

Reduction of TORC1 activity by means of either genetic or chemical manipulation has shown that the ability of yeast to proliferate in the presence of rapamycin does indeed require TORC1 activity. The measurement of rapamycin-insensitive growth rate in *tor1Δ*, *tco89Δ* and *kog1<sup>ts</sup>* mutants or a combined rapamycin/caffeine treatment of wild-type cultures has shown that reduction of TORC1 activity in addition to rapamycin treatment results in a slower rapamycin-insensitive growth rate. The slow rapamycin-insensitive growth rate of *ego-*

mutants is therefore likely to be due to low TORC1 activity in these cells, perhaps as a result of loss of signalling to TORC1 by the EGO complex.

TORC1 is a regulator of translation initiation (Barbet et al. 1996; Urban et al. 2007), we therefore measured the translation rate of wild-type and *ego1Δ* mutants treated with rapamycin as a measure of TORC1 activity. We found that translation rates were indeed lower in *ego1Δ* rapamycin treated cells compared to that of rapamycin treated wild-type cells. These results suggest that TORC1 activity is more severely reduced in *ego*- mutants in the presence of rapamycin compared to that of wild-type cells. It would be worth considering in the future to perform a time-course assay to monitor how long after the addition of rapamycin translation is inhibited and at what time after the addition of rapamycin the *ego1Δ* mutants have a slower translation rate compared to that of wild-type cells. It is possible that the slow translation rate of *ego1Δ* mutants treated with rapamycin is influencing the proliferation rate of these mutants. We find that there is an approximate 5.9 (+/- 3.5, SD) fold decrease in the translation rate of rapamycin treated *ego1Δ* cells compared to that of wild-type cells. We also find that the slow rapamycin-insensitive growth rate of *ego1Δ* cultures is approximately 4.9 (+/- 1.0, SD) times slower than that of wild-type cultures. Indeed, in the previous chapter (3.2.3), we found that *ego1Δ* cells treated with rapamycin for 24 hours resulted in a 4.7 (+/- 2.1, SD) fold decrease in amino acid uptake compared to that of *ego1Δ* cells treated with rapamycin for two hours. The similarity in the fold decrease in these three variables in *ego1Δ* cells suggests that these processes could be a result of a common denominator, one possibility being low TORC1 activity.

We propose that rapamycin treatment inactivates TORC1 activity which quickly results in a decrease in the translation rate. This decreased translation rate then has an almost immediate effect (within two hours) on slowing the proliferation rate. The defect in amino acid uptake of *ego1Δ* cells responds more slowly to reduced TORC1 activity as a result of rapamycin treatment, but eventually reaches a similar fold decrease as that seen for the translation rate and proliferation rate. The response of amino acid uptake to low TORC1 activity is not necessarily a result of the continued presence of rapamycin in the external media, we found that the uptake of amino acids into *ego1Δ* cells 24

hours after a “recovery period” was similar to that of cells following a 24 hour exposure to the drug. This observation suggests that TORC1 activity is maintained at a lower activity state in *ego1Δ* cells during a “recovery period” either as a result of persistence of the drug or an inability to reactivate TORC1. Either of these possibilities could impact the ability of *ego1Δ* cultures to recover from rapamycin treatment.

It is possible that the ability to proliferate in the presence of rapamycin impacts the ability of yeast cells to recover from rapamycin treatment. Our data imply that TORC1 activity is excessively reduced in *ego-* mutants, possibly with an approximately 5-fold decrease, compared to that of wild-type cells treated with the drug. The identification of a rapamycin-insensitive growth defect in *ego-* mutants and that the slow growth rate is potentially a result of decreased TORC1 activity could be used to further explore the inability of *ego-* mutants to recover from rapamycin treatment.

## 5 Rapamycin-insensitive proliferation underpins recovery from rapamycin

### 5.1 Introduction

We have identified a novel rapamycin-insensitive growth rate that is absolutely dependent on rapamycin-insensitive activity of TORC1. Mutants lacking a functional EGO complex are compromised in both rapamycin-insensitive TORC1 activity and in the ability to recover from the drug. Is it possible that the slow rapamycin-insensitive growth rate of *ego-* mutants in the presence of rapamycin somehow compromises their ability to recover following drug washout?

### 5.2 Results

#### 5.2.1 Can we invoke a rapamycin recovery defect in wild-type cells?

In the previous chapter we found that treatment of wild-type cultures with a sub-inhibitory concentration of caffeine selectively compromised rapamycin-insensitive growth. Caffeine treatment thus mimics *ego-* mutations in this regard. If the slow rapamycin-insensitive growth rate of *ego-* mutants compromises their ability to recover from the drug, then maintaining wild-type cells in the presence of a sub-inhibitory concentration of caffeine should be sufficient to invoke a rapamycin recovery defect.

Exponentially growing wild-type cultures were treated (or not) with rapamycin (200 ng/mL), caffeine (3 mM) or both in YPD at room temperature with agitation for two hours. Cells were washed three times in either plain YPD or YPD containing caffeine (3 mM) as appropriate before ten-fold serial dilutions were created in the appropriate media and spotted onto both a plain YPD plate and a YPD plate containing caffeine (3 mM). The plates were incubated at 30°C for two days.

The period in which cultures were exposed to the drug(s) we term the 'treatment' phase. Following the treatment phase, cells were washed, referred to as 'drug washout', to remove any external drug from the media, plated onto YPD plates and incubated; this incubation time is referred to as the 'recovery'

phase, *i.e.* the incubation period following washout of drugs from the media. We found that wild-type cells treated with both rapamycin and caffeine during the treatment phase were able to recover in the absence of any drug during the recovery phase (Figure 5.1). These results suggest that a slow rapamycin-insensitive growth rate during the treatment phase alone does not prevent recovery from rapamycin. To maintain low TORC1 activity during the recovery phase, *i.e.* mimicking the state of an *ego-* mutant, wild-type cells were maintained in the presence of caffeine (3 mM) for the duration of the recovery phase. Following a combined rapamycin and caffeine treatment phase and incubation in the constant presence of caffeine for the recovery phase, we found that wild-type cells were unable to recover (Figure 5.1). These results show that maintaining low TORC1 activity, due to the presence of a sub-inhibitory concentration of caffeine, during the treatment phase and recovery phase is sufficient to mimic the phenotype of *ego-* mutants in wild-type cells with regards to rapamycin recovery.

When is TORC1 activity required to permit recovery from rapamycin? The presence of caffeine during both the treatment and recovery phase prevents wild-type cells recovering from rapamycin. We tested the ability of cells to recover following treatment with rapamycin alone and the subsequent recovery phase occurring in the presence of caffeine. We found that wild-type cells were unable to recover from this treatment (Figure 5.1). These results suggest that TORC1 activity is specifically required during the recovery phase to enable cells to recover from rapamycin.

The ability of cells to recover from both a rapamycin and caffeine treatment suggests that it is not the slow growth rate of cultures in the drugs *per se* that prevents recovery, but rather insufficient TORC1 activity during the recovery phase. It is therefore possible that the inability of *ego-* mutants to recover from rapamycin treatment is a result of low TORC1 activity during the recovery phase.

Whilst it has been shown that TORC1 is the predominant target of caffeine in yeast (Reinke et al. 2006; Wanke et al. 2008) it is possible that off-target effects of the drug hinder the recovery of wild-type cells in the presence of both rapamycin and caffeine.

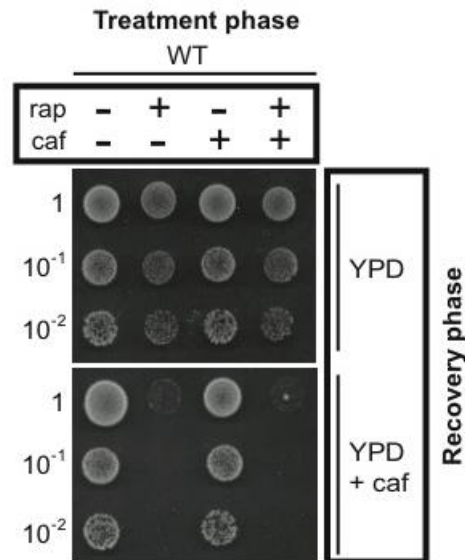


**Figure 5.1 Recovery of wild-type cells from rapamycin treatment in the presence of caffeine**

Exponentially growing wild-type cells at an  $OD_{600nm}$  of  $\sim 0.1$  were treated (or not) with rapamycin (200 ng/mL), caffeine (3 mM) or both in YPD at room temperature with agitation for two hours for the treatment phase. Cells were washed three times in fresh media or media containing caffeine (3 mM) as appropriate and ten-fold serial dilutions were plated (5  $\mu$ L) onto plain YPD or YPD plates containing caffeine (3 mM). Plates were incubated at 30°C for two days for the recovery phase.

To ensure that off-target effects of caffeine do not prevent the recovery of wild-type cells from rapamycin, we repeated the rapamycin recovery assay using wild-type cells expressing a caffeine resistant allele of *tor1* (*tor1*<sup>11954V</sup> (Reinke et al. 2006)).

Wild-type cells expressing either the wild-type *TOR1* gene or the caffeine resistant *tor1*<sup>11954V</sup> allele were grown overnight in selective media. Once in an exponential growth phase, cultures were treated (or not) with rapamycin (200 ng/mL), caffeine (3 mM) or both in YPD at 28°C with agitation for a two hour treatment phase. Cells were washed three times in YPD and ten-fold dilutions were spotted to either a plain YPD plate or a YPD plate containing caffeine (3 mM). Plates were incubated at 28° for two days for a recovery phase.

As seen in Figure 5.2 wild-type cells expressing either *pTOR1* or *ptor1*<sup>11954V</sup> were able to recover from all treatments tested when plated onto plain YPD. We found that wild-type cells expressing the caffeine resistant *tor1*<sup>11954V</sup>, but not the wild-type *TOR1* allele, recovered from rapamycin treatment when the recovery phase was carried out in the continuous presence of caffeine (Figure 5.2). We therefore conclude that caffeine is inhibiting the ability of wild-type cells to recover from rapamycin due to specifically targeting, and reducing, TORC1 activity.

### 5.2.2 The rapamycin-insensitive growth rate persists following washout of the drug

TORC1 activity is somehow required during the recovery phase for cells to recover from rapamycin. Is it possible that the effects of rapamycin (or rapamycin itself) are maintained following washout of rapamycin from the medium? Does the slow rapamycin-insensitive growth rate persist following washout of the drug?

Exponentially growing cultures of wild-type and *ego1Δ* cells were treated (or not) with a high concentration of rapamycin (40 ng/mL) in YPD and incubated at room temperature with agitation.

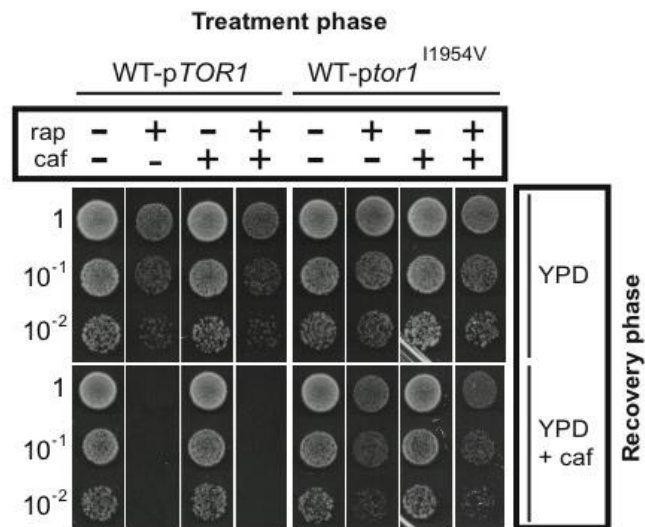


**Figure 5.2 Recovery of wild-type cells from rapamycin when expressing a caffeine resistant *tor1*<sup>I1954V</sup> allele in the presence of caffeine**

Wild-type cells containing either *pTOR1*, *ptor1*<sup>I1954V</sup> were grown overnight in selective media. Whilst in an exponential growth phase the cells were normalised to an OD<sub>600nm</sub> of ~0.1 and transferred into YPD. Normalised cultures were treated (or not) with rapamycin (200 ng/mL), caffeine (3 mM) or both and incubated at 28°C with agitation for a two hour treatment phase. Cells were washed three times in fresh YPD and ten-fold serial dilutions were plated (5 µL) onto plain YPD or YPD plates containing caffeine (3 mM). Plates were incubated at 30°C for two days for the recovery phase.

Two hours after the introduction of rapamycin, cells were washed three times with fresh drug-free media, inoculated into fresh YPD and incubated at room temperature with agitation for a 12 hour 'recovery phase'. Control cultures of untreated exponentially growing cultures in YPD, incubated at room temperature with agitation were included. The culture density was measured by Coulter counter and the  $\text{Log}_2$  of the relative culture density to the average at the time of rapamycin washout is shown.

As seen in Figure 5.3A we found that over the course of 12 hours after washout of rapamycin, the growth rate of wild-type cultures remained slow and stable. Indeed the growth rate of wild-type cultures observed during this recovery period looked remarkably similar to that of the rapamycin-insensitive growth rate of wild-type cultures seen in the constant presence of a high concentration of rapamycin (Figure 4.1). We also found that the growth rate of *ego1Δ* cultures during the recovery period remained slow and stable for the 12 hours monitored (Figure 5.3B). The growth rate of *ego1Δ* cultures following a two hour rapamycin treatment again resembled that of *ego1Δ* cultures in the constant presence of a high concentration of rapamycin (Figure 4.6). These observations suggest that the effects of rapamycin can persist for many hours following washout of the drug from the medium. Neither the growth rate of wild-type nor *ego1Δ* cultures appears to change over the 12 hours monitored.

### 5.2.3 Monitoring rapamycin in cells using mass spectrometry

Does rapamycin persist in cells following washout of the drug from the medium? We can use a mass spectrometry approach to monitor the cell-associated rapamycin pool (for example see Taylor & Johnson (1998)). Here, we measured the unmodified parent ion of cell-associated rapamycin extracted from yeast cultures, *i.e.* the chemically and metabolically unmodified drug.

During optimisation of the mass spectrometry experiment, we initially attempted to detect the presence of cell-associated rapamycin in yeast cells treated for two hours with rapamycin (200 ng/mL), our standard conditions. However, to maximise the detectable signal we chose to treat cells with a higher concentration of rapamycin (400 ng/mL) for four hours.

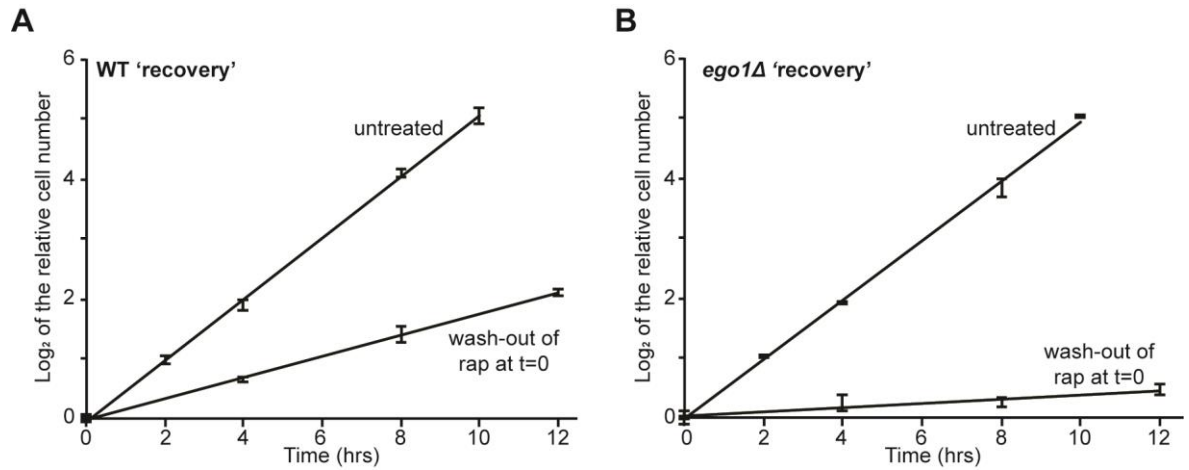


**Figure 5.3 The rapamycin-insensitive growth rate of cultures maintains after washout of the drug**

Exponentially growing cultures of wild-type and *ego1Δ* cells were normalised to an  $OD_{600nm}$  of  $\sim 0.1$  in YPD. Normalised cultures were treated (or not) with rapamycin (40 ng/mL) in YPD and incubated at room temperature with agitation for two hours. Rapamycin treated cells were subsequently washed three times in fresh YPD and inoculated into fresh media to 'recover' at room temperature with agitation (time of rapamycin washout:  $t=0$ ). Untreated cultures were maintained at room temperature with agitation as a control. Cultures were diluted as necessary with fresh media to maintain exponential growth. The culture density was measured by Coulter counter with time and the  $\text{Log}_2$  of the relative culture density (to the average at the time of rapamycin washout) is shown with a line of best fit plotted.  $N=3$  independent cultures; error bars denote S.E.M.

It is possible that altering the rapamycin concentration and treatment time affects the behaviour of cultures with regards to rapamycin recovery. A rapamycin recovery assay was carried out on wild-type and *ego1Δ* cultures following a four hour rapamycin (400 ng/mL) treatment: exponentially growing wild-type and *ego1Δ* cultures were treated (or not) with rapamycin (200 or 400 ng/mL) in YPD and incubated at 28°C with agitation for four hours. Cells were washed three times with fresh YPD before being spotted onto a YPD plate which was incubated at 28°C for two days. As seen in Figure 5.4 we found that wild-type cells were able to recover from a four hour rapamycin treatment (either 200 ng/mL or 400 ng/mL) whereas the *ego1Δ* mutant cells were unable to do so. Treatment of cells with a higher concentration of rapamycin for four hours does not therefore affect the ability of yeast cells to recover.

Detection of extracted cell-associated rapamycin was carried out in collaboration with Dr. Karl Burgess of the University of Glasgow Polyomics Facility. I ran many of the samples through the mass spectrometer myself (having been taught the procedure by Dr. Burgess) whilst others were run by Dr. Burgess. Optimisation of the conditions required to detect rapamycin by mass spectrometry were carried out by Dr. Burgess and myself. The identification of rapamycin peaks and determination of signal intensities was carried out by Dr. Burgess or Dr. Stephan Weidt (also of the University of Glasgow Polyomics Facility). Further analysis of the identified rapamycin signal peaks was carried out by myself.

To monitor the cell-associated pool of rapamycin, exponentially growing wild-type and *ego1Δ* cultures were treated with rapamycin (400 ng/mL) in YPD for four hours at room temperature with agitation. After four hours, cells were washed three times with fresh YPD, inoculated into fresh media and incubated at room temperature with agitation for the 'recovery phase'. Cell pellets equivalent to ~10 OD<sub>600nm</sub> units were collected at time 0 (the time of rapamycin washout), seven hours and 20 hours after drug washout. The pellets were washed three times in ice-cold water and cells lysed by vortexing in ice-cold water and an equal volume of glass beads. Rapamycin was extracted from the cell lysate into ethyl acetate. Detection of rapamycin by mass spectrometry was carried out in negative ionisation mode following retention on a C18 column.

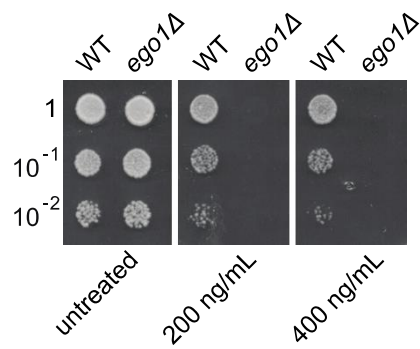


**Figure 5.4 Recovery of wild-type and *ego1Δ* from 400 ng/mL rapamycin**

Exponentially growing WT and *ego1Δ* cultures at an OD<sub>600nm</sub> of ~0.1 were treated (or not) with rapamycin (200 ng/mL or 400 ng/mL) in YPD at 28°C with agitation for four hours. Cells were washed three times in fresh YPD after which ten-fold serial dilutions were created and spotted (5 µL) onto a YPD plate to recover. Plates were incubated at 28°C for two days.

The identity of rapamycin signal peaks was confirmed by retention time, mass and fragment pattern compared to an authentic standard.

It is possible that loss of the EGO complex results in an increased uptake of rapamycin into these mutant cells compared to that of wild-type cells. The total cell-associated pool of rapamycin was measured for both wild-type and *ego1Δ* mutant cells at  $t=0$ , *i.e.* the time of washout of rapamycin following the treatment period. As seen in Figure 5.5 we found no significant difference ( $p=0.36$ ) in the cell-associated pool of rapamycin between wild-type and *ego1Δ* cells.

We found that the cell-associated pool of rapamycin in wild-type cells decreased slowly during the recovery period (Figure 5.6). Indeed, we found that 20 hours after washout of the drug the cell-associated pool of rapamycin in wild-type cells had only decreased to approximately a third of that at the time of washout ( $p=0.002$  at 20 hours compared to time 0) (Figure 5.6). We found that the cell-associated pool of rapamycin also decreased slowly, possibly more slowly, in *ego1Δ* mutants recovering from rapamycin treatment (Figure 5.6). We therefore conclude that rapamycin itself remains associated with cells for a long time following washout of the drug from the media, and to a significant extent in both wild-type and *ego1Δ* mutants. It is therefore likely that the persistence of the rapamycin-insensitive growth rate into the recovery phase is a result of the persistence of the drug in the cell.

The cell-associated pool of rapamycin decreased slowly during the recovery period. Is it possible that rapamycin is not actively detoxified in yeast, but is instead diluted among progeny cells due to continued, slow proliferation? The culture density of both wild-type and *ego1Δ* cultures was monitored during the above recovery experiment (Figure 5.7). The total amount of cell-associated rapamycin present in the culture during recovery was estimated by normalising the cell-associated pool of rapamycin for the culture density at each time point (Figure 5.8). We found that the density of wild-type cultures doubled approximately one and a half times during the 20 hour recovery phase (Figure 5.7), consistent with these cells proliferating very slowly.

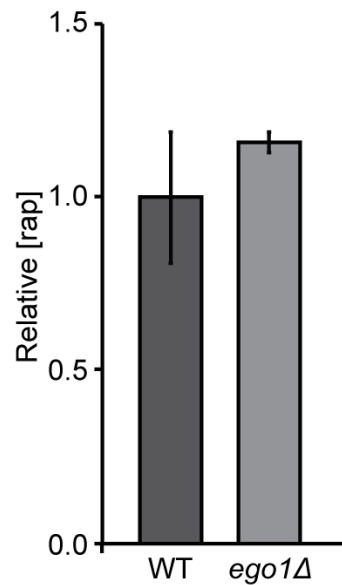


**Figure 5.5 Uptake of rapamycin into wild-type and *ego1Δ* cells**

Exponentially growing wild-type and *ego1Δ* cultures at an  $OD_{600nm}$  of ~0.6 were treated with rapamycin (400 ng/mL) in YPD at room temperature with agitation for four hours after which cells were washed three times in YPD. Cell pellets equivalent to ~10  $OD_{600nm}$  units were washed three times with ice-cold water before being physically lysed in an equal volume of glass beads and ice-cold water by vortexing. Rapamycin was extracted from the lysate into ethyl acetate and measured by mass spectrometry. Signal intensities were calculated relative to the average wild-type signal (1,124,479 a.u.). N=3 independent cultures, error bars denote S.E.M.

*Mass spectrometry was carried out in collaboration with Dr. Burgess and Dr. Weidt of the University of Glasgow Polyomics Facility.*

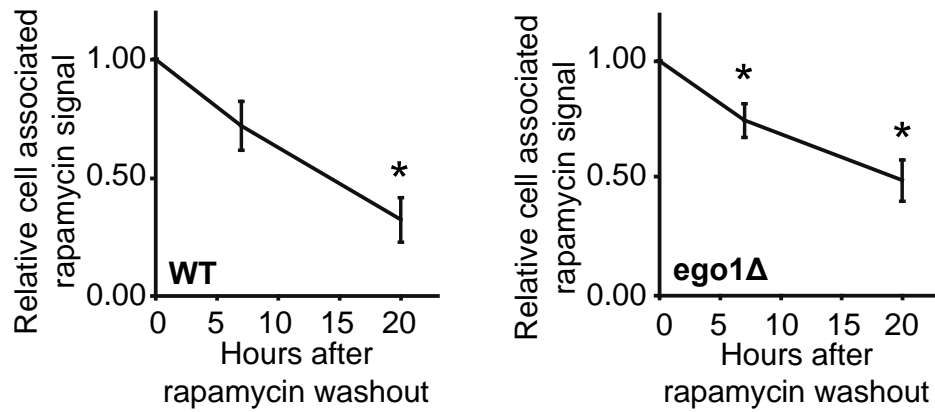


**Figure 5.6 Cell associated rapamycin during a ‘recovery phase’ from rapamycin treatment**

Exponentially growing wild-type and *ego1Δ* cultures at an  $OD_{600nm}$  of  $\sim 0.6$  were treated with rapamycin (400 ng/mL) in YPD and incubated at room temperature for four hours. Cells were then washed three times with YPD and inoculated into fresh media (time 0) and incubated at room temperature with agitation for the ‘recovery phase’. At time 0, 7 and 20 hours following the washout of rapamycin cell pellets equivalent to  $\sim 10 OD_{600nm}$  units were pelleted and washed three times in ice-cold water. Cells were lysed by vortexing in an equal volume of ice-cold water and glass beads. Rapamycin was extracted into ethyl acetate, a sample of which was passed through a mass spectrometer. The rapamycin mass spectrometry signal was calculated relative to that at time 0 (values ranged from 62,264 to 1,551,834 a.u.).  $N=5$  independent cultures; error bars denote S.E.M.; \*  $p < 0.05$  relative to time 0.

*Mass spectrometry was carried out in collaboration with Dr. Burgess and Dr. Weidt of the University of Glasgow Polyomics Facility.*

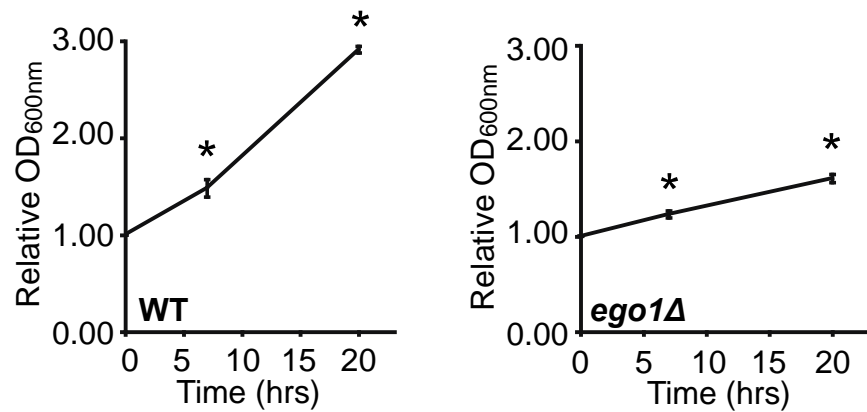


**Figure 5.7 Increase in culture density during recovery from rapamycin**

Exponentially growing wild-type and *ego1Δ* cultures at an OD<sub>600nm</sub> of ~0.6 were treated with rapamycin (400 ng/mL) in YPD and incubated at room temperature for four hours. Cells were then washed three times with fresh YPD and inoculated into fresh media (time 0) and incubated at room temperature with agitation for the 'recovery phase'. At time 0, 7 and 20 hours following the removal of rapamycin the density of each culture was measured by spectrometry at OD<sub>600nm</sub> and calculated relative to that at time 0 which ranged from 0.6-1.23 OD<sub>600nm</sub>. N=5 independent cultures; error bars denote S.E.M.; \* p<0.05 relative to time 0.

When the total amount of cell-associated rapamycin in wild-type cells was calculated we found that there was no significant change in the amount of cell-associated rapamycin during the 20 hours monitored ( $p=0.68$  at seven and  $0.8$  at 20 hours compared to time 0) (Figure 5.8). As the mass spectrometer is only able to detect the unmodified parent ion, these results imply that rapamycin is not metabolised in, nor exported from, wild-type cells during recovery. The growth rate of *ego1Δ* cultures was also monitored during the recovery phase and the cultures barely doubled during the recovery phase (Figure 5.7). The total amount of cell-associated rapamycin again did not appear to change significantly over the 20 hours monitored ( $p=0.41$  at seven and  $0.16$  at 20 hours compared to that at time 0) (Figure 5.8). The observable cell-associated pool of rapamycin is remarkably stable in both wild-type and *ego1Δ* cells, strongly suggesting that rapamycin is not actively detoxified in yeast cells.

We conclude that the observable pool of rapamycin is not significantly metabolised by yeast cells, but is slowly diluted between an increasing number of progeny cells. The lack of any apparently active detoxification within cells suggests that yeast may recover from the drug by a ‘dilution-by-proliferation’ mechanism. Such a ‘dilution-by-proliferation’ mechanism would rely on the ability of cells to maintain proliferation in the presence of the drug. Therefore the slow rapamycin-insensitive growth rate observed for *ego1Δ* mutants could help explain their inability to recover from rapamycin treatment.

#### 5.2.4 Can *ego*- mutants recover from rapamycin?

If rapamycin is detoxified by a dilution-by-proliferation mechanism, then the ability of cells to recover is dependent on both the size of the intracellular drug pool and on the rapamycin-insensitive growth rate. Cells lacking the EGO complex are still able to proliferate in the presence of high concentrations of the drug, albeit more slowly. Therefore, we predict that *ego*- mutants should be able to recover from lower concentrations of rapamycin, but concentrations that still induce hallmarks of inactive TORC1. The ability of *ego1Δ* and *gtr2Δ* mutants to recover from various high concentrations of rapamycin was tested.

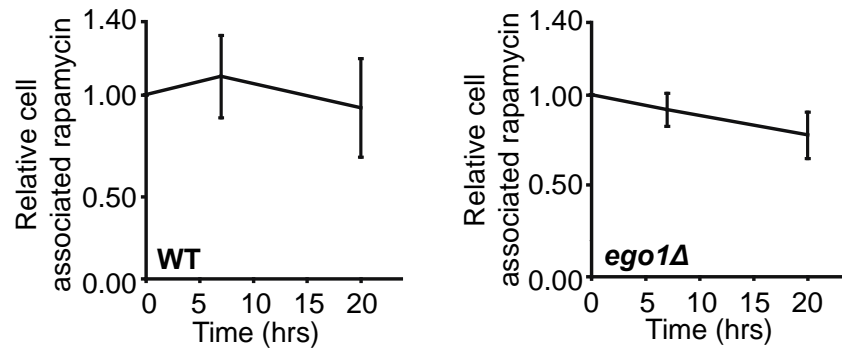


**Figure 5.8** The total intracellular concentration of rapamycin present during the ‘recovery phase’

The total cell-associated concentration of rapamycin was calculated by normalising the relative cell-associated rapamycin signal from Figure 5.6 to the increase in culture density from Figure 5.7 for each time point measured. The total concentration of cell associated rapamycin was calculated relative to that present at time 0 (values ranged from 62,264 to 1,551,834 a.u). N=5 independent cultures; error bars denote S.E.M.

*Mass spectrometry was carried out in collaboration with Dr. Burgess and Dr. Weidt of the University of Glasgow Polyomics Facility.*

Exponentially growing cultures of wild-type, *ego1Δ* and *gtr2Δ* cells were treated (or not) with rapamycin (20, 50, 100 and 200 ng/mL) in YPD at room temperature with agitation for two hours. Cells were washed three times with fresh YPD and ten-fold serial dilutions were spotted to a YPD plate. Plates were incubated at 30°C and colony formation was determined after two days. As seen in Figure 5.9 wild-type cells were able to recover from all concentrations of rapamycin tested consistent with our previous results. We found that cells lacking either Ego1p or Gtr2p failed to recover from concentrations of rapamycin greater than 50 ng/mL (Figure 5.9). However, we found that *ego1Δ* and *gtr2Δ* mutants were in fact able to recover from a 20 ng/mL rapamycin treatment. These results suggest that the ability of *ego*- mutants to recover from rapamycin is not an absolute property of the mutants but is potentially dependent on the size of the intracellular pool of the drug.

If, as it appears, the ability of *ego*- mutants to recover from rapamycin is dependent on the size of the intracellular pool of the drug, an alternative method to vary this pool would be to vary the treatment time. A rapamycin recovery spot assay was carried out as above using high concentrations of rapamycin (20-200 ng/mL) and treatment times of 15-240 minutes. The ability to recover was scored as full growth (+++) to no growth (-) and the results are shown in Table 5.1. Wild-type cells were able to recover from all treatments tested (Table 5.1). We found that *ego1Δ* and *gtr2Δ* cells could also recover from treatment with high (greater than 20 ng/mL) concentrations of rapamycin, but only if such treatments were for shorter amounts of time (Table 5.1). As the concentration of rapamycin increased in the media, the exposure time required to induce a recovery defect of *ego1Δ* and *gtr2Δ* cells decreased (Table 5.1). The discovery that the ability of *ego*- mutants to recover from rapamycin is dependent on both the treatment time and the drug concentration strongly implies that the size of the intracellular pool of rapamycin is crucial for recovery. These results also suggest that the *ego*- mutant recovery defect is a quantitative defect (*i.e.* varies by degree and as a function of the size of the cell-associated drug pool), rather than being a qualitative defect (*i.e.* yes or no).

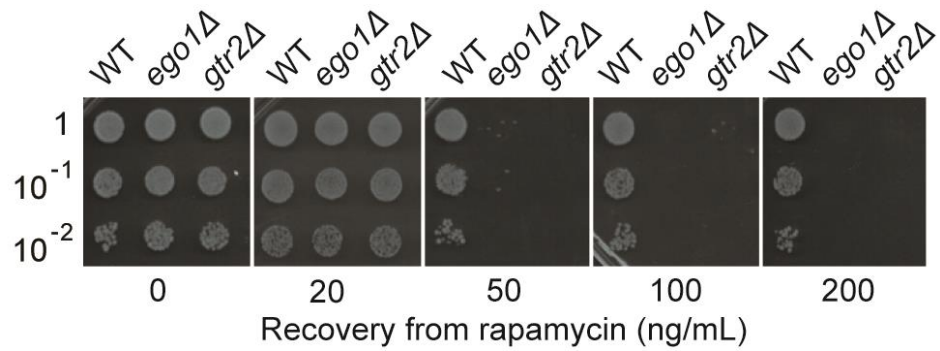


**Figure 5.9 Recovery of wild-type and *ego*- mutants from various concentrations of rapamycin**

Exponentially growing wild-type, *ego1Δ* and *gtr2Δ* cultures at an  $OD_{600nm}$  of  $\sim 0.1$  were treated (or not) with rapamycin (20-200 ng/mL) in YPD at room temperature with agitation for two hours. Cells were washed three times in fresh YPD, ten-fold serial dilutions were created and spotted (5  $\mu$ L) onto a YPD plate that was incubated at 30°C for two days.

|                                    |     | [rap]<br>ng/mL | Time (min) |     |     |     |     |     |
|------------------------------------|-----|----------------|------------|-----|-----|-----|-----|-----|
|                                    |     |                | 0          | 15  | 30  | 60  | 120 | 240 |
| WT                                 | 20  |                | +++        | +++ | +++ | +++ | +++ | +++ |
|                                    | 50  |                | +++        | +++ | +++ | +++ | +++ | +++ |
|                                    | 100 |                | +++        | +++ | +++ | +++ | +++ | +++ |
|                                    | 200 |                | +++        | +++ | +++ | +++ | +++ | +++ |
| <i>ego1Δ</i><br>or<br><i>gtr2Δ</i> | 20  |                | +++        | +++ | +++ | +++ | +++ | +++ |
|                                    | 50  |                | +++        | +++ | ++  | +   | -   | -   |
|                                    | 100 |                | +++        | ++  | +/- | -   | -   | -   |
|                                    | 200 |                | +++        | +/- | -   | -   | -   | -   |

**Table 5.1 Recovery from various concentrations of rapamycin with varying treatment times**

Exponentially growing wild-type, *ego1Δ* and *gtr2Δ* cultures at an OD<sub>600nm</sub> of ~0.1 were treated with rapamycin (20, 50, 100 or 200 ng/mL) in YPD at room temperature for 0, 15, 30, 60, 120 or 240 minutes. Cells were washed three times with fresh YPD, ten-fold serial dilutions were created and spotted to a YPD plate which was incubated for two days at 30°C. Colony formation was scored as full growth (+++) to no growth (-).

### 5.2.5 Can we quantify the recovery time?

We have found that the ability of *ego*<sup>-</sup> mutants to recover from rapamycin is concentration dependent (within a range of high concentrations of the drug). Is it possible to quantify the time at which cells, both wild-type and *ego*<sup>-</sup> mutants, recover from rapamycin treatment? Understanding the kinetics of recovery from rapamycin could help determine the underlying ‘detoxification’ mechanism.

Exponentially growing cultures of wild-type and *ego1Δ* cells were treated with various concentrations of rapamycin (20-200 ng/mL for wild-type cultures, 20-40 ng/mL for *ego1Δ* cultures) in YPD and incubated at room temperature with agitation for two hours. Cells were washed three times with fresh media, inoculated into fresh YPD and incubated at room temperature with agitation for a ‘recovery phase’. The culture density of each strain was measured by Coulter counter over a recovery period of 48 hours. The density of untreated cultures and those in the continuous presence of rapamycin (20 or 50 ng/mL) in YPD at room temperature with agitation were also measured for at least 14 hours after the introduction of rapamycin. Results are expressed as semi-Log<sub>2</sub> plots of the culture density with time, relative to the average culture density at the time of rapamycin washout.

Representative plots for both wild-type and *ego1Δ* cultures during a 48-hour recovery period are shown in Figure 5.10; in these particular examples, wild-type cultures were recovering from 100 ng/mL rapamycin whilst *ego1Δ* cultures were recovering from 30 ng/mL rapamycin. A line of best fit has been fitted to the control cultures (untreated and continuously rapamycin treated) and extrapolated where necessary. Each succeeding pair of data points for the relative culture density of recovering cultures were joined by a straight line (Figure 5.10). For the wild-type culture, the growth rate of the recovering culture initially resembled that of the culture in the continuous presence of the drug for up to 18-20 hours following washout of rapamycin (Figure 5.10). Between 18-20 hours, the growth rate of the wild-type culture appeared to switch from that resembling the culture in the continuous presence of the drug to that resembling the untreated culture (Figure 5.10).

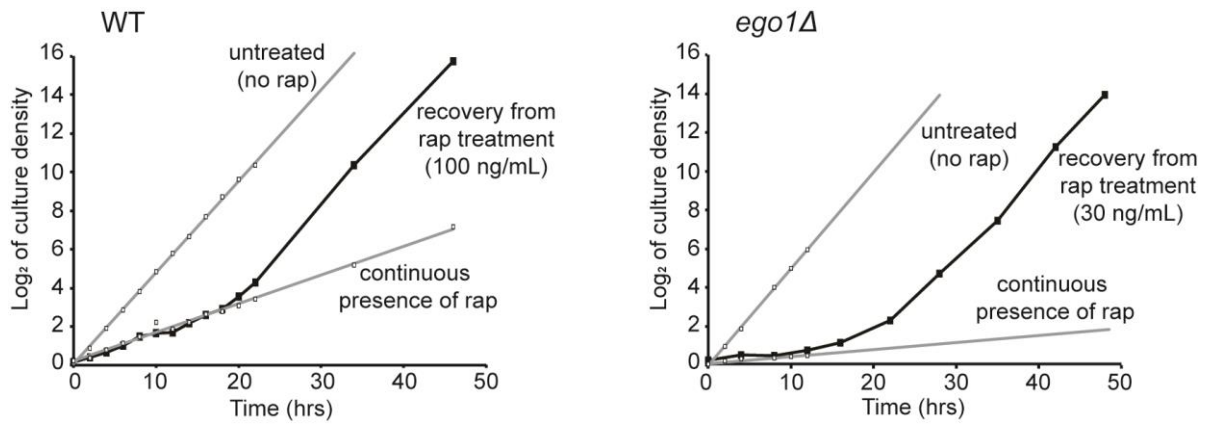


**Figure 5.10 Observing cultures recovering from rapamycin treatment**

Control cultures of exponentially growing wild-type and *ego1Δ* cultures at an  $OD_{600nm}$  of  $\sim 0.1$  were untreated or treated with rapamycin (50 ng/mL for wild-type, 20 ng/mL for *ego1Δ*) in YPD at room temperature with agitation. Cultures were maintained in an exponential growth phase for the duration of the experiment by dilution into the appropriate media, and the culture density adjusted by the appropriate dilution factor. The  $\text{Log}_2$  of the culture density, as measured by Coulter counter, was calculated relative to the culture density at two hours after the addition of rapamycin *i.e.* the time after which the rapamycin-insensitive growth rate is steady (Coulter counter values ranged from 19,901 to 34,927 a.u.). The culture density was measured up to at least 14 hours after the addition of the drug and a line of best fit for each plot is shown. For monitoring the recovery time, exponentially growing wild-type and *ego1Δ* cultures at an  $OD_{600nm}$  of  $\sim 0.1$  were treated with rapamycin (100 ng/mL for wild-type, 30 ng/mL for *ego1Δ*) in YPD at room temperature with agitation for two hours. Cells were subsequently washed three times with fresh media, inoculated into fresh YPD and incubated at room temperature with agitation for a 'recovery phase'. Cultures were maintained in an exponential growth phase for the duration of the experiment by dilution into the appropriate media and the culture density adjusted by the appropriate dilution factor. The  $\text{Log}_2$  of the culture density, as measured by Coulter counter for up to 48 hours after drug washout, was calculated relative the culture density at the time of rapamycin washout (Coulter counter values ranged from 10,953 to 24,656 a.u.) and each data-point is connected by a straight line.

The identification of a clear point of switching in growth rate of the recovering wild-type culture, that appears to occur within one culture doubling, suggests that most of the cells in the culture synchronously recover from the drug treatment, *i.e.* return to full, active proliferation at approximately the same time: the “recovery time”.

The *ego1Δ* cultures, in this case recovering from a lower concentration of the drug, behaved similarly to the recovering wild-type culture in switching from one growth rate to the other within a defined time window corresponding to approximately one cell doubling (Figure 5.10). The mutant culture also behaved as recovering at a particular point: the “recovery time”.

In subsequent systematic analysis, we estimated the recovery time by quantifying the observed lag time between a recovering culture and an equivalent untreated culture (measured in parallel) returning to, or remaining in, rapid exponential growth, see Figure 5.11. Note, in estimating the recovery time, we took into consideration the fact that recovering cells continued to proliferate slowly following washout of rapamycin, therefore we determined the lag time along the slope of the growth rate of continuously treated cultures, as illustrated in Figure 5.11. The lag time to recovery for each individual culture was estimated as the average of three measurements of the lag time on the same dataset, as shown in Figure 5.11. Three such measurements of lag time were made using three independent cultures (experimental replicates) which were averaged to arrive at the final recovery time for each strain.

### **5.2.6 How does the recovery time vary with concentration of rapamycin?**

We can estimate the time at which cultures behave as though recovering from rapamycin. How does this recovery time vary with the concentration of rapamycin treatment? Does a ‘dilution-by-proliferation’ model explain the kinetics of recovery?

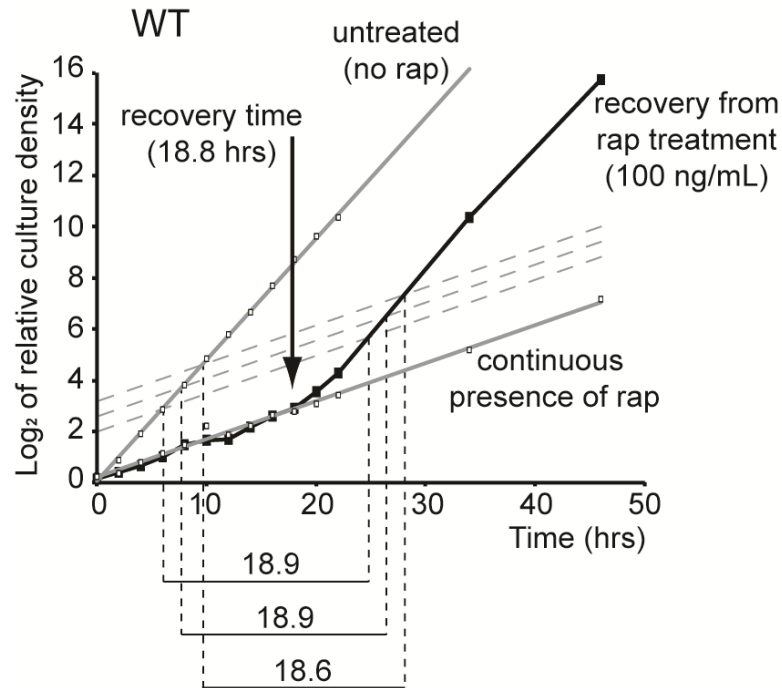


**Figure 5.11 Demonstrating how the lag time to recovery was determined**

The recovering wild-type culture from Figure 5.10 is used to illustrate how the recovery time was determined. The growth rate of the untreated and the continuously treated culture are plotted with a line of best fit for each, whilst each data point for the recovering culture is shown: each sequential pair of data points are joined by a straight line. Three estimates of lag time were measured in a region where the growth rate of the recovering culture clearly matches that of the untreated culture. The slope of the growth rate of the continuously rapamycin treated culture (grown in parallel) was used to estimate lag time: *i.e.* the time delay between points at which the untreated culture and the recovering culture intercept the dashed lines (at the slope of a culture growing in the continuous presence of a high concentration of rapamycin). The lag time was estimated three times and the average calculated to determine the recovery time for each individual culture.

Note that these three cultures: untreated, continuously treated and recovering, were grown in parallel for this experiment and originated from the same overnight culture. Washout of rapamycin occurred at  $t=0$ .

The recovery times of wild-type cultures were measured as described in the previous section (Figure 5.11) in cultures recovering from 20 to 200 ng/mL rapamycin, all high concentrations. As seen in Figure 5.12, the recovery times of wild-type cultures from concentrations of 20-50 ng/mL rapamycin increased with an increasing concentration of the drug in the media. The rate of increase of recovery time with concentration slows at 100 ng/mL rapamycin (Figure 5.12). It took wild-type cells ~20 hours to recover from the highest concentration of rapamycin tested (200 ng/mL) at which point the response seems to saturate (Figure 5.12). It would appear that the recovery time of wild-type cultures is dependent on the concentration of rapamycin present in the media during the (two hour) treatment phase but begins to saturate above approximately 100 ng/mL rapamycin. The discovery that wild-type cultures take approximately 20 hours to recover from rapamycin suggests that the mechanism of reducing the biologically active pool of the drug is incredibly slow, consistent with our model of dilution-by-proliferation.

The recovery times for *ego1Δ* cultures also increased with an increase in rapamycin concentration; however, the rate of increase in recovery time with increasing concentration of drug was much more dramatic compared to that of wild-type cultures (Figure 5.12). We found that *ego1Δ* cultures took much longer to recover from rapamycin than comparably treated wild-type cultures. Indeed, at the highest concentration of rapamycin used to treat *ego1Δ* cultures (40 ng/mL), recovery occurred ~35 hours after washout of the drug, whereas wild-type cultures recovered after ~15 hours from this concentration of rapamycin (40 ng/mL) (Figure 5.12). Due to the length of time it took for *ego1Δ* cultures to recover from 40 ng/mL rapamycin, we did not measure the recovery times from concentrations of rapamycin higher than this. We did not detect any sign of saturation within the concentration range measured for *ego1Δ* cultures (Figure 5.12) but have observed that *ego1Δ* cultures take much longer to recover from rapamycin than wild-type cultures.

Is rapamycin-inhibited TORC1 inherently difficult to reactivate, particularly in the absence of the EGO complex? Is there evidence in Figure 5.12 for an inherent, slow reactivation of TORC1 from rapamycin treatment?

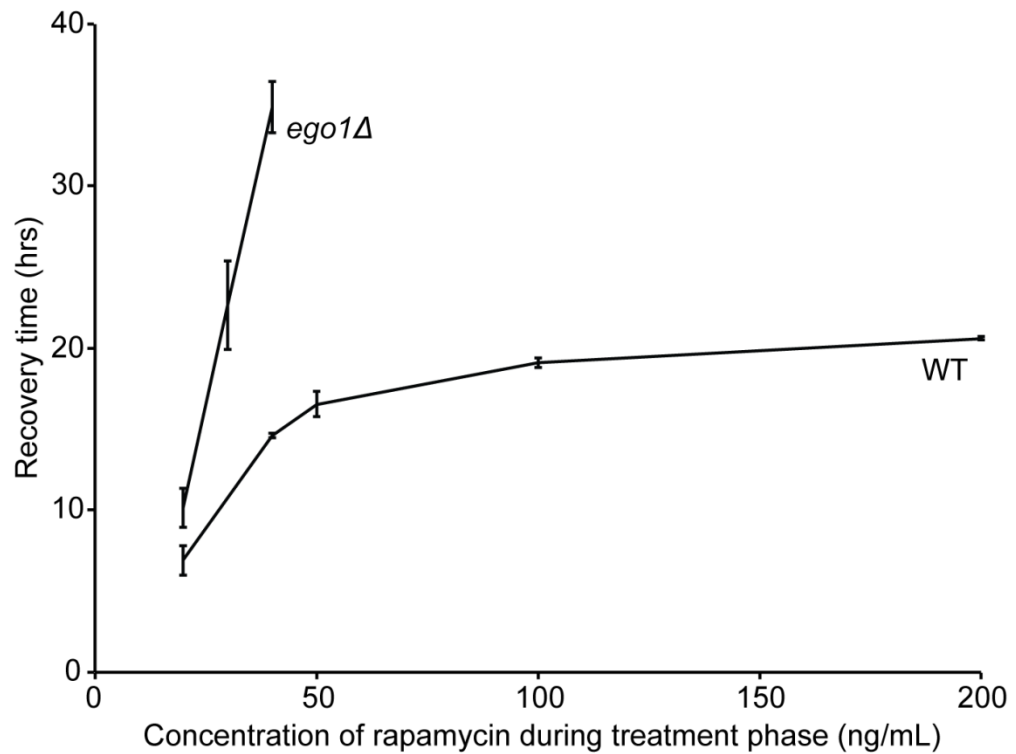


**Figure 5.12** The time at which wild-type and *ego1Δ* cells recover from various concentrations of rapamycin

The recovery times for wild-type and *ego1Δ* cultures from various high concentrations of rapamycin (between 20-200 ng/mL). The recovery times were measured as explained in section 5.2.5 and Figure 5.11. N=3 independent cultures; error bars denote S.E.M.

We linearly extrapolated the recovery time plots for both wild-type and *ego1Δ* mutants to the axes. If a lag in TORC1 reactivation exists, then we would expect each plot to extrapolate to the y-axis, *i.e.* a time needed to recover from rapamycin inhibited TORC1 at a theoretical but ‘inhibitory’ rapamycin concentration of 0 ng/mL. However, if no lag in TORC1 reactivation occurs we would expect the plots to extrapolate to the x-axis. We found that extrapolation of the recovery time plots for both wild-type and *ego1Δ* mutants extrapolated to the x-axis (Figure 5.13), consistent with there being no inherent lag time for TORC1 reactivation in the presence or absence of the EGO complex. Instead it is more likely that the slow recovery times from rapamycin, observed for both wild-type and *ego1Δ* cultures, are a result of the kinetics of reducing the biologically active rapamycin pool rather than in reactivating TORC1 itself.

### 5.2.7 Does the rapamycin-insensitive growth rate explain the recovery time?

It would appear that rapamycin is not actively detoxified in yeast and that there is no inherent lag for TORC1 reactivation following rapamycin treatment. We can test whether a model of dilution-by-proliferation explains the kinetics of recovery observed for both wild-type and *ego1Δ* cultures. A mechanism of dilution-by-proliferation is dependent on the ability of cells to maintain proliferation in the constant presence of rapamycin; *i.e.* the rapamycin-insensitive growth rate. This model predicts that doubling the size of the intracellular pool of rapamycin would extend the recovery time of a culture by one doubling time, at the rapamycin-insensitive growth rate. By knowing the doubling times for both the wild-type and *ego1Δ* cultures in the presence of rapamycin we can calculate a predicted recovery time from any concentration of rapamycin by the mechanism of dilution-by-proliferation.

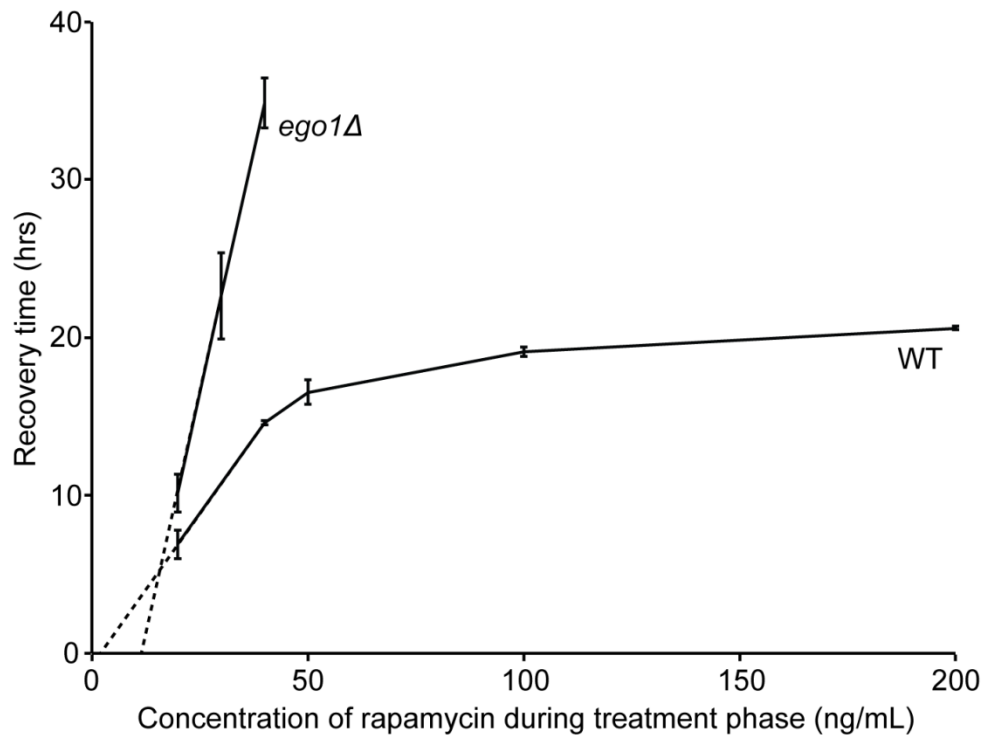


**Figure 5.13 Extrapolating recovery time to the origin**

The recovery time plots of Figure 5.12 for wild-type and *ego1Δ* mutants linearly extrapolated to intercept the axis.

To calculate the predicted recovery time, we used the following formula:

$$t^R = t^{DT} \times \log_2 [\text{rap}]_{\text{treatment}} + a$$

|        |                                   |  |
|--------|-----------------------------------|--|
| where: | $t^R$                             | predicted recovery time (hrs)  |
|        | $t^{DT}$                          | observed doubling time in the constant presence of a high concentration of rapamycin (far in excess of the minimum inhibitory concentration) (hrs) |
|        | $[\text{rap}]_{\text{treatment}}$ | the concentration of rapamycin in the media during the treatment phase (ng/mL)   |
|        | $a$                               | constant (hrs), a “fudge-factor” derived from the best fit of the initial trajectory of $t^R$ to the experimentally observed recovery times        |

Note, this calculation assumes that the extracellular concentration of rapamycin is proportional to the intracellular concentration of the drug, *i.e.* that doubling the extracellular concentration of rapamycin in the media will double the intracellular rapamycin pool.

The predicted recovery times for wild-type and *ego1Δ* cultures were calculated and plotted in Figure 5.14 (grey lines). The strain specific rapamycin-insensitive doubling times used in the calculation were measured in the constant presence of 20 ng/mL rapamycin (in parallel to cultures from which the experimentally observed recovery times were measured). As seen in Figure 5.14 the predicted recovery times for wild-type cultures appear very similar to the recovery times measured experimentally, particularly at concentrations of rapamycin up to 50 ng/mL rapamycin. We found that the predicted recovery times for *ego1Δ* mutants were indistinguishable from the experimentally observed recovery times (Figure 5.14).

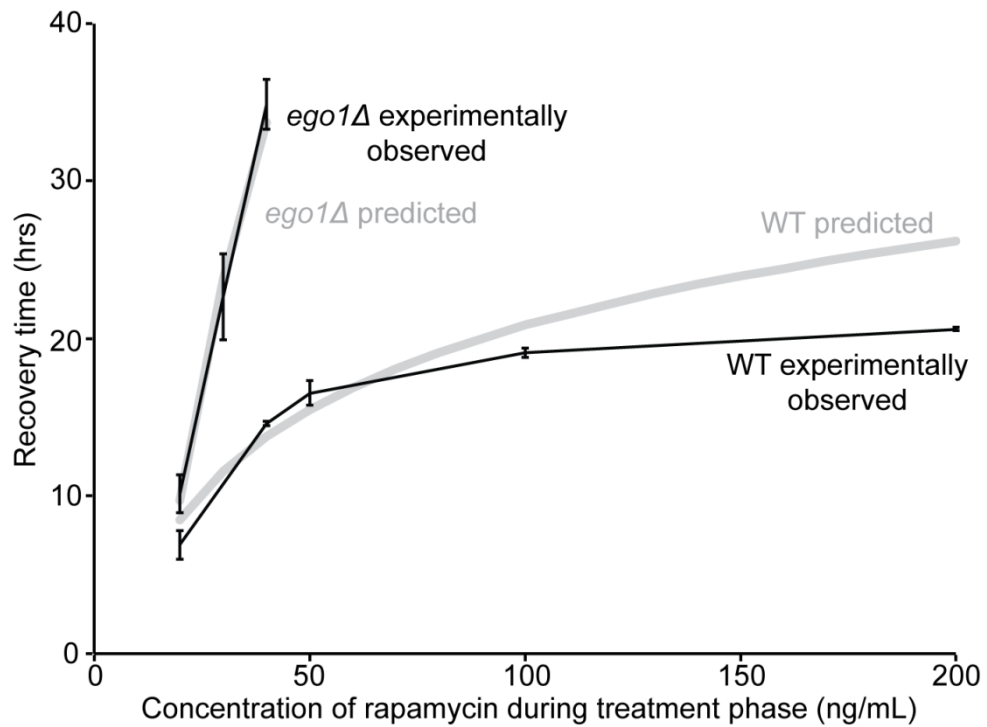


**Figure 5.14** The predicted and experimentally observed recovery times for wild-type and *ego1Δ* cultures from various high concentrations of rapamycin treatment

The recovery times for wild-type and *ego1Δ* cells were predicted using the following formula:

$$t^R = t^{DT} \times \log_2 [\text{rap}]_{\text{treatment}} + a$$

For wild-type cultures:

$$\begin{aligned} t^{DT} &= 5.32 \text{ (hrs)} \\ [\text{rap}] &= 20\text{-}200 \text{ ng/mL} \\ a &= -14.5 \text{ (hrs)} \end{aligned}$$

For *ego1Δ* mutants:

$$\begin{aligned} t^{DT} &= 23.79 \text{ (hrs)} \\ [\text{rap}] &= 20\text{-}40 \text{ ng/mL} \\ a &= -93 \text{ (hrs)} \end{aligned}$$

The predicted recovery times are shown in grey whilst the experimentally observed recovery times, from Figure 5.12, are plotted in black. Error bars denote S.E.M.

We conclude that a dilution-by-proliferation model is sufficient to explain:

- 1) The kinetics of recovery of wild-type cultures from rapamycin treatment.
- 2) The kinetics of recovery of *ego1Δ* cultures from rapamycin treatment.
- 3) The extent of the *ego1Δ* mutant, and by inference *ego*-mutant, recovery defect.

We can calculate the theoretical doubling time of cultures that would best explain the experimentally observed recovery time plots (Figure 5.12) if the dilution-by-proliferation model applies. The theoretical doubling times, for wild-type and *ego1Δ* cultures, were calculated as the initial slopes of the plots of recovery time versus the  $\log_2$  of the rapamycin concentration. As seen in Table 5.2 we found that the theoretical and observed doubling times for both wild-type and *ego1Δ* cultures were indistinguishable, within error, from the respective doubling times measured in the constant presence of rapamycin. The dilution-by-proliferation model indeed fits the experimentally observed data extremely closely.

### 5.2.8 Does a rapamycin-insensitive growth rate correlate with recovery?

It would appear that the inability of *ego*-mutants to recover from rapamycin treatment is a result of their slow rapamycin-insensitive growth rate. In the previous chapter we identified null mutants, in addition to those of the EGO complex, that exhibit a significantly slower rapamycin-insensitive growth rate compared to that of wild-type cultures. Does a slow rapamycin-insensitive growth rate impact the ability to recover from the drug for these null mutants? We tested the ability of *tor1Δ*, *tco89Δ* and *eap1Δ* null mutants, which we have shown to have a rapamycin-insensitive growth defect, to recover from rapamycin treatment (Figure 4.10 and Figure 4.16).

|              | Initial slope of recovery time vs Log <sub>2</sub> of rapamycin concentration (hrs) | Observed doubling time in the constant presence of rapamycin (20 ng/mL) (hrs) |
|--------------|---|---|
| WT           | 5.27 +/- 0.65   | 5.32 +/- 0.17   |
| <i>ego1Δ</i> | 24.52 +/- 0.97  | 23.79 +/- 5.51  |

**Table 5.2 Comparison of the calculated slope of the recovery time to the observed rapamycin-insensitive doubling time**

The slope for the initial region of the observed recovery times (between 20-50 ng/mL for wild-type cultures and 20-40 ng/mL for *ego1Δ* cultures) was calculated using the observed recovery times versus the Log<sub>2</sub> of rapamycin concentration. To compare, the doubling time of wild-type and *ego1Δ* cultures in the constant presence of rapamycin (20 ng/mL), as measured in parallel to cultures from which the recovery times were determined, is included. Results are shown +/- standard deviation.

A slow rapamycin-insensitive growth rate was also observed for wild-type strains in the EG123 genetic background (Figure 4.17). Testing the ability of these cultures to recover from rapamycin will give an indication as to whether our dilution-by-proliferation model also applies to all yeast strains and is not specific to cells in the BY4743 genetic background.

Exponentially growing cultures of wild-type (BY4743, W303 and EG123 genetic backgrounds), *ego1Δ*, *tor1Δ*, *tco89Δ* and *eap1Δ* cells (all mutant haploids were in a BY4743 genetic background) were treated (or not) with rapamycin (200 ng/mL) in YPD at 28°C with agitation for two hours. Cells were washed three times in fresh YPD from which ten-fold serial dilutions were created and spotted onto a YPD plate that was incubated at 28°C for two days.

We found that all strains with a slower rapamycin-insensitive growth rate in the presence of 200 ng/mL rapamycin, compared to that of wild-type (BY4743) cultures, struggled to recover from rapamycin treatment. As seen in Figure 5.15 *tor1Δ*, *tco89Δ* or *eap1Δ* null mutants and the wild-type (EG123) culture failed to efficiently recover from rapamycin treatment. These results are consistent with a slow rapamycin-insensitive growth rate impacting the ability of cultures to recover from the drug and appears independent of genetic background. By comparison the rapamycin-insensitive growth rate of wild-type (W303) was not significantly different to that of the wild-type (BY4743) culture in the constant presence of 200 ng/mL rapamycin (Figure 4.17). As seen in Figure 5.15 the wild-type (W303) culture could efficiently recover from rapamycin treatment. These results support our hypothesis that the ability to recover from rapamycin is primarily, but not exclusively, dependent on the growth rate of cultures in the presence of the drug.

### 5.3 Conclusion

In this chapter we have proposed a model to explain rapamycin detoxification in yeast cells; that is, rapamycin is not actively detoxified but instead the intracellular rapamycin pool is diluted by proliferation.

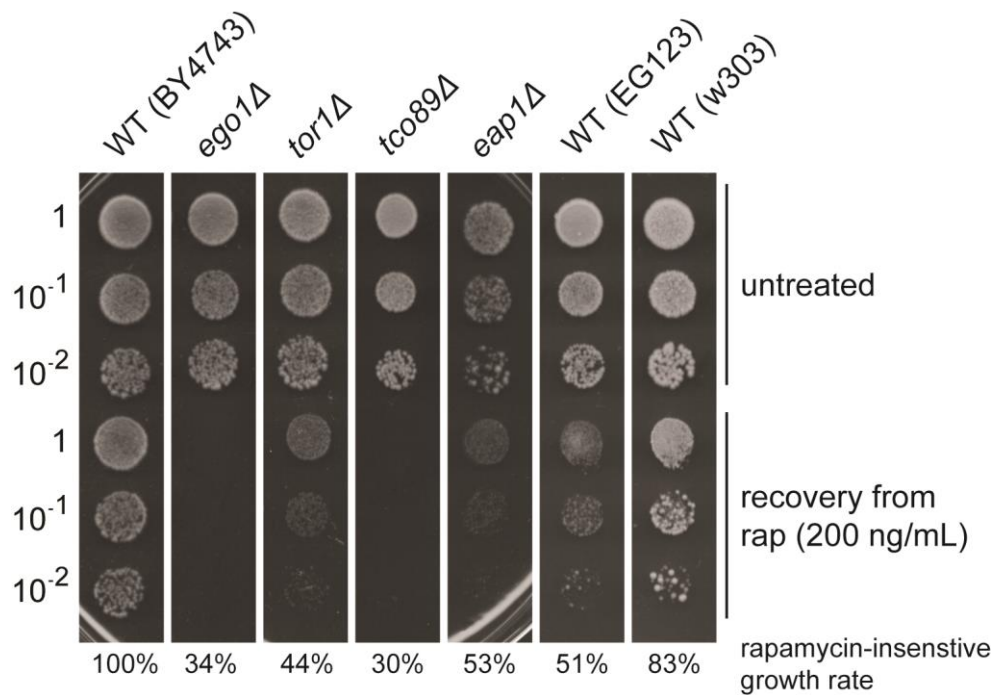


**Figure 5.15 Recovery of *tor1*Δ, *eap1*Δ wild-type (W303, EG123), and *tco89*Δ from rapamycin treatment**

Exponentially growing cultures of wild-type (By4743, W303 and EG123 genetic backgrounds), *ego1*Δ, *tor1*Δ, *eap1*Δ and *tco89*Δ cultures at an OD<sub>600nm</sub> of ~0.1 (0.05 for *tco89*Δ mutants) were treated (or not) with rapamycin (200 ng/mL) in YPD at 28°C with agitation for two hours. Cells were washed three times in fresh YPD before ten-fold serial dilutions were created and spotted (5 μL) onto a YPD plate which was incubated at 28°C for two days. The rapamycin-insensitive growth rates, as a percentage of that of BY4743 wild-type cultures, are also shown and were calculated from Figure 4.10, Figure 4.16 and Figure 4.17.

The dilution-by-proliferation model also explains why loss of the EGO complex results in a rapamycin recovery defect; *ego-* mutants are unable to proliferate quickly enough in the presence of rapamycin to reduce the drug to a sub-inhibitory concentration within the timings of our experiments.

Through the use of mass spectrometry analysis we have shown that the observable pool of rapamycin is not degraded in, nor exported from yeast cells: it would appear that rapamycin is not actively metabolised in yeast. Initially we found that the cell-associated pool of rapamycin decreased during a ‘recovery phase’. However, these results were based on culture samples that had been normalised for  $OD_{600nm}$  and therefore did not take into account the increase in culture density during the ‘recovery phase’. When the cell-associated pool of rapamycin, as measured by mass spectrometry, was normalised for the increase in culture density we found that the total cell-associated concentration of rapamycin present during the ‘recovery phase’ did not change over the 20 hours monitored. The decrease in cell-associated rapamycin per volume of culture, but stability over the whole culture, led us to conclude that the observable cell-associated pool of rapamycin is reduced by the slow mechanism of dilution-by-proliferation. The ability of yeast cells to maintain proliferation in the constant presence of rapamycin thus allows the drug to be diluted among an increasing number of progeny cells; the intracellular concentration eventually reaching a threshold concentration below that required to inactivate TORC1.

In the previous chapter we showed that *ego-* mutants were unable to recover from rapamycin (200 ng/mL). In this chapter, we found that the ability of *ego-* cells to recover from rapamycin was in fact concentration dependent: *ego-* cultures were in fact able to recover from treatments with lower, yet still TORC1 inhibiting, concentrations of rapamycin or from higher concentrations treated for a short time, consistent with the biologically-active pool of the drug also being diluted by proliferation. The knowledge that *ego-* cells were able to recover from lower, yet still inhibitory, concentrations of rapamycin allowed us to monitor the culture density, for both wild-type and *ego1Δ* mutants, during a ‘recovery phase’ from various concentrations of the drug. We discovered that the recovery time for both wild-type and *ego1Δ* cells increased with an increasing concentration of rapamycin and eventually saturated in wild-type

cultures. The length of time it took for wild-type cultures to recover from our standard two hour treatment with 200 ng/mL rapamycin was extremely long - approximately 20 hours and suggests that rapamycin is not easily 'detoxified' even in wild-type cells. Null *ego1Δ* mutants demonstrated a severe and slow defect in recovery times from rapamycin treatment, consistent with their over-reaction to the presence of rapamycin, other examples being: their slow rapamycin-insensitive growth rate, decreased translation rate and the eventual amino acid uptake rate compared to those of wild-type cultures.

To test our model that the biologically-active pool of rapamycin is 'detoxified' in a dilution-by-proliferation manner, we predicted the recovery times for both wild-type and *ego1Δ* cultures from various concentrations of rapamycin based on their individual rapamycin-insensitive growth rates. We found that the predicted and experimentally observed recovery times closely resembled each other, suggesting that dilution-by-proliferation is likely to be the mechanism by which rapamycin is 'detoxified'. We observed some divergence between the predicted and observed recovery times for wild-type cultures treated with higher concentrations of rapamycin. It is possible that this is due to saturation of the drug importer *in vivo*. We note however that the trend of the predicted recovery times closely matched that observed experimentally, suggesting that the observed saturation curve is an inherent property of the dilution-by-proliferation mechanism. We conclude that the inability of *ego1Δ* cultures, and by inference *ego-* mutants, to recover from rapamycin treatment is due to their slow rapamycin-insensitive growth rate, which is most likely a result of reduced TORC1 activity in these mutant strains. Indeed, we predict that it would take *ego1Δ* cultures ~90 hours to commence normal proliferation from a two hour treatment with 200 ng/mL rapamycin.

Having identified that a slow rapamycin-insensitive growth rate of *ego1Δ* cultures, and by inference *ego-* mutants, inhibits recovery from rapamycin we tested the ability of other null mutants (*tor1Δ*, *tco89Δ* and *eap1Δ*), that have a slow rapamycin-insensitive growth rate, to recover from rapamycin. We found that a slow rapamycin-insensitive growth rate, compared to that of wild-type cultures, correlated with the ability of cultures to recover from rapamycin treatment. Mutants lacking Tco89p have a rapamycin-insensitive growth rate similar to that of *ego1Δ* cultures and completely failed to recover from

rapamycin treatment. Null mutant cultures (or wild-type EG123) in which the rapamycin-insensitive growth rate is compromised, but not to the extent of that of *ego1Δ* mutants, struggled to recover from rapamycin treatment and only very small colonies were observed. These results imply that there is likely to be a rapamycin-insensitive growth rate threshold with regards to the ability to recover from rapamycin under our experimental conditions. Cultures with a rapamycin-induced growth rate slower than this threshold are perceived as being completely unable to recover from the drug. We therefore conclude that the rapamycin-insensitive proliferation rate, discovered in the previous chapter, underlies the ability of cells to recover.

## **6 Identifying other potential regulators of TORC1**

### **6.1 Introduction**

The focus of this project so far has been to understand how yeast cells recover from rapamycin and why TORC1, and its known activators, are required for this process. The EGO complex was identified by the De Virgilio group as an activator of TORC1. A number of additional upstream regulators of TORC1 that appear to respond to nutrient availability have also been identified: for example, the SEA complex (Panchaud et al. 2013b); Vam6p (Binda et al. 2009) and the leucyl-tRNA synthetase (Bonfils et al. 2012). It would appear that these regulators all act via the EGO complex to moderate TORC1 activity. However, the EGO complex is not essential: cells devoid of the complex are fully viable and are able to recover from periods of environmental and nutritional stress (Figure 3.6). It is therefore highly likely that additional, as yet unknown, regulators of TORC1 remain to be identified.

Prior to the start of this project, a large-scale, primary genetic screen was carried out by the Gray laboratory in collaboration with the Johnston laboratory (Dalhousie University, Canada) to identify null mutants that failed to recover from a long exposure time to high concentrations of rapamycin. Here, the results of the primary screen will be analysed and extended in an attempt to identify novel regulators of TORC1.

### **6.2 Results**

#### **6.2.1 Summary of the primary screen**

To identify null mutants that fail to recover from rapamycin treatment, the Johnston laboratory (Dr. Pak Poon, Dr. Richard Singer and Dr. Gerry Johnston) at Dalhousie University performed a large-scale genetic screen, testing ~4,700 null mutant haploids, each lacking a single non-essential gene, for their ability to recover from rapamycin treatment.

Although this portion of the work was not carried out by myself, here I will summarise how the primary screen was performed. This will provide background

information for my subsequent analysis of the primary data provided by the screen. Three independent robotic runs of the primary screen were performed on the arrayed BY4742 haploid deletion collection, which were freshly defrosted and grown prior to screening. The arrayed collection was pinned onto YPD plates containing 100 or 200 ng/mL rapamycin and incubated at 30°C for three or seven days. Following incubation, the arrayed collection was re-pinned (by robot) onto plain YPD plates which were incubated at 30°C for up to three days. The ability of each colony to resume proliferation on the plain YPD plates was then scored, by image analysis, as either unable to form colonies or formed small, mid-sized or full-sized colonies compared to that of the wild-type strain. Table 6.1 shows the number of null mutants identified with a colony size smaller than that of wild-type cultures following recovery from rapamycin treatment.

### 6.2.2 Analysis of the results of the primary screen

The following work is my analysis of the results of the primary screen. Of the ~4,700 null mutants tested, 172 were found in at least one of the three runs performed. Table 6.2 shows the number of null mutants identified in either one, two or all three runs. The average number of null mutants identified per run of the primary screen was 98, as calculated from Table 6.1, a small fraction of the collection screened. We can predict the frequency of null mutants expected to be found by chance in any two or all three runs of the screen. We predict that six null mutants would be identified by chance in any two runs of the screen (Table 6.2). As seen in Table 6.2, 39 null mutants were in fact identified in any two runs of the primary screen, which is an approximate 6.5-fold enrichment over the number expected by chance. If the primary screen only identified null mutants by chance then we would predict that no null mutant would be identified in all three runs of the screen (Table 6.2). We find that this is not the case and 49 null mutants were identified in all three runs, an approximate 1,200-fold enrichment over the number expected by chance (Table 6.2). Due to the fold enrichment of the null mutants identified in any two or all three runs of the primary screen, these null mutants shall be analysed further and are classed as the 'primary null mutant set'.

| Run | Concentration of rapamycin (ng/mL) | Treatment time (days) | Number of null mutants identified with a colony formation defect |
|-----|------------------------------------|-----------------------|--|
| 1   | 100                                | 3                     | 118  |
| 2   | 100                                | 7                     | 73   |
| 3   | 200                                | 7                     | 103  |

**Table 6.1** Null mutants identified from each run of the primary screen with a colony formation defect

Three runs of the primary screen were carried out by Dr. Poon. The ability of each strain to form a colony was scored by image analysis and the number of null mutants identified, per run, with a colony size smaller than that of wild-type cultures is shown.

*Note: All runs of the screen and identification of mutants with a recovery defect were carried out by Dr. Poon in the Johnston Laboratory at Dalhousie University, Canada.*

|                             | Identified only<br>in any one run | Identified only<br>in any two runs | Identified in<br>all three runs | Total |
|-----------------------------|-----------------------------------|------------------------------------|---------------------------------|-------|
| Experimentally<br>observed  | 84                                | 39                                 | 49                              | 172   |
| Mathematically<br>predicted | ~282                              | ~6<br>(6.2)                        | <1<br>(0.044)                   |       |
| Fold enrichment             | -                                 | ~6.5                               | ~1,200                          |       |

**Table 6.2** The number of null mutants identified across the three runs that were scored as having at least a mild rapamycin recovery defect

The number of null mutants experimentally observed as having a recovery defect (*i.e.* a colony size smaller than that of wild-type cultures following the recovery phase) in one run, any two runs or in all three runs is shown. The predicted number of null mutants that would be identified by chance is also included and was calculated as follows: The frequency of observing 98 null mutants (the average identified in one run of the screen) by chance in 4,700 genes tested is 0.021 ( $98/4,700$ ). The frequency of observing a null mutant by chance in any pair of three runs is therefore calculated as 6.2 mutants ( $3 \times ((0.021 \times 0.021) \times 4,700)$ ). The frequency of identifying a null mutant by chance in all three runs of the screen is  $9.3 \times 10^{-6}$  ( $3 \times 0.021$ ); in a deletion collection of 4,700 mutants this equates to less than one mutant (0.04) ( $4,700 \times (3 \times 0.021)$ ). The probability of identifying mutants by chance in only one screen was calculated by deducting the probability of identifying a mutant in either two or all three screens from the chance that they would be identified in one screen only, *i.e.*  $3 \times 98 - (6 \times 2) - (0.044 \times 3)$ .

*Note: All runs of the screen and identification of mutants with a recovery defect were carried out by Dr. Poon in the Johnston Laboratory at Dalhousie University, Canada.*

The 88 genes of the ‘primary gene set’ (corresponding to the primary mutant set) are shown in Table 6.3. We have successfully identified all four members of the EGO complex in our primary mutant set. This suggests that the primary screen was successful in identifying null mutants that potentially phenocopy *ego*-mutants (Table 6.3).

### 6.2.3 GO Term enrichment in the primary mutant set

Are particular biological processes or components enriched within our primary mutant set? Analysis of the 88 genes was carried out using the Gene Ontology (GO) Term Finder on the Saccharomyces Genome Database (SGD) website ([www.yeastgenome.org](http://www.yeastgenome.org)) and tested for enrichment in known GO process, GO component and GO function terms. The SGD GO Term Finder software identified GO terms that were significantly enriched ( $p < 0.01$ ) within our primary gene set. To account for multiple hypothesis testing, a Bonferroni Correction is automatically applied by SGD when calculating the p-value. For each enriched GO term, we also calculated the percentage of genes identified in our query set relative to the number of genes in the genome associated with that particular term; ‘percentage identification’. We set an arbitrary cut-off of 20% identification with the assumption that less than 20% identification was likely due to either non-specific GO terminology or poor enrichment.

Table 6.4 shows the GO terms that were found to be significantly enriched in our dataset by SGD and that were above our 20% identification cut-off. Twelve GO process terms were identified, which can be divided into three sub-categories, those involved in threonine biosynthesis, those involved in membrane trafficking and fusion and those involved in transcription and elongation. The GO process term ‘threonine biosynthetic process’ had the highest percentage identification within our mutant set, with 80% of the genes found in our primary screen (Table 6.4). The largest category of GO process terms identified was associated with membrane trafficking and fusion with 10 such terms found to have greater than 20% identification (Table 6.4). The GO process terms that related to transcription and elongation have the least percentage identified of all the GO Process Terms found (Table 6.4).

| Gene names of null mutants found in any two runs of the primary screen |         |              |         | Gene names of null mutants found in all three runs of the primary screen |         |              |           |
|--|---------|--------------|---------|--|---------|--------------|-----------|
| Gene Name  | ORF     | Gene Name    | ORF     | Gene Name  | ORF     | Gene Name    | ORF       |
| <i>BUD30</i>   | YDL151C | <i>PET54</i> | YGR222W | <i>ADH1</i>  | YOL086C | <i>PHO85</i> | YPL031C   |
| <i>BUD32</i>   | YGR262C | <i>RPA49</i> | YNL248C | <i>APQ13</i>   | YJL075C | <i>POC4</i>  | YPL144W   |
| <i>CNM67</i>   | YNL225C | <i>SAC3</i>  | YDR159W | <i>ATG11</i>   | YPR049C | <i>POP2</i>  | YNR052C   |
| <i>CTK1</i>  | YKL139W | <i>SER2</i>  | YGR208W | <i>BFR1</i>  | YOR198C | <i>PRO1</i>  | YDR300C   |
| <i>CTK2</i>  | YJL006C | <i>SIC1</i>  | YLR079W | <i>CCR4</i>  | YAL021C | <i>PRP18</i> | YGR006W   |
| <i>CTK3</i>  | YML112W | <i>SPC72</i> | YAL047C | <i>CDC40</i>   | YDR364C | <i>RLR1</i>  | YNL139C   |
| <i>DHH1</i>  | YDL160C | <i>SPS1</i>  | YDR523C | <i>CIN8</i>  | YEL061C | <i>ROX3</i>  | YBL093C   |
| <i>EGO3</i>  | YBR077C | <i>SSD1</i>  | YDR293C | <i>DEG1</i>  | YFL001W | <i>RPB4</i>  | YJL140W   |
| <i>ERG6</i>  | YML008C | <i>THR1</i>  | YHR025W | <i>DIA2</i>  | YOR080W | <i>SEM1</i>  | YDR363W-A |
| <i>GTR1</i>  | YML121W | <i>TMA23</i> | YMR269W | <i>EFG1</i>  | YGR272C | <i>SFP1</i>  | YLR403W   |
| <i>HEM14</i>   | YER014W | <i>UBA4</i>  | YHR111W | <i>EGO1</i>  | YKR007W | <i>SHP1</i>  | YBL058W   |
| <i>HOF1</i>  | YMR032W | <i>UBP15</i> | YMR304W | <i>ERG3</i>  | YLR056W | <i>SNX4</i>  | YJL036W   |
| <i>HOM2</i>  | YDR158W | <i>UME6</i>  | YDR207C | <i>FYV6</i>  | YNL133C | <i>SWI6</i>  | YLR182W   |
| <i>HSL7</i>  | YBR133C | <i>UMP1</i>  | YBR173C | <i>GON7</i>  | YJL184W | <i>THP1</i>  | YOL072W   |
| <i>KEM1</i>  | YGL173C | <i>VAM7</i>  | YGL212W | <i>GTR2</i>  | YGR163W | <i>THR4</i>  | YCR053W   |
| <i>LSM1</i>  | YJL124C | <i>VPS16</i> | YPL045W | <i>HOM3</i>  | YER052C | <i>TOM5</i>  | YPR133W-A |
| <i>LST4</i>  | YKL176C | <i>YKE2</i>  | YLR200W | <i>LUV1</i>  | YDR027C | <i>VAM6</i>  | YDL077C   |
| <i>MCH5</i>  | YOR306C | <i>YPT7</i>  | YML001W | <i>MNN10</i>   | YDR245W | <i>VMS1</i>  | YDR049W   |
| <i>MMS22</i>   | YLR320W | -            | YDL172C | <i>MNN11</i>   | YJL183W | <i>VPS15</i> | YBR097W   |
| <i>NPL3</i>  | YDR432W |              |         | <i>NCS6</i>  | YGL211W | <i>VPS33</i> | YLR396C   |
|  |         |              |         | <i>PAR32</i>   | YDL173W | <i>VPS34</i> | YLR240W   |
|  |         |              |         | <i>PAT1</i>  | YCR077C | <i>YDJ1</i>  | YNL064C   |
|  |         |              |         | <i>PEP3</i>  | YLR148W | <i>YME1</i>  | YPR024W   |
|  |         |              |         | <i>PEP5</i>  | YMR231W | -            | YDR417C   |
|  |         |              |         | <i>PIB2</i>  | YGL023C |              |           |

**Table 6.3** The gene name and ORF number of mutants identified in at least two runs of the primary screen

The gene names and ORF numbers for all 88 null mutants identified in at least two runs of the primary screen are listed in alphabetical order by gene name.

| GO Process   | Number in primary mutant set | Number in genome | p-value  | % identification in our screen of those in genome |
|--|------------------------------|------------------|----------|---|
| Threonine Biosynthetic Process                                 | 4/88                         | 5/7167           | 5.97E-05 | 80%   |
| Threonine Metabolic Process                                    | 4/88                         | 8/7167           | 0.00081  | 50%   |
| Regulation of SNARE Complex Assembly                           | 5/88                         | 9/7167           | 1.71E-05 | 56%   |
| Regulation of Vesicle Fusion                                   | 5/88                         | 10/7167          | 3.39E-05 | 50%   |
| SNARE Complex Assembly   | 5/88                         | 10/7167          | 3.39E-05 | 50%   |
| Regulation of Vacuole Fusion, Non-Autophagic                   | 6/88                         | 13/7167          | 2.62E-06 | 46%   |
| Regulation of Vacuole Organisation                             | 6/88                         | 16/7167          | 1.18E-05 | 38%   |
| Membrane Invagination  | 10/88                        | 43/7167          | 3.61E-08 | 23%   |
| Single Organism Membrane Invagination                          | 10/88                        | 43/7167          | 3.61E-08 | 23%   |
| Microautophagy   | 10/88                        | 43/7167          | 3.61E-08 | 23%   |
| Piecemeal Microautophagy of Nucleus                            | 7/88                         | 33/7167          | 6.19E-05 | 21%   |
| Nucleophagy  | 7/88                         | 34/7167          | 7.71E-05 | 21%   |
| Positive Regulation of DNA-Templated Transcription, Elongation | 9/88                         | 39/7167          | 3.72E-07 | 23%   |
| Regulation of DNA-Templated Transcription, Elongation          | 9/88                         | 41/7167          | 6.03E-07 | 22%   |
| <b>GO Component</b>  |                              |                  |          |   |
| HOPS Complex   | 5/88                         | 6/7167           | 2.15E-07 | 83%   |
| EGO Complex  | 4/88                         | 5/7167           | 1.53E-05 | 80%   |
| CORVET Complex   | 4/88                         | 6/7167           | 4.56E-05 | 67%   |
| Late Endosomal Membrane  | 4/88                         | 6/7167           | 4.56E-05 | 67%   |
| Cytoplasmic mRNA Processing Body                               | 8/88                         | 32/7167          | 4.51E-07 | 25%   |
| Endosomal Part   | 8/88                         | 36/7167          | 1.24E-06 | 22%   |
| <b>GO Function</b>   |                              |                  |          |   |
| Amino Acid Kinase Activity                                     | 3/88                         | 3/7167           | 0.00016  | 100%  |

**Table 6.4 Enrichment of GO terms identified in our primary mutant set**

The 88 primary gene set was tested for enrichment ( $p < 0.01$ ) in GO Terms by using the Saccharomyces Genome Database's GO Term Finder program. The percentage identification in our mutant set compared to the number of genes assigned to a particular term in the genome was calculated and only GO terms with over 20% identification are included. GO Term Finder analysis was run in January 2014.

Six GO component terms were found to be significantly enriched in our mutant set and three of these terms related to specific complexes; these were the HOPS and CORVET complexes and the EGO complex (Table 6.4). The remaining three GO component terms identified, whilst not relating to specific complexes, appear to encompass either endosomes or transcription thus complementing the results found when testing GO process terms. Only one GO function term was identified as significantly enriched within our mutant set (Table 6.4): all three of the genes annotated to the term ‘amino acid kinase activity’ were found in our screen and possibly relate to the genes involved in threonine biosynthesis and metabolism (Table 6.4).

GO term analysis identified 21 significantly and strongly enriched GO terms within our primary gene set. Thirty-four genes of the 88 primary gene set were identified by GO term analysis and are shown in Table 6.5. We can summarise the significant enrichment of genes found by GO Term analysis into three broad categories: ‘threonine biosynthesis’, ‘endosomal trafficking’ and ‘regulation of transcription’. Note that whilst *VPS15* and *VPS34* were originally identified in GO Term analysis as being involved in transcriptional regulation, these proteins are more often associated with autophagy and cytoplasm-to-vacuole trafficking (Kihara et al. 2001); the *vps15Δ* and *vps34Δ* null mutants will therefore be analysed in the category of ‘endosomal trafficking’.

#### **6.2.3.1 GO term enrichment in the ‘single-hit’ mutant set**

Were we justified in only analysing mutants found in two or more runs? To test this, we submitted the gene list corresponding to the mutants found only in any one run of the screen (our ‘single-hit mutant set’) to the SGD GO Term Finder. As seen in Table 6.6 we found no enrichment of GO process terms or of GO function terms. When testing GO component terms, we found two terms to be significantly enriched in the single-hit mutant set (Table 6.6). Both of these terms are broad with a large number of genes in the genome assigned to them (Table 6.6). Our initial run of the GO Term Finder software (January 2014) had identified significant enrichment of the GO component ‘mediator complex’ within our single-hit mutant set. However, a subsequent re-run of GO component enrichment in August 2014 did not identify the mediator complex as being enriched.

| Threonine biosynthesis<br>Genes identified in the primary screen        | Endosomal trafficking   |  | Regulation of transcription |  |
|---|-------------------------|--|-----------------------------|--|
|   | Known complex           | Genes identified in the primary screen | Known complex               | Genes identified in the primary screen |
| <i>PRO1</i><br><i>THR1</i><br><i>THR4</i><br><i>HOM2</i><br><i>HOM3</i> | EGO complex             | <i>EGO1</i>                            | CTDK-1 complex              | <i>CTK1</i>                            |
|   |                         | <i>EGO3</i>                            |                             | <i>CTK2</i>                            |
|   |                         | <i>GTR1</i>                            |                             | <i>CTK3</i>                            |
|   |                         | <i>GTR2</i>                            |                             |  |
|   |                         |  |                             | <i>CCR4</i>                            |
|   | HOPS/CORVET complex     | <i>PEP3</i>                            |                             | <i>PAT1</i>                            |
|   |                         | <i>PEP5</i>                            |                             | <i>DHH1</i>                            |
|   |                         | <i>VPS33</i>                           |                             | <i>SSD1</i>                            |
|   | HOPS complex            | <i>VPS16</i>                           |                             | <i>XRN1</i>                            |
|   |                         | <i>VAM6</i>                            |                             | <i>LSM1</i>                            |
|   | PtdIns 3-kinase complex | <i>VPS15</i>                           |                             | <i>RPB4</i>                            |
|   |                         | <i>VPS34</i>                           |                             | <i>POP2</i>                            |
|   |                         | <i>YPT7</i>                            |                             | <i>NPL3</i>                            |
|   |                         | <i>SHP1</i>                            |                             | <i>YKE2</i>                            |
|   |                         | <i>VAM7</i>                            |                             |  |
|   | <i>SNX4</i>             |  |                             |  |
|   | <i>ATG11</i>            |  |                             |  |

**Table 6.5** The gene names for which the null mutants were significantly enriched in the primary screen by GO Term analysis

The 34 of 88 genes in our primary gene set that were identified by GO term enrichment. We have grouped the genes within our categories of either ‘threonine biosynthesis’, ‘endosomal trafficking’ or ‘regulation of transcription. Known complexes associated with these genes are also shown.

| GO Process          | Number in single hit mutant set | Number in genome | p-value | % identification in our screen of those in genome |
|---------------------|---------------------------------|------------------|---------|---|
| NONE IDENTIFIED     | N/A                             | N/A              | N/A     | N/A   |
| <b>GO Component</b> |                                 |                  |         |   |
| Intracellular Part  | 76/84                           | 5226/7167        | 0.00712 | 1%  |
| Intracellular       | 76/84                           | 5240/7167        | 0.00828 | 1%  |
| <b>GO Function</b>  |                                 |                  |         |   |
| NONE IDENTIFIED     | N/A                             | N/A              | N/A     | N/A   |

**Table 6.6 Enrichment of GO Terms of the mutant set found only in any one run of the primary screen**

The 84 mutants of the single-hit mutant set were analysed using SGD's GO Term Finder. The percentage identification in the single-hit mutant set compared to the number of genes assigned to a particular term in the genome was calculated. GO Term Finder was tested in August 2014.

We account for the initial enrichment as a chance anomaly caused by database curation. The lack of any robust and significant enrichment within the single-hit mutant set for any specific terms implies that we were justified in eliminating this group of single hits from our analysis. We shall therefore continue to focus on the mutants identified in at least two runs of the primary screen for further testing.

#### **6.2.4 Protein-protein interactions among the gene products of the mutant set from the primary screen**

We utilised the “Osprey network analysis” software (Breitkreutz et al. 2003) to analyse physical interactions among our primary protein set of 88 proteins corresponding to the primary mutants identified in our screen. Osprey displays published interactions available on the SGD website.

We found that 45 of the 88 proteins tested interact with at least one other protein in our primary protein set. Of these 45, seven pairs of protein interactions were identified, of which the Vps15p-Vps34p interaction was particularly noteworthy (see below). The remaining 31 proteins were found to form three distinct, and dense, protein clusters (Figure 6.1).

##### **The “EGO” complex**

All four components of the EGO complex were identified as interacting with each other (Figure 6.1). In addition, another protein, Pib2p, in our primary protein set seems to be associated with members of the EGO complex (Figure 6.1). The function of Pib2p is currently unknown.

##### **The “HOPS/CORVET” complex**

All four shared members of the core HOPS and CORVET complexes (Pep3p, Pep5p, Vps16p and Vps33p) were identified and form a dense network among themselves and with the associated proteins Vam6p, Ypt7p and Vam7p (Figure 6.1). The HOPS complex (in association with Vps41p which was only detected in one of the three runs of the primary screen) is required for endosomal trafficking and fusion to the vacuole (Solinger & Spang 2013). Ytp7p is a Rab family GTPase that acts with the HOPS complex to aid maturation of endosomes to the vacuole (Wurmser et al. 2000).

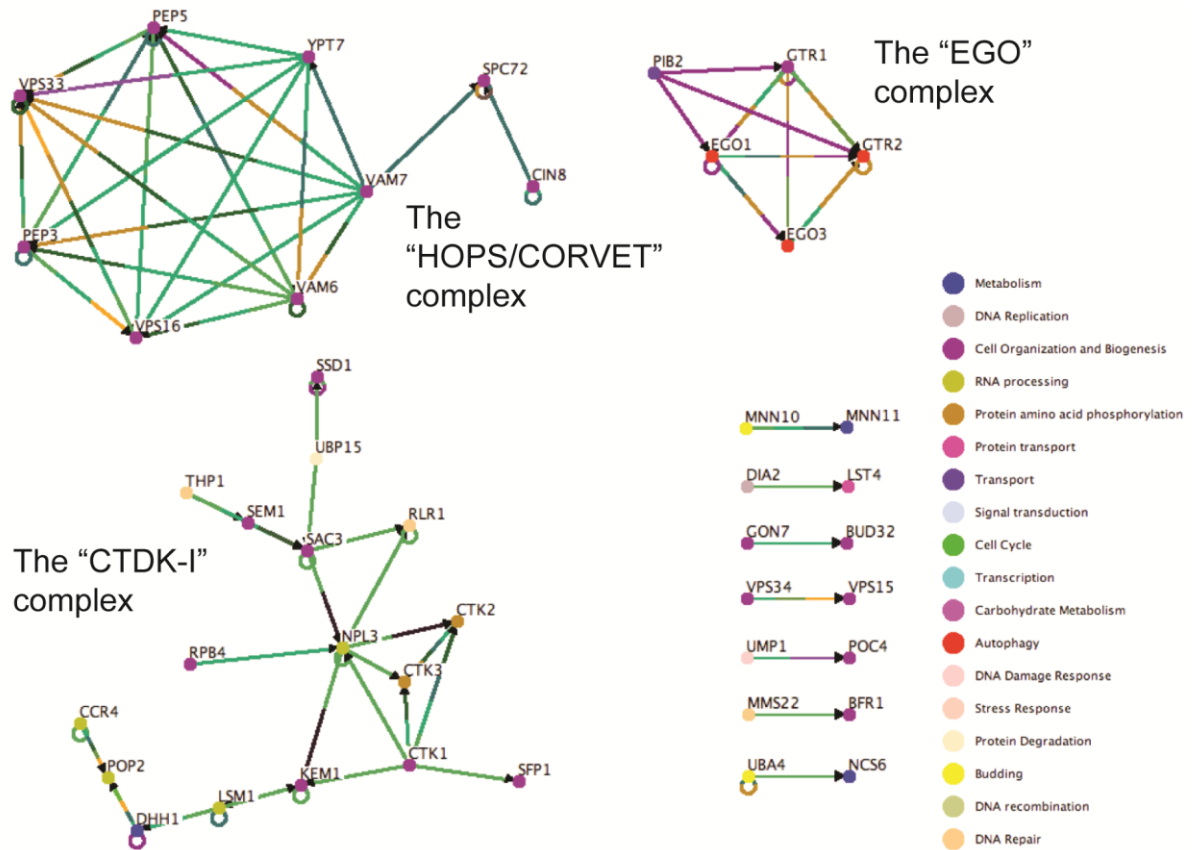


**Figure 6.1 Protein-protein interactions among the primary protein set**

Osprey software (Osprey 1.2.0, Version 5.0) was used to identify any known protein-protein interactions between the 88 proteins of the primary protein set. Only proteins which were shown to physically interact with at least one other protein in the dataset are shown. Each protein is coloured according to their predominant GO process term; the colour index is also shown. The variations in colour of the connecting interaction lines denote the experiment in which the interaction was identified. Experimental systems from which the interactions were identified were: protein-fragment complementation, affinity capture western, co-localisation, reconstituted complex, affinity capture mass spectrometry, yeast two-hybrid, co-fractionation, co-purification and FRET.

Vam7p is a vacuolar SNARE protein that aids membrane fusion and has also been shown to interact with the HOPS complex (Stroupe et al. 2006). Two other proteins (Spc72p and Cin8p) were identified to interact with Vam7p but not with any members of the core HOPS/CORVET complex (Figure 6.1).

### The “CTDK-I” complex

The third network identified involves the C-Terminal Kinase Domain 1 complex (CTDK-I) (Ctk1p, Ctk2p and Ctk3p) and involves 17 proteins (Figure 6.1). The CTDK-I complex is required for regulation of both transcription and translation (Hampsey & Kinzy 2007). The protein interaction network surrounding the CTDK-I complex was less dense than that seen for the HOPS/CORVET complex. Of the 17 proteins in the CTDK-I cluster, 11 were also identified by GO Term analysis: Ssd1p, Npl3p, Rpb4p, Ctk1p, Ctk2p, Ctk3p, Xrn1p (named Kem1p in Osprey), Lsm1p, Dhh1p, Pop2p and Ccr4p.

### The Vps15p-Vsp34p complex

The two interacting proteins, Vps15p and Vps34p, are the core of the PtdIns 3-kinase complex (Kihara et al. 2001) and were found in our primary protein set. The human homolog of Vps34p is thought to have a role in TORC1 signalling in a currently unknown manner (Suzuki & Inoki 2011) hence our focus on this particular protein pair.

## 6.2.5 Selection of mutants for secondary screening

We have identified protein interactions among 45 of the 88 proteins in our primary set. Of these, 31 were found to associate in one of three distinct clusters which appeared to be distinguished by a known complex. Each cluster was also distinct by the function of the associated proteins. As a result of GO term analysis and visualisation of physical interactions, representatives of each of our designated categories were selected for secondary screening.

The EGO complex is known to be required for recovery from rapamycin and will be discounted from further analysis. Of the remaining 84 mutants, 20 were chosen for secondary screening (Table 6.7). Two of the null mutants categorised as being involved in threonine biosynthesis were selected, these were *hom2Δ* and *hom3Δ* (Table 6.7).

| Category                    | Null mutant   | Identified by:   |                 |
|-----------------------------|---------------|------------------|-----------------|
|                             |               | GO Term analysis | Osprey analysis |
| Threonine biosynthesis      | <i>hom2Δ</i>  | ✓                | ✗               |
|                             | <i>hom3Δ</i>  | ✓                | ✗               |
| Endosomal trafficking       | <i>pep3Δ</i>  | ✓                | ✓               |
|                             | <i>pep5Δ</i>  | ✓                | ✓               |
|                             | <i>vps33Δ</i> | ✓                | ✓               |
|                             | <i>vps16Δ</i> | ✓                | ✓               |
|                             | <i>vam6Δ</i>  | ✓                | ✓               |
|                             | <i>vps15Δ</i> | ✓                | ✓               |
|                             | <i>vps34Δ</i> | ✓                | ✓               |
|                             | <i>shp1Δ</i>  | ✓                | ✗               |
|                             | <i>ypt7Δ</i>  | ✓                | ✓               |
|                             | <i>vam7Δ</i>  | ✓                | ✓               |
|                             | <i>snx4Δ</i>  | ✓                | ✗               |
|                             | <i>atg11Δ</i> | ✓                | ✗               |
|                             | <i>pib2Δ</i>  | ✗                | ✓               |
| Regulation of transcription | <i>ccr4Δ</i>  | ✓                | ✓               |
|                             | <i>dhh1Δ</i>  | ✓                | ✓               |
|                             | <i>npl3Δ</i>  | ✓                | ✓               |
|                             | <i>ctk1Δ</i>  | ✓                | ✓               |
|                             | <i>yke2Δ</i>  | ✓                | ✗               |

**Table 6.7 Null mutants selected for secondary screening**

The 20 null mutants selected from the primary mutant set that will be tested for their ability to recover from rapamycin. The analysis (GO Term and Osprey) in which the corresponding gene or protein was identified is also shown.

We would have liked to have included either *pro1Δ*, *thr1Δ* or *thr4Δ* mutants in addition to *hom2Δ* or *hom3Δ* mutants, but were unable to generate the null mutant haploid cells under our laboratory conditions. TORC1 has been shown to localise to the cytoplasmic face of the vacuolar membrane, therefore all null mutants categorised as endosomal trafficking, including *vps15Δ* and *vps34Δ*, were selected for secondary screening. The *pib2Δ* null mutant, the protein of which was found to interact with the EGO complex will also be included in this category (Table 6.7). Finally a selection of null mutants categorised as regulating transcription were also selected. We chose to test null *ctk1Δ*, *npl3Δ*, *ccr4Δ*, *dhh1Δ* and *yke2Δ* mutants, as identified by GO term and physical interaction analysis (Table 6.7). The 20 null mutants selected are termed our ‘secondary mutant set’.

### 6.2.6 Secondary screen: Recovery from rapamycin

It is possible that null mutants were identified in the primary screen for reasons other than a rapamycin recovery defect, for example an inability to survive the lengthy incubation or poor adherence to the robotic pins. We therefore tested the 20 representative null mutants for their ability to recover from a short period of treatment with rapamycin.

Fresh null mutant haploid cells were created by dissection of heterozygote diploids for each null mutant in the BY4743 background. Three independent null haploids of each mutant were tested for their ability to recover from rapamycin treatment. Exponentially growing liquid cultures were treated (or not) with rapamycin (200 ng/mL) in YPD and incubated at 28°C with agitation for two hours. Cells were subsequently washed three times in fresh YPD and ten-fold serial dilutions created and spotted onto a plain YPD plate. Plates were incubated at 28°C for two days prior to scanning. Of the 20 null mutants tested (which were originally identified in the primary screen), we found that 14 did indeed display a rapamycin recovery defect as shown in Figure 6.2, Figure 6.3 and Figure 6.4. Each category of null mutants will be discussed in more detail below.

### 6.2.6.1 Threonine biosynthesis mutants

As seen in Figure 6.2 we found that both of the two null mutants tested, *hom2Δ* and *hom3Δ*, had a rapamycin recovery defect. It would appear that Hom2p and Hom3p are somehow required for recovery from rapamycin.

### 6.2.6.2 Endosomal trafficking mutants

#### HOPS/CORVET mutants

We found that none of the five mutants tested efficiently recovered from rapamycin treatment (Figure 6.3). Cells lacking any of the four core proteins of the HOPS/CORVET complexes (Pep3p, Pep5p, Vps15p or Vps33p) were unable to recover from rapamycin treatment (Figure 6.3). Loss of the HOPS specific subunit, Vam6p, also results in a recovery defect from rapamycin, but appears less severe than that observed for cells lacking of any of the core proteins (Figure 6.3). It is therefore possible that the core HOPS/CORVET complex has a role in the TORC1 signalling pathway in addition to that of the Vam6p GEF in activating the EGO complex (Binda et al. 2009).

#### The Vps15p-Vsp34p complex

Of the two null mutants tested (*vps15Δ* or *vps34Δ*), neither was able to recover from rapamycin treatment (Figure 6.3). Phosphoinositide 3 kinase activity is therefore somehow required for recovery from rapamycin treatment.

#### Remaining endosomal trafficking mutants

Only one of the six remaining mutants classified as 'endosomal trafficking' had a rapamycin recovery defect (Figure 6.3). Loss of Shp1p resulted in a rapamycin recovery defect (Figure 6.3), Shp1p is a cofactor protein for Cdc48 and is involved in membrane fusion and autophagosome biogenesis (Dargemont & Ossareh-Nazari 2012). Loss of any one of Ypt7p, Vam7p, Snx4p, Atg11p, or Pib2p did not compromise rapamycin recovery (Figure 6.3). It is therefore likely that, with the exception of *shp1Δ*, these mutants were identified in the primary screen for reasons other than an inability to recover from rapamycin. It is possible that Shp1p on the other hand is required for recovery from rapamycin.

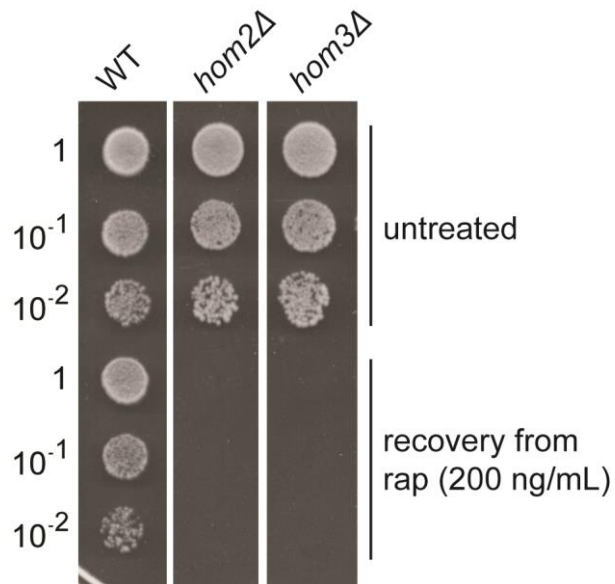


**Figure 6.2 Recovery from rapamycin of *hom2Δ* and *hom3Δ* mutants**

Exponentially growing wild-type, *hom2Δ* and *hom3Δ* cultures were normalised to an  $OD_{600nm}$  of  $\sim 0.1$  in YPD and treated (or not) with rapamycin (200 ng/mL) for two hours at 28°C with agitation. Cells were washed three times in fresh YPD prior to ten-fold serial dilutions being spotted (5  $\mu$ L) onto a YPD plate which was incubated at 30°C for two days. Representative images of three repeats of individual strains are shown.

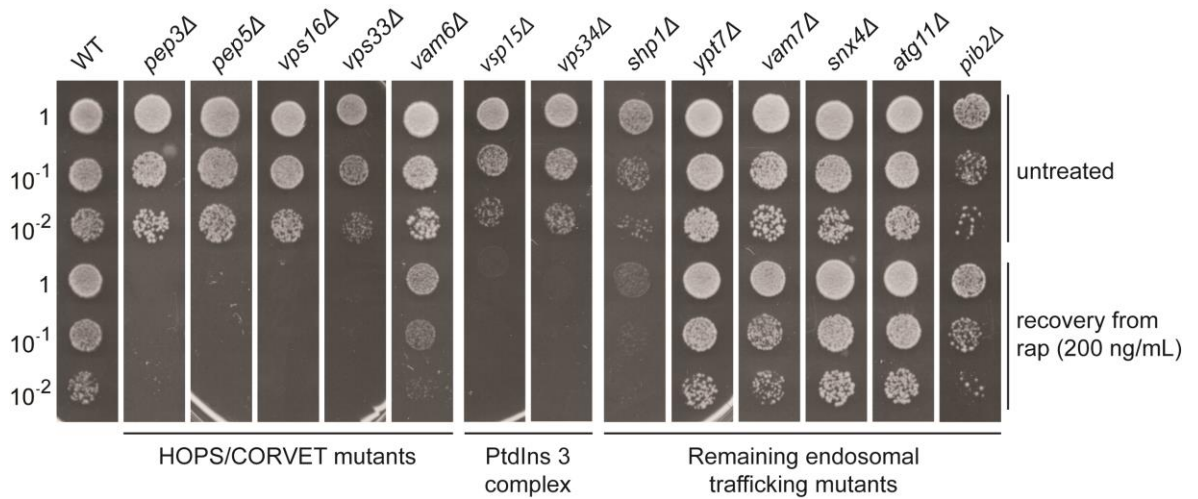


**Figure 6.3 Recovery from rapamycin of endosomal trafficking mutants**

Exponentially growing cultures of wild-type, *pep3Δ*, *pep5Δ*, *vps16Δ*, *vps33Δ*, *vam6Δ*, *vps15Δ*, *vps34Δ*, *shp1Δ*, *ypt7Δ*, *vam7Δ*, *snx4Δ*, *atg11Δ* and *pib2Δ* cells were normalised to an OD of  $\sim 0.1$  in YPD and treated (or not) with rapamycin (200 ng/mL) for two hours at 28°C with agitation. Cells were washed three times in fresh YPD prior to ten-fold serial dilutions being spotted (5  $\mu$ L) onto a YPD plate which was incubated at 30°C for two days. Representative images of three repeats of individual strains are shown.

### 6.2.6.3 Regulation of transcription mutants

We found that four of the five null mutants tested from the ‘regulation of transcription’ category failed to recover from rapamycin treatment. As seen in Figure 6.4, loss of any one of Ccr4p, Dhh1p, Npl3p or Ctk1p resulted in a rapamycin recovery defect. On the other hand, loss of Yke2p did not affect the ability of cells to recover (Figure 6.4). It is possible that the roles of Ccr4p, Dhh1p, Npl3p or Ctk1p are required for recovery from rapamycin

### 6.2.6.4 Summary

Of the 20 null mutants tested we have identified 14 that fail to efficiently recover from rapamycin treatment. It is known that Vam6p acts in the TORC1 signalling pathway via its GEF activity towards the EGO complex. We shall therefore not include *vam6Δ* mutants in our further phenotyping experiments. The remaining 13 null mutants that show a rapamycin recovery defect will be characterised further.

### 6.2.7 Tertiary screen I: Viability of null mutants in the presence of rapamycin

It is possible that the 13 null mutants fail to recover from rapamycin because they lose viability in the presence of rapamycin. We tested the viability of these 13 null mutants, using the methylene blue viability stain, in the absence and presence of a high concentration of rapamycin (200 ng/mL).

Exponentially growing cultures were treated (or not) with rapamycin (200 ng/mL) for two hours in YPD and incubated at 28°C with agitation. Following the two-hour rapamycin treatment, cells were washed three times with fresh YPD and inoculated into fresh YPD for a 24 hour “recovery period” at 28°C with agitation. Control cultures of untreated and continuously rapamycin (200 ng/mL) treated cells in YPD were also included and were incubated at 28°C with agitation for 24 hours. To observe methylene blue staining, cells were exposed to the stain and observed by microscopy.

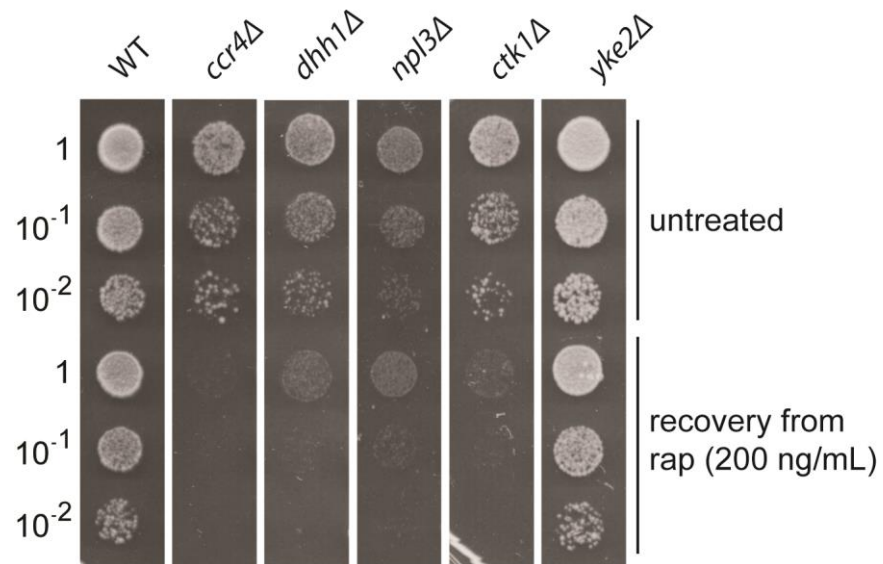


**Figure 6.4 Recovery from rapamycin of regulation of transcription representatives**

Exponentially growing cultures of wild-type, *ccr4Δ*, *dhh1Δ*, *npl3Δ*, *ctk1Δ* and *yke2Δ* cells were normalised to an  $OD_{600nm}$  of  $\sim 0.1$  in YPD and treated (or not) with rapamycin (200 ng/mL) for two hours at 28°C with agitation. Cells were washed three times with fresh YPD prior to ten-fold serial dilutions being spotted (5  $\mu$ L) onto a YPD plate which was incubated at 30°C for two days. Representative images of three repeats of individual strains are shown.

Control cultures of heat treated cells (aliquots of cells that had been exposed to rapamycin for 24 hours were heated to 85°C for 10 minutes) were also included to ensure rapamycin did not affect the methylene blue stain in these cells. A minimum of 200 cells were counted per culture.

Wild-type and *ego1Δ* cultures were included as controls and as expected we found no loss of viability in either of these cultures as a result of treatment with rapamycin (Table 6.8). By contrast, cells from heat-treated wild-type and heat-treated *ego1Δ* cultures fully stained with methylene blue (Table 6.8). We found that the presence of rapamycin did not result in a substantial proportion of cell death for any of the 13 null mutants tested (Table 6.8). Whilst loss of Ccr4p did appear to result in more cell death in the presence of rapamycin than any of the other null mutants, the percentage death observed cannot explain the profound recovery defect of *ccr4Δ* mutants. We therefore conclude that loss of viability is unable to explain the profound rapamycin recovery defect observed for any of the 13 null mutants tested, as assayed by methylene blue staining.

### 6.2.8 Tertiary screen II: Rapamycin-insensitive growth rate

Do the null mutants that are unable to recover from rapamycin display a slow rapamycin-insensitive proliferation rate? Exponentially growing cultures were treated (or not) with rapamycin (200 ng/mL) in YPD and incubated at 28°C with agitation. The culture density was measured by spectrometry at OD<sub>600nm</sub> three and six hours after the introduction of rapamycin and the growth rate calculated between these times. Growth rates were calculated relative to the average growth rate of untreated wild-type cultures. These results will be considered for each category in turn.

#### 6.2.8.1 Threonine biosynthesis mutants

Loss of either Hom2p or Hom3p did not compromise the vegetative growth rate compared to that of wild-type cultures (Figure 6.5). However, we found that the rapamycin-insensitive growth rate of *hom2Δ* mutants was significantly slower than that of wild-type cultures (p=0.0008) and looks comparable to that of *ego1Δ* mutants (Figure 6.5A & B).

|                             |               | Percentage of dead cells |  |   |                    |
|-----------------------------|---------------|--------------------------|--|---|--------------------|
|                             |               | Untreated cells          | 24 hours in constant rapamycin (200 ng/mL) | 24 hours following washout of rapamycin (200 ng/mL) | Heat treated cells |
|                             | WT            | <1%                      | <1%  | <1%   | >99%               |
|                             | <i>ego1Δ</i>  | <1%                      | <1%  | <1%   | >99%               |
| Threonine biosynthesis      | <i>hom2Δ</i>  | <1%                      | <1%  | <1%   | >99%               |
|                             | <i>hom3Δ</i>  | <1%                      | <1%  | <1%   | >99%               |
|                             | <i>pep3Δ</i>  | <2%                      | <1%  | <1%   | >99%               |
|                             | <i>pep5Δ</i>  | <1%                      | <1%  | <1%   | >99%               |
| Endosomal trafficking       | <i>vps33Δ</i> | <1%                      | <1%  | <1%   | >99%               |
|                             | <i>vps16Δ</i> | <1%                      | <1%  | <1%   | >99%               |
|                             | <i>vps15Δ</i> | <4%                      | <4%  | <7%   | >99%               |
|                             | <i>vps34Δ</i> | <1%                      | <1%  | <1%   | >99%               |
|                             | <i>shp1Δ</i>  | <3%                      | <17%                                       | <11%  | >99%               |
|                             | <i>ccr4Δ</i>  | <6%                      | <26%                                       | <30%  | >99%               |
|                             | <i>dhh1Δ</i>  | <3%                      | <8%  | <15%  | >99%               |
| Regulation of transcription | <i>npl3Δ</i>  | <5%                      | <11%                                       | <12%  | >99%               |
|                             | <i>ctk1Δ</i>  | <2%                      | <10%                                       | <6%   | >99%               |

**Table 6.8 Percentage of cell death following exposure to rapamycin**

The observed percentage of cell death in exponentially growing cultures, continuously rapamycin (200 ng/mL) treated cultures or after a recovery period from a two hour rapamycin (200 ng/mL) treatment. Heat treated cells were included as a control. Note that the percentage of dead cells for mutants labelled in bold is a combination of both methylene blue stained cells and those that had a 'ghost cell' like appearance which is an indicator that the cell has lysed (and therefore cannot retain the methylene blue stain).

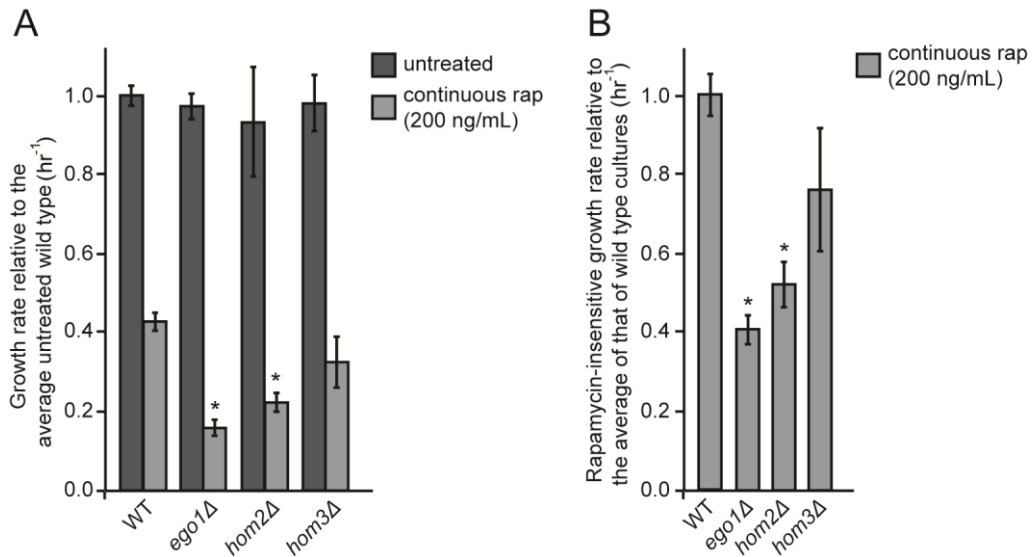


**Figure 6.5 The rapamycin-insensitive growth rate of *hom2Δ* and *hom3Δ* mutant cultures**

Exponentially growing cultures of wild-type, *ego1Δ*, *hom2Δ* and *hom3Δ* cells were normalised to an OD<sub>600nm</sub> of ~0.05 (untreated) or ~0.1 (rapamycin treated) in YPD. Normalised cultures were treated (or not) with rapamycin (200 ng/mL) in YPD and incubated at 28°C with agitation for six hours. At three and six hours after the introduction of rapamycin, the culture density was measured by spectrometry at OD<sub>600nm</sub> and the growth rate was calculated between these times for each culture.

A: The growth rates of all cultures were calculated relative to the average growth rate of untreated wild-type cultures (0.59 hr<sup>-1</sup>).

B: The rapamycin-insensitive growth rate of cultures was calculated relative to the average rapamycin-insensitive growth rate of wild-type cultures (0.25 hr<sup>-1</sup>).

N=13 independent cultures for wild-type, 11 for *ego1Δ* and 3 for *hom2Δ* and *hom3Δ* cultures. Error bars denote S.E.M.; \* p<0.05 relative to equivalently treated wild-type cultures.

Unfortunately the error bars for the rapamycin-insensitive growth rates for *hom3Δ* cultures are too large to draw a definitive conclusion (Figure 6.5A & B). Our data suggests that a slow rapamycin-insensitive growth rate of *hom2Δ* may underpin their inability to recover from the drug.

### 6.2.8.2 Endosomal trafficking mutants

#### HOPS/CORVET mutants

As seen in Figure 6.6, we found that loss of any one of the core HOPS/CORVET proteins did not result in a slow vegetative growth rate. However, loss of Pep3p, Pep5p, Vps16p or Vps33p resulted in a significantly slow rapamycin-insensitive growth rate compared to that of wild-type cultures ( $p=2.0 \times 10^{-5}$  for *pep3Δ*, 0.02 for *pep5Δ*, 0.02 for *vps16Δ*,  $1.2 \times 10^{-5}$  for *vps33Δ*) (Figure 6.6A & B). The slow rapamycin-insensitive growth rate of these core HOPS/CORVET null mutants is indistinguishable from that of *ego1Δ* cultures (Figure 6.6A & B). The compromised rapamycin-insensitive growth rate of the *hop/corvet*-cultures could therefore explain their inability to recover from rapamycin treatment.

#### The Vps15p-Vsp34p complex

We found that loss of Vps15p or Vps34p resulted in cultures with a modest, and significant in the case of *vps15Δ* cultures, defect in vegetative growth rate compared to that of wild-type cultures ( $p=8.6 \times 10^{-5}$  for *vps15Δ*) (Figure 6.6A). The rapamycin-insensitive growth rate of *vps15Δ* and *vps34Δ* mutant cultures was also significantly slower than that of wild-type cultures ( $p=0.02$  for *vps15Δ* and 0.02 for *vps34Δ*) (Figure 6.6A & B) and again appeared similar to that of rapamycin treated *ego1Δ* cultures (Figure 6.6 B). The slow rapamycin-insensitive growth rate of these null mutants could therefore explain their inability to recover from rapamycin.

#### Remaining endosomal trafficking mutants

Null *shp1Δ* cultures were found to have a significantly slower vegetative growth rate compared to that of wild-type cultures ( $p=3 \times 10^{-8}$ ) (Figure 6.6 A). In the presence of rapamycin, the growth rate of *shp1Δ* cultures was significantly slower than that of wild-type cultures ( $p=0.01$ ) and appeared similar to that of *ego1Δ* cultures (Figure 6.6 B). A slow rapamycin-insensitive growth rate could account for the inability of *shp1Δ* cultures to recover from the drug.

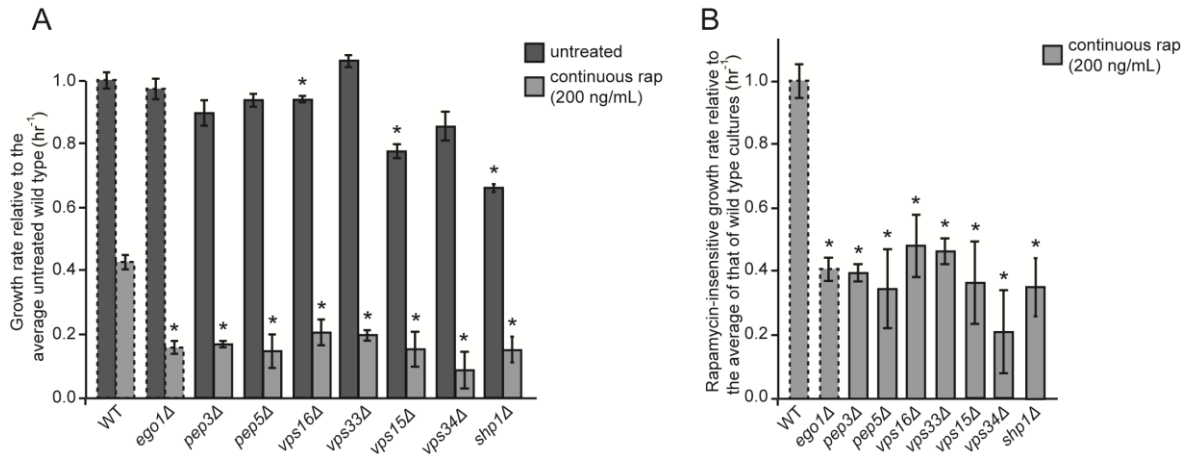


**Figure 6.6** The rapamycin-insensitive growth rate of *pep3Δ*, *pep5Δ*, *vps16Δ*, *vps33Δ*, *vps15Δ*, *vps34Δ* and *shp1Δ* mutant cultures

Exponentially growing cultures of *pep3Δ*, *pep5Δ*, *vps16Δ*, *vps33Δ*, *vps15Δ*, *vps34Δ* and *shp1Δ* cells were normalised to an OD<sub>600nm</sub> of ~0.05 (untreated) or ~0.1 (rapamycin treated) in YPD. Normalised cultures were treated (or not) with rapamycin (200 ng/mL) in YPD and incubated at 28°C with agitation for six hours. At three and six hours after the introduction of rapamycin, the culture density was measured by spectrometry at OD<sub>600nm</sub> and the growth rate was calculated between these times for each culture. The growth rates of wild-type and *ego1Δ* cultures from Figure 6.5 (indicated by a dashed border) are included for comparison; these growth rates were measured in parallel.

A: The growth rates of all cultures were calculated relative to that of the average growth rate of untreated wild-type cultures (0.59 hr<sup>-1</sup>) which were measured in parallel.

B: The rapamycin-insensitive growth rate of cultures was calculated relative to the average rapamycin-insensitive growth rate of wild-type cultures (0.25 hr<sup>-1</sup>), which were measured in parallel.

N=13 independent cultures for wild-type, 11 for *ego1Δ*, 7 for *pep3Δ* and 3 for all remaining cultures. Error bars denote S.E.M.; \* p<0.05 relative to equivalently treated wild-type cultures.

### 6.2.8.3 Regulation of transcription mutants

We found that loss of Ccr4p or Dhh1p resulted in a slow vegetative growth rate compared to that of wild-type cultures ( $p=0.006$  for *dhh1Δ* cultures; the difference was not significant in *ccr4Δ* cultures). The rapamycin-insensitive growth rate of *dhh1Δ* and *ccr4Δ* cultures was also significantly slower than that of wild-type cultures ( $p=0.007$  for *ccr4Δ*,  $9.8 \times 10^{-5}$  for *dhh1Δ* cultures) (Figure 6.7A & B). Unfortunately the error bars are too large for *ctk1Δ* cultures to draw any firm conclusions. Due to the initial inconsistency in the phenotype of different *npl3Δ* isolates, the rapamycin-insensitive growth rate of this mutant has not been measured. However, the identification of a slow rapamycin-insensitive growth rate of *ccr4Δ* and *dhh1Δ* cultures is consistent with the rapamycin-insensitive growth rate underlying the inability of cultures to recover.

### 6.2.8.4 Summary

All null mutants tested, that were confirmed to have a rapamycin recovery defect, also show a slow rapamycin-insensitive growth rate. Note that the results for *hom3Δ* and *ctk1Δ* are inconclusive and have not been included in this analysis. We have therefore identified null mutants from the initial primary screen that phenocopy *ego-* mutants, both in terms of their inability to recover from rapamycin treatment and their slow rapamycin-insensitive growth rate.

### 6.2.9 Selectivity to rapamycin treatment

We have shown that all null mutants tested (with the exception of *hom3Δ* and *ctk1Δ* mutants which were inconclusive) have a slow rapamycin-insensitive growth rate. Do these mutations selectively result in a slow rapamycin-insensitive growth rate? We re-calculated the results obtained in Section 6.2.8 to measure the fold decrease in growth rate of rapamycin-treated cultures compared that of the equivalently untreated cultures, measured in parallel. This re-calculation of the rapamycin-insensitive growth rates observed in Figure 6.5, Figure 6.6 and Figure 6.7 is shown in Figure 6.8A.

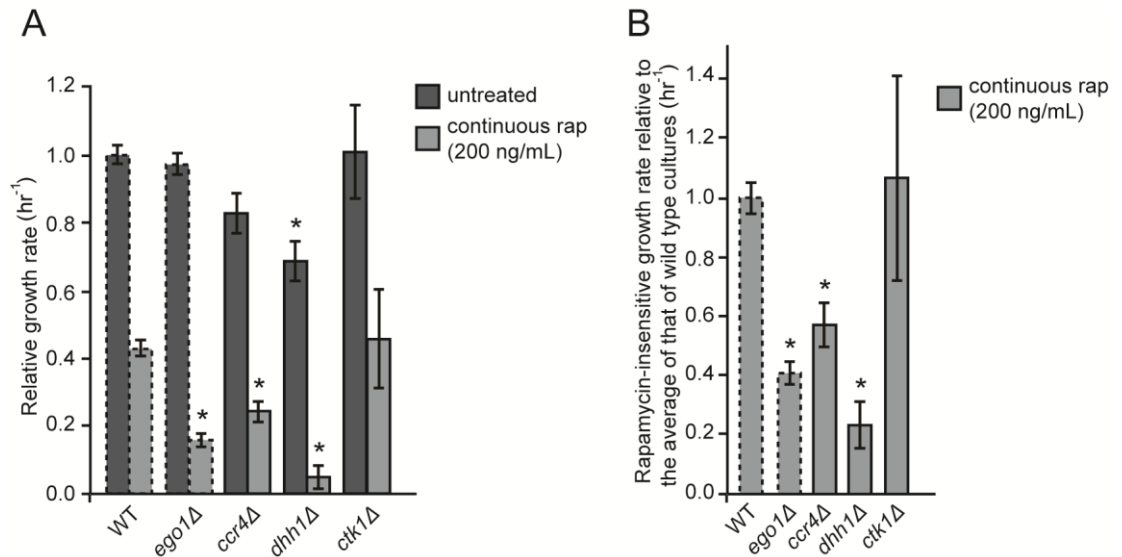


**Figure 6.7 The rapamycin-insensitive growth rate of *ccr4Δ*, *dhh1Δ* and *ctk1Δ* mutant cultures**

Exponentially growing cultures of *ccr4Δ*, *dhh1Δ* and *ctk1Δ* cells were normalised to an  $OD_{600nm}$  of  $\sim 0.05$  (untreated) or  $\sim 0.1$  (rapamycin treated) in YPD. Normalised cultures were treated (or not) with rapamycin (200 ng/mL) in YPD and incubated at  $28^{\circ}C$  with agitation for six hours. At three and six hours after the introduction of rapamycin, the culture density was measured by spectrometry at  $OD_{600nm}$  and the growth rate was calculated between these times for each culture. The growth rates of wild-type and *ego1Δ* cultures from Figure 6.5 (indicated by a dashed border) are included for comparison; these growth rates were measured in parallel.

A: The growth rates of all cultures were calculated relative to the average growth rate of untreated wild-type cultures ( $0.59 \text{ hr}^{-1}$ ), which were measured in parallel.

B: The rapamycin-insensitive growth rate of cultures was calculated relative to the average rapamycin-insensitive growth rate of wild-type cultures ( $0.25 \text{ hr}^{-1}$ ), which were measured in parallel.

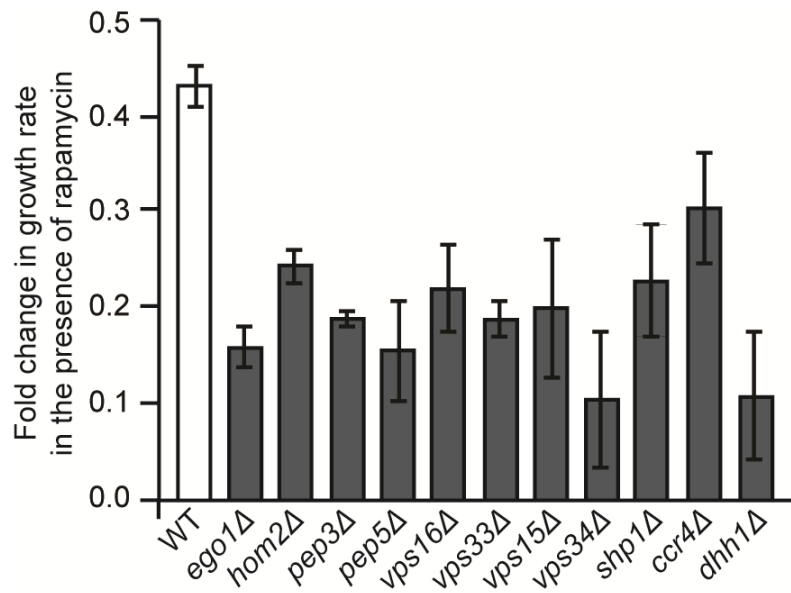
N=13 independent cultures for wild-type, 11 for *ego1Δ*, 4 for *dhh1Δ* and 3 for the remaining cultures. Error bars denote S.E.M.; \*  $p < 0.05$  relative to equivalently treated wild-type cultures.

We found that the slow rapamycin-insensitive growth rate is selectively affected by loss of seven of the 10 null mutants tested. The fold change in growth rate of *hom2Δ*, *pep3Δ*, *pep5Δ*, *vps16Δ*, *vps33Δ*, *vps34Δ* and *dhh1Δ* mutants in the presence of rapamycin was significantly slower than that of wild-type cultures (Figure 6.8A & B). The fold change in growth rate of these mutant cultures, with the exception of *hom2Δ* mutants, was not significantly different to that of *ego1Δ* cultures (Figure 6.8B). It is possible that loss of Hom2p results in a selectively slow rapamycin-insensitive growth rate, but that the defect is not as severe as that seen for *ego1Δ* cultures. The fold change in growth rate of the remaining three mutant cultures (*vps15Δ*, *shp1Δ* and *ccr4Δ*) was not significantly different from that of either wild-type or *ego1Δ* cultures (Figure 6.8B). These results are therefore inconclusive as to whether the slow rapamycin-insensitive growth rate is selective for loss of the protein in the presence of rapamycin. We have therefore identified seven null mutants which show a selectively slow rapamycin-insensitive growth rate; it is possible the corresponding proteins are required for TORC1 activity.

#### 6.2.10 Recovery from rapamycin of *ego1Δ pep3Δ* double mutants

The results of the primary and subsequent secondary and tertiary screens identified null mutants for any of the four members of the core HOPS/CORVET complex. The primary and secondary screens also identified the HOPS specific component Vam6p, which has GEF activity towards Gtr1p of the EGO complex (Binda et al. 2009). It has not previously been identified whether the core HOPS complex (shared with CORVET) also regulates TORC1. We found that the rapamycin recovery defect was more severe in cells lacking any one of the core complex than in cells lacking Vam6p, indicating that the core HOPS/CORVET complex has other function(s), independent of Vam6p, in modulating TORC1 activity. Does this additional function of the core HOPS/CORVET complex in TORC1 regulation also act via the EGO complex? Double mutants were created that lacked both the Ego1p subunit of the EGO complex and the Pep3p subunit of the core HOPS/CORVET complex. The ability of these double mutant cells to recover from low concentrations of rapamycin was tested.

A



B

|               | Compared to WT |                      | Compared to <i>ego1Δ</i> |      |
|---------------|----------------|----------------------|--------------------------|------|
|               | p<0.05         | p=                   | p<0.05                   | p=   |
| <i>hom2Δ</i>  | ✓              | 1.2x10 <sup>-4</sup> | ✓                        | 0.02 |
| <i>pep3Δ</i>  | ✓              | 3x10 <sup>-8</sup>   | ✗                        | 0.2  |
| <i>pep5Δ</i>  | ✓              | 0.021                | ✗                        | 0.97 |
| <i>vps16Δ</i> | ✓              | 0.024                | ✗                        | 0.31 |
| <i>vps33Δ</i> | ✓              | 2x10 <sup>-5</sup>   | ✗                        | 0.33 |
| <i>vps15Δ</i> | ✗              | 0.07                 | ✗                        | 0.63 |
| <i>vps34Δ</i> | ✓              | 0.033                | ✗                        | 0.53 |
| <i>shp1Δ</i>  | ✗              | 0.059                | ✗                        | 0.36 |
| <i>ccr4Δ</i>  | ✗              | 0.14                 | ✗                        | 0.11 |
| <i>dhh1Δ</i>  | ✓              | 0.03                 | ✗                        | 0.53 |

**Figure 6.8** The fold decrease in growth rate in the presence of rapamycin compared to equivalent untreated cultures

A: The fold decrease in growth rate was calculated for the rapamycin-insensitive growth rate of cultures shown in Figure 6.5, Figure 6.6 and Figure 6.7. The fold decrease of the rapamycin-insensitive growth rate was calculated relative to the untreated culture measured in parallel (values ranged from 0.41 to 0.63 hr<sup>-1</sup>). Error bars denote S.E.M.

B: The p-values of the fold change in growth rate of each mutant relative to that of either wild-type or *ego1Δ* cultures. A ✓ indicates that the p-value is less than 0.05 whilst a ✗ indicates that the p-value is above 0.05. The calculated p-values are also shown.

Exponentially growing cultures of wild-type, *ego1Δ*, *pep3Δ* and *ego1Δ pep3Δ* cells were treated (or not) with rapamycin (2, 5, 10 or 200 ng/mL) in YPD for two hours at 28°C with agitation. Cells were washed three times in fresh YPD, ten-fold dilutions were created and spotted to a YPD plate. Plates were incubated for two days at 28°C to allow for recovery.

As seen in Figure 6.9, we found that loss of both the EGO and core HOPS/CORVET complexes resulted in an indistinguishable phenotype from that of the single *pep3Δ* mutant at all concentrations of rapamycin tested. These results suggest that the EGO and core HOPS/CORVET complex do indeed act in the same pathway to promote recovery from rapamycin.

We found that loss of Pep3p resulted in cells with a more severe recovery defect than loss of Ego1p at low concentrations of rapamycin (10 ng/mL). This result suggests that the core HOPS/CORVET complex has a role in aiding recovery from rapamycin in addition to any role in the EGO pathway.

#### 6.2.11 The rapamycin-insensitive growth rate of *hops/corvet-ego*- double mutants

If the core HOPS/CORVET complex is required for maintaining TORC1 activity in addition to that of the EGO complex, does the double *ego- hops/corvet*- mutant have a slow rapamycin-insensitive growth rate in the presence of a high concentration of the drug? We can use the measurement of the rapamycin-insensitive growth rate as a proxy for TORC1 activity in strains lacking the EGO complex, core HOPS/CORVET complex or both.

Exponentially growing cultures of *ego1Δ pep3Δ* cells were treated (or not) with rapamycin (200 ng/mL) in YPD and incubated at 28°C with agitation. At three and six hours after the introduction of the drug the culture density was measured by OD<sub>600nm</sub> and the growth rate calculated between these time points. All growth rates were calculated relative to that of the average untreated wild-type culture from Figure 6.5, the growth rates of which were measured in parallel. The growth rates of *ego1Δ* and *pep3Δ* cultures from Figure 6.6 are included as comparisons; again these growth rates were also measured in parallel to that of the wild-type and double-mutant cultures.

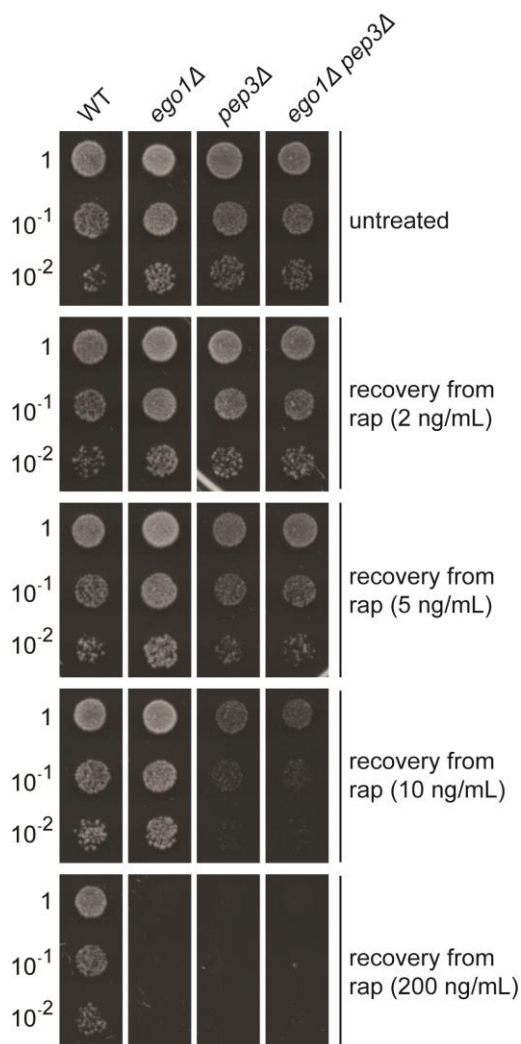


**Figure 6.9** Rapamycin recovery of *ego1Δ pep3Δ* double mutants from various concentrations of the drug

Exponentially growing cultures of wild-type, *ego1Δ*, *pep3Δ* and *ego1Δ pep3Δ* cells were treated (or not) with rapamycin (2, 5, 10 or 200 ng/mL) in YPD and incubated at 28°C with agitation for two hours. Cells were washed three times in fresh YPD, ten-fold serial dilutions created and spotted (5 μL) onto a plain YPD plate. Plates were incubated at 28°C for two days prior to scanning. These images represent one of two independent replicates.

We found that the rapamycin-insensitive growth rate of the double *ego1Δ pep3Δ* mutant was not significantly different to that of either the *ego1Δ* or the *pep3Δ* single mutant cultures ( $p=0.05$  compared to *ego1Δ* and  $0.07$  compared to *pep3Δ* cultures) (Figure 6.10).

We conclude that the core HOPS/CORVET and EGO complexes behave as if in a co-linear pathway; the core HOPS/CORVET complex supports TORC1 activity via the EGO complex alone. These results also suggest that the more severe rapamycin recovery defect phenotype of *pep3Δ* cultures is not due to loss of rapamycin-insensitive functions of TORC1, as assayed by growth rate. It is possible that loss of Pep3p, and by inference disruption of the core HOPS/CORVET complex, could affect the uptake of rapamycin into the cell or result in an altered threshold of TORC1 activity required for recovery.

#### **6.2.12 Could a vacuolar morphology defect explain the requirement of the core HOPS/CORVET complex in rapamycin recovery?**

The HOPS/CORVET complexes are required for vesicle trafficking and for maintaining the structure of the vacuole (Cai et al. 2007). It is thought that the TORC1 complex, along with key activators such as the EGO complex, are localised to the cytoplasmic face of the vacuolar membrane. Is it possible that the inability of *hops/corvet*- mutants to recover from rapamycin is due to malformed vacuoles and therefore potentially mislocalised TORC1, activators of the complex and downstream targets? If a loss of vacuole morphology results in a recovery defect, we would expect any mutant in which vacuole morphology, and potentially all endosomal trafficking, is disrupted would also have a recovery defect. Ypt7p is a Rab GTPase for the HOPS complex and is required for the homotypic fusion of late endosomes to the vacuole; mutants lacking Ypt7p have numerous fragmented vacuoles within the cell (Cai et al. 2007; Haas et al. 1995). Null *ypt7Δ* mutants were identified in our primary mutant set but exhibited a wild-type phenotype with regards to rapamycin recovery in our secondary screen (Figure 6.3). Is vacuolar trafficking indeed disrupted in this mutant? We used the vacuolar stain FM4-64 to visualise the vacuoles of wild-type, *ego1Δ*, *pep3Δ*, *ego1Δ pep3Δ* and *ypt7Δ* cells to test whether disruption of vacuolar morphology affects the ability of cells to recover from rapamycin.

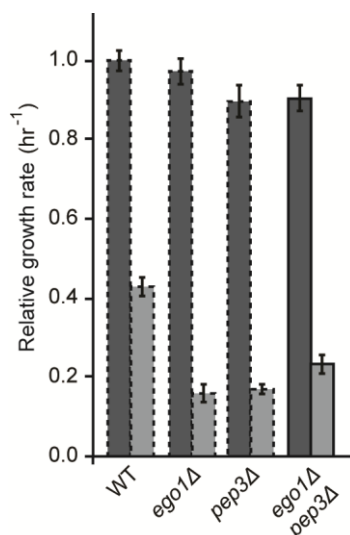


**Figure 6.10 The rapamycin-insensitive growth rate of *ego1Δ pep3Δ* double mutant cultures**

Exponentially growing cultures of *ego1Δ pep3Δ* cells were treated (or not) with rapamycin (200 ng/mL) in YPD and incubated at 28°C with agitation. The growth rate was calculated from the culture density, as measured by spectrometry at OD<sub>600nm</sub>, at three and six hours after the introduction of rapamycin. All growth rates were calculated relative to that of the average untreated wild-type culture (0.59 hr<sup>-1</sup>) from Figure 6.5, the growth rates of which were measured in parallel. The growth rates of *ego1Δ* and *pep3Δ* cultures from Figure 6.6 are included as comparisons, these growth rates were also measured in parallel to that of the wild-type and double mutant cultures. The vegetative growth rate of the *ego1Δ pep3Δ* culture was significantly slower than that of wild-type cultures (p=0.04) and the rapamycin-insensitive growth rates of *ego1Δ*, *pep3Δ* and *ego1Δ pep3Δ* cultures were significantly slower than that wild-type cultures (p=2.1×10<sup>-8</sup>, 2.0×10<sup>-8</sup> and 1.8×10<sup>-4</sup> respectively). N=13 independent cultures for wild-type, 11 for *ego1Δ*, 7 for *pep3Δ* and 5 for *ego1Δ pep3Δ* cultures. Error bars denote S.E.M.

Exponentially growing cultures of wild-type, *ego1Δ*, *pep3Δ*, *ego1Δ pep3Δ* and *ypt7Δ* cells were treated (or not) with rapamycin (200 ng/mL) in YPD at 28°C with agitation for two hours. Cells were pelleted, concentrated into YPD (with or without rapamycin (200 ng/mL) as appropriate) containing FM4-64 (2 μM) and incubated at 30°C for 30 minutes in the dark. Cells were diluted into fresh YPD, pelleted, then resuspended into YPD (with or without rapamycin (200 ng/mL) as appropriate) and incubated at 28°C with agitation for 90 minutes in the dark (to allow time for the stain to traffic to the vacuole). Cells were washed once with water and concentrated into complete synthetic media (which was used to reduce autofluorescence). All samples were kept on ice until assayed by microscopy.

We found that exponentially growing wild-type cells had predominantly one small-sized vacuole (Figure 6.11). Following rapamycin treatment however, the vacuole of wild-type cells increased in size and appeared to take up a large proportion of the cell (Figure 6.11). These observations are consistent with low TORC1 activity promoting autophagy. We found that the vacuolar morphology of *ego1Δ* mutants appeared no different from those of wild-type cells both in the absence or presence of rapamycin (Figure 6.11). Exponentially growing *pep3Δ* mutants did not appear to have any defined vacuolar structure, instead the FM4-64 was widely dispersed throughout the cytoplasm. When *pep3Δ* mutants were treated with rapamycin, the FM4-64 was found to remain dispersed through the cytoplasm but was concentrated in small puncta; no defined vacuole structure was observed (Figure 6.11). These results are consistent with loss of the core HOPS/CORVET complex preventing the formation of a vacuole. The concentrated puncta of FM4-64 stain in rapamycin treated *pep3Δ* cells is potentially due to the upregulation of autophagy and accumulation of late endosomal vesicles due to the lack of a vacuole with which to fuse. The dispersion of FM4-64 stain in double *ego1Δ pep3Δ* mutant cells both in the absence and presence of rapamycin appeared very similar to that of the single *pep3Δ* mutant (Figure 6.11). Consistent with the requirement of Ypt7p for fusion of endosomes to the vacuole, we found that loss of Ypt7p indeed resulted in cells that also had no identifiable vacuole; the FM4-64 stain was distributed throughout the cytoplasm both in the absence and presence of rapamycin (Figure 6.11).

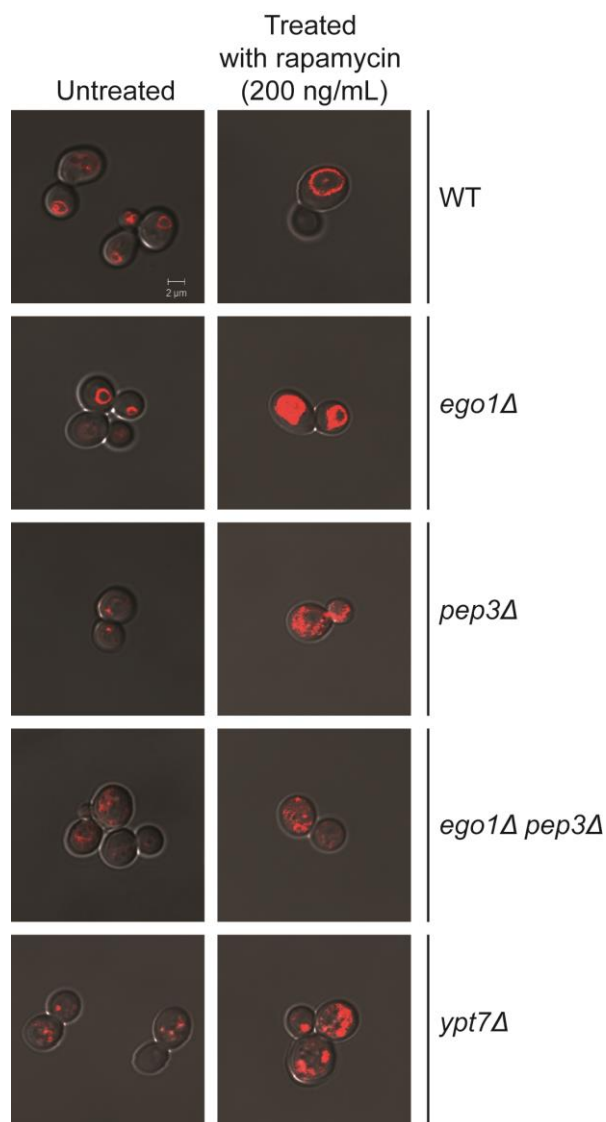


**Figure 6.11** Representative images of FM4-64 staining in wild-type, *ego1Δ*, *pep3Δ*, *ego1Δ pep3Δ* and *ypt7Δ* cells

Cultures of wild-type, *ego1Δ*, *pep3Δ*, *ego1Δ pep3Δ* and *ypt7Δ* cells were treated (or not) with rapamycin (200 ng/mL) in YPD for two hours at 28°C with agitation after which they were exposed to the vacuole stain FM4-64 for 30 min at 30°C. The cultures were washed into fresh media, either with or without rapamycin, and incubated for 90 minutes at 28°C with agitation to allow time for the stain to localise at the vacuole. Fluorescent microscopy images of mutant cells were taken with an excitation wavelength of 505-530 nm and an emission wavelength of 560 nm. All images were captured using a 63x oil immersion objective and a merge of the bright field and fluorescent image is shown.

As seen in the *pep3Δ* and *ego1Δ pep3Δ* mutant cells, treatment with rapamycin resulted in an increase in defined puncta of FM4-64 staining in *ypt7Δ* mutants, but no clear vacuolar structure was observed (Figure 6.11). The lack of vacuolar morphology in *pep3Δ* and *ypt7Δ* mutants is consistent with published results that these proteins are required for normal vacuole morphology (Cai et al. 2007).

Does a vacuolar morphology defect correlate with the inability to recover from rapamycin? We have shown that *ypt7Δ* mutants, like those lacking Pep3p, do not have a recognisable vacuolar structure (Figure 6.11). Yet unlike *pep3Δ* mutants, loss of Ypt7p does not result in a rapamycin recovery defect (Figure 6.3). These results alone suggest that the morphology of the vacuole does not correlate with an ability to recover from rapamycin. We have also shown that mutants lacking the EGO complex or those lacking Pep3p fail to recover from rapamycin treatment (Figure 3.1 and Figure 6.3), yet *ego1Δ* mutants have vacuoles that appear wild-type (Figure 6.11). We conclude that cells are able to recover from rapamycin regardless of the presence of a vacuolar structure. The core HOPS/CORVET complex must therefore have functions in addition to that required to maintain the vacuole and these functions appear to act, at least in part, via the EGO complex to regulate TORC1 activity.

### 6.3 Conclusion

A primary screen was carried out in an attempt to identify null mutants that failed to recover following incubation in the presence of rapamycin. Of the ~4,700 null mutants tested, 172 failed to recover in at least one run of the screen. We chose to analyse only those null mutants that had been identified in any two or more runs of the screen (88 null mutants in total). As a result of testing for GO term enrichment and known protein-protein interactions we identified 20 null mutants for further phenotyping. The results of our secondary and tertiary screens can be seen in Table 6.9. The results of the GO term analysis identified three categories of enriched genes which we termed threonine biosynthesis, endosomal trafficking and regulation of transcription. As seen in Table 6.9, null mutants were identified in each category that had a rapamycin recovery defect and a slow rapamycin-insensitive growth rate that was selective for loss of the protein.

| Category                    | Gene name    | Secondary screen:         | Tertiary screen:    |  |  |
|-----------------------------|--------------|---------------------------|---------------------|--|--|
|                             |              | Rapamycin recovery defect | Viable in rapamycin | Slow rapamycin-insensitive growth rate | Selectively affects growth rate in rapamycin |
| Threonine biosynthesis      | <i>HOM2</i>  | ✓                         | ✓                   | ✓                                      | ✓  |
|                             | <i>HOM3</i>  | ✓                         | ✓                   | ?                                      |  |
|                             | <i>PEP3</i>  | ✓                         | ✓                   | ✓                                      | ✓  |
|                             | <i>PEP5</i>  | ✓                         | ✓                   | ✓                                      | ✓  |
|                             | <i>VPS16</i> | ✓                         | ✓                   | ✓                                      | ✓  |
|                             | <i>VPS33</i> | ✓                         | ✓                   | ✓                                      | ✓  |
|                             | <i>VAM6</i>  | ✓                         |                     |  |  |
| Endosomal trafficking       | <i>VPS15</i> | ✓                         | ✓                   | ✓                                      | ?  |
|                             | <i>VPS34</i> | ✓                         | ✓                   | ✓                                      | ✓  |
|                             | <i>SHP1</i>  | ✓                         | ✓                   | ✓                                      | ?  |
|                             | <i>YPT7</i>  | ✗                         |                     |  |  |
|                             | <i>VAM7</i>  | ✗                         |                     |  |  |
|                             | <i>SNX4</i>  | ✗                         |                     |  |  |
|                             | <i>ATG11</i> | ✗                         |                     |  |  |
|                             | <i>PIB2</i>  | ✗                         |                     |  |  |
| Regulation of transcription | <i>CCR4</i>  | ✓                         | ✓                   | ✓                                      | ?  |
|                             | <i>DHH1</i>  | ✓                         | ✓                   | ✓                                      | ✓  |
|                             | <i>NPL3</i>  | ✓                         | ✓                   |  |  |
|                             | <i>CTK1</i>  | ✓                         | ✓                   | ?                                      |  |
|                             | <i>YKE2</i>  | ✗                         |                     |  |  |

**Table 6.9 Summary of the results of the secondary screens**

A summary of the results for each of the 20 null mutants tested in the secondary and tertiary screens. An indication of whether the slow rapamycin-insensitive growth rate is selective for the presence of rapamycin is also shown. ✓=positive result observed; ✗=negative result observed; ?=inconclusive result.

From our initial analysis and secondary testing we have confirmed seven null mutants that phenocopy loss of the EGO complex.

By carrying out GO term analysis and protein-protein interaction analysis, as well as only selecting representatives of each category, we have potentially overlooked additional null mutants from the primary screen that could have a rapamycin recovery defect. It would be worth performing a rapamycin recovery secondary screen on the remaining 64 null mutants identified in two or more runs of the primary screen to test their ability to recover from the drug. A screen carried out by the De Virgilio group to identify null mutants unable to recover from a 24 hour incubation in the presence of rapamycin (200 ng/mL) identified eight mutants, all of which were also identified in our primary mutant set: *ego1Δ*, *ego3Δ*, *gtr2Δ*, *pib2Δ*, *sac3Δ*, *ydj1Δ* and *ydl172cΔ* (Dubouloz et al. 2005). It would appear that three of the eight mutants identified in both our screen and the De Virgilio screen, *sac3Δ*, *ydj1Δ* and *ydl172cΔ*, received little attention in either our or De Virgilio's subsequent analysis. Testing the ability of these null mutants to recover from rapamycin might identify yet more potential regulators of TORC1.

Null mutants of the core HOPS/CORVET complex survived the primary, secondary and tertiary aspects of the screen. The slow rapamycin-insensitive growth rate of core *hops/corvet*- mutants appears to be selective for loss of any one of the four proteins (Table 6.9). Vam6p, is a known activator of the EGO complex (Binda et al. 2009) and is also a subunit of the HOPS complex, however it has not been clear whether Vam6p acts independently of the HOPS complex to regulate EGO. We have shown here that loss of the core HOPS/CORVET proteins results in a more profound rapamycin recovery defect than loss of Vam6p. We concluded that the core HOPS/CORVET complex therefore has a function in TORC1 signalling independent of the HOPS subunit Vam6p. All known regulators of TORC1 identified so far appear to act via the EGO complex. We used a double *ego- hops/corvet*- mutant to test whether the core HOPS/CORVET complex also acts via the EGO complex to signal to TORC1. It would appear that the core HOPS/CORVET complex function in regulating TORC1 also acts via the EGO complex alone. Loss of both the EGO and core HOPS/CORVET complexes does not result in a slower rapamycin-insensitive growth rate than loss of the core

HOPS/CORVET complex alone. However loss of the core HOPS/CORVET complex does result in a more severe recovery defect at low concentrations of rapamycin than loss of the EGO complex. It would therefore appear that the core HOPS/CORVET complex has a minor additional role that acts independently of the EGO complex.

It is possible that the additional role of the core HOPS/CORVET complex is involved in the uptake of rapamycin; the ability of core *hops/corvet*- mutants to recover from 10 ng/mL rapamycin was less efficient than that of *ego*- cultures yet these two mutants have indistinguishable rapamycin-insensitive growth rates, which should dictate the ability to recover. It is therefore unlikely that the additional role of the core HOPS/CORVET complex is affecting the rapamycin-insensitive function of TORC1. One possibility is that loss of vacuolar structure and endosomal trafficking in a core *hops/corvet*- mutant, but only in addition to loss of signalling to TORC1 by the complex, impacts the sensitivity of cells to the drug.

The identification of the core HOPS/CORVET complex in regulating TORC1 has provided us with a number of questions including: What is the role of the core HOPS/CORVET complex in signalling to the EGO complex? What is the EGO independent function of the core HOPS/CORVET complex? Does loss of the core HOPS/CORVET complex alter drug uptake? We address some of these questions in the final discussion chapter.

## 7 Discussion

Here, we found that rapamycin-insensitive proliferation is key to efficient recovery from rapamycin. Furthermore, we found that rapamycin-insensitive activity of TORC1 exists, drives this residual proliferation and accounts for the requirement for the EGO complex during recovery. Finally, we identified novel genes whose products may, like the EGO complex, activate TORC1 activity *in vivo*.

### 7.1 Rapamycin does not fully inactivate TORC1

Wild-type cells treated with rapamycin are able to maintain proliferation in the constant presence of the drug. However, proliferation is completely abolished in cells lacking the TORC1 subunit Kog1p and, by inference, TORC1 activity. We therefore conclude that rapamycin is only a partial inhibitor of yeast TORC1 activity. The identification of rapamycin-insensitive functions of yeast TORC1 brings the yeast complex in line with that of mammalian cells; mTORC1 has been shown to have functions that are not inhibited by rapamycin (Feldman et al. 2009; Thoreen et al. 2009). The identification of rapamycin-insensitive functions of yeast TORC1 suggests that there is likely to be a whole aspect of yeast TORC1 signalling that has been hidden from analysis, until now.

What are the functions of TORC1 that are insensitive to rapamycin? We have shown that proliferation is lowered but not completely abolished by rapamycin treatment. We found that loss of the EGO complex combined with rapamycin treatment results in almost no rate of translation in these cells; these results suggest that maintaining translation could be a rapamycin-insensitive function of yeast TORC1. One key downstream function insensitive to rapamycin in mammalian cells is the activation of the translation repressor 4EBP1 (Feldman et al. 2009). It is therefore probable that aspects of translation are also regulated by yeast TORC1 in a rapamycin-insensitive manner. We found that loss of a functional homolog of 4EBP1, Eap1p, resulted in cells with a slow rapamycin-insensitive proliferation rate. Whilst the role of Eap1p is thought to be that of a translational repressor, it is possible that the protein also functions to positively regulate translation via TORC1 in a rapamycin-insensitive manner. The identification of Eap1p as a potential regulator of translation in the TORC1

signalling pathway is consistent with previous studies, however the exact role of Eap1p in response to TORC1 remains elusive (Cosentino et al. 2000).

## 7.2 Is rapamycin-insensitive activity due to a subset of TORC1 not bound to rapamycin?

Is it possible that we observe rapamycin-insensitive functions in yeast due to incomplete binding of the Fpr1p-rapamycin binary complex to TORC1? We believe that this is not the case. Firstly, Fpr1p is one of the most abundant 10% of proteins in the cell, whilst the TORC1 specific subunits are within the least 25% abundant proteins, as estimated by quantitative proteomics (Wang et al. 2012). It is therefore highly unlikely that Fpr1p is limiting for formation of the binary Fpr1p-rapamycin complex. Second, we can estimate the fold increase in the amount of intracellular rapamycin compared to the estimated minimum inhibitory threshold. We know that wild-type cultures double approximately every five hours in the presence of a high concentration of rapamycin, meaning the intracellular pool of rapamycin in cells during recovery is halved every five hours. We found that it took approximately 20 hours for wild-type cultures to recover from 200 ng/mL rapamycin (Figure 5.12), suggesting that the intracellular pool of rapamycin had halved four times before becoming sub-inhibitory. We can therefore predict that the intracellular pool of rapamycin in wild-type cells treated with 200 ng/mL rapamycin is 16 ( $2^4$ ) times greater than the minimum required to inhibit TORC1. It is highly unlikely that TORC1 is not being saturated under these conditions. Whilst it appears rapamycin is not limiting for binding to TORC1, is it possible there is a subset of TOR1 complexes that cannot bind rapamycin?

It is possible that we see rapamycin-insensitive activity due to elevated levels of reactive oxygen species (ROS) which can disrupt the ability of TORC1 to bind to Fpr1p-rapamycin under stressed conditions (Neklesa & Davis 2008), meaning a fraction of TORC1 may not be bound to Fpr1p-rapamycin under our experimental conditions. We do not think this is the case; ROS damage to TORC1 has not been detected under normal nutrient-rich conditions (Neklesa & Davis 2008). Furthermore, we have carried out preliminary tests of the rapamycin-insensitive growth rate of cultures overexpressing a superoxide dismutase in combination with a catalase and do not see a change in the rapamycin-insensitive growth rate

of these cultures compared to that of wild-type cultures. We therefore conclude that the rapamycin-insensitive growth rate observed is due to inherent rapamycin-insensitive functions of TORC1 and not a result of only a fraction of the TORC1 complexes being inactivated.

### 7.3 The mechanism of rapamycin ‘detoxification’

The mechanism of rapamycin detoxification has received little attention. Here we show that rapamycin is not in fact actively metabolised in nor exported from the yeast cell, instead the drug is diluted between an increasing number of progeny cells: *i.e.* diluted-by-proliferation. It must be the case that any drug in which residual proliferation occurs is also partially ‘detoxified’ by a mechanism of dilution-by-proliferation; however, we are not aware of any other xenobiotic for which this mechanism is predominant in reducing drug toxicity.

It is worth mentioning that, whilst we have identified a mechanism by which rapamycin is cleared from cells, it is still unclear how rapamycin enters the cell. It is likely that the import mechanism of rapamycin is also regulated by TORC1 activity. We have found that wild-type cultures are able to recover from a prolonged, at least a 24 hour, treatment period with high concentrations of rapamycin. If rapamycin continues to be taken up by cells throughout this treatment period then the intracellular drug pool would grow with time, resulting in an increased recovery time. Knowing that recovery of rapamycin is dependent on the incredibly slow mechanism of dilution-by-proliferation, the ability of cells to recover from an extremely long treatment time suggests that the intracellular amount of the drug is limited. It is possible that rapamycin enters the cell via an amino-acid transporter. If rapamycin enters via an importer that is subsequently removed from the cell surface following the inactivation of TORC1 it could explain why intracellular rapamycin potentially has a threshold limit. It may be interesting to test whether maintaining amino acid permeases, which are normally degraded following TORC1 inactivation, at the cell surface results in an increase in recovery time.

This work was initially carried out to observe whether or not cells were able to recover from rapamycin treatment; however, our assay evolved to measure the rapamycin-insensitive growth rate. We subsequently found that the rapamycin-

insensitive growth rate dictated whether or not we saw a recovery defect, *i.e.*, a continuous phenotype (rapamycin-insensitive growth rate) reflected a discontinuous phenotype (ability to recover). In fact we now rename the 'ability' of cells to recover as the 'efficiency' of cells to recover. We have identified a number of null mutants in which the rapamycin-insensitive growth rate is significantly slower than that of wild-type cultures yet they do not exhibit as profound a recovery defect as that observed for *ego-* mutants. It is possible that there is a threshold of proliferation rate, influenced by TORC1 activity, that dictates the ability of a cell to recover within a specified time. Cells that proliferate slower than the threshold would be classified as having a profound recovery defect under the conditions of our experiment. On the other hand, cells that proliferate faster than the threshold would appear able to recover from rapamycin treatment, even though their rapamycin-insensitive proliferation rate may be slower than that of wild-type cells. Note that due to the nature of recovery from rapamycin, *i.e.* the mechanism of dilution-by-proliferation, if the conditions of the experiment are altered, for example the concentration of rapamycin used during treatment, the recovery defect of a mutant may be classified differently.

## 7.4 Identifying other potential regulators of TORC1

### 7.4.1 Mutants of translational regulators

We found that loss of Ccr4p or Dhh1p resulted in a slow rapamycin-insensitive growth rate that was selectively due to loss of either of the proteins. Ccr4p functions in the CCR4-NOT complex to both positively and negatively regulate transcription and translation (Liu et al. 1998) whilst Dhh1p functions in decapping mRNAs and has been shown to be regulated by the CCR4-NOT complex (Coller et al. 2001; Maillet & Collart 2002). We know, from measuring the translation rate of *ego1Δ* mutants, that maintaining translation is required for the ability of cells to proliferate in the presence of rapamycin and therefore recover from the drug. It is therefore possible that cells which have lost either of these two proteins (Ccr4p or Dhh1p) fail to recover from rapamycin due to excessively low translation rates in the presence of rapamycin. Measuring the translation rates of these mutants, both in the absence and presence of rapamycin, will provide an insight into whether this is the case. If the inability

of *ccr4Δ* and *dhh1Δ* mutants is due to slow translation, it would suggest that these proteins act downstream of TORC1 and are not necessarily regulators of the complex.

#### 7.4.2 Mutations of the HOM proteins

Four null mutants, the proteins of which are involved in threonine biosynthesis, were identified in the primary screen. Whilst we were only able to test the rapamycin recovery phenotype of *hom2Δ* and *hom3Δ* mutants, we found that loss of either one of these proteins results in a rapamycin recovery defect. It has been shown that Fpr1p acts as part of a feedback loop in the threonine biosynthesis pathway to prevent accumulation of the toxic aspartate β-semialdehyde intermediate (Figure 7.1) (Arévalo-Rodríguez et al. 2004). Fpr1p, activated by threonine, binds to Hom3p, the first enzyme in the aspartate to threonine (and methionine) biosynthesis pathway (Arévalo-Rodríguez et al. 2004). TORC1 is a regulator of cell growth in response to nutrient availability; it is possible that when our wild-type strain is treated with rapamycin, Fpr1p is saturated and unable to modulate the threonine (and methionine) biosynthesis pathway (Figure 7.1). If this is the case, a wild-type cell treated with rapamycin could result in elevated levels of threonine and methionine that could elevate TORC1 activity due to the cell sensing high intracellular amino acids. Therefore in cells lacking Hom2p or Hom3p, threonine (and methionine) levels are not elevated following rapamycin treatment resulting in less TORC1 activity, a slow rapamycin-insensitive growth rate and an inability to recover (Figure 7.1). It would be interesting to observe the phenotype of an *ego- hom2Δ* or *hom3Δ* double mutant to observe whether disruption of threonine biosynthesis pathway signals to TORC1 independently of, or via, the EGO complex.

#### 7.4.3 The Vps15-Vps34 complex

We found that both *vps15Δ* and *vps34pΔ* null mutants were unable to recover from rapamycin treatment. The human homolog of Vps34p has for some time been implemented in the mTORC1 signalling pathway, yet the role of hVps34 remains unclear (De Virgilio & Loewith 2006a). The identification of both *vps15Δ* and *vps34pΔ* null mutants in our screen suggests that these two proteins could be required for TORC1 activity.

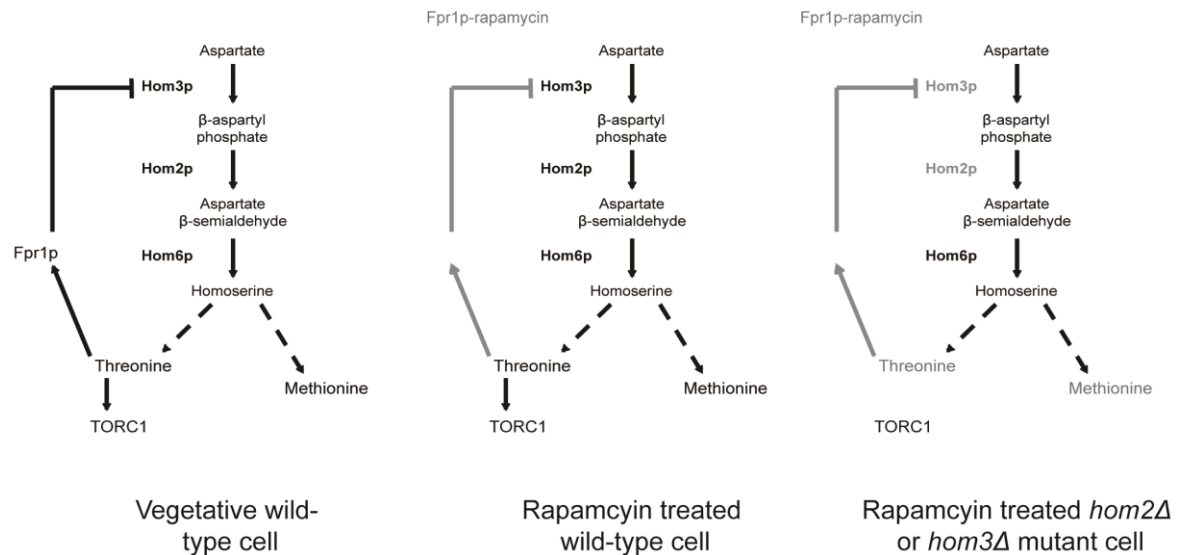


**Figure 7.1 The role of Hom2p and Hom3p in threonine biosynthesis and their potential role in TORC1 activation**

In vegetatively growing cells Fpr1p is regulated by threonine to inhibit the homoserine biosynthesis pathway. We predict that following rapamycin treatment this feedback loop is deregulated resulting in an increase in threonine production which could signal to TORC1 via amino acid sensing mechanisms promoting TORC1 activity. Loss of either Hom2p or Hom3p would prevent the synthesis of threonine in cells treated with rapamycin resulting in decreased TORC1 stimulation. Dashed lines indicate a number of enzymatic steps are involved that are not shown on this diagram

Vps34p is the only phosphatidylinositol 3-kinase in yeast (Obara & Ohsumi 2011). The signalling molecule phosphatidylinositol 3,5-bisphosphate (PI(3,5)P<sub>2</sub>) has been implicated in localising the TORC1 downstream target Sch9p to the vacuolar membrane (Jin et al. 2014). Is it possible that loss of the phosphatidylinositol 3-kinase activity of the Vps15p-Vps34p complex results in a loss of this PI(3,5)P<sub>2</sub> signalling molecule and therefore disrupts downstream TORC1 signalling? Fab1p is the only protein in yeast that converts PI(3)P into PI(3,5)P<sub>2</sub> and loss of Fab1p results in rapamycin hypersensitivity (Jin et al. 2014). It is possible that the role of the Vps15p-Vps34p complex is to provide the PI(3)P precursor for Fab1p to create PI(3,5)P<sub>2</sub> that is potentially required for TORC1 activity in a number of ways, one of which could be to recruit TORC1, its regulators and targets to the vacuolar membrane (see Chapter 1). If PI(3,5)P<sub>2</sub> is required for TORC1 localisation with its downstream targets, and PI(3,5)P<sub>2</sub> is lost in cells lacking either Vps15p or Vps34p it would suggest that these proteins are in fact implemented in regulating downstream functions of TORC1 rather than modulating TORC1 activity itself.

#### 7.4.4 The core HOPS/CORVET complex

We identified that loss of any of the four of the core HOPS/CORVET complex proteins resulted in a profound recovery defect. Loss of one of the core complex proteins resulted in a more severe phenotype than loss of the HOPS specific subunit, Vam6p, which has been shown to act as a GEF towards Gtr1p of the EGO complex (Binda et al. 2009). These results suggest that the core HOPS/CORVET complex has a role in TORC1 signalling in addition to providing a platform for the Vam6p subunit (Figure 7.2).

The TORC1 complex, its regulators and targets localise to the vacuolar membrane. Disruption of either endosomal trafficking or the vacuolar structure in a *hops/corvet*- mutant could disrupt TORC1 signalling. We found that this was unlikely; we tested both the vacuolar morphology and the ability to recover from rapamycin treatment of a *ypt7Δ* mutant. We found that the vesicle structure of a *ypt7Δ* mutant appeared similar to that of a *pep3Δ* null mutant, in that there was no defined vacuole. However, loss of Ypt7p did not compromise the ability of these cells to recover from rapamycin treatment.

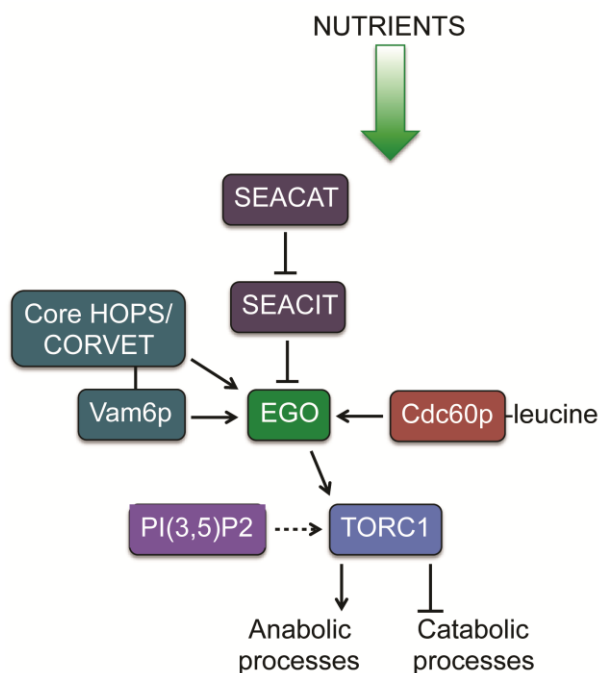


**Figure 7.2** The upstream TORC1 signalling pathway showing the role of the core HOPS/CORVET complex

The core HOPS/CORVET complex has two roles in signalling to TORC1, both of which act via the EGO complex: 1) the HOPS complex acts as a GEF to Gtr1p via the Vam6p subunit. 2) The core HOPS/CORVET proteins signal to the EGO complex in a currently unknown mechanism.

We therefore conclude that the core HOPS/CORVET complex has a role in TORC1 signalling that is different to its role for vesicle trafficking and proper vacuolar morphology.

Whilst the mammalian V-ATPase has been shown to have a role in regulating mTORC1, it would appear that this is unlikely to be the case in yeast. Preliminary studies from the Gray laboratory have found that mutants lacking a functional V-ATPase, and therefore defective vacuole function (Li & Kane 2009), are able to fully recover from rapamycin treatment. These results are consistent with other studies that find the V-ATPase is not required for rapamycin recovery in yeast (for example Kingsbury et al. 2014). The ability of cells with no functional V-ATPase to recover from rapamycin supports our conclusion that the inability of core *hops/corvet*- mutants to recover from rapamycin is due to a function of the complex in addition to that involved in maintaining vacuole morphology and function.

All nutrient signalling to TORC1 identified so far appears to act via the EGO complex. Is this also true for the core HOPS/CORVET complex? Genetic analysis of a double *ego1Δ pep3Δ* mutant suggests that the signalling of the HOPS/CORVET core complex acts via the EGO complex; the phenotype of a double *ego1Δ pep3Δ* mutant was no different to that of a single *pep3Δ* mutant. It would therefore appear that the core HOPS/CORVET complex has two roles in activating TORC1; firstly the Vam6p component of the HOPS complex acts as a GEF towards Gtr1p of the EGO complex. Second, the core HOPS/CORVET complex has an, as yet unidentified, role in TORC1 signalling that also appears to somehow act via the EGO complex. This conclusion is consistent with a recent study that has also shown that the core HOPS/CORVET complex may act via the EGO complex to regulate TORC1 (Kingsbury et al. 2014).

It is also possible that a *hops/corvet*- core mutant disrupts downstream signalling of TORC1. It has recently been shown that translocation of the GATA transcription factors, Gat1p and Gln3p, to the nucleus following TORC1 inactivation is dependent on at least three of the four core HOPS/CORVET proteins (Pep3p, Pep5p and Vps16p; Vps33p was not tested) (Fayyadkazan et al. 2014). It is therefore possible that whilst loss of endosomal trafficking does not appear to dictate the ability to recover from rapamycin *per se*, it is possible that

loss of upstream signalling and disruption of downstream signalling could explain why loss of the core HOPS/CORVET complex results in a profound recovery defect.

## 7.5 How much TORC1 activity is insensitive to rapamycin?

Why do *ego-* mutants have no vegetative growth defect? It appears that TORC1 activity is ~60% less in exponentially growing *ego-* mutants compared to wild-type cells as measured by the phosphorylation state of Sch9p (Binda et al. 2009; Panchaud et al. 2013b). The amount of TORC1 activity in the wild-type cell appears to be significantly higher than is required to maintain proliferation under normal conditions. Furthermore, *ego-* mutant cells do not display any other characteristics of cells with low TORC1 activity. It is possible that different consequences of inactive TORC1 are initiated at different thresholds of TORC1 activity. Sch9p phosphorylation aside, it would appear that all other hallmarks of inactive TORC1 measured in *ego-* cells (including the proliferation rate, translation rate, autophagy, glycogen accumulation and phosphorylation of eIF2 $\alpha$  (our results and Dubouloz et al. (2005)) require a larger reduction in TORC1 activity. However, these hallmarks have only been measured in high concentrations of rapamycin. Indeed, in this thesis we have not tested the induction of autophagy or the rapamycin-insensitive growth rate in concentrations of rapamycin less than 20 ng/mL. It is possible that different downstream events are triggered by different threshold concentrations of rapamycin.

What percentage of TORC1 is insensitive to rapamycin? Sch9p is a rapamycin-sensitive target of TORC1; in the presence of rapamycin Sch9p is fully dephosphorylated (Binda et al. 2009). Loss of the EGO complex lowers rapamycin-insensitive TORC1 activity by at least 60% (Binda et al. 2009; Panchaud et al. 2013b). The absence of a vegetative growth rate defect in *ego-* mutants suggests that ~40% of rapamycin-sensitive TORC1 activity in cells is still sufficient to maintain normal proliferation. The total TORC1 activity is a combination of the rapamycin-sensitive activity and the rapamycin-insensitive activity. The phosphorylation state of Sch9p only reports on the rapamycin-sensitive activity, but we can estimate the rapamycin-insensitive activity from

the reduced growth rate of wild-type cultures in the presence of rapamycin. If we assume, as is reasonable, that loss of the EGO complex reduces the total TORC1 activity to a level near to a threshold required for normal growth and that rapamycin brings the total TORC1 activity down to ~40% below the threshold required for normal growth (as estimated by the rapamycin-insensitive growth rate of wild-type cultures), then we arrive at the following estimates:

1. That rapamycin reduces total TORC1 activity by at least 80% in wild-type cells.
2. The corollary is that the rapamycin-insensitive activity of TORC1 is due to at most 20% of the total TORC1 activity in a wild-type cell.
3. The loss of the EGO complex alone reduces the total TORC1 activity by at least 50% relative to that in untreated wild-type cells.
4. That the addition of rapamycin to an *ego*- mutant results in a maximum of 5% of TORC1 activity remaining compared to that of an untreated wild-type cell.

These results suggest that the EGO complex is a significant contributor to total TORC1 activity, even in a wild-type cell in rich media. However, it would also appear that there is a two-fold overabundance in the total TORC1 activity in a cell, under normal conditions, which could explain why *ego*- mutants do not have an obvious phenotype. These estimations of TORC1 activity also suggest that the rapamycin-insensitive functions of TORC1 are only a minor fraction of the total TORC1 activity in the cell.

## 7.6 Does all nutrient signalling to TORC1 act via the EGO complex?

All nutrient-controlled regulators of TORC1 identified so far appear to act via the EGO complex. Yet *ego*- mutants are viable and do not have a phenotype resembling that of starved cells, as would be expected if the EGO complex was the only nutrient sensor. Is it possible that the TORC1 complex is not the predominant or sole mechanism by which nutrient availability is sensed by a cell?

If TORC1 acts in a signalling network, the modulation of TORC1 activity by ~50% afforded by the EGO complex could report on nutrient status in the context of other components in the network that are being independently modulated by nutrients.

Tate & Cooper (2013) have demonstrated that five different TORC1 inactivating treatments - nitrogen starvation, methionine sulfoximine addition, nitrogen limitation, rapamycin addition and leucine starvation, all result in different responses with regards to the nuclear relocalisation of the TORC1-regulated translation regulator Gln3p. They argue that context is key to how lowered TORC1 activity is interpreted by the cell, *i.e.*, nutrients are sensed via a network, only one component of which is TORC1.

If TORC1 does not act alone to modulate the behaviour of a cell in response to nutrients, what other pathways could be involved? The PKA pathway is one likely candidate to act with TORC1 in a larger network. Numerous studies have probed the relationship between the TORC1 and PKA pathways but the details are complex and the overall picture remains unclear, as might be expected for interactions between hubs acting in a larger network (for example see: Ramachandran & Herman 2011; Roosen et al. 2005; Schmelzle et al. 2004; Zurita-Martinez & Cardenas 2005). Both the PKA and TORC1 pathways regulate cell growth in response to nutrients and similarly to the TORC1 pathway, the PKA pathway also regulates ribosome biogenesis and stress responses (De Virgilio 2012). Loss of the downstream target Sch9p is lethal in combination with reduced PKA signalling suggesting that these two pathways act independently, although it would appear some redundancy does occur between the TORC1 and PKA pathways (Roosen et al. 2005).

## **7.7 Future work**

### **7.7.1 The large-scale genetic screen**

Our analysis of the data from the large-scale screen presented in CHAPTER has so far identified 10 null mutants that fail to recover from rapamycin treatment and have a slow rapamycin-insensitive growth rate. These 10 gene products may have a role in supporting TORC1 signalling. A combination of GO term and

known physical interaction analysis was used to select an initial subset of the primary mutant set to study in depth. However, both of these strategies have drawbacks resulting in potentially interesting genes being overlooked; this is especially true for genes that have yet to be fully characterised and therefore are not well annotated with GO terms. It would be very worthwhile testing all of the remaining 64 null mutants, identified in two or more runs of the primary screen, for their ability to recover from rapamycin. A subsequent test of the rapamycin-insensitive growth rate of those identified with a rapamycin recovery defect might highlight other potential novel regulators of TORC1.

Our analysis has so far indicated that the core HOPS/CORVET complex has a role in TORC1 signalling, independently of the known GEF function of the HOPS component Vam6p but potentially via the EGO complex. What is the function of the core HOPS/CORVET complex in TORC1 signalling? A co-immunoprecipitation assay could be performed to test whether any of the four core HOPS/CORVET complex proteins physically interacts with any of the components of the EGO complex. An interaction could indicate that the core HOPS/CORVET complex is physically modulating EGO activity and consequently TORC1 activity. If any protein-protein interactions are identified it would be worth testing whether the strength of these interactions is different in response to nutrient availability. The strength of interactions between regulators of mTORC1 changes depending on the presence of nutrients (Bar-Peled et al. 2012). It is postulated that these different binding states are a method of regulating mTORC1 activity in response to nutrient availability (Bar-Peled et al. 2012). Is it possible that yeast also using different binding strengths of upstream regulators to modulate TORC1 activity?

The results of our secondary and tertiary screens of mutants identified in the primary screen identified that loss of either Vps34p or Vps15p resulted in both a rapamycin recovery defect and a slow rapamycin-insensitive growth rate. As described in the Introduction, it is currently thought that the human homolog of Vps34p has an as yet unidentified role in mTORC1 signalling (Yang et al. 2013) and that the signalling molecule PI(3,5)P<sub>2</sub>, the synthesis of which requires PI3 (synthesised by Vps34p (Obara & Ohsumi 2011)), has a role in TORC1 signalling in yeast (Jin et al. 2014). It is postulated that PI(3,5)P<sub>2</sub> provides a platform for TORC1 and its downstream target Sch9p to reside at the vacuole membrane (Jin

et al. 2014). It is therefore unclear whether the role of the Vps34p-Vps15p complex is to act upstream of TORC1, as thought to be the case in mammalian cells, or whether it is to provide a membrane-bound platform for the TORC1 complex and its downstream targets. If the Vps34p-Vps15p complex acts upstream of TORC1 (and EGO) then the phenotype of *vps34Δ* or *vps15Δ* null mutants should be rescued by the presence of a constitutively active allele of Gtr1p (Nakashima et al. 1999). Whilst the work carried out by Jin et al. (2014) suggests that loss of Fab1p, and therefore the PI(3,5)P2 signalling molecule, results in rapamycin hypersensitivity of *fab1Δ* mutants, our preliminary results suggest that *fab1Δ* mutants are in fact able to recover from rapamycin treatment. Recovery of *fab1Δ* mutants from rapamycin treatment indicates that Vps34p-Vps15p has a role in supporting TORC1 signalling over and above that supported by PI(3,5)P2. Further work is needed to determine whether it is the Vps34p-Vps15p proteins themselves, or the PI3 signalling molecule synthesised by Vps34p-Vps15p that is required for TORC1 signalling. The use of catalytically inactive mutants of *VPS34* or *VPS15* would result in cells that contained the proteins but not the PI3 signalling molecule; the ability of these cells to recover from rapamycin treatment could then be tested.

### 7.7.2 TORC1 activity

The ability to quantify TORC1 activity within a cell could greatly extend our work. Sch9p is a direct downstream target of TORC1 and is phosphorylated when TORC1 is active (Urban et al. 2007). Previous studies have utilised a gel shift assay to determine the phosphorylation status of the C-terminal region of Sch9p, following chemical cleavage *in vitro*, as an indication of TORC1 activity (Binda et al. 2009; Panchaud et al. 2013a; Urban et al. 2007). Alternatively, eIF2 $\alpha$  is phosphorylated when TORC1 is inactivated and the phosphorylation status of eIF2 $\alpha$  can be assayed using anti-phosphorylated site-specific antibodies on a western blot (Dubouloz et al. 2005). A combination of measuring the phosphorylation status of Sch9p and eIF2 $\alpha$  would give a detailed insight into the level of TORC1 activity within specific strains and under various conditions. The ability to assay TORC1 activity would indicate whether mutants, such as *hops/corvet*- mutants, have intrinsically low levels of TORC1 activity in the presence or absence of rapamycin.

### 7.7.3 Identify new regulators of TORC1

The results of our large-scale genetic screen have identified potentially novel regulators of TORC1; however the screen was only carried out using the non-essential deletion collection. How can essential gene products be identified that have a role in TORC1 signalling? Tandem affinity purification (TAP) could be performed using known and potential regulators of TORC1, indeed the presence of Tco89p in the TOR1 complex was identified by this method (Reinke et al. 2004). By identifying protein-protein interactions, additional novel components of the TORC1 signalling complex, which may be overlooked by analysing viable null mutants alone, could be identified.

Our results, and those of others, indicate that all nutrient sensing may act via the EGO complex. However, the EGO complex is not essential in yeast. A genetic screen could be performed in which null mutants of every gene are screened in an *ego*-mutant background to identify double mutants that are synthetic sick, or lethal, under normal conditions or following either nutrient starvation or rapamycin treatment. It is possible that some null mutants that are synthetic sick or lethal in combination with loss of the EGO complex are lacking genes required to support TORC1 activity independently of the EGO complex. Such large-scale screens could be performed using, for example, a synthetic genetic array (SGA) approach (Tong et al. 2001).

### 7.7.4 How does rapamycin enter the cell?

We have shown during this thesis how rapamycin is detoxified in yeast; rapamycin is not actively metabolised but is instead detoxified by dilution-by-proliferation. But how does rapamycin enter the cell? The answer is not known; however, as speculated in this chapter it is likely that the import mechanism is linked to TORC1 activity: we predict that the uptake of rapamycin into a cell decreases following treatment with the drug; but is this true? By utilising a radiolabelled version of rapamycin (for example see Levin et al. 2005), the uptake of the drug into cells could be directly monitored over time. It is possible that rapamycin enters the cell via an amino acid transporter, in particular one that is removed from the cell surface following rapamycin treatment. A number of large-scale studies have tested single null mutants for

sensitivity to rapamycin, however none so far have found evidence of single null mutants lacking amino-acid transporters that convey rapamycin resistance (for examples see Hillenmeyer et al. 2008; Neklesa & Davis 2009). It is therefore likely that rapamycin is entering the cell via multiple amino-acid transporters. Firstly, a screen of mutant strains containing combinations of multiple deletions of known and potential amino-acid transporters could be performed seeking those with strong resistance to rapamycin. Overexpression of transporters through which rapamycin is imported into the cell could result in hypersensitivity to the drug, or an inability of cells to recover from a long treatment time with rapamycin due to excessive import of the drug. Therefore a second large-scale screen of strains over-expressing amino acid transporters in wild-type cells could be performed seeking those that are hypersensitive to the drug.

#### **7.7.5 What are the rapamycin-insensitive functions of TORC1?**

We have demonstrated within this thesis that rapamycin is not a complete inhibitor of TORC1; but what functions of TORC1 are insensitive to rapamycin treatment? Metabolomic, proteomic and transcriptomic profiles could be generated for wild-type and *ego*- mutants both in the absence and presence of rapamycin and might indicate what functions of TORC1 are resistant to the presence of rapamycin. Any such rapamycin-insensitive functions of TORC1 identified are likely to be completely new additions to our knowledge of the TORC1 signalling pathway.

### **7.8 Conclusion**

In over two decades of research into rapamycin action and the TORC1 pathway, it appears that much remains to be explored and understood. We have shown that TORC1 has in fact rapamycin-insensitive functions that have yet to be uncovered. How nutrients are signalled to TORC1 remains elusive. TORC1 likely acts as part of a much larger signalling network to control the response of cells to environmental change. Some of the genes identified in Chapter 6 may illuminate part of the answers.

## References

- Alibhoy, A. a & Chiang, H.-L., 2010. The TOR complex 1 is required for the interaction of multiple cargo proteins selected for the vacuole import and degradation pathway. *Communicative & integrative biology*, 3(6), pp.594-6.
- Altmann, M., Schmitz, N., Berset, C. & Trachsel, H., 1997. A novel inhibitor of cap-dependent translation initiation in yeast: p20 competes with eIF4G for binding to eIF4E. *The EMBO journal*, 16(5), pp.1114-21.
- Andréasson, C., Neve, E.P.A. & Ljungdahl, P.O., 2004. Four permeases import proline and the toxic proline analogue azetidine-2-carboxylate into yeast. *Yeast*, 21(3), pp.193-9.
- Anzenbacher, P. & Anzenbacherova, E., 2001. Cytochromes P450 and metabolism of xenobiotics. *Cellular and Molecular Life Sciences*, 58, pp.737-747.
- Arévalo-Rodríguez, M., Pan, X., Boeke, J.D. & Heitman, J., 2004. FKBP12 controls aspartate pathway flux in *Saccharomyces cerevisiae* to prevent toxic intermediate accumulation. *Eukaryotic cell*, 3(5), pp.1287-1296.
- Aronova, S. & Wedaman, K., 2007. Probing the membrane environment of the TOR kinases reveals functional interactions between TORC1, actin, and membrane trafficking in *Saccharomyces cerevisiae*. *Molecular biology of the cell*, 18(August), pp.2779-2794.
- Barbet, N.C., Schneider, U., Helliwell, S.B., Stansfield, I., Tuite, M.F. & Hall, M.N., 1996. TOR controls translation initiation and early G1 progression in yeast. *Molecular biology of the cell*, 7(1), pp.25-42.
- Bar-Peled, L., Chantranupong, L., Cherniack, A.D., Chen, W.W., Ottina, K. a, Grabiner, B.C., Spear, E.D., Carter, S.L., Meyerson, M. & Sabatini, D.M., 2013. A Tumor suppressor complex with GAP activity for the Rag GTPases that signal amino acid sufficiency to mTORC1. *Science*, 340(6136), pp.1100-6.
- Bar-Peled, L., Schweitzer, L.D., Zoncu, R. & Sabatini, D.M., 2012. Ragulator is a GEF for the rag GTPases that signal amino acid levels to mTORC1. *Cell*, 150(6), pp.1196-208.
- Beck, T. & Hall, M.N., 1999. The TOR signalling pathway controls nuclear localization of nutrient-regulated transcription factors. *Nature*, 402(6762), pp.689-92.
- Beck, T., Schmidt, a & Hall, M.N., 1999. Starvation induces vacuolar targeting and degradation of the tryptophan permease in yeast. *The Journal of cell biology*, 146(6), pp.1227-38.
- Benjamin, D., Colombi, M., Moroni, C. & Hall, M.N., 2011. Rapamycin passes the torch: a new generation of mTOR inhibitors. *Nature reviews. Drug discovery*, 10(11), pp.868-80.

- Berchtold, D. & Walther, T., 2009. TORC2 plasma membrane localization is essential for cell viability and restricted to a distinct domain. *Molecular biology of the cell*, 20, pp.1565-1575.
- Berset, C., Trachsel, H. & Altmann, M., 1998. The TOR (target of rapamycin) signal transduction pathway regulates the stability of translation initiation factor eIF4G in the yeast *Saccharomyces cerevisiae*. *Proceedings of the National Academy of Sciences of the United States of America*, 95(8), pp.4264-9.
- Binda, M., Péli-Gulli, M.-P., Bonfils, G., Panchaud, N., Urban, J., Sturgill, T.W., Loewith, R. & De Virgilio, C., 2009. The Vam6 GEF controls TORC1 by activating the EGO complex. *Molecular cell*, 35(5), pp.563-73.
- Bonfils, G., Jaquenoud, M., Bontron, S., Ostrowicz, C., Ungermann, C. & De Virgilio, C., 2012. Leucyl-tRNA synthetase controls TORC1 via the EGO complex. *Molecular cell*, 46(1), pp.105-10.
- Bossche, H. Vanden & Koymans, L., 1998. Review Article Cytochromes P450 in fungi. *Mycoses*, 41, pp.32-38.
- Breitkreutz, B.-J., Stark, C. & Tyers, M., 2003. Osprey: a network visualization system. *Genome biology*, 4(3), p.R22.
- Brown, C.R., Hung, G.-C., Dunton, D. & Chiang, H.-L., 2010. The TOR complex 1 is distributed in endosomes and in retrograde vesicles that form from the vacuole membrane and plays an important role in the vacuole import and degradation pathway. *The Journal of biological chemistry*, 285(30), pp.23359-70.
- Buchan, J.R. & Parker, R., 2009. Eukaryotic Stress Granules: The Ins and Out of Translation What are Stress Granules? *Molecular cell*, 36(6).
- Butcher, R.A., Bhullar, B.S., Perlstein, E.O., Marsischky, G., LaBaer, J. & Schreiber, S.L., 2006. Microarray-based method for monitoring yeast overexpression strains reveals small-molecule targets in TOR pathway. *Nature chemical biology*, 2(2), pp.103-9.
- Cai, H., Reinisch, K. & Ferro-Novick, S., 2007. Coats, tethers, Rabs, and SNAREs work together to mediate the intracellular destination of a transport vesicle. *Developmental cell*, 12(5), pp.671-82.
- Cardenas, M.E., Cutler, N.S., Lorenz, M.C., Di Como, C.J. & Heitman, J., 1999. The TOR signaling cascade regulates gene expression in response to nutrients. *Genes & development*, 13(24), pp.3271-9.
- Cherkasova, V. a & Hinnebusch, A.G., 2003. Translational control by TOR and TAP42 through dephosphorylation of eIF2alpha kinase GCN2. *Genes & development*, 17(7), pp.859-72.
- Coller, J.M., Tucker, M., Sheth, U., Valencia-Sanchez, M.A. & Parker, R., 2001. The DEAD box helicase, Dhh1p, functions in mRNA decapping and interacts with both the decapping and deadenylase complexes. *RNA*, 7, pp.1717-1727.

- Di Como, C.J. & Arndt, K.T., 1996. Nutrients, via the Tor proteins, stimulate the association of Tap42 with type 2A phosphatases. *Genes & development*, 10(15), pp.1904-16.
- Cosentino, G.P., Schmelzle, T., Haghghat, a, Helliwell, S.B., Hall, M.N. & Sonenberg, N., 2000. Eap1p, a novel eukaryotic translation initiation factor 4E-associated protein in *Saccharomyces cerevisiae*. *Molecular and cellular biology*, 20(13), pp.4604-13.
- Crešnar, B. & Petrič, S., 2011. Cytochrome P450 enzymes in the fungal kingdom. *Biochimica et biophysica acta*, 1814(1), pp.29-35.
- Dargemont, C. & Ossareh-Nazari, B., 2012. Cdc48/p97, a key actor in the interplay between autophagy and ubiquitin/proteasome catabolic pathways. *Biochimica et biophysica acta*, 1823(1), pp.138-44.
- De Virgilio, C., 2012. The essence of yeast quiescence. *FEMS microbiology reviews*, 36(2), pp.306-39.
- De Virgilio, C. & Loewith, R., 2006a. Cell growth control: little eukaryotes make big contributions. *Oncogene*, 25(48), pp.6392-6415.
- De Virgilio, C. & Loewith, R., 2006b. The TOR signalling network from yeast to man. *The international journal of biochemistry & cell biology*, 38(9), pp.1476-81.
- Dokudovskaya, S., Waharte, F., Schlessinger, A., Pieper, U., Devos, D.P., Cristea, I.M., Williams, R., Salamero, J., Chait, B.T., Sali, A., Field, M.C., Rout, M.P. & Dargemont, C., 2011. A conserved coatmer-related complex containing Sec13 and Seh1 dynamically associates with the vacuole in *Saccharomyces cerevisiae*. *Molecular & cellular proteomics*, 10(6), p.M110.006478.
- Dubouloz, F., Deloche, O., Wanke, V., Cameroni, E. & De Virgilio, C., 2005. The TOR and EGO protein complexes orchestrate microautophagy in yeast. *Molecular cell*, 19(1), pp.15-26.
- Düvel, K., Santhanam, A., Garrett, S., Schneper, L. & Broach, J.R., 2003. Multiple roles of Tap42 in mediating rapamycin-induced transcriptional changes in yeast. *Molecular cell*, 11(6), pp.1467-78.
- Fayyadkazan, M., Tate, J.J., Vierendeels, F., Cooper, T.G., Dubois, E. & Georis, I., 2014. Components of Golgi-to-vacuole trafficking are required for nitrogen- and TORC1-responsive regulation of the yeast GATA factors. *MicrobiologyOpen*, 1, pp.1-17.
- Feldman, M.E., Apsel, B., Uotila, A., Loewith, R., Knight, Z. a, Ruggiero, D. & Shokat, K.M., 2009. Active-site inhibitors of mTOR target rapamycin-resistant outputs of mTORC1 and mTORC2. *PLoS biology*, 7(2), p.e38.
- Gao, M. & Kaiser, C., 2006. A conserved GTPase-containing complex is required for intracellular sorting of the general amino-acid permease in yeast. *Nature Cell Biology*, 8(7), pp.657-667.

- Gao, X.-D., Wang, J., Keppler-Ross, S. & Dean, N., 2005. ERS1 encodes a functional homologue of the human lysosomal cystine transporter. *The FEBS journal*, 272(10), pp.2497-511.
- Giaever, G., Chu, A.M., Ni, L., Connelly, C., Riles, L., Véronneau, S., Dow, S., Lucau-Danila, A., Anderson, K., André, B., Arkin, A.P., Astromoff, A., El-Bakkoury, M., Bangham, R., Benito, R., Brachat, S., Campanaro, S., Curtiss, M., Davis, K., Deutschbauer, A., Entian, K.-D., Flaherty, P., Foury, F., Garfinkel, D.J., Gerstein, M., Gotte, D., Güldener, U., Hegemann, J.H., Hempel, S., Herman, Z., Jaramillo, D.F., Kelly, D.E., Kelly, S.L., Kötter, P., LaBonte, D., Lamb, D.C., Lan, N., Liang, H., Liao, H., Liu, L., Luo, C., Lussier, M., Mao, R., Menard, P., Ooi, S.L., Revuelta, J.L., Roberts, C.J., Rose, M., Ross-Macdonald, P., Scherens, B., Schimmack, G., Shafer, B., Shoemaker, D.D., Sookhai-Mahadeo, S., Storms, R.K., Strathern, J.N., Valle, G., Voet, M., Volckaert, G., Wang, C., Ward, T.R., Wilhelmy, J., Winzeler, E.A., Yang, Y., Yen, G., Youngman, E., Yu, K., Bussey, H., Boeke, J.D., Snyder, M., Philippsen, P., Davis, R.W. & Johnston, M., 2002. Functional profiling of the *Saccharomyces cerevisiae* genome. *Nature*, 418(6896), pp.387-91.
- Gietz, R.D., Schiestl, R.H., Willems, a R. & Woods, R. a, 1995. Studies on the transformation of intact yeast cells by the LiAc/SS-DNA/PEG procedure. *Yeast*, 11(4), pp.355-60.
- Goldstein, A. & McCusker, J., 1999. Three new dominant drug resistance cassettes for gene disruption in *Saccharomyces cerevisiae*. *Yeast*, 1553, pp.1541-1553.
- Guengerich, F.P., 1999. Cytochrome P-450 3A4: regulation and role in drug metabolism. *Annual review of pharmacology and toxicology*, 39, pp.1-17.
- Guertin, D. a & Sabatini, D.M., 2007. Defining the role of mTOR in cancer. *Cancer cell*, 12(1), pp.9-22.
- Haas, A., Scheglmann, D. & Lazar, T., 1995. The GTPase Ypt7p of *Saccharomyces cerevisiae* is required on both partner vacuoles for the homotypic fusion step of vacuole inheritance. *The EMBO journal*, 14(21), pp.5258-5270.
- Hampsey, M. & Kinzy, T.G., 2007. Synchronicity: policing multiple aspects of gene expression by Ctk1. *Genes & development*, 21(11), pp.1288-91.
- Han, J.M., Jeong, S.J., Park, M.C., Kim, G., Kwon, N.H., Kim, H.K., Ha, S.H., Ryu, S.H. & Kim, S., 2012. Leucyl-tRNA synthetase is an intracellular leucine sensor for the mTORC1-signaling pathway. *Cell*, 149(2), pp.410-24.
- Hardwick, J.S., Kuruvilla, F.G., Tong, J.K., Shamji, a F. & Schreiber, S.L., 1999. Rapamycin-modulated transcription defines the subset of nutrient-sensitive signaling pathways directly controlled by the Tor proteins. *Proceedings of the National Academy of Sciences of the United States of America*, 96(26), pp.14866-70.
- Heitman, J., Movva, N.R. & Hall, M.N., 1991. Targets for cell cycle arrest by the immunosuppressant rapamycin in yeast. *Science*, 253(5022), pp.905-9.

- Hillenmeyer, M.E., Fung, E., Wildenhain, J., Pierce, S.E., Hoon, S., Lee, W., Proctor, M., St Onge, R.P., Tyers, M., Koller, D., Altman, R.B., Davis, R.W., Nislow, C. & Giaever, G., 2008. The chemical genomic portrait of yeast: uncovering a phenotype for all genes. *Science*, 320(587), pp.362-5.
- Hirose, E., Nakashima, N., Sekiguchi, T. & Nishimoto, T., 1998. RagA is a functional homologue of *S. cerevisiae* Gtr1p involved in the Ran/Gsp1-GTPase pathway. *Journal of cell science*, 111, pp.11-21.
- Huber, A., Bodenmiller, B., Uotila, A., Stahl, M., Wanka, S., Gerrits, B., Aebersold, R. & Loewith, R., 2009. Characterization of the rapamycin-sensitive phosphoproteome reveals that Sch9 is a central coordinator of protein synthesis. *Genes & development*, 23(16), pp.1929-43.
- Inoki, K. & Guan, K.-L., 2006. Complexity of the TOR signaling network. *Trends in cell biology*, 16(4), pp.206-12.
- Jacinto, E., Guo, B., Arndt, K.T., Schmelzle, T. & Hall, M.N., 2001. TIP41 Interacts with TAP42 and Negatively Regulates the TOR Signaling Pathway. *Molecular Cell*, 8(5), pp.1017-1026.
- Jewell, J.L. & Guan, K.-L., 2013. Nutrient signaling to mTOR and cell growth. *Trends in biochemical sciences*, 38(5), pp.233-42.
- Jin, N., Mao, K., Jin, Y., Tevzadze, G., Kauffman, E.J., Park, S., Bridges, D., Loewith, R., Saltiel, A.R., Klionsky, D.J. & Weisman, L.S., 2014. Roles for PI(3,5)P<sub>2</sub> in nutrient sensing through TORC1. *Molecular biology of the cell*, 25(7), pp.1171-85.
- Jorgensen, P. & Rupeš, I., 2004. A dynamic transcriptional network communicates growth potential to ribosome synthesis and critical cell size. *Genes & development*, pp.2491-2505.
- Kamada, Y., Funakoshi, T., Shintani, T., Nagano, K., Ohsumi, M. & Ohsumi, Y., 2000. Tor-Mediated Induction of Autophagy via an Apg1 Protein Kinase Complex. *The Journal of Cell Biology*, 150(6), pp.1507-1513.
- Kamada, Y., Yoshino, K., Kondo, C., Kawamata, T., Oshiro, N., Yonezawa, K. & Ohsumi, Y., 2010. Tor directly controls the Atg1 kinase complex to regulate autophagy. *Molecular and cellular biology*, 30(4), pp.1049-58.
- Kelly, S.L., Lamb, D.C., Baldwin, B.C., Corran, A.J. & Kelly, D.E., 1997. Characterization of *Saccharomyces cerevisiae* CYP61, sterol delta<sup>22</sup>-desaturase, and inhibition by azole antifungal agents. *The Journal of biological chemistry*, 272(15), pp.9986-9988.
- Kihara, a, Noda, T., Ishihara, N. & Ohsumi, Y., 2001. Two distinct Vps34 phosphatidylinositol 3-kinase complexes function in autophagy and carboxypeptidase Y sorting in *Saccharomyces cerevisiae*. *The Journal of cell biology*, 152(3), pp.519-30.

- Kim, E., Goraksha-Hicks, P., Li, L., Neufeld, T.P. & Guan, K.-L., 2008. Regulation of TORC1 by Rag GTPases in nutrient response. *Nature cell biology*, 10(8), pp.935-45.
- Kingsbury, J.M., Sen, N.D., Maeda, T., Heitman, J. & Cardenas, M.E., 2014. Endolysosomal membrane trafficking complexes drive nutrient-dependent TORC1 signaling to control cell growth in *Saccharomyces cerevisiae*. *Genetics*, 196(4), pp.1077-89.
- Kira, S., Tabata, K., Shirahama-Noda, K., Nozoe, A., Yoshimori, T. & Noda, T., 2014. Reciprocal conversion of Gtr1 and Gtr2 nucleotide-binding states by Npr2-Npr3 inactivates TORC1 and induces autophagy. *Autophagy*, 10(9), pp.1-14.
- Kogan, K., Spear, E.D., Kaiser, C. a & Fass, D., 2010. Structural conservation of components in the amino acid sensing branch of the TOR pathway in yeast and mammals. *Journal of molecular biology*, 402(2), pp.388-98.
- Koltin, Y., Faucette, L., Bergsma, D.J., Levy, M. a, Cafferkey, R., Koser, P.L., Johnson, R.K. & Livi, G.P., 1991. Rapamycin sensitivity in *Saccharomyces cerevisiae* is mediated by a peptidyl-prolyl cis-trans isomerase related to human FK506-binding protein. *Molecular and cellular biology*, 11(3), pp.1718-23.
- Korolchuk, V.I., Saiki, S., Lichtenberg, M., Siddiqi, F.H., Roberts, E. a, Imarisio, S., Jahreiss, L., Sarkar, S., Futter, M., Menzies, F.M., O’Kane, C.J., Deretic, V. & Rubinsztein, D.C., 2011. Lysosomal positioning coordinates cellular nutrient responses. *Nature cell biology*, 13(4), pp.453-60.
- Krause, S.A. & Gray, J. V, 2002. The protein kinase C pathway is required for viability in quiescence in *Saccharomyces cerevisiae*. *Current biology*, 12(7), pp.588-93.
- Kunz, J., Schneider, U., Howald, I., Schmidt, a & Hall, M.N., 2000. HEAT repeats mediate plasma membrane localization of Tor2p in yeast. *The Journal of biological chemistry*, 275(47), pp.37011-20.
- Laplante, M. & Sabatini, D.M., 2009. mTOR signaling at a glance. *Journal of cell science*, 122, pp.3589-94.
- Levin, A.D., Jonas, M., Hwang, C.-W. & Edelman, E.R., 2005. Local and systemic drug competition in drug-eluting stent tissue deposition properties. *Journal of controlled release*, 109(1-3), pp.236-43.
- Li, a P., Kaminski, D.L. & Rasmussen, A., 1995. Substrates of human hepatic cytochrome P450 3A4. *Toxicology*, 104, pp.1-8.
- Li, H., Tsang, C.K., Watkins, M., Bertram, P.G. & Zheng, X.F.S., 2006. Nutrient regulates Tor1 nuclear localization and association with rDNA promoter. *Nature*, 442, pp.1058-61.
- Li, S.C. & Kane, P.M., 2009. The yeast lysosome-like vacuole: endpoint and crossroads. *Biochimica et biophysica acta*, 1793(4), pp.650-63.

- Linardi, R. & Natalini, C., 2006. Multi-drug resistance (MDR1) gene and P-glycoprotein influence on pharmacokinetic and pharmacodynamic of therapeutic drugs. *Ciência Rural*, 36, pp.336-341.
- Liu, H.Y., Badarinarayana, V., Audino, D.C., Rappsilber, J., Mann, M. & Denis, C.L., 1998. The NOT proteins are part of the CCR4 transcriptional complex and affect gene expression both positively and negatively. *The EMBO journal*, 17(4), pp.1096-106.
- Liu, Q., Ren, T. & Fresques, T., 2012. Selective ATP-competitive Inhibitors of TOR Suppress Rapamycin Insensitive Function of TORC2 in *S. cerevisiae* Qingsong. *ACS chemical biology*, 7(6), pp.982-987.
- Loewith, R. & Hall, M.N., 2011. Target of rapamycin (TOR) in nutrient signaling and growth control. *Genetics*, 189(4), pp.1177-201.
- Loewith, R., Jacinto, E., Wullschleger, S., Lorberg, A., Crespo, J.L., Bonenfant, D., Oppliger, W., Jenoe, P. & Hall, M.N., 2002. Two TOR complexes, only one of which is rapamycin sensitive, have distinct roles in cell growth control. *Molecular cell*, 10(3), pp.457-68.
- Long, X., Lin, Y., Ortiz-Vega, S., Yonezawa, K. & Avruch, J., 2005. Rheb binds and regulates the mTOR kinase. *Current biology*, 15(8), pp.702-13.
- Lorenz, M.C. & Heitman, J., 1995. TOR Mutations Confer Rapamycin Resistance by Preventing Interaction with FKBP12-Rapamycin. *Journal of Biological Chemistry*, 270(46), pp.27531-27537.
- Maillet, L. & Collart, M. a, 2002. Interaction between Not1p, a component of the Ccr4-not complex, a global regulator of transcription, and Dhh1p, a putative RNA helicase. *The Journal of biological chemistry*, 277(4), pp.2835-42.
- Mallory, J., Crudden, G. & Johnson, B., 2005. Dap1p, a heme-binding protein that regulates the cytochrome P450 protein Erg11p/Cyp51p in *Saccharomyces cerevisiae*. *Molecular and cellular biology*, 25(5), pp.1669-1679.
- Martin, D.E. & Hall, M.N., 2005. The expanding TOR signaling network. *Current opinion in cell biology*, 17(2), pp.158-66.
- Martin, D.E., Powers, T. & Hall, M.N., 2006. Regulation of ribosome biogenesis: where is TOR? *Cell metabolism*, 4(4), pp.259-60.
- Moye-Rowley, W., 2003. Transcriptional control of multidrug resistance in the yeast *Saccharomyces*. *Progress in nucleic acid research and molecular biology*, 73, pp.251-79.
- Nada, S., Hondo, A., Kasai, A., Koike, M., Saito, K., Uchiyama, Y. & Okada, M., 2009. The novel lipid raft adaptor p18 controls endosome dynamics by anchoring the MEK-ERK pathway to late endosomes. *The EMBO journal*, 28(5), pp.477-89.

- Nakashima, A., Maruki, Y., Imamura, Y., Kondo, C., Kawamata, T., Kawanishi, I., Takata, H., Matsuura, A., Lee, K.S., Kikkawa, U., Ohsumi, Y., Yonezawa, K. & Kamada, Y., 2008. The yeast Tor signaling pathway is involved in G2/M transition via polo-kinase. *PLoS one*, 3(5), p.e2223.
- Nakashima, N., Noguchi, E. & Nishimoto, T., 1999. *Saccharomyces cerevisiae* putative G protein, Gtr1p, which forms complexes with itself and a novel protein designated as Gtr2p, negatively regulates the Ran/Gsp1p G protein cycle through Gtr2p. *Genetics*, 152(3), pp.853-67.
- Neklesa, T.K. & Davis, R.W., 2009. A genome-wide screen for regulators of TORC1 in response to amino acid starvation reveals a conserved Npr2/3 complex. *PLoS genetics*, 5(6), p.e1000515.
- Neklesa, T.K. & Davis, R.W., 2008. Superoxide anions regulate TORC1 and its ability to bind Fpr1:rapamycin complex. *Proceedings of the National Academy of Sciences of the United States of America*, 105(39), pp.15166-71.
- Obara, K. & Ohsumi, Y., 2011. PtdIns 3-Kinase Orchestrates Autophagosome Formation in Yeast. *Journal of lipids*, 2011, p.498768.
- Obrig, T. & Culp, W., 1971. The mechanism by which cycloheximide and related glutarimide antibiotics inhibit peptide synthesis on reticulocyte ribosomes. *Journal of Biological Chemistry*, 246, pp.174-181.
- Ozaki, K., Tanaka, K. & Imamura, H., 1996. Rom1p and Rom2p are GDP/GTP exchange proteins (GEPs) for the Rho1p small GTP binding protein in *Saccharomyces cerevisiae*. *The EMBO Journal*, 15(9), pp.2196-2207.
- Painting, K. & Kirsop, B., 1990. A quick method for estimating the percentage of viable cells in a yeast population, using methylene blue staining. *World journal of microbiology & biotechnology*, 6(3), pp.346-7.
- Panchaud, N., Péli-Gulli, M. & Virgilio, C. De, 2013a. SEACing the GAP that nEGOCiates TORC1 activation. *Cell Cycle*, 12(18), pp.2948-2952.
- Panchaud, N., Péli-Gulli, M.-P. & De Virgilio, C., 2013b. Amino acid deprivation inhibits TORC1 through a GTPase-activating protein complex for the Rag family GTPase Gtr1. *Science signaling*, 6(277), p.ra42.
- Poüs, C. & Codogno, P., 2011. Lysosome positioning coordinates mTORC1 activity and autophagy. *Nature cell biology*, 13(4), pp.342-4.
- Powers, R.W., Kaeberlein, M., Caldwell, S.D., Kennedy, B.K. & Fields, S., 2006. Extension of chronological life span in yeast by decreased TOR pathway signaling. *Genes & development*, 20(2), pp.174-84.
- Powers, T. & Walter, P., 1999. Regulation of ribosome biogenesis by the rapamycin-sensitive TOR-signaling pathway in *Saccharomyces cerevisiae*. *Molecular biology of the cell*, 10(4), pp.987-1000.

- Prasad, R. & Goffeau, A., 2012. Yeast ATP-binding cassette transporters conferring multidrug resistance. *Annual review of microbiology*, 66, pp.39-63.
- Ramachandran, V. & Herman, P.K., 2011. Antagonistic interactions between the cAMP-dependent protein kinase and Tor signaling pathways modulate cell growth in *Saccharomyces cerevisiae*. *Genetics*, 187(2), pp.441-54.
- Raught, B., Gingras, a C. & Sonenberg, N., 2001. The target of rapamycin (TOR) proteins. *Proceedings of the National Academy of Sciences of the United States of America*, 98(13), pp.7037-44.
- Reinke, A., Anderson, S., McCaffery, J.M., Yates, J., Aronova, S., Chu, S., Fairclough, S., Iverson, C., Wedaman, K.P. & Powers, T., 2004. TOR complex 1 includes a novel component, Tco89p (YPL180w), and cooperates with Ssd1p to maintain cellular integrity in *Saccharomyces cerevisiae*. *The Journal of biological chemistry*, 279(15), pp.14752-62.
- Reinke, A., Chen, J.C.-Y., Aronova, S. & Powers, T., 2006. Caffeine targets TOR complex I and provides evidence for a regulatory link between the FRB and kinase domains of Tor1p. *The Journal of biological chemistry*, 281(42), pp.31616-26.
- Rohde, J., Heitman, J. & Cardenas, M.E., 2001. The TOR kinases link nutrient sensing to cell growth. *The Journal of biological chemistry*, 276(13), pp.9583-6.
- Roosen, J., Engelen, K., Marchal, K., Mathys, J., Griffioen, G., Cameroni, E., Thevelein, J.M., De Virgilio, C., De Moor, B. & Winderickx, J., 2005. PKA and Sch9 control a molecular switch important for the proper adaptation to nutrient availability. *Molecular microbiology*, 55(3), pp.862-80.
- Sancak, Y., Bar-Peled, L., Zoncu, R., Markhard, A.L., Nada, S. & Sabatini, D.M., 2010. Ragulator-Rag complex targets mTORC1 to the lysosomal surface and is necessary for its activation by amino acids. *Cell*, 141(2), pp.290-303.
- Sancak, Y., Peterson, T.R., Shaul, Y.D., Lindquist, R. a, Thoreen, C.C., Bar-Peled, L. & Sabatini, D.M., 2008. The Rag GTPases bind raptor and mediate amino acid signaling to mTORC1. *Science*, 320(5882), pp.1496-501.
- Sancak, Y., Thoreen, C.C., Peterson, T.R., Lindquist, R. a, Kang, S. a, Spooner, E., Carr, S. a & Sabatini, D.M., 2007. PRAS40 is an insulin-regulated inhibitor of the mTORC1 protein kinase. *Molecular cell*, 25(6), pp.903-15.
- Schmelzle, T., Beck, T., Martin, D.E. & Hall, M.N., 2004. Activation of the RAS/cyclic AMP pathway suppresses a TOR deficiency in yeast. *Molecular and cellular biology*, 24(1), pp.338-51.
- Schmelzle, T. & Hall, M.N., 2000. TOR, a central controller of cell growth. *Cell*, 103(2), pp.253-62.

- Schmidt, a, Beck, T., Koller, a, Kunz, J. & Hall, M.N., 1998. The TOR nutrient signalling pathway phosphorylates NPR1 and inhibits turnover of the tryptophan permease. *The EMBO journal*, 17(23), pp.6924-31.
- Segev, N. & Hay, N., 2012. Hijacking leucyl-tRNA synthetase for amino acid-dependent regulation of TORC1. *Molecular cell*, 46(1), pp.4-6.
- Sehgal, S., 2003. Sirolimus: its discovery, biological properties, and mechanism of action. *Transplantation Proceedings*, 35(3), pp.S7-S14.
- Sekiguchi, T., Hirose, E., Nakashima, N., Ii, M. & Nishimoto, T., 2001. Novel G proteins, Rag C and Rag D, interact with GTP-binding proteins, Rag A and Rag B. *The Journal of biological chemistry*, 276(10), pp.7246-57.
- Sekiguchi, T., Kamada, Y., Furuno, N., Funakoshi, M. & Kobayashi, H., 2014. Amino acid residues required for Gtr1p-Gtr2p complex formation and its interactions with the Ego1p-Ego3p complex and TORC1 components in yeast. *Genes to cells : devoted to molecular & cellular mechanisms*, 19(6), pp.449-63.
- Shimobayashi, M., Oppliger, W., Moes, S., Jenö, P. & Hall, M.N., 2013. TORC1-regulated protein kinase Npr1 phosphorylates Orm to stimulate complex sphingolipid synthesis. *Molecular biology of the cell*, 24(6), pp.870-81.
- Shin, C. & Huh, W., 2011. Bidirectional regulation between TORC1 and autophagy in *Saccharomyces cerevisiae*. *Autophagy*, 7(8), pp.854-862.
- Solinger, J. a. & Spang, A., 2013. Tethering complexes in the endocytic pathway: CORVET and HOPS. *FEBS Journal*, 280(12), pp.2743-2757.
- Springael, J.Y. & André, B., 1998. Nitrogen-regulated ubiquitination of the Gap1 permease of *Saccharomyces cerevisiae*. *Molecular biology of the cell*, 9(6), pp.1253-63.
- Stracka, D., Jozefczuk, S., Rudroff, F., Sauer, U. & Hall, M.N., 2014. Nitrogen Source Activates TOR Complex 1 via Glutamine and Independently of Gtr/Rag. *The Journal of biological chemistry*, 289, pp.25010-25020.
- Stroupe, C., Collins, K.M., Fratti, R. a & Wickner, W., 2006. Purification of active HOPS complex reveals its affinities for phosphoinositides and the SNARE Vam7p. *The EMBO journal*, 25(8), pp.1579-89.
- Suzuki, K. & Ohsumi, Y., 2010. Current knowledge of the pre-autophagosomal structure (PAS). *FEBS letters*, 584(7), pp.1280-6.
- Suzuki, T. & Inoki, K., 2011. Spatial regulation of the mTORC1 system in amino acids sensing pathway. *Acta Biochimica et Biophysica Sinica*, 43(9), pp.671-679.
- Swinnen, E., Ghillebert, R., Wilms, T. & Winderickx, J., 2013. Molecular mechanisms linking the evolutionary conserved TORC1-Sch9 nutrient signalling branch to lifespan regulation in *Saccharomyces cerevisiae*. *FEMS yeast research*, 14(1), pp.17-32.

- Szczyпка, M., 1996. The Yeast Cadmium Factor Protein (YCF1) Is a Vacuolar Glutathione S-Conjugate Pump. *Journal of Biological Chemistry*, 271(11), pp.6509-6517.
- Takahara, T. & Maeda, T., 2012. Transient sequestration of TORC1 into stress granules during heat stress. *Molecular cell*, 47(2), pp.242-52.
- Tate, J.J. & Cooper, T.G., 2013. Five conditions commonly used to down-regulate tor complex 1 generate different physiological situations exhibiting distinct requirements and outcomes. *The Journal of biological chemistry*, 288(38), pp.27243-62.
- Taylor, P.J. & Johnson, a G., 1998. Quantitative analysis of sirolimus (Rapamycin) in blood by high-performance liquid chromatography-electrospray tandem mass spectrometry. *Journal of chromatography B*, 718(2), pp.251-7.
- Thomas, G. & Hall, M., 1997. TOR signalling and control of cell growth. *Current opinion in cell biology*, 9, pp.782-787.
- Thoreen, C.C., Kang, S. a, Chang, J.W., Liu, Q., Zhang, J., Gao, Y., Reichling, L.J., Sim, T., Sabatini, D.M. & Gray, N.S., 2009. An ATP-competitive mammalian target of rapamycin inhibitor reveals rapamycin-resistant functions of mTORC1. *The Journal of Biological Chemistry*, 284(12), pp.8023-8032.
- Tong, A.H., Evangelista, M., Parsons, A.B., Xu, H., Bader, G.D., Pagé, N., Robinson, M., Raghibizadeh, S., Hogue, C.W., Bussey, H., Andrews, B., Tyers, M. & Boone, C., 2001. Systematic genetic analysis with ordered arrays of yeast deletion mutants. *Science*, 294(5550), pp.2364-8.
- Urban, J., Soulard, A., Huber, A., Lippman, S., Mukhopadhyay, D., Deloche, O., Wanke, V., Anrather, D., Ammerer, G., Riezman, H., Broach, J.R., De Virgilio, C., Hall, M.N. & Loewith, R., 2007. Sch9 is a major target of TORC1 in *Saccharomyces cerevisiae*. *Molecular cell*, 26(5), pp.663-74.
- Vézina, C., Kudelski, A. & Sehgal, S.N., 1975. Rapamycin (AY-22,989), a new antifungal antibiotic. I. Taxonomy of the producing streptomycete and isolation of the active principle. *The Journal of antibiotics*, 28(10), pp.721-726.
- Wang, M., Weiss, M., Simonovic, M., Haertinger, G., Schrimpf, S.P., Hengartner, M.O. & von Mering, C., 2012. PaxDb, a database of protein abundance averages across all three domains of life. *Molecular & cellular proteomics*, 11(8), pp.492-500.
- Wanke, V., Cameroni, E., Uotila, A., Piccolis, M., Urban, J., Loewith, R. & De Virgilio, C., 2008. Caffeine extends yeast lifespan by targeting TORC1. *Molecular Microbiology*, 69(1), pp.277-285.
- Wedaman, K. & Reinke, A., 2003. Tor kinases are in distinct membrane-associated protein complexes in *Saccharomyces cerevisiae*. *Molecular biology of the cell*, 14, pp.1204-1220.

- Welter, E., Thumm, M. & Krick, R., 2010. Quantification of nonselective bulk autophagy in *S. cerevisiae* using Pgc1-GFP. *Autophagy*, 6(6), pp.794-797.
- Werck-reichhart, D. & Feyereisen, R., 2000. Protein family review Cytochromes P450 : a success story. *Genome biology*, pp.3003.1-3003.9.
- Wolfe, K.H. & Shields, D.C., 1997. Molecular evidence for an ancient duplication of the entire yeast genome. *Nature*, 387(6634), pp.708-13.
- Wu, X. & Tu, B.P., 2011. Selective regulation of autophagy by the Iml1-Npr2-Npr3 complex in the absence of nitrogen starvation. *Molecular biology of the cell*, 22(21), pp.4124-33.
- Wullschleger, S., Loewith, R. & Hall, M.N., 2006. TOR signaling in growth and metabolism. *Cell*, 124(3), pp.471-84.
- Wurmser, A., Sato, T. & Emr, S., 2000. New component of the vacuolar class C-Vps complex couples nucleotide exchange on the Ypt7 GTPase to SNARE-dependent docking and fusion. *The Journal of cell biology*, 151(3), pp.551-562.
- Yan, G., Lai, Y. & Jiang, Y., 2012a. The TOR complex 1 is a direct target of Rho1 GTPase. *Molecular cell*, 45(6), pp.743-753.
- Yan, G., Lai, Y. & Jiang, Y., 2012b. TOR Under Stress: Targeting TORC1 by Rho1 GTPase. *Cell Cycle*, 11(18), pp.3384-3388.
- Yang, H., Gong, R. & Xu, Y., 2013. Control of cell growth: Rag GTPases in activation of TORC1. *Cellular and molecular life sciences*, 70(16), pp.2873-85.
- Zaman, S., Lippman, S.I., Zhao, X. & Broach, J.R., 2008. How *Saccharomyces* responds to nutrients. *Annual review of genetics*, 42, pp.27-81.
- Zaragoza, D., Ghavidel, a, Heitman, J. & Schultz, M.C., 1998. Rapamycin induces the G0 program of transcriptional repression in yeast by interfering with the TOR signaling pathway. *Molecular and cellular biology*, 18(8), pp.4463-70.
- Zhang, T., Péli-Gulli, M., Yang, H., Virgilio, C. De & Ding, J., 2012. Ego3 Functions as a Homodimer to Mediate the Interaction between Gtr1-Gtr2 and Ego1 in the EGO Complex to Activate TORC1. *Structure*, 1, pp.2151-2160.
- Zoncu, R., Bar-Peled, L., Efeyan, A., Wang, S., Sancak, Y. & Sabatini, D.M., 2011. mTORC1 senses lysosomal amino acids through an inside-out mechanism that requires the vacuolar H(+)-ATPase. *Science*, 334(6056), pp.678-83.
- Zurita-Martinez, S.A. & Cardenas, M.E., 2005. Tor and cyclic AMP-protein kinase A: two parallel pathways regulating expression of genes required for cell growth. *Eukaryotic cell*, 4(1), pp.63-71.

Zurita-Martinez, S.A., Puria, R., Pan, X., Boeke, J.D. & Cardenas, M.E., 2007. Efficient Tor signaling requires a functional class C Vps protein complex in *Saccharomyces cerevisiae*. *Genetics*, 176(4), pp.2139-50.